

Critical Phenomena and Renormalization-Group Theory

Andrea Pelissetto

Dipartimento di Fisica and INFN – Sezione di Roma I

Università degli Studi di Roma “La Sapienza”

I-00185 Roma, ITALIA

E-mail: Andrea.Pelissetto@roma1.infn.it

Ettore Vicari

Dipartimento di Fisica and INFN – Sezione di Pisa

Università degli Studi di Pisa

I-56127 Pisa, ITALIA

E-mail: Ettore.Vicari@df.unipi.it

February 7, 2020

Abstract

We review results concerning the critical behavior of spin systems at equilibrium. We consider the Ising and the general $O(N)$ -symmetric universality class. For each of them, we review the estimates of the critical exponents, of the equation of state, of several amplitude ratios, and of the two-point function of the order parameter. We report results in three and two dimensions. We discuss the crossover phenomena that are observed in this class of systems. In particular, we review the field-theoretical and numerical studies of systems with medium-range interactions.

Moreover, we consider several examples of magnetic and structural phase transitions, which are described by more complex Landau-Ginzburg-Wilson Hamiltonians, such as N -component systems with cubic anisotropy, $O(N)$ -symmetric systems in the presence of quenched disorder, frustrated spin systems with noncollinear or canted order, and finally, a class of systems described by the tetragonal Landau-Ginzburg-Wilson Hamiltonian with three quartic couplings. The results for the tetragonal Hamiltonian are original, in particular we present the six-loop perturbative series for the β -functions and the critical exponents.

Contents

1	The theory of critical phenomena	6		
1.1	Introduction	6		
1.2	The models and the basic thermodynamic quantities	7		
1.3	Critical indices and scaling relations	9		
1.4	Rigorous results for $N = 1$	11		
1.5	Scaling behavior of the free energy and of the equation of state	12		
1.5.1	Renormalization-group scaling	12		
1.5.2	Normalized Helmholtz free energy	13		
1.5.3	Expansion of the equation of state	14		
1.5.4	The behavior at the coexistence curve for scalar systems	15		
1.5.5	The behavior at the coexistence curve for vector systems	15		
1.5.6	Parametric representations	16		
1.5.7	Corrections to scaling	17		
1.6	The two-point function of the order parameter	18		
1.6.1	The high-temperature critical behavior	18		
1.6.2	The low-temperature critical behavior	18		
1.6.3	Scaling function associated with the correlation length	19		
1.6.4	Scaling corrections	19		
2	Numerical determination of critical quantities	20		
2.1	High-temperature expansions	20		
2.2	Monte Carlo methods	22		
2.2.1	Infinite-volume methods	22		
2.2.2	Monte-Carlo renormalization group	23		
2.2.3	Finite-size scaling	23		
2.3	Improved Hamiltonians	25		
2.3.1	Determinations of the improved Hamiltonians	25		
2.3.2	List of improved Hamiltonians	26		
2.4	Field-theoretical methods	27		
2.4.1	The fixed-dimension expansion	28		
2.4.2	The ϵ expansion	29		
2.4.3	Resummation of the perturbative series	29		
3	The Ising universality class	31		
3.1	The critical exponents	32		
3.1.1	Theoretical results	32		
3.1.2	Experimental results.	36		
3.2	The zero-momentum four-point coupling constant	36		
3.3	The critical equation of state of Ising-like systems	38		
3.3.1	Small-magnetization expansion of the (Helmholtz) free energy in the HT phase.	38		
3.3.2	Approximate parametric representations of the equation of state: The general formalism	38		
3.3.3	Approximate critical equation of state and amplitude ratios	41		
3.3.4	Trigonometric parametric representations	43		
3.4	The two-dimensional Ising universality class	45		
3.4.1	General results	45		
3.4.2	The critical equation of state: exact results	46		
3.4.3	Approximate representations of the equation of state	46		
3.5	The two-point function of Ising-like systems.	49		
3.5.1	High-temperature phase	49		
3.5.2	Low-temperature phase	50		
4	The XY universality class	51		
4.1	The three-dimensional XY universality class	51		
4.2	The critical exponents	51		
4.3	The critical equation of state	53		
4.3.1	Small-magnetization expansion of the free energy in the HT phase.	53		
4.3.2	Approximate representations of the equation of state.	53		
4.4	The two-point function in the high-temperature phase	55		
4.5	The two-dimensional XY universality class.	55		
4.5.1	The Kosterlitz-Thouless critical behavior	55		
4.5.2	The roughening transition and Solid-on-Solid models	56		
4.5.3	Numerical studies	57		
5	Critical behavior of N-vector models with $N \geq 3$	57		
5.1	Three-dimensional models	57		
5.1.1	The Heisenberg universality class	58		
5.1.2	The O(4) universality class	58		
5.2	Two-dimensional systems	58		
5.2.1	The critical behavior	60		
5.2.2	Amplitude ratios and two-point function	61		

6	The Limit $N \rightarrow 0$	62
6.1	Walk models	62
6.2	N -vector model for $N \rightarrow 0$ and self-avoiding walks	63
6.3	Critical exponents, universal amplitudes, and scaling functions	64
7	Critical crossover between the Gaussian and the Wilson-Fisher fixed point	66
7.1	Critical crossover as a two-scale problem	66
7.2	Critical crossover functions in field theory	67
7.3	Critical crossover in spin models with medium-range interaction	68
7.4	Critical crossover in self-avoiding walk models with medium-range jumps	70
8	Critical phenomena described by Landau-Ginzburg-Wilson Hamiltonians	71
8.1	Introduction	71
8.2	The field-theoretical method for generic ϕ^4 theories	72
8.3	The LGW Hamiltonian with cubic anisotropy	73
8.4	The randomly dilute spin models.	75
8.5	The critical behavior of frustrated spin models with noncollinear order	79
8.6	The tetragonal Landau-Ginzburg-Wilson Hamiltonian	84

Plan of the review

In this review, we discuss the critical behavior of spin systems at equilibrium.

In Sec. 1 we introduce the notations and the basic renormalization-group results for the critical exponents, the equation of state, and the two-point function of the order parameter, which are used throughout the paper.

In Sec. 2 we briefly outline the most important methods that are used in the study of equilibrium spin systems: high-temperature expansions, Monte Carlo methods, and field-theoretical perturbative methods. It is not a comprehensive review of these techniques; the purpose is to present the most efficient methods and to discuss their possible systematic errors.

In the following sections we focus on specific models. Secs. 3 and 4 are dedicated to the Ising and XY universality classes respectively. In Sec. 5 we consider spin models with $O(N)$ symmetry and $N \geq 3$, with special emphasis on the physically important cases $N = 3$ and $N = 4$. Finally, in Sec. 6 we discuss the limit $N \rightarrow 0$ that describes the asymptotic properties of self-avoiding walk models and of polymers in dilute solutions and in the good-solvent regime. For each of these models, we review the estimates of the critical exponents, of the equation of state, of several amplitude ratios, and of the two-point function of the order parameter. We report results in three and two dimensions.

In Sec. 7 we discuss the crossover phenomena that are observed in this class of systems. In particular, we review the field-theoretic and numerical studies of systems with medium-range interactions.

In Sec. 8 we consider several examples of magnetic and structural phase transitions, which are described by more complex Landau-Ginzburg-Wilson Hamiltonians. We present field-theoretical results and we compare them with other theoretical and experimental estimates. In Sec. 8.3 we discuss N -component systems with cubic anisotropy, and in particular the stability of the $O(N)$ -symmetric fixed point in the presence of cubic perturbations. In Sec. 8.4 we consider $O(N)$ -symmetric systems in the presence of quenched disorder, focusing on the randomly dilute Ising model that shows a different type of critical behavior. In Sec. 8.5 we discuss the critical behavior of frustrated spin systems with noncollinear or canted order, reviewing recent field-theoretical results that confirm the presence of a new chiral universality class. Finally, in Sec. 8.6 we discuss a class of systems described by the tetragonal Landau-Ginzburg-Wilson Hamiltonian with three quartic couplings. We show that all these systems have a critical behavior described by the XY model. This

section contains original results, in particular the six-loop perturbative series of the β -functions and the critical exponents.

Acknowledgements

We thank Tomeu Allés, Pasquale Calabrese, Massimo Campostrini, Sergio Caracciolo, José Carmona, Michele Caselle, Serena Causo, Alessio Celi, Robert Edwards, Martin Hasenbusch, Gustavo Mana, Tereza Mendes, Andrea Montanari, Paolo Rossi, Alan Sokal, for collaborating with us on the issues considered in this review.

1 The theory of critical phenomena

1.1 Introduction

The theory of critical phenomena has quite a long history. Probably we should put the starting point in the XIX century with the discovery by Andrews [38] of a peculiar point in the $P - T$ plane of carbon dioxide, where the properties of the liquid and of the vapor become indistinguishable and the system shows critical opalescence: It was the first observation of a critical point. Thirty years later, Pierre Curie [234] discovered the ferromagnetic transition in iron and realized the similarities of the two phenomena. However, a quantitative theory was still to come. Landau [497] was the first one proposing a general framework that provided a unified explanation of these phenomena. His model, which we now know to correspond to the mean-field approximation, gave a good qualitative description of the transitions in fluids and magnets. However, after Onsager's solution [613] of the two-dimensional Ising model [422], it was clear that Landau's model was not quantitatively correct. In the early 60's the modern notations were introduced by Fisher [299], and several scaling relations among critical exponents were derived [279, 338, 766]. Also a scaling form for the equation of state was proposed [259, 626, 768]. A more general framework was introduced by Kadanoff [445] but a complete understanding was reached only when the scaling ideas were understood in the general renormalization-group (RG) framework by Wilson [771, 772, 775]. Within the new framework it was possible to explain the nonclassical behavior of most of the systems and the universality of the behavior observed in many of them; for instance, why fluids and uniaxial antiferromagnets behave quantitatively in an identical way at the critical point.

Since then, critical phenomena have been the object of extensive studies and many new ideas have been developed in order to understand the critical behavior of increasingly complex systems. Moreover, the concepts that first appeared in this area of condensed-matter physics have been applied to completely different areas of physics, and even outside, e.g. to computer science, biology, economics, and social sciences.

The prototype of the models with a critical phase transition with nonclassical exponents is the celebrated Ising model [422]. It is defined on a regular lattice with Hamiltonian

$$\mathcal{H} = -J \sum_{\langle ij \rangle} s_i s_j - H \sum_i s_i, \quad (1.1)$$

where $s_i = \pm 1$, and the first sum is extended over all

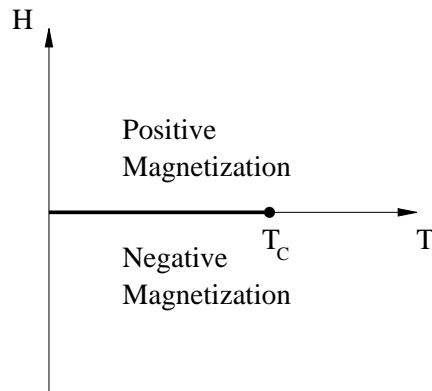


Figure 1: The phase diagram of a magnetic system.

nearest-neighbor pairs $\langle ij \rangle$. The partition function is defined by

$$Z = \sum_{\{s_i\}} e^{-\mathcal{H}/T}. \quad (1.2)$$

The Ising model provides a very simplified description of a uniaxial magnet in which the spins align along a specific direction. The phase diagram of this system is well known, see Fig. 1. For zero magnetic field, there is a paramagnetic phase for $T > T_c$ and a ferromagnetic phase for $T < T_c$, separated by a critical point at $T = T_c$. We are interested in the behavior near the critical point where long-range correlations develop and thus it is possible to give a universal description of the large-scale behavior of the system.

The Ising model can easily be mapped into a lattice gas. Consider the Hamiltonian

$$\mathcal{H} = -4J \sum_{\langle ij \rangle} \rho_i \rho_j - \mu \sum_i \rho_i, \quad (1.3)$$

where $\rho_i = 0, 1$ depending if the site is empty or occupied, and μ is the chemical potential. If we define $s_i = 2\rho_i - 1$, we reobtain the Ising-model Hamiltonian with $H = 2qJ + \mu/2$, where q is the coordination number of the lattice. Thus, for $\mu = -4qJ$, there is an equivalent transition separating the gas phase for $T > T_c$ from a liquid phase for $T < T_c$.

The lattice gas is a very crude approximation of a real fluid. Nonetheless, because of the universality of the behavior around a critical phase-transition point, certain quantities, e.g., critical exponents, amplitude ratios, scaling functions, and so on, are identical in a real fluid and in a lattice gas, and hence in the Ising model. Thus, the study of the Ising model provides *exact* predictions for real fluids at the transition point.

FLUID	MAGNET
density: $\rho - \rho_c$ chemical potential: $\mu - \mu_c$	magnetization M magnetic field H
$C_P = -T \left(\frac{\partial^2 \mathcal{F}}{\partial T^2} \right)_P$	$C_H = -T \left(\frac{\partial^2 \mathcal{F}}{\partial T^2} \right)_H$
$C_V = -T \left(\frac{\partial^2 \mathcal{A}}{\partial T^2} \right)_V$	$C_M = -T \left(\frac{\partial^2 \mathcal{A}}{\partial T^2} \right)_M$
$\kappa_T = \frac{1}{\rho} \left(\frac{\partial \rho}{\partial P} \right)_T = -\frac{1}{V} \left(\frac{\partial^2 \mathcal{F}}{\partial P^2} \right)_T$	$\chi = \left(\frac{\partial M}{\partial H} \right)_T = -\left(\frac{\partial^2 \mathcal{F}}{\partial H^2} \right)_T$

Table 1: Relation between fluid and magnetic quantities. Here \mathcal{F} and \mathcal{A} are respectively the Gibbs and the Helmholtz free energy, C_P and C_V the isobaric and isochoric specific heats, C_M and C_H the specific heats at fixed magnetization and magnetic field, κ_T the isothermic compressibility, and χ the magnetic susceptibility. ρ_c and μ_c are the values of the density and of the chemical potential at the critical point.

In the following, we will always use a magnetic “language”. In Table 1 we write down the correspondences between fluid and magnetic quantities. The quantity that is related to the magnetic field is the chemical potential. However, such a quantity is not easily accessible experimentally, and thus one uses the pressure as second thermodynamic variable. The phase diagram of a real fluid is shown in Fig. 2. It should be compared to Fig. 1. The boldface line in Fig. 1 corresponds here to the liquid-gas transition line between the triple and the critical point. Of course, our description is only valid in a neighborhood of the critical point. Note that in magnetic systems there is a symmetry $M \rightarrow -M$, $H \rightarrow -H$ which is absent in fluids. This implies that, although the leading universal behavior is identical, in fluids one observes subleading corrections that are not present in magnets, due to the different symmetry structure of the two models. This review will mostly focus on the critical behavior of systems with an N -vector order parameter without disorder. This is certainly the oldest class of systems to which the theory was applied and indeed it is meant to describe classical phenomena, like the critical behavior of simple liquids, multicomponent mixtures, and magnets. But it should be observed that these models have also found applications outside the classical condensed-matter area, and now they are used to describe transitions, e.g., in nuclear and subnuclear matter, in cosmology, etc.

The critical behavior of these models has been amply reviewed in the literature, see, e.g., Refs. [200,304,307,424,533,623,792]. Other reviews can be found in the Domb-Green-Lebowitz book series. In our review we will mainly focus on the most recent developments.

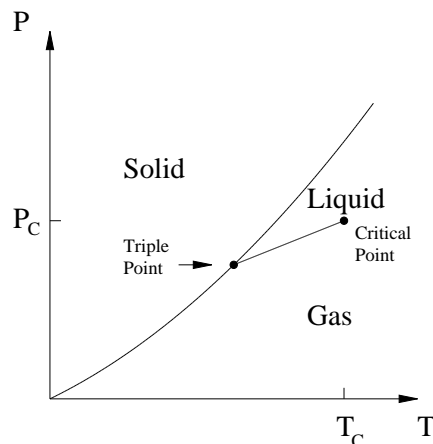


Figure 2: The phase diagram of a simple fluid.

1.2 The models and the basic thermodynamic quantities

In this review we mainly deal with systems whose critical behavior can be described by the Heisenberg Hamiltonian (in Sec. 8 we will consider some more general theories that can be studied with similar techniques). More precisely, we consider a regular lattice, N -vector unit spins defined at the sites of the lattice, and the

Hamiltonian¹

$$\mathcal{H} = -\beta \sum_{\langle ij \rangle} \vec{s}_i \cdot \vec{s}_j - \sum_i \vec{H} \cdot \vec{s}_i, \quad (1.4)$$

where the summation is extended over all lattice nearest-neighbor pairs $\langle ij \rangle$, and β is the inverse temperature. This model represents the natural generalization of the Ising model, which corresponds to the case $N = 1$. One may also consider more general Hamiltonians of the form

$$\mathcal{H} = -\beta \sum_{\langle ij \rangle} \vec{\phi}_i \cdot \vec{\phi}_j + \sum_i V(\phi_i) - \sum_i \vec{H} \cdot \vec{\phi}_i, \quad (1.5)$$

where $\vec{\phi}_i$ is an N -dimensional vector, and $V(x)$ is a generic potential such that

$$\int_{-\infty}^{\infty} e^{bx^2 - V(x)} < +\infty, \quad (1.6)$$

for all real b . An important particular case is the ϕ^4 Hamiltonian

$$\mathcal{H} = -\beta \sum_{\langle ij \rangle} \vec{\phi}_i \cdot \vec{\phi}_j + \sum_i \left[\lambda (\vec{\phi}_i^2 - 1)^2 + \phi_i^2 \right] - \sum_i \vec{H} \cdot \vec{\phi}_i, \quad (1.7)$$

which is the lattice discretization of the continuum theory

$$\mathcal{H} = \int dx \left[\frac{1}{2} \partial_\mu \vec{\varphi}(x) \cdot \partial_\mu \vec{\varphi}(x) + \frac{1}{2} r \vec{\varphi}(x)^2 + \frac{1}{4!} u (\vec{\varphi}(x)^2)^2 - \vec{H} \cdot \vec{\varphi}(x) \right], \quad (1.8)$$

where, on a hypercubic lattice,

$$\varphi = \beta^{1/2} \phi, \quad r = \frac{1 - 2\lambda}{\beta} - d, \quad u = \frac{4! \lambda}{\beta^2}. \quad (1.9)$$

The partition function is given by

$$Z(H, T) = \int \left[\prod_i d\mu(\vec{\phi}_i) \right] e^{-\mathcal{H}}, \quad (1.10)$$

where $d\mu(\vec{\phi}) = d^N \phi$ when ϕ is an unconstrained vector and $d\mu(\vec{s}) = d^N s \delta(s^2 - 1)$ for the Heisenberg Hamiltonian. We will only consider the classical case, and thus our spins will always be classical fields and not quantum operators.

As usual, we introduce the Gibbs free-energy density

$$\mathcal{F}(H, T) = -\frac{1}{V} \log Z(H, T), \quad (1.11)$$

¹Note that here and in the following our definitions differ by powers of the temperature from the standard thermodynamic definitions. It should be easy for the reader to reinstate these factors any time they are needed. See Sec. 2.1 of Ref. [655] for a discussion of the units.

and the related Helmholtz free-energy density

$$\mathcal{A}(M, T) = \vec{M} \cdot \vec{H} + \mathcal{F}(H, T), \quad (1.12)$$

where V is the volume. Here \vec{M} is the magnetization density defined by

$$\vec{M} = - \left(\frac{\partial \mathcal{F}}{\partial \vec{H}} \right)_T. \quad (1.13)$$

General arguments of thermal and mechanical stability imply $C_P \geq 0$, $C_V \geq 0$, and $\kappa_T \geq 0$, so that one also has $C_H \geq 0$, $C_M \geq 0$, and² $\chi \geq 0$. These results allow us to prove the convexity³ properties of the free energy. The positivity of the specific heats at constant magnetic field and magnetization and of the susceptibility implies that the Gibbs free energy is concave in T and H , and the Helmholtz free energy is concave in T and convex in M . For the models we have introduced above these properties can be proved easily by using Hölder's inequality [351].

We consider several thermodynamic quantities:

1. The magnetic susceptibility χ :

$$\chi = - \frac{\partial^2 \mathcal{F}}{\partial \vec{H} \cdot \partial \vec{H}} = \sum_x \left[\langle \vec{\phi}_x \cdot \vec{\phi}_0 \rangle - \langle \vec{\phi}_0 \rangle^2 \right]. \quad (1.14)$$

For vector systems we can also define

$$\chi^{ab} = - \frac{\partial^2 \mathcal{F}}{\partial H^a \partial H^b}, \quad (1.15)$$

and, if $H^a = H \delta^{a1}$, the transverse and longitudinal susceptibilities

$$\chi_L = \chi^{11}, \quad (1.16)$$

$$\chi_T = \frac{1}{(N-1)} (\chi - \chi_L). \quad (1.17)$$

Note that $\chi^{ab} = \delta^{ab} \chi_T$ for $a, b \neq 1$, because of the residual $O(N-1)$ invariance.

2. The $2n$ -point connected correlation function χ_{2n} at zero momentum:

$$\chi_{2n} = - \frac{\partial^{2n} \mathcal{F}}{(\partial \vec{H} \cdot \partial \vec{H})^n}. \quad (1.18)$$

For the Ising model in the low-temperature phase we also consider odd derivatives of the Gibbs free energy χ_{2n+1} .

²Note that it is not generically true that the magnetic susceptibility is positive. For instance, in diamagnets $\chi < 0$.

³We remind the reader that a function $f(x)$ is *convex* if $f(ax+by) \leq af(x) + bf(y)$ for all $x, y, 0 \leq a, b \leq 1$ with $a+b=1$. If the opposite inequality holds, the function is *concave*.

3. The specific heat at fixed magnetic field and at fixed magnetization:

$$C_H = -T \left(\frac{\partial^2 \mathcal{F}}{\partial T^2} \right)_H, \quad (1.19)$$

$$C_M = -T \left(\frac{\partial^2 \mathcal{A}}{\partial T^2} \right)_M. \quad (1.20)$$

4. The two-point correlation function:

$$G(x) = \langle \vec{\phi}_x \cdot \vec{\phi}_0 \rangle - \langle \vec{\phi}_0 \rangle^2, \quad (1.21)$$

whose zero-momentum component is the magnetic susceptibility, i.e. $\chi = \sum_x G(x)$. In the low-temperature phase, for vector models, one distinguishes transverse and longitudinal contributions. If $H^a = H\delta^{a1}$ we define

$$G_L(x) = \langle \phi_x^1 \phi_0^1 \rangle - M^2, \quad (1.22)$$

$$G_T(x) = \langle \phi_x^a \phi_0^a \rangle, \quad (1.23)$$

where $a \neq 1$ is not summed over.

5. The exponential or true correlation length (inverse mass gap)

$$\xi_{\text{gap}} = -\lim_{|x| \rightarrow \infty} \sup \frac{|x|}{\log G(x)}. \quad (1.24)$$

6. The second-moment correlation length

$$\xi = \left[\frac{1}{2d} \frac{\sum_x |x|^2 G(x)}{\sum_x G(x)} \right]^{1/2}. \quad (1.25)$$

1.3 Critical indices and scaling relations

In this section we describe the critical behavior of the systems we have introduced before, and define the critical indices and the universal amplitude ratios that characterize it. In three dimensions and for $H = 0$, they display a low-temperature magnetized phase separated from a paramagnetic phase by a critical point. For the ϕ^4 Hamiltonian and the Heisenberg Hamiltonian such a transition is a second-order one with an infinite correlation length. However, this is not always true for generic theories defined by the Hamiltonian (1.5). Indeed, for some choices of the potential, the transition is of first order, while for some very specific cases (they require the tuning of one parameter) one observes a tricritical transition. In three dimensions such a transition has classical exponents with logarithmic corrections. In this review we only consider the standard transition; the reader interested in the tricritical behavior should consult Ref. [503]. In two dimensions a standard critical behavior is observed only

for $N < 2$. For $N \geq 3$ there is no finite-temperature phase transition and correlations are finite for all temperatures $T \neq 0$, diverging for $T \rightarrow 0$. Some properties of these systems are described in Sec. 5.2. For $N = 2$ the systems show a Kosterlitz-Thouless transition [491] with a different type of scaling behavior. This is described in Sec. 4.5. In this section we do not consider these somewhat special cases and we confine ourselves to the ‘‘standard’’ critical behavior characterized by power laws.

When the reduced temperature

$$t \equiv \frac{T - T_c}{T_c} = \frac{\beta_c - \beta}{\beta} \quad (1.26)$$

goes to zero and the magnetic field vanishes, all quantities show power-law singularities. It is customary to consider three different trajectories in the (t, H) plane.

- The high-temperature phase at zero field: $t > 0$ and $H = 0$. For $t \rightarrow 0$ we have

$$T_c C_H \approx A^+ t^{-\alpha}, \quad (1.27)$$

$$\chi \approx N C^+ t^{-\gamma}, \quad (1.28)$$

$$\chi_{2n} \approx R_{n,N} C_{2n}^+ t^{-\gamma_{2n}}, \quad (1.29)$$

$$\xi \approx f^+ t^{-\nu}, \quad (1.30)$$

$$\xi_{\text{gap}} \approx f_{\text{gap}}^+ t^{-\nu}, \quad (1.31)$$

where the normalization factor $R_{n,N}$ is given by

$$R_{n,N} = \frac{N(N+2) \dots (N+2n-2)}{(2n-1)!!}. \quad (1.32)$$

Note that $R_{n,1} = 1$. In this phase, the magnetization vanishes.

- The coexistence curve: $t < 0$ and $H = 0$. In this case we should distinguish scalar systems ($N = 1$) from vector systems ($N \geq 2$). Indeed, on the coexistence line vector systems show Goldstone excitations that make infinite the two-point function at zero momentum. Therefore, χ , χ_{2n} , ξ , and ξ_{gap} become infinite at the coexistence curve, i.e. for $|H| \rightarrow 0$ and any $t < 0$. For a scalar system we define

$$T_c C_H \approx A^- (-t)^{-\alpha'}, \quad (1.33)$$

$$|M| \approx B(-t)^\beta, \quad (1.34)$$

$$\chi \approx C^- (-t)^{-\gamma'} \quad (1.35)$$

$$\chi_n \approx C_n^- (-t)^{-\gamma'_n}. \quad (1.36)$$

$$\xi \approx f^- (-t)^{-\nu'}, \quad (1.37)$$

$$\xi_{\text{gap}} \approx f_{\text{gap}}^- (-t)^{-\nu'}. \quad (1.38)$$

The formulae for C_H and $|M|$ apply also to vector systems.

- The critical isotherm $t = 0$. For $|H| \rightarrow 0$ we have

$$\vec{M} \approx B^c \vec{H} |H|^{(1-\delta)/\delta}, \quad (1.39)$$

$$\xi \approx f^c |H|^{-\nu_c}, \quad (1.40)$$

$$\xi_{\text{gap}} \approx f_{\text{gap}}^c |H|^{-\nu_c}. \quad (1.41)$$

The scaling of the n -point connected correlation functions is easily obtained from that of \vec{M} by taking derivatives with respect to \vec{H} . For instance

$$\chi \approx C^c |H|^{(1-\delta)/\delta}, \quad (1.42)$$

$$\chi_L \approx C_L^c |H|^{(1-\delta)/\delta}, \quad (1.43)$$

where

$$C^c = \frac{B^c}{\delta} (1 + N\delta - \delta), \quad (1.44)$$

$$C_L^c = \frac{B^c}{\delta}. \quad (1.45)$$

The relations we have introduced above are valid asymptotically close to the critical point and are obtained neglecting corrections that are controlled by a universal exponent ω , which is related to the RG dimension of the leading irrelevant operator. Explicitly, for $H = 0$, both in the high- and in the low-temperature phase we neglect corrections of order $|t|^\Delta$ with $\Delta = \omega\nu$, while on the critical isotherm we neglect terms of order $|H|^{\Delta_c}$ with $\Delta_c = \omega\nu_c$.

We also remark that the scaling behavior of the specific heat given above is correct only if $\alpha > 0$. If $\alpha < 0$ we should add an analytic background, i.e.

$$T_c C_H \approx A^\pm |t|^{-\alpha} + B, \quad (1.46)$$

valid for $\alpha > -1$. Moreover, there are interesting cases, for instance the two-dimensional Ising model, in which the specific heat diverges logarithmically, i.e.

$$T_c C_H \approx -A^\pm \log |t|. \quad (1.47)$$

The exponents we have introduced are not independent. Indeed the RG predicts several relations among them. First, the exponents in the high-temperature phase and on the coexistence curve are identical, i.e.

$$\alpha = \alpha', \quad (1.48)$$

$$\gamma = \gamma', \quad (1.49)$$

$$\gamma_{2n} = \gamma'_{2n}, \quad (1.50)$$

$$\nu = \nu'. \quad (1.51)$$

Second, the following relations hold:

$$\alpha + 2\beta + \gamma = 2, \quad (1.52)$$

$$2 - \alpha = \beta(\delta + 1), \quad (1.53)$$

$$\gamma_{2n} = \gamma + 2(n-1)\Delta_{\text{gap}}, \quad (1.54)$$

$$\beta\delta\nu_c = \nu, \quad (1.55)$$

where Δ_{gap} is the “gap” exponent—the name is due to the fact that Δ_{gap} controls the radius of the disk in the complex-temperature plane without zeroes, i.e. the gap, of the partition function (Yang-Lee theorem). Finally, below the upper critical dimension, i.e. for $d < 4$, also the following “hyperscaling” relations are supposed to be valid:

$$2 - \alpha = d\nu, \quad (1.56)$$

$$2\Delta_{\text{gap}} = d\nu + \gamma. \quad (1.57)$$

There is no rigorous proof of the validity of these equalities, although for $N = 1$ some of them are proved as inequalities. In the following we will always assume $d < 4$ and thus we will use the hyperscaling relations.

The critical exponents we have introduced are universal in the sense that they have the same value for all systems belonging to a given universality class. The amplitudes instead are not universal and depend on the microscopic parameters. Nonetheless, RG predicts that some combinations are universal. Some universal amplitude ratios are reported in Table 2. Those involving the amplitudes of the susceptibilities and of the correlation lengths on the coexistence curve, and the amplitude of the interface tension are defined only for a scalar theory.

Another important exponent, η , is defined from the behavior of the two-point function at the critical point $T = T_c$, $H = 0$:

$$G(x) \sim \frac{1}{|x|^{d-2+\eta}}. \quad (1.58)$$

The exponent η measures the deviations from a purely Gaussian behavior. It is not an independent exponent and it is related to γ and ν by the scaling relation

$$\gamma = \nu(2 - \eta). \quad (1.59)$$

In the low-temperature phase of the Ising model another interesting quantity is the interface tension σ , which, for $t \rightarrow 0^-$, behaves as

$$\sigma = \sigma_0 t^\mu. \quad (1.60)$$

The exponent μ satisfies the hyperscaling relation [767]

$$\mu = (d-1)\nu. \quad (1.61)$$

Thus, the quantity $\sigma\xi^{d-1}$ is expected to have a finite universal critical limit: $R_\sigma = \sigma_0(f^-)^{d-1}$.

In the low-temperature phase of the vector models ($N \geq 2$) correlation lengths such as ξ or ξ_{gap} cannot be defined. In this case, one introduces a transverse correlation length ξ_T defined from the stiffness constant ρ_s (see Eq. (1.161) below for the definition). Then, one

$U_0 \equiv A^+/A^-$	$U_2 \equiv C^+/C^-$
$U_4 \equiv C_4^+/C_4^-$	$R_4^+ \equiv -C_4^+ B^2/(C^+)^3$
$R_c^+ \equiv \alpha A^+ C^+/B^2$	$R_c^- \equiv \alpha A^- C^-/B^2$
$R_4^- \equiv C_4^- B^2/(C^-)^3$	$R_\chi \equiv C^+ B^{\delta-1}/(B^c)^\delta$
$v_3 \equiv -C_3^- B/(C^-)^2$	$v_4 \equiv -C_4^- B^2/(C^-)^3 + 3v_3^2$
$F_0^\infty \equiv (C^+)^{(3\delta-1)/2} (B^c)^{-\delta} (-C_4^+)^{(1-\delta)/2}$	$f_0^\infty \equiv R_\chi^{-1}$
$g_4^+ \equiv -C_4^+ / [(C^+)^2 (f^+)^d]$	$w^2 \equiv C^- / [B^2 (f^-)^d]$
$U_\xi \equiv f^+ / f^-$	$U_{\xi_{\text{gap}}} \equiv f_{\text{gap}}^+ / f_{\text{gap}}^-$
$Q^+ \equiv \alpha A^+ (f^+)^d$	$Q^- \equiv \alpha A^- (f^-)^d$
$R_\xi^+ \equiv (Q^+)^{1/d}$	$Q_\xi^+ \equiv f_{\text{gap}}^+ / f^+$
$Q_\xi^- \equiv f_{\text{gap}}^- / f^-$	$Q_\xi^c \equiv f_{\text{gap}}^c / f^c$
$Q_c \equiv B^2 (f^+)^d / C^+$	$Q_2 \equiv (f^c / f^+)^{2-\eta} C^+ / C^c$
$R_\sigma \equiv \sigma_0 (f^-)^{d-1}$	$R_\sigma^+ \equiv \sigma_0 (f^+)^{d-1}$

Table 2: Definitions of several universal amplitude ratios. Those involving C^- , C_n^- , f^- , f_{gap}^- , and σ_0 are defined only for $N = 1$.

may consider an additional hyperuniversal combination [285]

$$R_\xi^T \equiv (A^-)^{1/d} f_T^-, \quad (1.62)$$

where f_T^- is the amplitude of ξ_T . For $N = 2$, the constant R_ξ^T is determined directly from experiments below T_c on the superfluid ^4He , see, e.g., Ref. [655].

An important quantity is the four-point renormalized coupling constant g_4 defined in the high-temperature phase by

$$g_4 = -\frac{3N}{N+2} \frac{\chi_4}{\chi_2^2 \xi^d}, \quad (1.63)$$

which, in the critical limit, converges to the hyperuniversal constant

$$g_4^+ = -\frac{C_4^+}{(C^+)^2 (f^+)^d}. \quad (1.64)$$

This quantity is of interest in quantum field theory since it is related to the strength of the four-field interaction. In particular, if the critical limit of g_4 vanishes, the theory is considered trivial, since no particle scattering exists.

Finally, we want to mention the relation between ferromagnetic and antiferromagnetic models on bipartite lattices, such as simple cubic and bcc lattices. Because of the structure of the lattice, one can write down an exact relation between the two models. In an antiferromagnetic model the relevant critical quantities are the staggered ones. For instance, the relevant susceptibility

is the staggered susceptibility, defined on a hypercubic lattice by

$$\chi_{\text{stagg}} = \sum_x (-1)^{p(x)} \langle \sigma_0 \sigma_x \rangle, \quad (1.65)$$

where $p(x) = \text{mod}(x_1 + \dots + x_d, 2)$ is the parity of x . The exact mapping we mentioned implies $\chi_{\text{stagg}} = \chi_{\text{ferro}}$ where χ_{ferro} is the ordinary susceptibility in the ferromagnetic model. Thus, the critical behavior of the staggered quantities is identical to the critical behavior of the zero-momentum quantities in the ferromagnetic model. The critical behavior of the usual thermodynamic quantities is different, although still related to that of the ferromagnetic model. For instance, the susceptibility behaves as [298]

$$\chi \approx c_0 + c_1 t + \dots + b_0 |t|^{1-\alpha} + \dots \quad (1.66)$$

1.4 Rigorous results for $N = 1$

Several rigorous results have been obtained for spin systems with $N = 1$. We report here only the most relevant ones and refer the reader to Refs. [66, 290] for a detailed presentation of the subject. Most of the results deal with the general ferromagnetic Hamiltonian

$$\mathcal{H} = -\sum_{i<j} K_{ij} \phi_i \phi_j - \sum_i h_i \phi_i, \quad (1.67)$$

where K_{ij} , h_i are arbitrary positive numbers, and the first sum is extended over all lattice pairs. The parti-

tion function is given by

$$Z = \int \prod_i [d\phi_i F(\phi_i)] e^{-\mathcal{H}}, \quad (1.68)$$

where $F(x)$ is an even function satisfying

$$\int_{-\infty}^{\infty} dx F(x) e^{bx} < +\infty, \quad (1.69)$$

for all real b . For this class of Hamiltonians the following results have been obtained:

- Fisher [303] proved the inequality:

$$\gamma \leq (2 - \eta)\nu. \quad (1.70)$$

- Sokal [706] proved for $T > T_c$ that $\chi \leq \text{const}(1 + \xi^2)$ so that

$$\gamma \leq 2\nu. \quad (1.71)$$

If we *assume* the scaling relation $\gamma = (2 - \eta)\nu$ this implies $\eta\nu \geq 0$, and, since $\nu > 0$, $\eta \geq 0$.

- The following Buckingham-Gunton inequalities have been proved [155, 303]:

$$2 - \eta \leq d\gamma'/(2\beta + \gamma') \leq d\gamma'/(2 - \alpha'); \quad (1.72)$$

$$2 - \eta \leq d(\delta - 1)/(\delta + 1). \quad (1.73)$$

- Sokal [705] also proved that

$$d\nu' \geq \gamma' + 2\beta \geq 2 - \alpha'. \quad (1.74)$$

For the ϕ^4 theory it was proved [64, 343] additionally that $\gamma \geq 1$, from which, using Eq. (1.71) we have $\nu \geq 1/2$.

Several additional results have been proved for $d > 4$, showing that the exponents are classical. In particular, Aizenman [20] proved that $\gamma = 1$, and then [21] that $\beta = 1/2$ and $\delta = 3$ for all $d \geq 5$. Moreover, for the four-point renormalized coupling the inequality [20]

$$g_4 \leq \frac{\text{const}}{\xi^{d-4}} \rightarrow 0 \quad (1.75)$$

holds, implying the absence of scattering (triviality) above the four dimensions. For $d = 4$ the RG predictions [139, 501, 761] have been proved for the weakly coupled ϕ^4 theory [377, 378]:

$$\chi(t) \sim t^{-1} |\log t|^{1/3}, \quad (1.76)$$

$$\xi_{\text{gap}}(t) \sim t^{-1/2} |\log t|^{1/6}, \quad (1.77)$$

$$g_4 \sim \frac{1}{n_0 + |\log t|}, \quad (1.78)$$

where n_0 is a positive constant.

1.5 Scaling behavior of the free energy and of the equation of state

1.5.1 Renormalization-group scaling

According to the RG, the Gibbs free energy obeys a general scaling law. Indeed, we can write it in terms of the nonlinear scaling fields associated with the RG eigenoperators at the fixed point. If u_i are the scaling fields—they are analytic functions of t , H , and of any parameter appearing in the Hamiltonian—we have

$$\mathcal{F}(H, t) = \mathcal{F}_{\text{reg}}(H, t) + \mathcal{F}_{\text{sing}}(u_1, u_2, \dots, u_n, \dots), \quad (1.79)$$

where $\mathcal{F}_{\text{reg}}(H, t)$ is an analytic (also at the critical point) function of H and t which is usually called background or bulk contribution. The function $\mathcal{F}_{\text{sing}}$ obeys a scaling law of the form [759]:⁴

$$\mathcal{F}_{\text{sing}}(u_1, u_2, \dots, u_n, \dots) = b^{-d} \mathcal{F}_{\text{sing}}(b^{y_1} u_1, b^{y_2} u_2, \dots, b^{y_n} u_n, \dots), \quad (1.80)$$

where b is any positive number and y_n are the RG dimensions of the scaling fields. In the models we consider there are two relevant fields, i.e. such that $y_i > 0$, and an infinite set of irrelevant fields with $y_i < 0$. The relevant scaling fields are associated with the temperature and the magnetic field. We assume that they correspond to u_1 and u_2 . Then $u_1 \sim t$ and $u_2 \sim |H|$ for $t, |H| \rightarrow 0$. If we fix b by requiring $b^{y_1} |u_1| = 1$, we obtain from Eq. (1.80)

$$\mathcal{F}_{\text{sing}}(u_1, u_2, \dots, u_n, \dots) = |u_1|^{d/y_1} \times \mathcal{F}_{\text{sing}}(\text{sign } u_1, u_2 |u_1|^{-y_2/y_1}, \dots, u_n |u_1|^{-y_n/y_1}, \dots). \quad (1.81)$$

For $n > 2$, $y_i < 0$, so that $u_n |u_1|^{-y_n/y_1} \rightarrow 0$ for $t \rightarrow 0$. Thus, provided that $\mathcal{F}_{\text{sing}}$ is finite and nonvanishing in this limit,⁵ we can rewrite

$$\mathcal{F}_{\text{sing}}(u_1, u_2, \dots, u_n, \dots) \approx |t|^{d/y_1} \mathcal{F}_{\text{sing}}(\text{sign } t, |H| |t|^{-y_2/y_1}, 0, 0, \dots). \quad (1.82)$$

Using Eqs. (1.79) and (1.82) we obtain all scaling and hyperscaling relations provided that we identify

$$y_1 = \frac{1}{\nu}, \quad y_2 = \frac{\beta + \gamma}{\nu}. \quad (1.83)$$

⁴This is the generic scaling form. However, in certain specific cases, the behavior is more complicated with the appearance of logarithmic terms. This may be due to resonances between the RG eigenvalues, to the presence of marginal operators, ..., see Ref. [759]. The simplest example which shows such a behavior is the two-dimensional Ising model.

⁵This is expected to be true below the upper critical dimension, but not above it [305]. The breakdown of this hypothesis causes a breakdown of the hyperscaling relations and allows the recovery of the classical exponents for all dimensions above the upper critical one.

Note that the scaling part of the free energy is expressed in terms of two different functions, depending on the sign of t . However, the presence of two functions is only apparent. Indeed, since the free energy is analytic along the critical isotherm for $H \neq 0$, the two functions are analytically related. Indeed it is also possible to rewrite

$$\mathcal{F}_{\text{sing}}(u_1, u_2, \dots, u_n, \dots) \approx t^{d\nu} \widehat{\mathcal{F}}_1(|H|t^{-\beta-\gamma}). \quad (1.84)$$

where we have introduced a single function, such that the region $t > 0$ corresponds to real values of the argument and the region $t < 0$ to a line in the complex plane.

It is also possible to avoid these problems by fixing b from $b^{y_2}|u_2| = 1$. In this case we obtain for $t \rightarrow 0$ and $|H| \rightarrow 0$

$$\mathcal{F}_{\text{sing}}(u_1, u_2, \dots, u_n, \dots) \approx |H|^{d/y_2} \mathcal{F}_{\text{sing}}(t|H|^{y_1/y_2}, 1, 0, 0, \dots). \quad (1.85)$$

where we have used the fact that the free energy does not depend on the direction of \vec{H} .

In conclusion, for $|t| \rightarrow 0$, $|H| \rightarrow 0$, $t|H|^{-1/(\beta+\gamma)}$ fixed, we can write

$$\begin{aligned} \mathcal{F}(H, t) - \mathcal{F}_{\text{reg}}(H, t) &\approx \\ |t|^{d\nu} \widehat{\mathcal{F}}_1(Ht^{-\beta-\gamma}) &= |H|^{d\nu/(\beta+\gamma)} \widehat{\mathcal{F}}_2(t|H|^{-1/(\beta+\gamma)}). \end{aligned} \quad (1.86)$$

The functions $\widehat{\mathcal{F}}_1$ and $\widehat{\mathcal{F}}_2$ are universal apart from trivial rescalings. Eq. (1.86) is valid in the critical limit. Two types of corrections are expected: analytic corrections due to the fact that u_1 and u_2 are analytic functions of t and $|H|$, and nonanalytic ones due to the leading irrelevant operator, of order $|u_1|^{-y_3/y_1} \sim t^\Delta$, or $|u_2|^{-y_3/y_2} \sim |H|^{\Delta_c}$, where we have identified $y_3 = -\omega$, $\Delta = \omega\nu$, $\Delta_c = \omega\nu_c$.

The Helmholtz free energy obeys similar laws. In the critical limit, for $t \rightarrow 0$, $|M| \rightarrow 0$, and $t|M|^{-1/\beta}$ fixed, it can be written as

$$\begin{aligned} \Delta\mathcal{A} = \mathcal{A}(M, t) - \mathcal{A}_{\text{reg}}(M, t) &\approx \\ t^{d\nu} \widehat{\mathcal{A}}_1(|M|t^{-\beta}) &= |M|^{\delta+1} \widehat{\mathcal{A}}_2(t|M|^{-1/\beta}). \end{aligned} \quad (1.87)$$

where $\mathcal{A}_{\text{reg}}(M)$ is a regular background contribution. The functions $\widehat{\mathcal{A}}_1$ and $\widehat{\mathcal{A}}_2$ are universal apart from trivial rescalings.

1.5.2 Normalized Helmholtz free energy

In this section we fix the scales and define universal functions from $\widehat{\mathcal{A}}_1$ and $\widehat{\mathcal{A}}_2$. The function $\widehat{\mathcal{A}}_1(|M|t^{-\beta})$ may be written in terms of a function $A_1(z)$ normalized in the high-temperature phase. Indeed, the analyticity of the free energy outside the critical point

and the coexistence curve (Griffiths' analyticity) implies that $\widehat{\mathcal{A}}_1(|M|t^{-\beta})$ has a regular expansion in powers of $|M|^2 t^{-2\beta}$. Then, we introduce a new variable

$$z = b_1 |M| t^{-\beta}, \quad (1.88)$$

and we write

$$\widehat{\mathcal{A}}_1(|M|t^{-\beta}) = a_{10} + a_{11} A_1(z), \quad (1.89)$$

where the constants are fixed by the requirement

$$A_1(z) = \frac{z^2}{2} + \frac{z^4}{4!} + O(z^6). \quad (1.90)$$

The constants a_{10} , a_{11} , and b_1 can be expressed in terms of the amplitudes defined before:

$$a_{10} = -\frac{A^+}{(2-\alpha)(1-\alpha)}, \quad (1.91)$$

$$a_{11} = -\frac{(C^+)^2}{C_4^+}, \quad (1.92)$$

$$b_1 = \left[-\frac{C_4^+}{(C^+)^3} \right]^{1/2}. \quad (1.93)$$

The constants a_{10} , a_{11} , and b_1 are not universal since they are normalization factors. On the other hand, the ratio a_{11}/a_{10} and the function $A_1(z)$ are universal. It is worth mentioning that the ratio a_{11}/a_{10} can be computed from the function $A_1(z)$ alone. Indeed, given the function $A_1(z)$, there is a unique constant c such that $t^{2-\alpha}(c+A_1(z))$ is analytic on the critical isotherm. Such a constant is the ratio a_{10}/a_{11} .

The function $\widehat{\mathcal{A}}_2(t|M|^{-1/\beta})$ is usually normalized by considering the free energy at the coexistence curve and on the critical isotherm. First, we introduce

$$x = B^{1/\beta} t|M|^{-1/\beta}, \quad (1.94)$$

where B is the amplitude of the magnetization, so that $x = -1$ corresponds to the coexistence curve. Then, we define

$$\widehat{\mathcal{A}}_2(t|M|^{-1/\beta}) = a_{20} A_2(x), \quad (1.95)$$

requiring $A_2(0) = 1$. This fixes the constant a_{20} :

$$a_{20} = \frac{(B^c)^{-\delta}}{\delta+1}. \quad (1.96)$$

Again, a_{20} is nonuniversal while $A_2(x)$ is universal.

The functions $A_1(z)$ and $A_2(x)$ are related:

$$A_1(z) = -\frac{a_{10}}{a_{11}} + B^{\delta+1} \frac{a_{20}}{a_{11}} x^{-d\nu} A_2(x). \quad (1.97)$$

Using the definitions given above, the equation of state can be written as

$$\vec{H} = \frac{\partial \mathcal{A}}{\partial \vec{M}} = a_{11} b_1 \frac{\vec{M}}{|M|} t^{\beta \delta} F(z) = (B^c)^{-\delta} \vec{M} |M|^{\delta-1} f(x) \quad (1.98)$$

where we have neglected analytic terms and

$$\begin{aligned} F(z) &\equiv \frac{dA_1}{dz}, \\ f(x) &\equiv A_2(x) - \frac{x}{d\nu} \frac{dA_2}{dx}. \end{aligned} \quad (1.99)$$

Note that $f(0) = 1$, since $A_2(0) = 1$, and $f(-1) = 0$ since $x = -1$ corresponds to the coexistence curve.

By solving Eq. (1.99) with the appropriate boundary conditions, it is possible to reobtain the free energy. It is trivial in the case of $A_1(z)$. For $A_2(x)$ we have for $\alpha > 0$:

$$A_2(x) = 1 - (\text{sign } x) d\nu |x|^{2-\alpha} \int_0^x dy |y|^{\alpha-1} f(y). \quad (1.100)$$

For $\alpha < 0$ one writes down a similar formula by means of an appropriate subtraction within the integral.

1.5.3 Expansion of the equation of state

Since the free energy is analytic in the (T, H) plane outside the critical point and the coexistence curve, the functions $A_1(z)$ and $F(z)$ have a regular expansion in powers of z , with the appropriate symmetry under $z \rightarrow -z$. Because of Eq. (1.90) we can write

$$F(z) = z + \frac{1}{6} z^3 + \sum_{n=3} \frac{r_{2n}}{(2n-1)!} z^{2n-1}. \quad (1.101)$$

The constants r_{2n} can be computed in terms of the $2n$ -point functions χ_{2n} for $H = 0$ and $t \rightarrow 0^+$. Explicitly

$$r_6 = 10 - \frac{C_6^+ C^+}{(C_4^+)^2}, \quad (1.102)$$

$$r_8 = 280 - 56 \frac{C_6^+ C^+}{(C_4^+)^2} + \frac{C_8^+ (C^+)^2}{(C_4^+)^3},$$

$$\begin{aligned} r_{10} &= 15400 - 4620 \frac{C_6^+ (C^+)}{(C_4^+)^2} + 126 \frac{(C_6^+)^2 (C^+)^2}{(C_4^+)^4} \\ &\quad + 120 \frac{C_8^+ (C^+)^2}{(C_4^+)^3} - \frac{C_{10}^+ (C^+)^3}{(C_4^+)^4}, \end{aligned}$$

etc... The coefficients r_{2n} are related to the $2n$ -point renormalized coupling constants g_{2n}^+ :

$$g_{2n}^+ \equiv r_{2n} (g_4^+)^{n-1}. \quad (1.103)$$

Because of Griffiths' analyticity, $\mathcal{A}(M)$ has also a regular expansion in powers of t for $|M|$ fixed. This implies

the following large- z expansion of $F(z)$:

$$F(z) = z^\delta \sum_{k=0} F_k^\infty z^{-k/\beta}. \quad (1.104)$$

The function $F(z)$ is defined only for $t > 0$, and thus, in order to describe the low-temperature region $t < 0$, one should perform an analytic continuation in the complex t -plane [358, 792]. The coexistence curve corresponds to a complex $z_0 = |z_0| e^{-i\pi\beta}$ such that $F(z_0) = 0$. Therefore, the behavior near the coexistence curve is related to the behavior of $F(z)$ in the neighborhood of z_0 . The constants F_0^∞ and $|z_0|$ can be expressed in terms of universal amplitude ratios, by using the asymptotic behavior of the magnetization along the critical isotherm and at the coexistence curve. One obtains

$$\begin{aligned} F_0^\infty &= (\delta + 1) \frac{a_{20} b_1^{-\delta-1}}{a_{11}} \\ &= (B^c)^{-\delta} (C^+)^{(3\delta-1)/2} (-C_4^+)^{-(\delta-1)/2} \\ &= R_\chi (R_4^+)^{(1-\delta)/2}, \end{aligned} \quad (1.105)$$

and

$$|z_0|^2 = b_1^2 B^2 = R_4^+ \equiv -\frac{C_4^+ B^2}{(C^+)^3}. \quad (1.106)$$

Let us now consider the function $f(x)$, which is normalized in such a way that $f(-1) = 0$ and $f(0) = 1$. Of course, the two functions $f(x)$ and $F(z)$ are related:

$$z^{-\delta} F(z) = F_0^\infty f(x), \quad (1.107)$$

$$z = |z_0| x^{-\beta}. \quad (1.108)$$

Griffiths' analyticity implies that $f(x)$ is regular everywhere for $x > -1$. The regularity of $F(z)$ for $z \rightarrow 0$ implies a large- x expansion of the form

$$f(x) = x^\gamma \sum_{n=0}^\infty f_n^\infty x^{-2n\beta}. \quad (1.109)$$

The coefficients f_n^∞ can be expressed in terms of r_{2n} using Eq. (1.101). We have

$$f_n^\infty = |z_0|^{2n+1-\delta} \frac{r_{2n+2}}{F_0^\infty (2n+1)!}, \quad (1.110)$$

where we set $r_2 = r_4 = 1$. In particular, using Eqs. (1.105) and (1.106)

$$f_0^\infty = R_\chi^{-1} \equiv \frac{B}{C^+} \left(\frac{B}{B^c} \right)^\delta. \quad (1.111)$$

$f(x)$ has a regular expansion in powers of x :

$$f(x) = 1 + \sum_{n=1}^\infty f_n^0 x^n, \quad (1.112)$$

where the coefficients are related to those appearing in Eq. (1.104):

$$f_n^0 = \frac{F_n^\infty}{F_0^\infty} |z_0|^{-n/\beta}. \quad (1.113)$$

1.5.4 The behavior at the coexistence curve for scalar systems

For a scalar theory, the free energy $\mathcal{A}(M, t)$ admits a power-series expansion⁶ also near the coexistence curve, i.e. for $t < 0$ and $H = 0$. If $M_0 = \lim_{H \rightarrow 0^+} M(H)$, for $M > M_0$ (i.e. for $H \geq 0$) we can write

$$\mathcal{A}(M, t) = \sum_{j=2}^{\infty} \frac{1}{j!} a_j(t) (M - M_0)^j. \quad (1.114)$$

For the singular part of the free energy this implies an expansion of the form

$$\mathcal{A}_{\text{sing}}(M, t) = (-t)^{2-\alpha} [a_0 + b_2 \mathcal{B}(u)] \quad (1.115)$$

where

$$a_0 = -\frac{A^-}{(\alpha-1)(\alpha-2)}, \quad (1.116)$$

$$b_2 = \frac{B^2}{C^-}, \quad (1.117)$$

$$u = B^{-1} M (-t)^{-\beta}, \quad (1.118)$$

and $\mathcal{B}(u)$ is normalized so that:

$$\mathcal{B}(u) = \frac{1}{2}(u-1)^2 + \sum_{j=3}^{\infty} \frac{v_j}{j!} (u-1)^j. \quad (1.119)$$

The function $\mathcal{B}(u)$ is universal, as well as the ratio b_2/a_0 . The universal constants v_j can be related to critical ratios of the correlation functions χ_n . Explicit formulae are reported in Table 2. Note that $u = |z|/|z_0|$ for $t < 0$ and thus Eq. (1.119) is related to the expansion of $A_1(z)$ near $z = z_0$. We mention that the constants v_j are related to the low-temperature renormalized coupling constants

$$g_n^- \equiv v_n w^{n-2}, \quad (1.120)$$

where

$$w^2 \equiv \frac{C^-}{B^2 (f^-)^d}. \quad (1.121)$$

Finally, the relation between $f(x)$ and $\mathcal{B}(u)$ is

$$f(x) = b_0 u^{-\delta} \frac{d\mathcal{B}(u)}{du}, \quad (1.122)$$

$$x = -u^{-1/\beta},$$

where

$$b_0 = \frac{B}{C^-} \left(\frac{B^c}{B} \right)^\delta = \frac{U_2}{R_\chi}. \quad (1.123)$$

⁶ Note that we are not claiming that the free energy is analytic on the coexistence curve. Indeed, essential singularities are expected [36, 301, 316, 421, 499]. Thus, the expansion (1.114) should be intended as a formal power series.

In particular, for $x \rightarrow -1$ we have

$$f(x) = b_{f,1}(x+1) + b_{f,2}(x+1)^2 + O((x+1)^3). \quad (1.124)$$

where $b_{f,1} = b_0 \beta$.

1.5.5 The behavior at the coexistence curve for vector systems

In this section we discuss the behavior of $f(x)$ for $x \rightarrow -1$ for vector systems. Since the free energy \mathcal{A} is a function of $|M|$, we have

$$\chi_T = \frac{|M|}{|H|}, \quad (1.125)$$

$$\chi_L = \frac{\partial |M|}{\partial |H|}. \quad (1.126)$$

The leading behavior of χ_L at the coexistence curve can be computed from the behavior of $f(x)$ for $x \rightarrow -1$. The presence of the Goldstone singularities drastically changes the behavior of $f(x)$ with respect to the scalar case. The singularity is now controlled by the zero-temperature infrared-stable Gaussian fixed point [145, 147, 502]. This leads to the prediction

$$f(x) \approx c_f (1+x)^{2/(d-2)} \quad \text{for } x \rightarrow -1. \quad (1.127)$$

Using this result we obtain near the coexistence curve

$$\chi_L^{-1} = \delta \frac{|H|}{|M|} - \frac{(B^c)^\delta}{\beta} |M|^{\delta-1} x f'(x)$$

$$\propto (-t)^{\beta \delta (d-2)/2 - \beta} |H|^{(4-d)/2}, \quad (1.128)$$

which shows that χ_L diverges as $|H| \rightarrow 0$.

The nature of the corrections to the behavior (1.127) is less clear. Setting $v \equiv 1+x$ and $y \equiv |H| |M|^{-\delta}$, it has been conjectured that v has a double expansion in powers of y and $y^{(d-2)/2}$ near the coexistence curve [502, 681, 753], i.e., for $y \rightarrow 0$,

$$v \equiv 1+x = c_1 y + c_2 y^{1-\epsilon/2} + d_1 y^2 + d_2 y^{2-\epsilon/2} + d_3 y^{2-\epsilon} + \dots \quad (1.129)$$

where $\epsilon = 4-d$. This expansion has been derived essentially from an ϵ -expansion analysis. Note that in three dimensions this conjecture predicts an expansion in powers of $y^{1/2}$, or equivalently an expansion of $f(x)$ in powers of v for $v \rightarrow 0$.

The asymptotic expansion of the d -dimensional equation of state at the coexistence curve was computed analytically in the framework of the large- N expansion [642], using the $O(1/N)$ formulae reported in Ref. [145]. It turns out that the expansion (1.129) does not strictly hold for values of the dimension d such that

$$2 < d = 2 + \frac{2m}{n} < 4, \quad \text{for } 0 < m < n, \quad m, n \in \mathbb{N}. \quad (1.130)$$

In particular, in three dimensions one finds [642]

$$f(x) = v^2 \left[1 + \frac{1}{N} (f_1(v) + \log v f_2(v)) + O(N^{-2}) \right], \quad (1.131)$$

where the functions $f_1(v)$ and $f_2(v)$ have a regular expansion in powers of v . Moreover,

$$f_2(v) = O(v^2), \quad (1.132)$$

so that logarithms affect the expansion only at the next-next-to-leading order. A possible interpretation of the large- N analysis is that the expansion (1.131) holds for all values of N , so that Eq. (1.129) is not correct due to the presence of logarithms. The reason of their appearance is unclear, but it does not contradict the conjecture that the behavior near the coexistence curve is controlled by the zero-temperature infrared-stable Gaussian fixed point. In this case logarithms would not be unexpected, as they usually appear in reduced-temperature asymptotic expansions around Gaussian fixed points (see, e.g., Ref. [55]).

1.5.6 Parametric representations

The analytic properties of the equation of state can be implemented in a simple way by introducing appropriate parametric representations [442,686,687]. One may parametrize M and t in terms of two new variables R and θ according to⁷

$$\begin{aligned} |M| &= m_0 R^\beta m(\theta), \\ t &= R(1 - \theta^2), \\ |H| &= h_0 R^{\beta\delta} h(\theta), \end{aligned} \quad (1.133)$$

where h_0 and m_0 are normalization constants. The variable R is nonnegative and measures the distance from the critical point in the (t, H) plane; the critical behavior is obtained for $R \rightarrow 0$. The variable θ parametrizes the displacements along the lines of constant R . The line $\theta = 0$ corresponds to the high-temperature phase $t > 0$ and $H = 0$, the line $\theta = 1$ to the critical isotherm $t = 0$, and $\theta = \theta_0$, where θ_0 is the smallest positive zero of $h(\theta)$, to the coexistence curve $T < T_c$ and $H \rightarrow 0$. Of course, one should have $\theta_0 > 1$, $m(\theta) > 0$ for $0 < \theta \leq \theta_0$, and $h(\theta) > 0$ for $0 < \theta < \theta_0$. The functions $m(\theta)$ and $h(\theta)$ must be analytic in the physical interval $0 \leq \theta < \theta_0$ in order to satisfy the requirements of regularity of the equation of state (Griffiths' analyticity). Note that the mapping

⁷It is also possible to generalize the expression for t , writing $t = Rk(\theta)$. The function $k(\theta)$ must satisfy the obvious requirements: $k(0) > 0$, $k(\theta_0) < 0$, $k(\theta)$ decreasing in $0 \leq \theta \leq \theta_0$.

(1.133) is not invertible when its Jacobian vanishes, which occurs when

$$Y(\theta) \equiv (1 - \theta^2)m'(\theta) + 2\beta\theta m(\theta) = 0. \quad (1.134)$$

Thus, the parametric representation is acceptable only if $\theta_0 < \theta_l$, where θ_l is the smallest positive zero of the function $Y(\theta)$. The functions $m(\theta)$ and $h(\theta)$ are odd⁸ in θ , and can be normalized so that $m(\theta) = \theta + O(\theta^3)$ and $h(\theta) = \theta + O(\theta^3)$. Since

$$\vec{H} = a_{11} b_1^2 t^\gamma \vec{M} \quad (1.135)$$

for $|M| \rightarrow 0$, $t > 0$, see Eqs. (1.98) and (1.101), these normalization conditions imply $h_0 = a_{11} b_1^2 m_0 = m_0/C^+$. Following Ref. [358], we introduce a new arbitrary constant ρ by writing

$$m_0 = \frac{\rho}{b_1}, \quad h_0 = \rho b_1 a_{11}. \quad (1.136)$$

Using Eqs. (1.98) and (1.133), one can relate the functions $h(\theta)$, $m(\theta)$ to the scaling function $F(z)$:

$$z = \rho m(\theta) (1 - \theta^2)^{-\beta}, \quad (1.137)$$

$$F(z(\theta)) = \rho (1 - \theta^2)^{-\beta\delta} h(\theta). \quad (1.138)$$

The constant ρ is arbitrary, since it corresponds to a very specific choice of m_0 and h_0 . Thus, in the exact parametric equation the value of ρ may be chosen arbitrarily. But when adopting an approximation procedure the dependence on ρ is not eliminated, and it may become important to choose the value of this parameter properly in order to optimize the approximation.

The scaling function $f(x)$ is obtained from

$$\begin{aligned} x &= \frac{1 - \theta^2}{\theta_0^2 - 1} \left[\frac{m(\theta_0)}{m(\theta)} \right]^{1/\beta}, \\ f(x) &= \left[\frac{m(\theta)}{m(1)} \right]^{-\delta} \frac{h(\theta)}{h(1)}. \end{aligned} \quad (1.139)$$

For $\theta \rightarrow 0$, $h(\theta)$ and $m(\theta)$ can be expanded in odd powers of θ . The coefficients can be related to the expansion of $F(z)$ for $z \rightarrow 0$, see Eq. (1.101). Analogously $h(\theta)$ and $m(\theta)$ can be expanded in powers of $(1 - \theta)$. The corresponding coefficients can again be related to the expansion (1.104).

Finally, let us consider the behavior at the coexistence curve. For the Ising model, the expansion (1.114)

⁸This requirement guarantees that the equation of state has an expansion in odd powers of $|M|$, see Eq. (1.101), in the high-temperature phase for $|M| \rightarrow 0$. In the Ising model, this requirement can be understood directly, since in Eq. (1.133) one can use H and M instead of their absolute values, and thus it follows from the Z_2 symmetry of the theory.

implies a regular expansion in powers of $(\theta - \theta_0)$, with

$$\begin{aligned} m(\theta) &\approx m_{f,0} + m_{f,1}(\theta - \theta_0) + \dots \\ h(\theta) &\approx h_{f,1}(\theta - \theta_0) + \dots \end{aligned} \quad (1.140)$$

with $m_{f,0} \neq 0$. For three-dimensional models with $N \geq 2$, Eq. (1.127) implies

$$\begin{aligned} m(\theta) &\approx m_{f,0} + m_{f,1}(\theta - \theta_0) + \dots \\ h(\theta) &\approx h_{f,2}(\theta - \theta_0)^2 + \dots \end{aligned} \quad (1.141)$$

with $m_{f,0} \neq 0$. The logarithmic corrections we mentioned in Sec. 1.5.5 imply that $h(\theta)$ and/or $m(\theta)$ cannot be expanded in powers of $(\theta - \theta_0)$. Indeed, logarithmic terms should be present to reproduce $\log(1+x)$.

The singular part of the free energy is given by

$$\mathcal{F}_{\text{sing}} = h_0 m_0 R^{2-\alpha} g(\theta), \quad (1.142)$$

where $g(\theta)$ is the solution of the first-order differential equation

$$(1 - \theta^2)g'(\theta) + 2(2 - \alpha)\theta g(\theta) = [(1 - \theta^2)m'(\theta) + 2\beta\theta m(\theta)] h(\theta) \quad (1.143)$$

that is regular at $\theta = 1$.

The parametric representations are useful because the functions $h(\theta)$ and $m(\theta)$ can be chosen analytic in all the interesting domain $0 \leq \theta < \theta_0$. This is at variance with the functions $f(x)$ and $F(z)$ which display a nonanalytic behavior for $x \rightarrow \infty$ and $z \rightarrow \infty$ respectively. This fact is very important from a practical point of view. Indeed, in order to obtain approximate expressions of the equation of state, one can approximate $h(\theta)$ and $m(\theta)$ with analytic functions. The structure of the parametric representation automatically ensures that the analyticity properties of the equation of state are satisfied.

1.5.7 Corrections to scaling

In the preceding sections we have only considered the leading critical behavior. Now, we discuss the corrections to the scaling behavior. They are due to the nonlinear scaling fields in Eq. (1.80) with $y_i < 0$.

Using Eq. (1.81) and keeping only one irrelevant field, that with the largest y_i (we identify it with u_3), we have

$$\begin{aligned} \mathcal{F}_{\text{sing}}(u_1, u_2, u_3) = & \\ & |u_1|^{d/y_1} \mathcal{F}_{\text{sing}}(\text{sign } u_1, u_2|u_1|^{-y_2/y_1}, u_3|u_1|^{-y_3/y_1}) = \\ & |u_1|^{d\nu} \sum_{n=0}^{\infty} f_{n,\pm}(u_2|u_1|^{-\beta-\gamma})(u_3|u_1|^\Delta)^n, \end{aligned} \quad (1.144)$$

where we have used the standard notations $\omega = -y_3$, $\Delta = \omega\nu$. The presence of the irrelevant operator induces nonanalytic corrections proportional to $|u_1|^{n\Delta}$.

The nonlinear scaling fields are analytic functions of t , H , and of any parameter appearing in the Hamiltonian—we indicate them collectively by λ . Therefore, we can write

$$\begin{aligned} u_1 &= t + t^2 g_{11}(\lambda) + H^2 g_{21}(\lambda) + O(t^3, tH^2, H^4), \\ u_2 &= H [1 + t g_{12}(\lambda) + H^2 g_{22}(\lambda) + O(t^2, tH^2, H^4)], \\ u_3 &= g_{13}(\lambda) + t g_{23}(\lambda) + H^2 g_{33}(\lambda) + O(t^2, tH^2, H^4). \end{aligned} \quad (1.145)$$

Substituting these expressions into Eq. (1.144), we see that, if $g_{13}(\lambda) \neq 0$, the singular part of the free energy has corrections of order $t^{m\Delta+m}$. These singular corrections appear also in the other quantities. Additional singularities are due to the background term. For instance, for the susceptibility in zero magnetic field we obtain the explicit formula [16]

$$\begin{aligned} \chi &= t^{-\gamma} \sum_{m,n=0}^{\infty} \chi_{1,mn}(\lambda) t^{m\Delta+n} \\ &+ t^{1-\alpha} \sum_{m,n=0}^{\infty} \chi_{2,mn}(\lambda) t^{m\Delta+n} + \sum_{n=0}^{\infty} \chi_{3,n}(\lambda) t^n, \end{aligned} \quad (1.146)$$

where the contribution proportional to $t^{1-\alpha}$ stems from the terms of order H^2 appearing in the expansion of u_1 and u_3 , and the last term is the contribution of the regular part of the free energy. Notice that the regular part of the free energy is often assumed not to depend on H . If this were the case, we would have $\chi_{3,n}(\lambda) = 0$. However, for the two-dimensional Ising model, one can prove rigorously that $\chi_{3,0} \neq 0$ [335, 488], showing the incorrectness of this conjecture. For a discussion, see Ref. [677].

Analogous corrections are due to the other irrelevant operators present in the theory, and therefore we expect corrections proportional to t^ρ with $\rho = n_1 + n_2\Delta + \sum_i m_i \Delta_i$, where Δ_i are the exponents associated with the additional irrelevant operators.

In many interesting instances, it is possible to cancel the leading correction due to the irrelevant operator by choosing a specific value λ^* of a parameter λ appearing in the Hamiltonian. It is enough to choose λ^* such that $g_{13}(\lambda^*) = 0$. In this case, $u_3|u_1|^\Delta \sim t^{1+\Delta}$, so that no term of the form $t^{m\Delta+n}$, with $n < m$, are present. In particular the leading term proportional to t^Δ does not appear in the expansion. This class of models is particularly useful in numerical work. We will call them *improved* models, and the corresponding Hamiltonians will be named *improved* Hamiltonians.

1.6 The two-point function of the order parameter

The critical behavior of the two-point correlation function $G(x)$ of the order parameter is relevant to the description of scattering phenomena with light and neutron sources.

The discussion we have presented for the free energy extends to the correlation function as well. If $\tilde{G}(q)$ is the Fourier transform of $G(x)$ we expect a general scaling form [727]:

$$\tilde{G}(q) \approx |t|^{-\gamma} Z(t|M|^{-1/\beta}, q|t|^{-\nu}), \quad (1.147)$$

where $Z(y_1, y_2)$ is a universal function apart from trivial rescalings.

1.6.1 The high-temperature critical behavior

We describe here some general properties of the two-point function in the high-temperature phase and on the line $H = 0$. If ξ is the second-moment correlation length, we can write for $t > 0$ [309, 310, 314, 727]

$$\tilde{G}(q) \approx \frac{\chi}{g^+(y)}, \quad (1.148)$$

where $y \equiv q^2 \xi^2$. In this definition we have fixed the scales and $g^+(y)$ is a universal function. Classically, the function $\tilde{G}(q)$ has a very simple form, the so-called Ornstein-Zernicke behavior,

$$\tilde{G}(q) \approx \frac{\chi}{1 + q^2 \xi^2}. \quad (1.149)$$

Such a formula is by definition exact for $q \rightarrow 0$. However as q increases one observes significant deviations.

For $y \rightarrow 0$, $g^+(y)$ has a regular expansion in powers of y , i.e.

$$g^+(y) = 1 + y + \sum_{n=2} c_n^+ y^n, \quad (1.150)$$

where c_n^+ , $n \geq 2$, are universal constants.

For $y \rightarrow \infty$, the function $g^+(y)$ follows the Fisher-Langer law [317]

$$g^+(y)^{-1} \approx \frac{A_1^+}{y^{1-\eta/2}} \left(1 + \frac{A_2^+}{y^{(1-\alpha)/(2\nu)}} + \frac{A_3^+}{y^{1/(2\nu)}} \right). \quad (1.151)$$

Finally, there are two other important quantities that characterize the large-distance behavior of $G(x)$. Indeed, outside the critical point the function decays exponentially for large x according to:

$$G(x) \approx \frac{Z_{\text{gap}}}{2(\xi_{\text{gap}})^d} \left(\frac{2\pi|x|}{\xi_{\text{gap}}} \right)^{-(d-1)/2} e^{-|x|/\xi_{\text{gap}}}. \quad (1.152)$$

Then, we can define the ratios

$$S_M^+ \equiv \lim_{t \rightarrow 0^+} \frac{\xi^2}{\xi_{\text{gap}}^2} = \left(\frac{f^+}{f_{\text{gap}}^+} \right)^2, \quad (1.153)$$

$$S_Z^+ \equiv \lim_{t \rightarrow 0^+} \frac{\chi}{\xi_{\text{gap}}^2 Z_{\text{gap}}}, \quad (1.154)$$

and $Q_\xi^+ = (S_M)^{-1/2}$. If y_0 is the negative zero of $g^+(y)$ that is closest to the origin, then

$$S_M^+ = |y_0|, \quad (1.155)$$

$$S_Z^+ = \left. \frac{\partial g^+(y)}{\partial y} \right|_{y=y_0}. \quad (1.156)$$

1.6.2 The low-temperature critical behavior

For scalar models, the behavior in the low-temperature phase is analogous, and the same formulae hold. In particular, Eqs. (1.150) and (1.151) are valid, but of course with different functions and coefficients, i.e. $g^-(y)$, c_i^- , A_i^- , and so on. The coefficients A_n^- are related to the coefficients A_n^+ . A short-distance expansion analysis [141, 408] gives

$$\begin{aligned} \frac{A_1^+}{A_1^-} &= U_2^{-1} U_\xi^{-\gamma/\nu}, \\ \frac{A_2^+}{A_2^-} &= -U_0 U_\xi^{(1-\alpha)/\nu}, \\ \frac{A_3^+}{A_3^-} &= U_\xi^{1/\nu}, \end{aligned} \quad (1.157)$$

where U_0 , U_2 , and U_ξ have been defined in Table 2.

For vector systems, the behavior is more complicated since the correlation function at zero momentum diverges on the coexistence line [146, 410, 627]. For small H , $t < 0$, and $q \rightarrow 0$, the transverse two-point function behaves as [313, 627]

$$\tilde{G}_T(q) \approx \frac{M^2}{MH + \rho_s q^2}, \quad (1.158)$$

where ρ_s is the stiffness constant.⁹ For $t \rightarrow 0$ the stiffness constant goes to zero as [313, 373]

$$\rho_s = \rho_{s0} (-t)^s, \quad (1.159)$$

where the exponent s is given by the hyperscaling relation

$$s = (d-2)\nu. \quad (1.160)$$

From the stiffness constant one may define a correlation length on the coexistence curve by

$$\xi_T = \rho_s^{-1/(d-2)} = \rho_{s0}^{-1/(d-2)} (-t)^{-\nu}. \quad (1.161)$$

⁹We mention that the stiffness constant can be also written in terms of the helicity modulus [313].

For $H \rightarrow 0$ the correlation function diverges for $q \rightarrow 0$ as $1/q^2$, implying the algebraic decay of $G_T(x)$ for large x , i.e.

$$G_T(x) \approx M^2 \frac{\Gamma(d/2)\pi^{-d/2}}{2(d-2)} \left(\frac{\xi_T}{|x|}\right)^{d-2}. \quad (1.162)$$

For $|x| \rightarrow \infty$ and $|H| \rightarrow 0$, the longitudinal correlation function is directly related to the transverse one. On the coexistence curve we have [627]

$$\tilde{G}_L(q) \sim \frac{M^2 \xi_T^d}{(q \xi_T)^{d-4}}, \quad (1.163)$$

and, in real space,

$$G_L(x) \sim M^2 \left(\frac{\xi_T}{|x|}\right)^{2d-4}. \quad (1.164)$$

The short-distance behavior of $G(x)$ and the corresponding large- q behavior of $\tilde{G}(q)$ in the whole plane (t, H) are discussed in Ref. [141].

1.6.3 Scaling function associated with the correlation length

From the two-variable scaling function (1.147) of the two-point function one may derive scaling functions associated with the correlation lengths ξ_{gap} and ξ defined in Eqs. (1.24) and (1.25). One may write in the scaling limit

$$\xi^2(M, t) = (B^c)^{2\delta/d} M^{-2\nu/\beta} f_\xi(x), \quad (1.165)$$

$$\xi_{\text{gap}}^2(M, t) = (B^c)^{2\delta/d} M^{-2\nu/\beta} f_{\text{gap}}(x), \quad (1.166)$$

where $x = B^{1/\beta} t M^{-1/\beta}$ is the variable introduced in Sec. 1.5.2. The normalization of the functions is such to make $f_\xi(x)$ and $f_{\text{gap}}(x)$ universal. This follows from two-scale-factor universality, i.e. the assumption that the singular part of the free energy in a correlation volume is universal. Using the scaling relations (1.87) and (1.95) for the Helmholtz free-energy density we obtain in the scaling limit

$$\mathcal{A}_{\text{sing}}(M, t) [\xi(M, t)]^d = \frac{1}{\delta + 1} A_2(x) f_\xi(x). \quad (1.167)$$

Since $A_2(x)$ is universal, it follows that also $f_\xi(x)$ is universal. The same argument proves that $f_{\text{gap}}(x)$ is universal. Note the following limits:

$$\lim_{x \rightarrow \infty} x^{2\nu} f_\xi(x) = (R_\chi Q_c)^{2/d}, \quad (1.168)$$

$$\begin{aligned} f_\xi(0) &= (f^c)^2 (B^c)^{2/d} \\ &= \left(\frac{R_4^+}{g_4}\right)^{2/d} \left(\frac{Q_2}{\delta}\right)^{2\nu/\gamma} (R_\chi)^{-4\beta/d\gamma}, \end{aligned} \quad (1.169)$$

$$f_\xi(-1) = U_\xi^{-2} (R_\chi Q_c)^{2/d}. \quad (1.170)$$

Similar equations hold for $f_{\text{gap}}(x)$. Of course, Eq. (1.170) applies only to scalar systems.

One may also define a scaling function associated with the ratio ξ^2/χ , that is

$$\xi^2/\chi = (B^c)^{(2-d)\delta/d} M^{-\eta\nu/\beta} f_Z(x), \quad (1.171)$$

where $f_Z(x)$ is a new universal function which is related to the scaling functions $f_\xi(x)$ and $f(x)$ by

$$f_Z(x) = f_\xi(x) \left[\delta f(x) - \frac{1}{\beta} x f'(x) \right]. \quad (1.172)$$

For vector systems, in Eq. (1.171) one should consider the longitudinal susceptibility χ_L . We also introduce a scaling function in terms of the variable z defined in Eq. (1.88). We write

$$\xi^2/\chi = (-a_{11})^{2/d} g_4^{-2/d} t^{\eta\nu} F_Z(z), \quad (1.173)$$

where the normalization factor is chosen so that $F_Z(0) = 1$, and a_{11} is defined in Eq. (1.92). The function $F_Z(z)$ is universal and is simply related to the function $f_Z(x)$ defined in (1.171). Indeed, we have

$$z^{\eta\nu/\beta} F_Z(z) = \frac{1}{f_0^\infty} |z_0|^{\eta\nu/\beta} (R_\chi Q_c)^{-2/d} f_Z(x), \quad (1.174)$$

where the universal constants f_0^∞ and $|z_0|$ are defined in Sec. 1.5.3. Note that ξ^2/χ must always be positive by thermodynamic stability requirements (see, e.g., Ref. [351, 711]). Indeed, this combination is related to the intrinsically positive free energy associated with nonvanishing gradients $|\nabla M|$ throughout the critical region. Therefore, the scaling functions must be positive.

One may also consider parametric representations of the correlation lengths ξ and ξ_{gap} supplementing those for the equation of state, cf. Eq. (1.133), such as

$$\xi^2/\chi = R^{-\eta\nu} a(\theta), \quad (1.175)$$

$$\xi_{\text{gap}}^2/\chi = R^{-\eta\nu} a_{\text{gap}}(\theta). \quad (1.176)$$

Again, given the parametric representation (1.133) of the equation of state, the normalizations of $a(\theta)$ and $a_{\text{gap}}(\theta)$ are not arbitrary but are fixed by the two-scale-factor universality. We have

$$\begin{aligned} a(0) &= h_0^{1-2/d} m_0^{-1-2/d} g_4^{-2/d} [6(\gamma + h_3 - m_3)]^{2/d}, \\ a_{\text{gap}}(0) &= (Q_\xi^+)^2 a(0), \end{aligned} \quad (1.177)$$

where $h_3 = d^3 h / d\theta^3 (\theta = 0)$, $m_3 = d^3 m / d\theta^3 (\theta = 0)$.

1.6.4 Scaling corrections

The results we presented above apply only in the critical limit and are obtained neglecting subleading corrections. There are essentially two types of corrections:

- (a) Corrections due to operators that are rotationally invariant. Such corrections are always present, both in continuum systems and in lattice systems.
- (b) Corrections due to operators that have only the lattice symmetry. Such corrections are not present in rotationally invariant systems, but only in models and experimental systems on a lattice. The operators which appear depend on the type of lattice. These corrections control the recovery of rotational invariance of the correlation functions.

In three dimensions, corrections of type (b), controlled by an exponent ω_{NR} , are much weaker than corrections of type (a) that are controlled by the exponent ω , i.e. $\omega < \omega_{\text{NR}}$. Therefore, rotational invariance is recovered before the disappearance of the rotationally-invariant scaling corrections. In two dimensions instead and on the square lattice, corrections of type (a) and (b) have exactly the same exponent [169].

2 Numerical determination of critical quantities

In this section we wish to review the numerical methods that are used in the study of statistical systems at criticality. In two dimensions many nontrivial models can be solved exactly, and moreover there exists a very powerful tool, conformal field theory, that gives exact predictions for the critical exponents and for the behavior at the critical point. In three dimensions the situation is worse: No nontrivial model has been solved exactly and there is no theory providing exact predictions at the critical point. In all these cases, one must resort to numerical methods. For the class of models we consider the most precise results have been obtained from the analysis of high-temperature (HT) expansions, from Monte Carlo (MC) simulations, and by using perturbative field-theoretical (FT) methods. For the Ising model, one can also consider low-temperature (LT) expansions (see, e.g., Ref. [623]). The results of their analysis are not so precise as those obtained using HT expansions. Nonetheless, LT series are important since they give direct access to LT quantities. We will not review them here since they are conceptually very similar to the HT expansions.¹⁰

2.1 High-temperature expansions

The HT expansion is one of the most efficient approaches to the study of critical phenomena. For the

¹⁰The interested reader can find LT expansions in Refs. [49, 93, 120, 366, 717, 744] and references therein.

models we are considering, present-day computers and a careful use of graph techniques [170, 530, 603, 664, 781] allow the generation of quite long series. In three dimensions, for χ and

$$\mu_2 \equiv \sum_x |x|^2 G(x), \quad (2.1)$$

the two quantities that are used in the determination of the critical exponents, the longest available series are the following:

- (a) Ising model: 25 orders on the body-centered cubic (bcc) lattice and 23 on the simple cubic (sc) lattice [170];
- (b) Klauder, double-Gaussian, and Blume-Capel model for generic values of the coupling, spin- S Ising model for $S = 1/2, 1, 2$, and $S = \infty$: 21 orders on the bcc lattice [603];
- (c) N -vector model for generic values of N : 21 orders on the bcc, sc, and diamond lattices [164, 176];
- (d) Improved Hamiltonians¹¹ in the Ising and XY universality classes, see Sec. 2.3.2: 20 orders on the sc lattice [171, 177, 179];
- (e) N -vector model for $N = 0$ (the generation of the HT series is equivalent to the enumeration of self-avoiding walks): 26 orders for χ on the sc lattice [535].

Series for the $2n$ -point correlation functions at zero momentum can be found in Refs. [165, 170, 171, 177, 179]. Other HT series can be found in Refs. [455, 556]. In two dimensions, the longest series for the N -vector model for generic N are the following: triangular lattice, 15 orders [172, 174]; square lattice, 21 orders [162, 172, 174]; honeycomb lattice, 30 orders [172, 174].

The analysis of the HT series requires an extrapolation to the critical point. Several different methods have been developed in the years. They are reviewed, e.g., in Refs. [66, 364].

In this approach the confluent corrections with non-integer exponents discussed in Sec. 1.5.7 are the main obstacle for a precise determination of universal quantities. The presence of these nonanalytic terms causes a slow convergence and introduces a large (and dangerously undetectable) systematic error in the results of the HT series analyses. In order to obtain precise estimates of the critical parameters, the approximants

¹¹Series were generated for the most general model on the sc lattice in the Ising and XY universality classes, but such series were too long to be published. They can be requested to the authors of Refs. [177, 178].

of the HT series should properly allow for the confluent nonanalytic corrections [6, 220, 315, 337, 341, 597, 793]. Second- or higher-order integral (also called differential) approximants [311, 368, 419, 662] are, in principle, able to describe a nonanalytic correction term. However, the extensive numerical work that has been done shows that in practice, with the series of moderate length that are available today, no unbiased analysis is able to take effectively into account nonanalytic correction-to-scaling terms [6, 220, 597, 601, 603, 793]. In order to effectively keep into account the leading scaling corrections, one should use biased methods in which the presence of a nonanalytic term with exponent Δ is imposed (see, e.g., Refs. [8, 164, 165, 167, 601, 640, 653, 666]).

There are several different methods that try to handle properly the nonanalytic corrections. For instance, one may use the method proposed in Ref. [666] and generalized in Refs. [8, 653]. The idea is to perform the change of variables—we will call it Roskies transform—

$$z = 1 - (1 - \beta/\beta_c)^\Delta, \quad (2.2)$$

so that the nonanalytic terms in $(\beta_c - \beta)$ become analytic in $(1 - z)$. The new series has weaker nonanalytic corrections, of order $(1 - z)^{\Delta_2/\Delta}$ and $(1 - z)^{1/\Delta}$ (here Δ_2 is the second irrelevant exponent, $\Delta_2 = \nu\omega_2$), and thus analyses of these new series should provide more reliable estimates. Note, however, that the change of variable (2.2) requires the knowledge of β_c and Δ . Therefore, one should also consider an additional systematic error to keep into account the uncertainty on these two quantities. An equivalent possibility consists in using suitably biased integral approximants [164, 165, 167], again fixing Δ and β_c . It is also possible to fit the coefficients with the expected large-order behavior, fixing the subleading exponents, as it was done, e.g., in Ref. [535]. All these methods work reasonably and appear to effectively take into account the corrections to scaling.

A significant improvement of the HT results is obtained by using improved Hamiltonians (see Sec. 1.5.7), i.e. Hamiltonians for which the leading correction to scaling vanishes. As we shall see, such Hamiltonians can be determined with high accuracy by means of MC simulations. For the theories we consider, the analyses of the HT series for the improved models provide the most accurate estimates of the critical exponents and of other infinite-volume HT quantities obtained so far.

In order to illustrate the role played by the nonanalytic corrections, we consider the zero-momentum four-point coupling $g_4(t)$ defined in Eq. (1.63) for $N = 1$. We consider the ϕ^4 Hamiltonian (1.7) on a cubic lattice and, for several values of λ , we analyze the 18-th

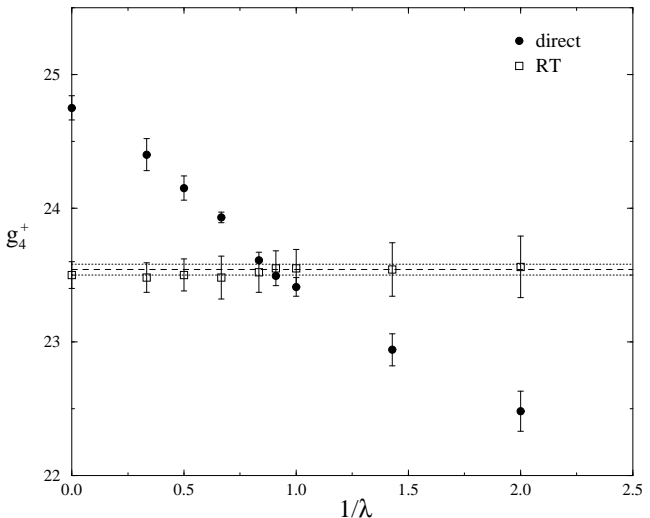


Figure 3: Estimates of g_4^+ obtained from an unbiased analysis (direct) of the HT series and from the analysis (RT) of the series obtained by means of the Roskies transform (2.2), for the ϕ^4 lattice model. The dashed line marks the more precise estimate (with its error) derived from the analysis of an improved HT expansion, i.e. $g_4^+ = 23.54(4)$, see Table 8.

order series of $g_4(t)$ by using different methods (details can be found in Ref. [177]). In Fig. 3 we report the results for g_4^+ obtained from an analysis without biasing the value of the exponent Δ —effectively this corresponds to extrapolate linearly at the critical point—and from an analysis that uses the transformation (2.2) with $\Delta = 1/2$ and β_c determined from the analysis of the susceptibility (21 orders). It is evident that the first type of analysis is unreliable: The result for g_4^+ should be independent of λ . Instead, it varies with λ , and the variation is much larger than the quoted error obtained as usual from the spread of the approximants. For instance, the analysis of the series of the standard Ising model, corresponding to $\lambda = \infty$, gives results that differ by more than 5% from the estimate obtained from the second analysis, while the spread of the approximants is much smaller. The estimates obtained from the transformed series are independent of λ within error bars, giving the estimate $g_4^+ \approx 23.5$. Such independence clearly indicates that the transformation (2.2) is effectively able to take into account the nonanalytic behavior. However, this result is much less precise than a standard analysis using series for improved Hamiltonians with suppressed leading scaling corrections. Indeed, in this case we obtain $g_4^+ = 23.54(4)$ (see Sec. 3.2), which is consistent with the estimate re-

ported above but more precise. By using series for improved Hamiltonians—we will call them *improved* HT (IHT) series—the results are significantly more precise.

2.2 Monte Carlo methods

The MC method is a very powerful technique for the simulation of statistical systems. Its main advantage is its flexibility. Indeed, for essentially any system it is possible to devise a MC algorithm for its simulation. Of course, results will be more or less precise depending on the efficiency of the algorithm. Systems with an N -vector order parameter and $O(N)$ symmetry are quite a special case, since there exists a very efficient algorithm with practically no critical slowing down: the Wolff algorithm [779], a generalization of the Swendsen-Wang algorithm [722] for the Ising model (see Ref. [188] for a general discussion). The original algorithm was defined for the N -vector model, but it can be applied to general $O(N)$ models by simply adding a Metropolis test [150].

In this section we describe different methods for obtaining critical quantities from MC simulations. After discussing the standard infinite-volume methods, we present two very successful techniques. One is based on real-space RG transformations, the second one makes use of the finite-size scaling (FSS) theory.

2.2.1 Infinite-volume methods

Traditional MC simulations determine the critical behavior from infinite-volume data. In this case, the analysis of the MC data is done in two steps. In order to determine the critical behavior of a quantity S , one first computes $S(\beta, L)$ for fixed β and several values of L and determines

$$S_\infty(\beta) = \lim_{L \rightarrow \infty} S(\beta, L), \quad (2.3)$$

by performing an extrapolation in L . For the systems we consider here such a step is usually simple. Indeed, for $L \rightarrow \infty$,

$$S(\beta, L) \approx S_\infty(\beta) + aL^p e^{-L/\xi_{\text{gap}}}, \quad (2.4)$$

where ξ_{gap} is the exponential correlation length. Such a rapid convergence usually makes the finite-size effects negligible compared to the statistical errors for moderately large values of L/ξ_{gap} already. In the HT phase a ratio $L/\xi_{\text{gap}} \lesssim 5$ -7 is usually sufficient, while in the LT phase larger values must be considered: for the three-dimensional Ising model, Ref. [206] used $L/\xi_{\text{gap}} \approx 20$. Finite-size effects introduce a severe limitation in the values of ξ_{gap} that can be reached, since the size L of actual MC simulations is at most of order 10^2 in three dimensions.

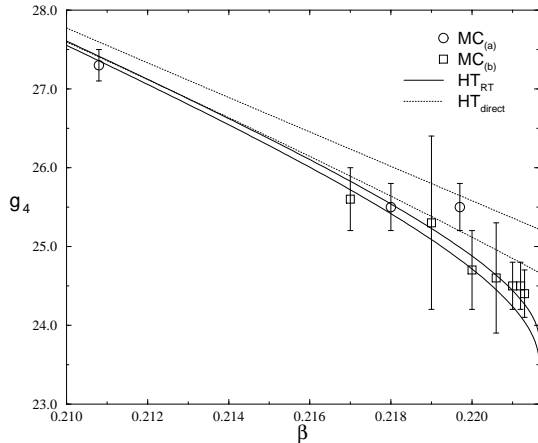


Figure 4: MC results for the four-point coupling $g_4(t)$ for the three-dimensional Ising model: (a) from Ref. [68]; (b) from Ref. [472]. For comparison we also report the extrapolation of the HT series by means of a direct analysis ($\text{HT}_{\text{direct}}$) and of an analysis that uses the transformation (2.2) (HT_{RT}). For each of these extrapolations we report two lines corresponding to the one-error-bar interval.

Once the infinite-volume quantities $S_\infty(\beta)$ are determined, exponents and amplitudes are obtained by fitting the numerical results with the expected form:

$$S_\infty(\beta) = a|\beta_c - \beta|^{-\sigma} + b|\beta_c - \beta|^{-\sigma+\Delta} + \dots \quad (2.5)$$

Of course, one cannot use too many unknown parameters in the fit and often only the leading term in Eq. (2.5) is kept. However, this is the origin of large systematic errors: It is essential to keep into account the leading nonanalytic correction with exponent Δ .

Again, in order to show the importance of the non-analytic scaling corrections, we present in Fig. 4 some numerical results [68, 472] for the four-point coupling $g_4(t)$. A simple extrapolation to a constant gives $g_4^+ = 24.5(2)$ [472] which is inconsistent with the result $g_4^+ = 23.54(4)$ we mentioned above. On the other hand, a fit that takes into account the leading correction to scaling gives $g_4^+ = 23.7(2)$ [640] which is now in perfect agreement with the previous results.

2.2.2 Monte-Carlo renormalization group

Here we briefly outline the real-space RG which has been much employed in numerical MC RG studies.¹² This method has been amply reviewed in the literature, see, e.g., Refs. [723, 775].

The main idea of the RG approach is to reduce the number of degrees of freedom of the system by integrating out the short-range fluctuations. In the real-space RG this is performed by block-field transformations [445]. In a block-field transformation, a block with l^d sites on the original lattice is mapped into a site of the blocked lattice. A block field ϕ_B is then constructed from the field ϕ of the original lattice, according to rules that should leave unchanged the critical modes, eliminating only the noncritical ones. The Hamiltonian \mathcal{H}_B of the blocked system is defined as

$$\exp[-\mathcal{H}_B(\phi_B)] = \int D\phi \mathcal{M}(\phi_B, \phi) \exp[-\mathcal{H}(\phi)], \quad (2.6)$$

where $\mathcal{M}(\phi_B, \phi)$ denotes the kernel of the block-field transformation. Then, the lattice spacing of the blocked lattice is rescaled to one.

The RG transformations are defined in the infinite-dimensional space of all possible Hamiltonians. If \mathcal{H} is written as

$$\mathcal{H}(K_1, K_2, \dots; O) = \sum_a K_a O_a, \quad (2.7)$$

where O_a are translation-invariant functions of the field ϕ and K_a are the corresponding couplings, the RG transformation induces a mapping

$$K \rightarrow K' = R(K). \quad (2.8)$$

The renormalized couplings K' are assumed to be analytic functions of the original ones.¹³

The nonanalytic behavior at the critical point is obtained by iterating the RG transformation an infinite number of times. Continuous phase transitions are associated with the fixed points K^* of the RG transformation. The critical exponents are determined by the

¹²There exist other numerical methods based on the real-space RG. Among others, we should mention the works on approximate RG transformations that followed the ideas of Kadanoff and Migdal [446, 447, 564]. For a general review, see, e.g., Refs. [156, 606].

¹³This assumption should be taken with care. Indeed, it has been proved [352, 423, 741, 742] that in many specific cases real-space RG transformations are singular. These singularities reflect the mathematical fact that RG transformations may transform a Gibbs measure into a new one which is non-Gibbsian [741, 742]. In approximate RG studies, these singularities appear as discontinuities of the RG map, see, e.g., Ref. [676].

RG flow in the neighborhood of the fixed point. If we define

$$T_{ab} = \left. \frac{\partial K'_a}{\partial K_b} \right|_{K=K^*}, \quad (2.9)$$

the eigenvectors of T give the linearized scaling fields. The corresponding eigenvalues can be written as $\lambda_i = l^{y_i}$, where y_i are the RG dimensions of the scaling fields.

An exact RG transformation is defined in the space of Hamiltonians with an infinite number of couplings. However, in practice a numerical implementation of the method requires a truncation of the Hamiltonians considered. Therefore, any method that is based on real-space RG transformations chooses a specific basis, trying to keep those terms that are more important for the description of the critical modes. As a general rule, one keeps only terms in which a small number of fields is involved and that are localized (see, e.g., Ref. [128]). The precision of the method depends crucially on the choice for the truncated Hamiltonian and on the choice of the RG transformation.

In numerical MC studies, given a MC generated configuration $\{\phi\}$, one generates a series of blocked configurations $\{\phi^{(i)}\}$, with $i = 0$ corresponding to the original configuration, by applying the block-field transformation. Correspondingly, one computes the operators $O^{(i)} \equiv O(\phi^{(i)})$. Then, one determines the matrices

$$A_{ab}^{(i)} = \left\langle \left(O_a^{(i)} - \langle O_a^{(i)} \rangle \right) \left(O_b^{(i)} - \langle O_b^{(i)} \rangle \right) \right\rangle, \quad (2.10)$$

$$B_{ab}^{(i)} = \left\langle \left(O_a^{(i)} - \langle O_a^{(i)} \rangle \right) \left(O_b^{(i-1)} - \langle O_b^{(i-1)} \rangle \right) \right\rangle,$$

and the matrix $T^{(i)}$ [721]

$$A_{ab}^{(i)} T_{bc}^{(i)} = B_{ac}^{(i)}. \quad (2.11)$$

If all possible couplings were considered, the matrix $T^{(i)}$ would converge to T defined in Eq. (2.9) for $i \rightarrow \infty$. In practice, only a finite number of couplings and a finite number of iterations is used. These approximations can be partially controlled by checking the convergence of the results with respect to the number of couplings and of RG iterations.

2.2.3 Finite-size scaling

Finite-size effects in critical phenomena have been the object of theoretical studies for a long time: see, e.g., Refs. [87, 199, 200, 652] for reviews. Only recently, due to the progress in the preparation of thin films, this issue has begun being investigated experimentally, see, e.g., Refs. [31, 32, 75, 272, 333, 417, 504, 514, 559]. FSS techniques are particularly important in numerical work. With respect to the infinite-volume methods, they do not need to satisfy the condition $\xi_{\text{gap}} \ll L$.

One can work with $\xi_{\text{gap}} \sim L$ and thus is better able to probe the critical regime. FSS MC simulations are at present one of the most effective techniques for the determination of critical quantities. Here, we will briefly review the main ideas behind FSS and report the results that are used in numerical studies to determine critical quantities.

The starting point of FSS is the generalization of Eq. (1.80) for the singular part of the Helmholtz free energy of a sample of linear size L [87, 131, 312, 654]:

$$\mathcal{F}_{\text{sing}}(u_t, u_h, \{u_i\}, L) = b^{-d} \mathcal{F}_{\text{sing}}(b^{y_t} u_t, b^{y_h} u_h, \{b^{y_i} u_i\}, L/b), \quad (2.12)$$

where $u_t \equiv u_1$, $u_h \equiv u_2$, $\{u_i\}$ with $i \geq 3$ are the scaling fields associated respectively with the reduced temperature, magnetic field, and the other irrelevant operators. Choosing $b = L$, we obtain

$$\mathcal{F}_{\text{sing}}(u_t, u_h, \{u_i\}, L) = L^{-d} \mathcal{F}_{\text{sing}}(L^{y_t} u_t, L^{y_h} u_h, \{L^{y_i} u_i\}, 1), \quad (2.13)$$

from which, by performing the appropriate derivatives with respect to t and H , one finds the scaling behavior of the thermodynamically interesting quantities. As we explained in Sec. 1.5.1, in the models we consider u_t and u_h are the only relevant scaling fields, and thus, neglecting correction of order $L^{y_3} = L^{-\omega}$, we can simply set $u_i = 0$ in the previous equation. Using Eq. (2.13) one may obtain the FSS behavior of any thermodynamic quantity $S(\beta, L)$. If $S_{\infty}(\beta) \equiv S(\beta, \infty)$ behaves as $t^{-\sigma}$ for $t \rightarrow 0$, then we have

$$S(\beta, L) = L^{\sigma/\nu} [f_S(\xi_{\infty}/L) + O(L^{-\omega}, \xi_{\infty}^{-\omega})], \quad (2.14)$$

where $\xi_{\infty}(\beta)$ is the correlation length in the infinite-volume limit. We do not specify which definition we are using, since any definition can be used here. For numerical studies, it is convenient to rewrite this relation in terms of a correlation length $\xi(\beta, L)$ defined in a finite lattice. Then, one may rewrite the above equation as

$$S(\beta, L) = L^{\sigma/\nu} [\bar{f}_S(\xi(\beta, L)/L) + O(L^{-\omega}, \xi^{-\omega})]. \quad (2.15)$$

FSS methods can be used to determine β_c , critical exponents, and critical amplitudes. Below we will review a few of them (we assume everywhere $H = 0$, but much can be generalized to $H \neq 0$).

In order to determine β_c , a widely used method is the ‘‘crossing’’ method. Choose a thermodynamic quantity $S(\beta, L)$ for which $\sigma = 0$ or σ/ν is known and define $R(\beta, L) \equiv S(\beta, L)L^{-\sigma/\nu}$. Then consider pairs (L_1, L_2) and determine the solution β_{cross} of the equation [123]

$$R(\beta_{\text{cross}}, L_1) = R(\beta_{\text{cross}}, L_2). \quad (2.16)$$

If L_1, L_2 diverge, β_{cross} converges to β_c with corrections of order $L_1^{-\omega-1/\nu}$, $L_2^{-\omega-1/\nu}$, and thus it provides an estimate of β_c . A widely used quantity is the Binder cumulant Q ,

$$Q = \frac{\langle M^4 \rangle}{\langle M^2 \rangle^2}, \quad (2.17)$$

where M is the magnetization. Other choices are ξ/L , generalizations of the Binder cumulant using higher powers of the magnetization, and the ratio of the partition function with periodic and antiperiodic boundary conditions [171, 382, 390].

The determination of the critical exponents can be performed using several different methods. One of the oldest approaches is the phenomenological renormalization of Nightingale [608]. One fixes a temperature β_1 and two sizes L_1 and L_2 and then determines β_2 so that

$$\frac{\xi(\beta_2, L_2)}{\xi(\beta_1, L_1)} = \frac{L_2}{L_1}. \quad (2.18)$$

Neglecting scaling corrections, in the FSS regime β_1 and β_2 are related by

$$(\beta_2 - \beta_c) = \left(\frac{L_1}{L_2}\right)^{1/\nu} (\beta_1 - \beta_c). \quad (2.19)$$

In Ref. [608] the method is implemented iteratively, using $L_2 = L_1 + 1$. Starting from β_0, L_0 , by using Eq. (2.19) one obtains a sequence of estimates β_i, ν_i that converge to β_c and ν respectively. In the original papers, the transfer-matrix approach was used, but this is not really necessary: MC simulations combined with reweighting methods [280, 295] may work as well. It is also possible to consider a magnetic field, obtaining in this case also the exponent $(\beta + \gamma)/\nu$.

The critical exponents can also be determined by studying thermodynamic quantities at the critical point. In this case,

$$S(\beta_c, L) \sim L^{\sigma/\nu}, \quad (2.20)$$

neglecting scaling corrections. Thus, one can determine σ/ν by simply studying the L -dependence. For example, γ/ν and β/ν can be determined from

$$\begin{aligned} \chi(\beta_c, L) &\sim L^{\gamma/\nu}, \\ |M|(\beta_c, L) &\sim L^{\beta/\nu}. \end{aligned} \quad (2.21)$$

The exponent ν can be determined by studying the L -dependence of derivatives with respect to β . Indeed,

$$\left. \frac{\partial S(\beta, L)}{\partial \beta} \right|_{\beta=\beta_c} \sim L^{(\sigma+1)/\nu}, \quad (2.22)$$

which can be obtained from Eq. (2.14), using $\xi_{\infty} \sim |t|^{-\nu}$. This method has the drawback that an estimate

of β_c is needed. Moreover, since β_c is usually determined only at the end of the runs, one must keep into account the fact that the available numerical results correspond to $\beta \neq \beta_c$. There are then two possibilities: computing $S(\beta_c, L)$ using the reweighting method [280, 295], or including in the fit Ansatz [131, 132] correction terms proportional to $(\beta - \beta_c)L^{1/\nu}$. In both cases, the method requires $(\beta - \beta_c)L^{1/\nu}$ to be a small correction. Note that in the method of Refs. [131, 132] one can also keep β_c as a free parameter, obtaining in this way also an estimate of the critical point.

It is possible to avoid the use of β_c . In Refs. [76–79, 81] one fixes L_1 and L_2 and then determines β , for instance by reweighting the data, so that

$$\frac{\xi(\beta, L_1)}{\xi(\beta, L_2)} = \frac{L_1}{L_2}. \quad (2.23)$$

Then, the exponent σ is obtained from

$$\frac{S(\beta, L_1)}{S(\beta, L_2)} = \left(\frac{L_1}{L_2}\right)^{\sigma/\nu}, \quad (2.24)$$

neglecting the scaling corrections. When L_1 and L_2 go to infinity, this estimate converges towards the exact value. Because of cross-correlations this method gives results that are more precise than those obtained by studying the theory at the critical point.

A somewhat different approach is proposed in Ref. [382]. With respect to the approach of Refs. [76–79, 81], it has the advantage of avoiding a tuning on two different lattices. One introduces an additional quantity $R(\beta, L)$ such that $R(\beta_c, L) \rightarrow R^*$ for $L \rightarrow \infty$. Then, one fixes a value \bar{R} —for practical purposes it is convenient to choose $\bar{R} \approx R^*$ —and, for each L , determines $\beta_f(L)$ from

$$R(\beta_f(L), L) = \bar{R}. \quad (2.25)$$

Finally, one considers $S(\beta_f(L), L)$ which still behaves as $L^{\sigma/\nu}$ for large L . Because of cross-correlations, the error on S at fixed R turns out to be smaller than the error on S at fixed β .

The FSS methods we have described are effective in determining the critical exponents. However, they cannot be used to compute amplitude ratios or other infinite-volume quantities. For this purpose, however, we can still use FSS methods [94, 186, 189, 292, 468, 531, 541, 561, 619]. The idea consists in rewriting Eq. (2.15) as

$$\frac{S(\beta, sL)}{S(\beta, L)} = \hat{f}(\xi(\beta, L)/L) + O(L^{-\omega}, \xi^{-\omega}), \quad (2.26)$$

where s is an arbitrary (rational) number. In the absence of scaling corrections, one could proceed as follows. First, one performs several runs for fixed L ,

determining $S(\beta, sL)$, $S(\beta, L)$, $\xi(\beta, sL)$, and $\xi(\beta, L)$. By means of a suitable interpolation, this provides the function $\hat{f}(\xi(\beta, L)/L)$ for S and ξ . Then, $S_\infty(\beta)$ and $\xi_\infty(\beta)$ are obtained from $S(\beta, L)$ and $\xi(\beta, L)$ by iterating Eq. (2.26) and the corresponding equation for $\xi(\beta, L)$. Of course, in practice one must be very careful about scaling corrections, increasing systematically L till the results become independent of L within error bars.

In all these methods, scaling corrections represent the main source of error. They should not be neglected in order to get reliable estimates of the critical exponents. The leading scaling correction, which is $O(L^{-\omega})$, turns out to be important, and should be taken into account, performing fits with Ansatz

$$aL^{\sigma/\nu} + bL^{\sigma/\nu-\omega}. \quad (2.27)$$

As we have already stressed previously, these difficulties can be partially overcome if one uses an improved Hamiltonian. In this case the leading corrections are absent and a naive fit to the leading behavior gives reliable results at the level of present-day statistical accuracy. However, in practice improved Hamiltonians are known only approximately, so that one may be worried of the systematic error due to the residual correction terms. In the next section we will discuss how to keep this systematic error into account.

2.3 Improved Hamiltonians

As we already stressed, one of the main sources of systematic errors in the numerical methods we presented is the presence of nonanalytic corrections controlled by the RG eigenvalue $y_3 = -\omega$. A way out consists in using improved models, i.e. models for which there are no corrections with exponent ω : No terms of order $|t|^{\omega\nu}$ appear in infinite-volume quantities and no terms of order $L^{-\omega}$ in FSS variables. Such Hamiltonians cannot be determined analytically and one must use numerical methods. Some of them will be presented below.

2.3.1 Determinations of the improved Hamiltonians

In order to determine an improved Hamiltonian, one may consider a one-parameter family of models, parametrized, say, by λ , that belong to the given universality class. Then, one may consider a specific quantity and find numerically a value λ^* such that the leading correction to scaling is absent. According to the RG theory, at λ^* the leading scaling correction gets suppressed in *any* quantity. Note that, within a given one-parameter family of models, nothing guarantees that such a value of λ can be found. For instance, no λ^*

can be found for sufficiently large values of N in the lattice ϕ^4 theory (1.7) [177]. For a discussion in the continuum, see, e.g., Ref. [57, 792].

The first attempt to determine an improved Hamiltonian is due to Chen, Fisher, and Nickel [220], who studied two classes of two-parameter models, the bcc scalar double-Gaussian and Klauder models, that are expected to belong to the Ising universality class and that interpolate between the spin-1/2 Ising model and the Gaussian model. They showed that improved models with suppressed leading corrections to scaling could be obtained by tuning the parameters (see also Refs. [315, 603]). The main difficulty of the method is the precise determination of λ^* . In Refs. [220, 341] the partial differential approximant technique was used; however, the error on λ^* was relatively large, and the final results represented only a modest improvement with respect to standard (and much simpler) analyses using biased approximants.

One may determine the improved Hamiltonian by comparing the results of a “good” and of a “bad” analysis of the HT series [177, 315]. Considering again the four-point coupling $g_4(t)$, we can for instance determine λ^* from the results of the analyses presented in Sec. 2.1. The improved model corresponds to the value of λ for which the unbiased analysis gives results that are consistent with the analysis that takes into account the subleading correction. From Fig. 3, we see that in the interval $1.0 < \lambda < 1.2$ the two analyses coincide and thus, we can estimate $\lambda^* = 1.1(1)$. This estimate is consistent with the result of Ref. [382], i.e. $\lambda^* = 1.10(2)$ obtained using the MC method based on FSS, but is much less precise.

In the last few years many numerical studies [79, 81, 131, 171, 382, 383, 390] have shown that improved Hamiltonians can be accurately determined by means of MC simulations, using FSS methods that are very sensitive to confluent corrections.

There are several methods that can be used. A first class of methods is very similar in spirit to the crossing technique we presented in the previous section for the determination of β_c . In its simplest implementation [177] one considers a quantity $R(\beta, \lambda, L)$ such that, for $L \rightarrow \infty$, $R(\beta_c(\lambda), \lambda, L)$ converges to a universal constant R^* , which is supposed to be known. Standard scaling arguments predict for $L \rightarrow \infty$

$$R(\beta_c(\lambda), \lambda, L) \approx R^* + a_1(\lambda)L^{-\omega} + a_2(\lambda)L^{-2\omega} + \dots + b_1(\lambda)L^{-\omega_2} \dots \quad (2.28)$$

where $\omega_2 \equiv -y_4$ is the next-to-leading correction-to-scaling exponent. In order to determine λ^* , which is the value for which $a_1(\lambda) = 0$, we can determine $\lambda^{\text{eff}}(L)$

from the equation

$$R(\beta_c(\lambda^{\text{eff}}(L)), \lambda^{\text{eff}}(L), L) = R^*. \quad (2.29)$$

For $L \rightarrow \infty$, $\lambda^{\text{eff}}(L)$ converges to λ^* with corrections of order $L^{\omega-\omega_2}$. In practice, neither R^* nor $\beta_c(\lambda)$ are known exactly. It is possible to avoid these problems by considering two different quantities R_1 and R_2 which have a universal limit for $L \rightarrow \infty$ [171, 382]. First, we define $\beta_f(\lambda, L)$ by

$$R_1(\beta_f, \lambda, L) = \bar{R}_1, \quad (2.30)$$

where \bar{R}_1 is a fixed value taken from the range of R_1 . Approximate estimates of λ^* are obtained by solving the equation

$$R_2(\beta_f(\lambda, L), \lambda, L) = R_2(\beta_f(\lambda, bL), \lambda, bL). \quad (2.31)$$

for some value of b .

Another possibility [79, 81, 171, 382, 391] consists in determining the size of the corrections to scaling for two values of λ which are near, but not too near in order to have a good signal, to λ^* and perform a linear interpolation. In the implementation of Refs. [79, 81] one considers the corrections to Eq. (2.24), while Refs. [171, 382, 391] consider the corrections to a RG-invariant quantity at fixed β_f , see Eq. (2.30).

We should note that all these numerical methods provide only approximately improved Hamiltonians. Therefore leading corrections with exponent ω are actually depressed but not completely suppressed. However, it is possible to evaluate the residual systematic error due to these terms. The idea is the following [382]. First, one considers a specific quantity which behaves as

$$S(L) = aL^{\sigma/\nu}(1 + b(\lambda)L^{-\omega} + \dots). \quad (2.32)$$

Then, one studies numerically $S(L)$ in the approximately improved model, i.e. for $\lambda = \lambda_{\text{est}}^*$ (λ_{est}^* is the estimated value of λ), and in a model in which the corrections to scaling are large: for instance in the N -vector model $\lambda = \infty$. Finally, one determines numerically an upper bound on $b(\lambda_{\text{est}}^*)/b(\infty)$. The RG theory guarantees that this ratio is identical for any quantity. Therefore, one can obtain an upper bound on the residual irrelevant corrections, by computing the correction term in the N -vector model—this is easy since the corrections are large—and multiplying the result by the factor determined above.

2.3.2 List of improved Hamiltonians

We list here the improved models that have been determined so far. We write the partition function in the

form

$$Z = \int \prod_i d\mu(\phi_i) \exp \left[\beta \sum_{\langle ij \rangle} \phi_i \cdot \phi_j \right], \quad (2.33)$$

where ϕ_i is an N -dimensional vector and the sum is extended over all nearest-neighbor pairs $\langle ij \rangle$. For $N = 1$ the following improved models have been determined:

1. Double-Gaussian model:

$$d\mu(\phi) = d\phi \left\{ \exp \left[-\frac{(\phi + \sqrt{y})^2}{2(1-y)} \right] + \exp \left[-\frac{(\phi - \sqrt{y})^2}{2(1-y)} \right] \right\}, \quad (2.34)$$

with $0 < y < 1$. The improved model has been determined on the bcc lattice from the study of HT series. The improved model corresponds to $y^* = 0.87(4)$ [220], $y^* = 0.87(1)$ [341], $y^* = 0.90(3)$ [315], $y^* \approx 0.85$ [603].

2. Klauer model:

$$d\mu(\phi) = d\phi |\phi|^{y/(1-y)} \exp \left(-\frac{\phi^2}{2(1-y)} \right), \quad (2.35)$$

with $0 < y < 1$. The improved model has been determined on the bcc lattice from the study of HT series. The improved model corresponds to $y^* = 0.81(6)$ [220], $y^* = 0.815(35)$ [315].

3. ϕ^4 - ϕ^6 model:

$$d\mu(\phi) = d\phi \exp \left[-\phi^2 - \lambda(\phi^2 - 1)^2 - \lambda_6(\phi^2 - 1)^3 \right]. \quad (2.36)$$

The couplings corresponding to improved models have been determined by means of MC simulations. On the sc lattice, the Hamiltonian is improved for these values of the couplings: (a)¹⁴ $\lambda^* = 1.10(2)$, $\lambda_6^* = 0$ [382]; (b) $\lambda^* = 1.90(4)$, $\lambda_6^* = 1$ [177].

4. Blume-Capel model:

$$d\mu(\phi) = d\phi \left[\delta(\phi - 1) + \delta(\phi + 1) + e^D \delta(\phi) \right]. \quad (2.37)$$

The Hamiltonian is improved for $D^* \approx 0.7$ [131], $D^* = 0.641(8)$ [383].

¹⁴ This is the estimate used in Ref. [177], which was derived from the MC results of Ref. [382]. There, the result $\lambda^* = 1.095(12)$ was obtained by fitting the data for the lattices of size $L \geq 16$. Since fits using also data for smaller lattices, i.e. with $L \geq 12$ and $L \geq 14$, gave consistent results, one might expect that the systematic error is at most as large as the statistical one [384].

For $N = 2, 3, 4$, the ϕ^4 theory (1.7) has been considered and λ^* has been determined [171, 385, 391] by means of FSS simulations. The values of λ^* are the following [171, 385]:

$$\lambda^* = 2.07(5) \quad \text{for } N = 2, \quad (2.38)$$

$$\lambda^* = 4.4(7) \quad \text{for } N = 3, \quad (2.39)$$

$$\lambda^* = 12.5(4.0) \quad \text{for } N = 4. \quad (2.40)$$

For $N \rightarrow \infty$, it can be shown that no positive value of λ corresponds to an improved model.

For $N = 2$ the dynamically dilute XY model has also been considered:

$$d\mu(\phi) = d^2\phi \left[\delta(\phi_1)\delta(\phi_2) + \frac{e^D}{2\pi} \delta(1 - |\phi|) \right], \quad (2.41)$$

where $\phi = (\phi_1, \phi_2)$. The Hamiltonian is improved for $D^* = 1.02(3)$ [171]. Again, the improved theory has been determined by means of MC simulations.

Finally, in Refs. [131, 390] a model with extended interactions was considered:

$$\mathcal{H} = \beta \left[\sum_{\langle ij \rangle} \sigma_i \sigma_j + y \sum_{[ij]} \sigma_i \sigma_j \right], \quad (2.42)$$

where $\sigma_i = \pm 1$, the first sum is extended over all nearest-neighbor pairs $\langle ij \rangle$, and the second over all third nearest-neighbor pairs $[ij]$. In Ref. [131] a significant reduction of the subleading corrections was observed for $y \approx 0.4$. However, this cannot be taken as a good estimate of y^* . Indeed, the subsequent analysis of Ref. [390] finds $y^* \lesssim 0.25$.

2.4 Field-theoretical methods

FT methods provide very accurate estimates of critical quantities. They can be divided into two classes: (a) perturbative approaches based on the ϕ^4 continuum Hamiltonian

$$\mathcal{H} = \int d^d x \left[\frac{1}{2} \partial_\mu \phi(x) \partial_\mu \phi(x) + \frac{r}{2} \phi(x)^2 + \frac{u}{4!} \phi(x)^4 \right]; \quad (2.43)$$

(b) nonperturbative approaches based on approximate solutions of Wilson's RG equations.

The oldest perturbative method is the ϵ -expansion in which the expansion parameter is $\epsilon = 4 - d$ [774]. Subsequently, Parisi [620] pointed out the possibility of using perturbation theory directly at the physical dimensions $d = 3$ and $d = 2$. In the original works [70, 620] the theory was renormalized at zero momentum. Later, a four-dimensional minimal subtraction scheme without ϵ -expansion was also proposed [257, 683, 684]. With

a slight abuse of language, we will call the first “traditional” method the fixed-dimension expansion approach, although also in the second case the dimension is fixed. The second approach will be named the minimal subtraction scheme without ϵ -expansion.

The nonperturbative approach has a very long history [345, 594, 595, 760, 775] and it has been the subject of extensive work even recently, see, e.g., Refs. [61, 113, 571] and references therein. We will not describe it here, since the method has been recently reviewed in Refs. [61, 113]. We only mention that in general the numerical estimates that can be found in the literature are less precise than those obtained by the perturbative approaches.

2.4.1 The fixed-dimension expansion

In the fixed-dimension expansion one works directly in $d = 3$ or $d = 2$. In this case the theory is super-renormalizable and the number of primitively divergent diagrams is finite. One may regularize the corresponding integrals by keeping d arbitrary and performing an expansion in $\epsilon = 3 - d$ or $\epsilon = 2 - d$. In divergent diagrams poles in ϵ appear. Such divergences are related to the necessity of performing an infinite renormalization of the parameter r appearing in the bare Hamiltonian, see e.g. the discussion in Ref. [55]. This problem can be avoided by replacing r with the mass m defined by

$$m^{-2} = \frac{1}{\Gamma^{(2)}(0)} \left. \frac{\partial \Gamma^{(2)}(p^2)}{\partial p^2} \right|_{p^2=0}, \quad (2.44)$$

where the function $\Gamma^{(2)}(p^2)$ is related to the one-particle irreducible two-point function by

$$\Gamma_{ab}^{(2)}(p) = \delta_{ab} \Gamma^{(2)}(p^2). \quad (2.45)$$

Perturbation theory in terms of m and u is finite. The critical limit is obtained for $m \rightarrow 0$. To handle it, one determines appropriate RG functions. Specifically, one defines the zero-momentum four-point coupling g and the field-renormalization constant Z_ϕ by

$$\begin{aligned} \Gamma_{ab}^{(2)}(p) &= \delta_{ab} Z_\phi^{-1} [m^2 + p^2 + O(p^4)], \quad (2.46) \\ \Gamma_{abcd}^{(4)}(0) &= Z_\phi^{-2} m^{4-d} \frac{g}{3} (\delta_{ab} \delta_{cd} + \delta_{ac} \delta_{bd} + \delta_{ad} \delta_{bc}), \quad (2.47) \end{aligned}$$

where $\Gamma_{a_1, \dots, a_n}^{(n)}$ are one-particle irreducible correlation functions. Using Eq. (1.63) and noting that m can be identified with the inverse second-moment correlation length, one can verify that g is exactly g_4 . Then, one defines a coupling-renormalization constant Z_u and a mass-renormalization constant Z_t by

$$u = m^{4-d} g Z_u Z_\phi^{-2}, \quad (2.48)$$

$$\Gamma_{ab}^{(1,2)}(0) = \delta_{ab} Z_t^{-1},$$

where $\Gamma_{ab}^{(1,2)}(p)$ is the one-particle irreducible two-point function with an insertion of $\frac{1}{2}\phi^2$. The renormalization constants are determined as perturbative expansions in powers of g . The fixed point of the model is determined by the nontrivial zero g^* of the β -function

$$\beta(g) = m \left. \frac{\partial g}{\partial m} \right|_u = (d-4)g \left[1 + g \frac{d}{dg} \log(Z_u Z_\phi^{-2}) \right]^{-1}. \quad (2.49)$$

Then, one defines

$$\eta_\phi(g) = \left. \frac{\partial \ln Z_\phi}{\partial \ln m} \right|_u = \beta(g) \frac{\partial \ln Z_\phi}{\partial g}, \quad (2.50)$$

$$\eta_t(g) = \left. \frac{\partial \ln Z_t}{\partial \ln m} \right|_u = \beta(g) \frac{\partial \ln Z_t}{\partial g}. \quad (2.51)$$

Finally, the critical exponents are given by

$$\eta = \eta_\phi(g^*), \quad (2.52)$$

$$\nu = [2 - \eta_\phi(g^*) + \eta_t(g^*)]^{-1}, \quad (2.53)$$

$$\omega = \beta'(g^*), \quad (2.54)$$

where ω is the exponent associated to the leading irrelevant operator.¹⁵ All other exponents are obtained by using the scaling relations. The fixed-point value g^* coincides with the critical value g_4^+ of g_4 .

The longest available series for the critical exponents can be found in Refs. [46, 70, 584] for $d = 3$ and in Ref. [616] for $d = 2$. More precisely, in three-dimensions the critical exponents and the β -function are known to six loops for generic values of N [46]. For $N = 0, 1, 2, 3$ seven-loop series for η_ϕ and η_t were computed in Ref. [584]. They are reported in the Appendix of Ref. [359]. In two dimensions, five-loop series are available for all values of N [616]. Perturbative expansions for universal amplitude ratios of subleading corrections [55] and for the $2n$ -point renormalized coupling constants [708] were also computed. For the Ising model, one can extend the method [62] obtaining the free energy below the critical temperature and therefore all universal amplitude ratios defined from zero-momentum quantities. For the study of the LT phase of the Ising model, a slightly different approach was developed in Refs. [361, 582], which allowed also the computation of ratios involving the correlation length.

The scheme we have presented is based on zero-momentum renormalization conditions and therefore,

¹⁵This is not always correct [169]. Indeed, $\beta'(g)$ is always equal to the exponent of the first nonanalytic correction in g . Usually, the first correction is due to the leading irrelevant operator, but this is not necessarily the case. In the two-dimensional Ising model, the first correction in $g(m)$ is related to the presence of an analytic background in the free energy, and $\beta'(g) = \gamma/\nu$.

it is not well suited for the study of vector models in the LT phase. In this case, the minimal-subtraction scheme without ϵ -expansion can be used. Since it is strictly related to the ϵ -expansion, it will be presented in the next section.

2.4.2 The ϵ expansion

The ϵ expansion [774] is based on the observation that, for $d = 4$, the theory is essentially Gaussian. One can then consider the standard perturbative expansion, that is then transformed into an expansion in powers of $\epsilon \equiv 4 - d$. In practice, the method works as in the fixed-dimension expansion. One first determines the renormalization constants Z_u , Z_ϕ , and Z_t . Initially, they were obtained by requiring the normalization conditions (2.46), (2.47), and (2.48). However, in this framework it is simpler to use the minimal-subtraction scheme. Once the renormalization constants are determined, one computes $\beta(g)$, $\eta_\phi(g)$, and $\eta_t(g)$ as before. The fixed-point value g^* is obtained by solving perturbatively in ϵ the equation $\beta(g) = 0$. Once the expansion of g^* is available, one obtains the expansion of the exponents, by expressing $\eta_\phi(g^*)$ and $\eta_t(g^*)$ in powers of ϵ . Notice that, in the minimal-subtraction scheme, g is not related to g_4 .

In this scheme five-loop series were computed in Ref. [223] for the exponents. A small error was later found and the revised series appeared in Ref. [482]. The equation of state and several amplitude ratios were determined in Refs. [116, 146, 604, 643, 752].

The minimal-subtraction scheme without ϵ -expansion [257, 683, 684] is strictly related. The functions $\beta(g)$, $\eta_\phi(g)$, and $\eta_t(g)$ are the minimal-subtraction functions. However, here ϵ is no longer considered as a small quantity but it is set to its physical value¹⁶, i.e. in three dimensions one simply sets $\epsilon = 1$. Then, the procedure is identical to that presented for the fixed-dimension expansion. A nontrivial zero g^* of the β -function is determined and the exponent series are computed for this value of g^* . The method is well suited for the study of universal LT properties of vector systems, and indeed, extensive perturbative series have been obtained for amplitude ratios [159, 500, 715].

2.4.3 Resummation of the perturbative series

FT perturbative expansions are divergent, and thus, in order to obtain accurate results, an appropriate resummation is required. This can be done exploiting

¹⁶ Note that the dependence on ϵ of the above-defined RG functions is trivial. The exponents $\eta_\phi(g)$ and $\eta_t(g)$ are independent of ϵ , $\beta(g) = -\epsilon g + b(g)$ and $b(g)$ is independent of ϵ .

Borel summability, which has been proved for the fixed-dimension expansion [266, 284, 537, 538], and it has been conjectured for the ϵ expansion. Therefore, accurate results can be obtained by using a Borel transform. The idea is the following. Consider a function $S(g)$ that has a perturbative expansion

$$S(g) \approx \sum s_k g^k, \quad (2.55)$$

in which the coefficients diverge as

$$s_k \sim k! (-a)^k k^b [1 + O(k^{-1})], \quad (2.56)$$

with $a > 0$. Here, the perturbative coupling is the renormalized coupling constant of the fixed-dimension expansion. But the same discussion applies to the ϵ expansion, replacing g by ϵ . Then, we consider the Borel-Leroy transform $B(t)$ of $S(g)$. Its perturbative expansion is given by

$$B_{\text{exp}}(t) = \sum_k \frac{s_k}{\Gamma(k+c+1)} t^k, \quad (2.57)$$

where c is an arbitrary number. Using Eq. (2.56), one can prove that the series $B_{\text{exp}}(t)$ is convergent in the disk $|t| < t_c \equiv 1/a$ of the complex plane, and also on the boundary if $c > b$. In this domain, one can compute $B(t)$ using $B_{\text{exp}}(t)$. However, in order to perform an inverse Borel transform, we need $B(t)$ for all positive values of t . It is thus necessary to perform an analytic continuation of $B_{\text{exp}}(t)$. Two methods have been used for this purpose. If the value of a is unknown, one can use Padé approximants to the series [70]. If a is known, one can use an Euler transformation [505]

$$y(t) = \frac{\sqrt{1+at} - 1}{\sqrt{1+at} + 1}, \quad (2.58)$$

and rewrite

$$B(t) = \sum_k f_k [y(t)]^k. \quad (2.59)$$

It is also possible to use Eq. (2.59) when a is not known, considering a as a free parameter that can be optimized in the resummation procedure [574].

If all the singularities belong to the interval $[-\infty, -t_c]$, the expansion (2.59) converges everywhere in the complex t -plane except on the negative axis for $t < -t_c$. After these transformations, we obtain a new expansion for the function $S(g)$:

$$S(g) \approx \int_0^\infty dt e^{-t} t^c \sum_k f_k [y(tg)]^k. \quad (2.60)$$

This sequence of operations has transformed the original divergent series into an integral of a convergent one, which can then be studied numerically. Notice that

the convergence of the integral (2.60), which is controlled by the analytic properties of $S(g)$, is not guaranteed. For instance, if $S(g)$ has a cut for $g \geq g^*$ —we will show below that this occurs in the fixed-dimension expansion—, then the integral does not converge for $g > g^*$.

The constant a that characterizes the large-order behavior of the original series is directly related to the singularity $t_b = -1/a$ of the Borel transform $B(t)$ that is nearest to the origin. Such a constant can be determined by means of a steepest-descent calculation in which the relevant saddle point is a finite-energy solution (instanton) of the classical field equations with negative coupling [144, 515].

A different resummation method is used by Kleiner [435, 478, 479]. Instead of using the perturbative series in terms of the renormalized coupling constant g , he considers the expansion in terms of the bare coupling u . Since perturbative series in three dimensions are expressed in terms of $\bar{u} = u/m$, the critical results are obtained by evaluating the perturbative expressions in the limit $\bar{u} \rightarrow \infty$. Similar extrapolations are used in the context of polymers, i.e. in the ϕ^4 theory in the limit $N \rightarrow 0$, see, e.g., Ref. [249]. Of course, the extrapolation is here a tricky point. Refs. [478, 479] use a variational method. Essentially, one introduces a new parameter such that the exact expressions are independent of it. In the truncated series the new parameter is a nontrivial variable that is fixed by requiring the results to be stationary with respect to its variation. The variational method transforms an initially divergent series in a convergent sequence of approximations.

The convergence of all the resummation methods depends on the analytic behavior at $g = g^*$. If the function is regular, a simple extrapolation works correctly, but, if nonanalyticities are present, deviations are expected. For the ϵ -expansion it has been argued that no nonanalyticities are present in the universal quantities. This has also been argued for the fixed-dimension expansion in the minimal subtraction scheme [58, 680], but this is difficult to check in the absence of a nonperturbative definition of the scheme.

Singularities—predicted long ago in Refs. [597, 598, 620]—do appear in the fixed-dimension expansion renormalized at zero momentum. To understand the problem, following Nickel [597], let us consider the four-point renormalized coupling g_4 —which, as we already remarked, coincides with the perturbative coupling g in Eq. (2.47)—as a function of the reduced temperature t . For $t \rightarrow 0$ we can write down an expansion of the form

$$g_4 = g_4^+ \left[1 + a_1 t + a_2 t^2 + \dots + b_1 t^\Delta + b_2 t^{2\Delta} + \dots + \right. \tag{2.61}$$

$$\left. c_1 t^{\Delta+1} + \dots + d_1 t^{\Delta^2} + \dots + e_1 t^\gamma + \dots \right], \tag{2.61}$$

where Δ, Δ_2, \dots are subleading exponents. The corrections proportional to t^γ are due to the presence of an analytic background in the free energy. We expect on general grounds that $a_1 = a_2 = a_3 = \dots = 0$. Indeed, these analytic corrections arise from the nonlinearity of the scaling fields and their effect can be eliminated in the Green's functions by an appropriate change of variables [16]. For dimensionless RG-invariant quantities such as g_4 , the leading term is universal and therefore independent of the scaling fields, so that no analytic term can be generated. Analytic correction factors to the singular correction terms are generally present, and therefore the constants c_i in Eq. (2.61) are expected to be nonzero.

Starting from Eq. (2.61), one may easily compute the β -function. Since the mass gap m scales analogously, for $\Delta < \gamma$ —this condition is usually, but not always, satisfied¹⁷—, we obtain the following expansion:

$$\begin{aligned} \beta(g_4) \equiv m \frac{\partial g_4}{\partial m} &= \alpha_1 \Delta g + \alpha_2 (\Delta g)^2 + \dots + \\ &\beta_1 (\Delta g)^{\frac{1}{\Delta}} + \beta_2 (\Delta g)^{\frac{2}{\Delta}} + \dots + \\ &\gamma_1 (\Delta g)^{1+\frac{1}{\Delta}} + \dots + \\ &\delta_1 (\Delta g)^{\frac{\Delta^2}{\Delta}} + \dots + \zeta_1 (\Delta g)^{\frac{\Delta}{\Delta}} + \dots, \end{aligned} \tag{2.62}$$

where $\Delta g = g_4^+ - g_4$. It is easy to verify that $\alpha_1 = -\Delta/\nu \equiv -\omega$ and that, if $a_1 = a_2 = \dots = 0$ in Eq. (2.61), then $\beta_1 = \beta_2 = \dots = 0$. Eq. (2.62) clearly shows the presence of several nonanalytic terms with exponents depending on $1/\Delta, \Delta_i/\Delta$, and γ/Δ .

As pointed out by Sokal [508, 707] (see also Ref. [60] for a discussion in the Wilson's RG setting), the nonanalyticity of the RG functions can also be understood within Wilson's RG approach. We repeat his argument here. Consider the Gaussian fixed point which, for $3 \leq d < 4$, has a two-dimensional unstable manifold \mathcal{M}_u : The two unstable directions correspond to the interactions ϕ^2 and ϕ^4 . The continuum field theories are in a one-to-one correspondence with Hamiltonians on \mathcal{M}_u . Thus the FT RG is nothing but Wilson's RG restricted to \mathcal{M}_u . The point is that there is no reason why it should approach the fixed point along a direction orthogonal to all other subleading irrelevant operators. Barring miracles, the approach should have nonzero components along any of the irrelevant

¹⁷ In some models, for instance in the two-dimensional Ising model, $\Delta > \gamma$. In this case, Eq. (2.62) is still correct [169] if γ and Δ are interchanged. Also $\alpha_1 = -\gamma/\nu$ in this case.

directions. But, if this happens, nonanalytic terms are present in any RG function.

In order to clarify the issue, Ref. [640] determined the asymptotic behavior of $\beta(g)$ for $g \rightarrow g^*$ in the continuum field theory for $N \rightarrow \infty$ and $2 < d < 4$, showing that Eq. (2.62) holds and the expected nonanalytic terms are present. In Ref. [169] the computation was extended to two dimensions, finding again nonanalytic terms.

These singularities are known to give rise to systematic deviations in the resummations of the perturbative series. In Refs. [169, 212] the results of the resummations of some simple test functions have been reported, showing that large discrepancies should be expected if the first nonanalytic exponent is small. For instance, if a function $f(g)$ behaves as the β function, i.e.

$$f(g) \approx a(g - g_0) + b(g - g_0)^{1+p} \quad (2.63)$$

for $g \rightarrow g_0$, a relatively precise estimate of a is obtained if $p \gtrsim 1$, while for small values of p the estimate is largely incorrect and, even worse, any estimate of the error is also incorrect. It is important to note that these discrepancies are not related to the fact that the series are divergent. They would be present even if the perturbative expansions were convergent.¹⁸

Of course, the interesting question is whether these nonanalyticities are relevant in the ϕ^4 perturbative series. In three dimensions $\Delta \approx 0.5$ and Δ_2/Δ is approximately 2 [345, 595]. Thus, the leading nonanalytic term has exponent Δ_2/Δ and is not very different from an analytic one. Therefore, we expect small corrections and indeed the FT results are in substantial agreement with the estimates obtained in MC and HT studies.

The situation worsens in the two-dimensional case. Indeed, in the Ising model Ref. [169] predicted a nonanalytic term $(\Delta g)^{8/7}$ while for $N \geq 3$ logarithmic corrections $(\Delta g)/\log \Delta g$ are predicted on general grounds and found in a large- N calculation [169]. Since the first nonanalytic term has a very small exponent, large deviations are expected [169]. Indeed, two-dimensional estimates differ significantly from the theoretically expected results [505, 616].

Finally, we mention that it is possible to improve the results of the ϵ -expansion if the value of a quantity R is known for some values of the dimensions. The method was originally proposed in Refs. [248, 251, 507] where exact values in two or one dimension were used in the analysis of the ϵ -expansion. The method of Ref. [507]

works as follows. One considers a quantity R such that for $\epsilon = \epsilon_1$ the exact value $R_{\text{ex}}(\epsilon_1)$ is known. Then, one defines

$$\overline{R}(\epsilon) = \left[\frac{R(\epsilon) - R_{\text{ex}}(\epsilon_1)}{(\epsilon - \epsilon_1)} \right], \quad (2.64)$$

and a new quantity

$$R_{\text{imp}}(\epsilon) = R_{\text{ex}}(\epsilon_1) + (\epsilon - \epsilon_1)\overline{R}(\epsilon). \quad (2.65)$$

New estimates of R at $\epsilon = 1$ can then be obtained by resumming the ϵ expansion of $\overline{R}(\epsilon)$ and then computing $R_{\text{imp}}(1)$. The idea behind this method is very simple. If, for instance, the value of R for $\epsilon = 2$ is known, one uses as zeroth-order approximation at $\epsilon = 1$ the value of the linear interpolation between $\epsilon = 0$ and $\epsilon = 2$ and then uses the series in ϵ to compute the deviations. If the interpolation is a good approximation, one should find that the series which gives the deviations has smaller coefficients than the original one. Consequently, also the errors in the resummation are reduced.

In Ref. [640] this strategy was generalized to the case in which one knows the exact value of R for more than one value of ϵ . If exact values $R_{\text{ex}}(\epsilon_1), \dots, R_{\text{ex}}(\epsilon_k)$ are known for a set of dimensions $\epsilon_1, \dots, \epsilon_k$, $k \geq 2$, then one defines

$$Q(\epsilon) = \sum_{i=1}^k \left[\frac{R_{\text{ex}}(\epsilon_i)}{(\epsilon - \epsilon_i)} \prod_{j=1, j \neq i}^k (\epsilon_i - \epsilon_j)^{-1} \right], \quad (2.66)$$

and

$$\overline{R}(\epsilon) = \frac{R(\epsilon)}{\prod_{i=1}^k (\epsilon - \epsilon_i)} - Q(\epsilon), \quad (2.67)$$

and finally

$$R_{\text{imp}}(\epsilon) = [Q(\epsilon) + \overline{R}(\epsilon)] \prod_{i=1}^k (\epsilon - \epsilon_i). \quad (2.68)$$

One can easily verify that the expression

$$[Q(\epsilon) + \overline{R}(0)] \prod_{i=1}^k (\epsilon - \epsilon_i) \quad (2.69)$$

represents the k th-order polynomial interpolation among the points $\epsilon = 0, \epsilon_1, \dots, \epsilon_k$. Again the resummation procedure is applied to the ϵ expansion of $\overline{R}(\epsilon)$ and the final estimate is obtained by computing $R_{\text{imp}}(1)$. Such a technique was successfully used in many different cases, see Refs. [640–643].

3 The Ising universality class

The Ising model is one of the most studied models in the theory of phase transitions, not only because it is

¹⁸ The reader may consider $f(g) = (1-g)^p$ and try to compute $f(1)$ from its Taylor expansion around $g = 0$. Since for $p \rightarrow 0^+$, $f(g) \rightarrow 1$ pointwise for all $g < 1$, for small values of p any extrapolation provides an estimate $f(1) \approx 1$, clearly different from the exact value $f(1) = 0$.

the simplest nontrivial model which has a critical behavior with nonclassical exponents, but also because it describes the critical behavior of many physical systems. Indeed, many systems characterized by short-range interactions and a scalar order parameter undergo a critical transition belonging to the Ising universality class. We mention the liquid-vapor transition in simple fluids and the critical transitions in multicomponent fluid mixtures, in uniaxial antiferromagnetic materials, and in micellar systems.

Continuous transitions belonging to the three-dimensional Ising universality class are also expected in some theories relevant for high-energy physics. We mention:

- (i) The finite-temperature transition in the electroweak theory, which is relevant for the initial evolution of the universe. Lattice simulations [674] show that in the plane of the temperature and of the Higgs mass there is a line of first-order transitions, which eventually ends at a second-order transition point. Such a transition is argued to belong to the Ising universality class.
- (ii) An Ising-like continuous transition is predicted at finite temperature and finite baryon-number chemical potential in the theory of strong interactions (QCD) [111, 370].
- (iii) For large values of the quark mass, the finite-temperature transition of QCD is of first order. With decreasing the quark mass, the first-order transition should persist up to a critical value, where the transition becomes continuous and is expected to be Ising-like [647].
- (iv) The chiral phase transition with three massless flavored quarks is known to be of first order [339, 340]. The first-order phase transition should persist for $m_{\text{quark}} > 0$ up to a critical value of the quark mass. At this critical point, the transition is continuous and it has been conjectured to belong to the Ising universality class [453, 454].
- (v) The finite-temperature transition of the four-dimensional $SU(2)$ gauge theory [647], which has been much studied as a prototype of nonabelian gauge theories, belongs to the Ising universality class.

3.1 The critical exponents

3.1.1 Theoretical results

The Ising universality class has been studied using several theoretical approaches. In Tables 3, 4, 5, and 6 we

present the most recent estimates of the critical exponents obtained by various methods, such as HT expansions, MC simulations, FT methods, etc...

Let us begin by discussing the results obtained by employing HT expansion techniques. The most recent ones are reported in Table 3. Older estimates are reviewed in Ref. [6]. Ref. [177] considers three specific improved Hamiltonians, see Sec. 2.3.2: the ϕ^4 - ϕ^6 lattice model (2.36) for $\lambda^* = 1.10(2)$, $\lambda_6^* = 0$ [382], and $\lambda^* = 1.90(4)$, $\lambda_6^* = 1$ [177]; the Blume-Capel model (2.37) for $D^* = 0.641(8)$ [383]. For each improved model, the 20-th order HT expansions were analyzed using integral approximants of various order. The results of each analysis were very stable, showing that, once a precise estimate of the improved parameter is available, the quality of the HT series analysis greatly improves, even for moderately long series. In order to check whether the observed stability corresponded really to a better accuracy of the final estimates, the results for the three lattice models were carefully compared and found to be in perfect agreement. This confirms the significant increase in precision and supports the basic assumption that most of the systematic error in the analyses of HT expansions of nonimproved models is due to the confluent corrections, and is thus significantly reduced when analyzing series for improved models. The estimates of the critical exponents obtained in such a way are denoted by IHT in Table 3. One can make even more effective the combination of MC simulations and HT expansion techniques by exploiting the effectiveness of MC simulations based on FSS to determine β_c . Using the MC estimate of β_c to bias the IHT analyses, a further improvement in precision is obtained. For example, for the ϕ^4 lattice model (1.7) one may use the MC result $\beta_c = 0.3750966(4)$ for $\lambda = 1.10$ [382] to bias the IHT analysis [177], and obtain the results denoted by MC+IHT ϕ^4 in Table 3.

Recently, the HT expansions of χ and μ_2 , cf. Eq. (2.1), for the standard Ising model ($s-\frac{1}{2}$ in the Tables) on the simple cubic and bcc lattice were extended respectively to 23rd and 25th order [170] (almost at the same time, Ref. [167] presented the 23rd-order expansions for both lattices). An analysis of these extended series was presented in Ref. [167]. The results reported in Table 3 were obtained by using biased approximants, with β_c and Δ taken as external inputs. The errors however do not take into account the uncertainties on β_c and Δ . One may compare these results with those obtained earlier by analyzing series to 21st order [164, 166], using essentially the same method. The errors do not change significantly while the central estimates decrease towards the IHT results. The estimates of Refs. [220, 315, 341, 601, 603] were obtained from the analysis of 21st-order expan-

Ref.	info	order	γ	ν	η	α	β	ω
[177] 1999	MC+IHT ϕ^4	20th	1.2372(3)	0.6301(2)	0.0364(4)	0.1097(6)*	0.32652(15)*	
[167] 2000	IHT $\phi^4, \phi^6, s-1$	20th	1.2371(4)	0.63002(23)	0.0364(4)	0.1099(7)*	0.32648(18)*	
[164] 1997	$s-\frac{1}{2}$ bcc	25th	1.2375(6)	0.6302(4)	0.036(2)*	0.1094(12)*	0.3265(7)*	
[167] 2000	$s-\frac{1}{2}$ bcc	21st	1.2384(6)	0.6308(5)	0.037(2)*	0.1076(15)*	0.3270(8)*	
[164] 1997	$s-\frac{1}{2}$ sc	23rd	1.2378(10)	0.6306(8)	0.037(3)*	0.1082(24)*	0.3270(13)*	
[166] 1999	$s-\frac{1}{2}$ sc	21st	1.2388(10)	0.6315(8)	0.038(3)*	0.1055(24)*	0.3278(13)*	
[367] 1994	$s-\frac{1}{2}$ sc,bcc	21st		0.631(2)*		0.106(6)		
[119] 1994	$s-\frac{1}{2}$ sc	25th		0.6330(13)*		0.101(4)		
[603] 1990	$s-\frac{1}{2}$ sc	23rd		0.6320(13)*		0.104(4)		
[603] 1990	DG bcc	21st	1.237(2)	0.6300(15)	0.0359(7)	0.11(2) _a	0.3263(8)*	0.825(48)
[362] 1987	$s-\frac{1}{2}, 1, 2$, bcc	21st	1.239(3)	0.632 ⁺² ₋₃	0.040(9)	0.104 ⁺⁹ ₋₆ *	0.328(4)*	
[315] 1985	DG,K bcc	21st	1.2395(4)	0.632(1)	0.039(4)*	0.105(7) _a	0.3283(15)*	0.85(8)
[341] 1984	DG bcc	21st	1.2378(6)	0.63115(30)	0.0375(5)	0.1066(9)*	0.3278(6)*	0.82(5)
[289] 1983	$s-S$ bcc	21st	1.242 ⁺³ ₋₅	0.634 ⁺³ ₋₄		0.098 ⁺¹² ₋₉ *		
[220] 1982	DG,K bcc	21st	1.2385(15)					
[793] 1981	$s-S$ bcc	21st	1.2385(25)	0.6305(15)	0.0357(6)*	0.1085(45)*	0.3265(26)*	
[601] 1981	DG bcc	21st	1.237(3)	0.630(3)	0.036(2)*	0.110(9)*	0.327(5)*	
[666] 1981	$s-S$ bcc	21st	1.240(2)	0.628(2)	0.025(7)*	0.116(6)*	0.322(3)*	

Table 3: Theoretical estimates of the critical exponents obtained from HT expansions for the three-dimensional Ising universality class. See text for explanation of symbols in the column “info”. We indicate with an asterisk (*) the estimates that have been obtained by using the scaling relations $\gamma = (2 - \eta)\nu$, $2 - \alpha = 3\nu$, $\beta = \nu(1 + \eta)/2$ (when the error was not reported by the authors, we used the independent-error formula to estimate it).

Ref.	info	γ	ν	η	α	β
[49] 1995	LT $s-\frac{1}{2}$		0.624(10)		0.13(3)*	
[366] 1993	LT $s-\frac{1}{2}$	1.251(28)	0.625(2)	0.05(3)*	0.125(6)*	0.329(9)
[120] 1992	LT $s-\frac{1}{2}$				0.207(4)	0.308(5)
[645] 1995	CVM $s-\frac{1}{2}$	1.239(3)				0.325(4)
[487] 1995	CAM $s-\frac{1}{2}$	1.237(4)	0.631(2)*	0.039(8)*	0.108(5)	0.327(4)

Table 4: Other theoretical estimates of the critical exponents for the three-dimensional Ising universality class. See text for explanation of symbols in the column “info”. We indicate with an asterisk (*) the estimates that have been obtained by using the scaling relations $\gamma = (2 - \eta)\nu$, $2 - \alpha = 3\nu$, $\beta = \nu(1 + \eta)/2$.

Ref.	info	γ	ν	η	α	β	ω
[30] 2000	FSS DS $s^{-\frac{1}{2}}$		0.6280(15)		0.1160(45)*		0.745(74)
[383] 1999	FSS ϕ^4	1.2366(15)*	0.6297(5)	0.0362(8)	0.1109(15)*	0.3262(4)*	0.845(10)
[132] 1999	FSS $s^{-\frac{1}{2}nm, 3n}$	1.2372(13)*	0.63032(56)	0.0372(10)	0.1090(17)*	0.3269(5)*	0.82(3)
[382] 1999	FSS ϕ^4	1.2367(11)*	0.6296(7)	0.0358(9)	0.1112(21)*	0.3261(5)*	0.845(10)
[81] 1999	FSS $s^{-\frac{1}{2}}$	1.2353(25)*	0.6294(10)	0.0374(12)	0.1118(30)*	0.3265(4)*	0.87(9)
[390] 1999	FSS ϕ^4	1.2366(11)*	0.6298(5)	0.0366(8)	0.1106(15)*	0.3264(4)*	
[436] 1999	STCD $s^{-\frac{1}{2}}$		0.6327(20)	0.035(6)*	0.102(6)*	0.3273(17)	
[224] 1999	FSS $s^{-\frac{1}{2}}$			0.036(2)			
[389] 1998	FSS $s^{-\frac{1}{2}}$		0.6308(10)*		0.1076(30)		
[726] 1996	S $s^{-\frac{1}{2}}$					0.3269(6)	
[129] 1996	MCRG $s^{-\frac{1}{2}nn, 2n, 3n}$	1.2378(27)*	0.6309(12)	0.038(2)	0.1073(36)*	0.3274(9)	
[360] 1996	MCRG $s^{-\frac{1}{2}}$	1.234(4)*	0.625(1)	0.025(6)	0.125(3)*	0.320(2)	0.7
[131] 1995	FSS $s^{-\frac{1}{2}nn, 3n, s-1}$	1.237(2)*	0.6301(8)	0.037(3)	0.110(2)*	0.3267(10)*	0.82(6)
[73] 1992	MCRG $s^{-\frac{1}{2}}$	1.232(4)*	0.624(2)	0.026(3)	0.128(6)*	0.3201(13)*	0.80–0.85
[294] 1991	FSS $s^{-\frac{1}{2}}$	1.239(7)*	0.6289(8)	0.030(11)	0.1133(24)*	0.3258(44)*	
[29] 1990	FSS DS $s^{-\frac{1}{2}}$		0.6285(19)		0.1145(57)*		
[128] 1989	MCRG $s^{-\frac{1}{2}}$	1.242(10)*	0.6285(40)	0.024(8)	0.114(12)*	0.3218(32)*	
[630] 1984	MCRG $s^{-\frac{1}{2}}$	1.238(11)*	0.629(4)	0.031(5)	0.113(12)*	0.324(3)*	
[542] 1984	FSS DS $s^{-\frac{1}{2}}$		0.62(1)		0.14(3)*		

Table 5: Estimates of the critical exponents from MC simulations for the three-dimensional Ising universality class. See text for explanation of symbols in the column “info”. We indicate with an asterisk (*) the estimates that have been obtained by using the scaling relations $\gamma = (2 - \eta)\nu$, $2 - \alpha = 3\nu$, $\beta = \nu(1 + \eta)/2$ (when the error was not reported by the authors, we used the independent-error formula to estimate it).

Ref.	info	γ	ν	η	α	β	ω
[359] 1998	$d = 3$ exp	1.2396(13)	0.6304(13)	0.0335(25)	0.109(4)	0.3258(14)	0.799(11)
[435] 1999	$d = 3$ exp	1.2403(8)	0.6303(8)	0.0335(6)	0.1091(24)	0.3257(5)	0.792(3)
[584] 1991	$d = 3$ exp	1.2378(6){18}	0.6301(5){11}	0.0355(9){6}	0.1097(15){33}		
[505] 1977	$d = 3$ exp	1.241(2)	0.6300(15)	0.031(4)	0.1100(45)	0.3250(15)	0.79(3)
[359] 1998	ϵ -exp _{free}	1.2355(50)	0.6290(25)	0.0360(50)	0.113(7)	0.3257(25)	0.814(18)
[359] 1998	ϵ -exp _{bc}	1.2380(50)	0.6305(25)	0.0365(50)	0.108(7)	0.3265(15)	
[595] 1984	SFM	1.23(2)	0.626(9)	0.040(7)	0.122(27)	0.326(5)	0.85(7)
[691] 1999	CRG	1.2322	0.6307	0.0467	0.1079	0.3300	
[570] 1997	CRG	1.203	0.618(14)	0.054	0.146(42)	0.326(7)	
[729] 1994	CRG	1.258	0.645	0.045	0.065	0.336	

Table 6: FT estimates of the critical exponents for the three-dimensional Ising universality class. See text for explanation of symbols in the column “info”.

sions for two families of models, the Klauder (K) and the double-Gaussian (DG) models on the bcc lattice, see Eqs. (2.35) and (2.34), which depend on an irrelevant parameter y and interpolate between the Gaussian model and the spin-1/2 Ising model. In Refs. [220,315] the double expansion of χ in the inverse temperature β and the irrelevant parameter y was analyzed by employing two-variable partial differential approximants, devised to reproduce the expected scaling behavior in a neighborhood of $(y^*, \beta_c(y^*))$ in the (y, β) plane. The estimate of γ of Ref. [315] is significantly higher than the IHT result. The same series were analyzed by using a different method in Ref. [603]: the estimate of γ was lower and in perfect agreement with the IHT result. As pointed out in Ref. [603], the discrepancy is strictly correlated to the estimate of y^* : the estimates of γ increase with y^* , and thus the larger values of γ of Ref. [315] is due to the fact that a larger value of y^* is used. The results of Refs. [289,666,793] were obtained by analyzing 21st-order expansions for spin- S models on the bcc lattice, computed by Nickel [597].

The HT expansion analyses usually focus on χ and μ_2 , or equivalently $\xi^2 = \mu_2/(2d\chi)$, and thus they provide direct estimates of γ and ν . The other exponents can be obtained by using the scaling relations. The specific heat exponent α can be also estimated independently, although the results are not as precise as those obtained using the hyperscaling relation $\alpha = 2 - 3\nu$. One can obtain α from the analysis of the HT expansion of the specific heat [119,166,367], and, on bipartite lattices, from the analysis of the magnetic susceptibility χ at the antiferromagnetic singularity $\beta = -\beta_c$ [315,603]. In Table 3 we have added a subscript a to these latter estimates of α .

Results obtained by analyzing the LT expansions of the Ising model (see, e.g., Refs. [49,120,366]) are consistent with, although much less precise than, the HT results. They are reported in Table 4. There, we also report results obtained by using the so-called cluster variation method (CVM) [467,645], and a generalization of the mean-field approach, the so-called coherent-anomaly method (CAM) [487].

There are several MC determinations of the critical exponents. The most precise results have been obtained by using the FSS methods described in Sec. 2.2.3, see, e.g., Refs. [81,130–132,224,294,381–383,389,390] and the results denoted by FSS in Table 5. The results of Refs. [382,390] were obtained by simulating an improved ϕ^4 lattice Hamiltonian and an improved Blume-Capel model, see Sec. 2.3.2. Ref. [383] reports the estimates resulting from the combination of these results. In Refs. [129,131,132] the Ising model (2.42) with nearest-neighbor (nn) and third-neighbor ($3n$) spin interactions were considered, using values of y that

reduce the scaling corrections. The critical exponents have been also computed by using the MC RG method presented in Sec. 2.2.2 (MCRG) [73,128,129,360,630], by fitting the infinite-volume data close to the critical point to the expected scaling behavior (S) [726], by studying the short-time critical dynamics (STCD) [434,436], and from the FSS of the partition-function zeros in the complex-temperature plane [425] determined from the density of states (FSS DS) [29,30,542].

Let us turn to the results obtained in the FT approaches that are presented in Table 6. In the fixed-dimension approach, the perturbative series of Refs. [70,584] were reanalyzed in Ref. [359], using essentially the resummation method of Ref. [505] (see also Ref. [795]). Comparing with the HT and MC results, we note that there are small discrepancies for γ , η , and ω . These deviations are probably due to the non-analyticity of the RG functions for $g = g^*$ which we discussed in Sec. 2.4.3. Similar results were obtained in Refs. [435,480], using different methods of analysis, but still neglecting the confluent singularities at the infrared-stable fixed point. The errors reported there seem to be rather optimistic, especially if compared with those obtained in Ref. [359]. The analysis of Ref. [584] allowed for a more general nonanalytic behavior of the β -function [584]. In Table 6, we quote two errors for the results of Ref. [584]: the first one (in parentheses) is the resummation error, and the second one (in braces) takes into account the uncertainty of g^* , which is estimated to be $\sim 1\%$. To estimate the second error we used the results of Ref. [359] where the dependence of the exponents on g^* is given.

The results of the analyses of the ϵ expansion are presented in Table 6. We report estimates obtained by standard analyses (denoted as “free”) and constrained analyses [506] (denoted by “bc”) that make use of the exact two-dimensional values, employing the method discussed in Sec. 2.4.3.

Other estimates of the critical exponents have been obtained by nonperturbative FT methods based on approximate solutions of continuous RG equations (CRG). They are much less precise than the above-presented methods although much work has been dedicated to their improvement (see, e.g., the recent review [113] and references therein). The starting point of this approach is an exact RG equation for the generator of the connected correlation functions or for its Legendre transform, the generator of one-particle irreducible correlation functions (such a quantity is called effective action in the FT language and coincides with the Helmholtz free energy in the presence of a position-dependent magnetic field). Except for a few trivial cases, these functional equations cannot be solved exactly. On the other hand, numerical methods require

the use of approximations and/or truncations, such as the derivative expansion, that is a functional expansion of the effective action in powers of momenta. The first order of the derivative expansion is the local potential approximation (see e.g. Ref. [61]), which implies $\eta = 0$, and thus it is expected to provide a good starting point only when $\eta \ll 1$.¹⁹ Moreover the convergence properties of the derivative expansion are not clear, and therefore, it is difficult to estimate the errors on the results obtained by this approach. However, the results seem to improve (in the sense that they get closer to the more precise estimates obtained by other methods) when better truncations are considered, see, e.g., Refs. [113, 570]. The results of Ref. [595] were obtained using a similar approach, called the scaling-field method (SFM). While the results for the critical exponents γ , ν and η (see Table 6) are considerably less precise than the perturbative ones, the authors were able to estimate also additional subleading exponents, such as the next-to-leading irrelevant exponent, obtaining $\omega_2 = 1.67(11)$.

Finally, we mention the results obtained for the universal critical exponent ω_{NR} describing how the spatial anisotropy, which is present in physical systems with cubic symmetry such as uniaxial magnets, vanishes when approaching the rotationally-invariant fixed point [176], see Sec. 1.6. The most accurate estimate of ω_{NR} was obtained by analyzing the IHT expansions of the first non-spherical moments of the two-point function of the order parameter [177], obtaining²⁰

$$\omega_{\text{NR}} = 2.0208(12), \quad (3.1)$$

which is very close to the Gaussian value $\omega_{\text{NR}} = 2$. FT methods provided consistent although considerably less precise estimates [176, 177].

3.1.2 Experimental results.

Many experimental results can be found in the literature. For recent reviews, see, e.g., Refs. [39, 98, 131, 655]. The most important physical systems belonging to the Ising universality class may be divided into four classes:

- (a) **Liquid-vapor transitions (lv).** The order parameter is $\rho - \rho_c$, where ρ is the density and ρ_c its value at the critical point. The Ising-like continuous transition occurs at the end of the first-order liquid-gas transition line in the pressure-temperature plane; see Fig. 2. The liquid-vapor

¹⁹For example in the two-dimensional Ising case, where $\eta = 1/4$ is not particularly small, the local potential approximation is unable to display the expected fixed point structure [296, 569].

²⁰We signal the presence of a misprint in Ref. [177] concerning the estimate of ω_{NR} , which is there called ρ .

transition does not have the Z_2 symmetry which is present in magnetic systems, except at the critical point. Therefore, in fluids one observes Z_2 -noninvariant corrections to scaling, which are absent in magnets. For a general review see, e.g., [625].

- (b) **Binary mixtures (bm).** One considers here two fluids at fixed temperature. The order parameter is the concentration and the transition corresponds to the mixing of the two liquids (or gases): on the one side of the transition the two fluids are separated, on the other side they are mixed. Note that binary mixtures also undergo a liquid-vapor transition as described in (a). Similar transitions also occur in solids, for instance in β -brass.
- (c) **Uniaxial magnetic systems (ms).** These are the systems that inspired the Ising Hamiltonian. They are magnetic systems in which the crystalline structure favors the alignment along a specific direction. The experimental systems usually display antiferromagnetism, but, as we discussed in Sec. 1.3, on bipartite lattices ferromagnetic and antiferromagnetic criticality are closely related. Because of the crystalline structure, these systems are not rotationally invariant. Thus, there are corrections to scaling that are not present in fluids.
- (d) **Micellar systems (mi).** Micellization is the process of aggregation of certain surfactant molecules in dilute aqueous solutions. The onset of micellization, i.e. the concentration at which the aggregation process begins, can be regarded as a second-order phase-transition point [39, 372].

In Table 7 we report some experimental results for the critical exponents, most of them published after 1990. It is not a complete list of the published results, but it may be useful to get an overview of the experimental state of the art. Even if the considered systems are quite different, the results substantially agree, although, looking in more detail, one may find small discrepancies. The agreement with the theoretical results supports the RG theory of critical phenomena, although experimental results are substantially less accurate than the theoretical ones.

3.2 The zero-momentum four-point coupling constant

The zero-momentum four-point coupling constant g_4 defined in Eq. (1.63) plays an important role in the FT perturbative expansion at fixed dimension [620].

	Ref.	γ	ν	η	α	β
lv	[400] 1999				0.1105 ^{+0.0250} _{-0.0270}	
	[236] 1998			0.042(6)		
	[495] 1995					0.341(2)
	[1] 1994				0.111(1)	0.324(2)
	[713] 1993				0.1075(54)	
	[268] 1984				0.1084(23)	
	[646] 1984	1.233(10)				0.327(2)
bm	[661] 1998				0.104(11)	
	[462] 1994	1.09(3)				
	[33] 1994					0.324(5)
	[33] 1994					0.329(2)
	[34] 1994					0.329(4)
	[34] 1994					0.333(2)
	[688] 1993		0.610(6)			
	[784] 1992				0.105(8)	
	[74] 1992					0.336(30)
	[235] 1989	1.228(39)	0.628(8)	0.0300(15)		
	[429] 1986	1.26(5)	0.64(2)			
[374] 1985	1.24(1)	0.606(18)		0.077(44)	0.319(14)	
ms	[546] 1994					0.325(2)
	[678] 1993				0.11(3)	
	[716] 1993	1.25(2)				0.315(15)
	[102] 1987	1.25(2)	0.64(1)			
	[543] 1985				0.11(3)	
	[101] 1983				0.110(5)	0.331(6)
mi	[682] 1994	1.216(13)	0.623(13)	0.039(4)		
	[789] 1994	1.237(7)	0.630(12)			
	[51] 1993					0.34(8)
	[52] 1993	1.18(3)	0.60(2)			
	[700] 1992	1.17(11)	0.65(4)			
	[375] 1991	1.25(2)	0.63(1)			

Table 7: Experimental estimates of critical exponents for the three-dimensional Ising universality class. lv denotes the liquid-vapor transition in simple fluids, bm refers to a binary fluid mixture, ms to a uniaxial magnetic system, and mi to a micellar system.

In this approach, any universal quantity is obtained from a perturbative expansion in powers of $g \equiv g_4$ computed at $g = g^* \equiv g_4^+$, see Sec. 2.4.1. Therefore, a precise determination of g_4^+ is crucial in order to obtain precise estimates of universal critical quantities.

In Table 8 we review the estimates of g_4^+ obtained by exploiting various approaches.

In Ref. [177] an accurate estimate of g_4^+ was obtained from the analysis of the 18th-order IHT expansions of g_4 for three improved models: the ϕ^4 - ϕ^6 model (2.36) and the Blume-Capel model (2.37), see Sec. 2.3.2. Here, we have reanalyzed the series of g_4 and obtained a slightly larger value than that reported in Ref. [177]. The difference is due to the fact that here we use a different analysis which we believe to be more reliable. Such analysis was used in Ref. [171] (see App. B.3) in order to determine g_4^+ for the XY universality class. All other results are in substantial agreement. The HT estimates of Refs. [163, 165, 640] were obtained by using appropriate biased approximants (using β_c and Δ as external inputs) to reduce the systematic effects due to confluent singularities. The authors of

Ref. [107] performed a dimensional expansion of the Green's functions around $d = 0$ (d -exp.). The analysis of these series allowed them to obtain a quite precise estimate of g_4^+ in three dimensions.

Results of MC simulations are reported in Ref. [471], where a FSS technique was used to obtain g_4 for large correlation lengths. An estimate of g_4^+ —in perfect agreement with the IHT result—was obtained by fitting the data with an Ansatz that takes into account the leading scaling correction. Ref. [79] reports MC results obtained from simulations of the ϕ^4 lattice Hamiltonian (1.7) with $\lambda = 1$, which is close to the optimal value $\lambda^* \simeq 1.10$. In Ref. [79] no final estimate is reported. The value we quote in Table 8 is the result of our fit to their data. The result of Ref. [736] was obtained by studying the probability distribution of the average magnetization (see also Ref. [672] for a work employing a similar approach). The other estimates were obtained from fits to data in the neighborhood of β_c . The MC estimates of Refs. [68, 472] were larger because the effects of scaling corrections were neglected, as shown in Ref. [640].

FT estimates are substantially consistent. In the $d=3$ fixed-dimension approach g_4^+ is determined from the zero of the corresponding Callan-Symanzik β -function, obtained by resumming its perturbative six-loop series [70]. The results of Refs. [359, 505], which used a Borel transformation and a conformal mapping to take into account the large-order behavior (see Sec. 2.4.3), are slightly larger than the IHT one.²¹ The more general analysis of the g -expansion of Ref. [584] led to a smaller value $g_4^+ = 23.46$, with an uncertainty estimated by the authors to be about 1%. The ϵ -expansion result of Refs. [640, 643] was obtained from a constrained analysis—see Sec. 2.4.3—of the $O(\epsilon^4)$ series that took into account the known values of g_4^+ for $d = 0, 1, 2$. In Table 8 we also report estimates obtained by using the nonperturbative continuous RG (CRG) approach [570, 691, 729]. Other estimates of g_4^+ , which do not appear in Table 8, can be found in Refs. [65, 67, 69, 108, 330, 331, 476, 596, 763, 765].

3.3 The critical equation of state of Ising-like systems

The equation of state relates the external (magnetic) field H , the expectation value M of the order parameter (magnetization), and the reduced temperature $t \equiv (T - T_c)/T_c$. In fluids the variables playing the roles of H and M are $\mu - \mu_c$ and $\rho - \rho_c$ respectively, where μ is the chemical potential and ρ the density, and the subscript c indicates the values at the critical point.

3.3.1 Small-magnetization expansion of the (Helmholtz) free energy in the HT phase.

As discussed in Sec. 1.5.2, for small values of M and $t > 0$ the scaling function $A_1(z)$, that corresponds to the Helmholtz free energy, and the equation-of-state scaling function $F(z)$ can be parametrized in terms of the universal constants r_{2n} , see Eqs. (1.101) and (1.102).

Table 9 reports the available estimates of r_6 , r_8 , and r_{10} . The results of Ref. [177] were obtained by analyzing the IHT expansions of r_6 , r_8 , and r_{10} to order 17, 16, and 15 respectively for three improved lattice models, the ϕ^4 - ϕ^6 model (2.36) and the improved Blume-

²¹This difference may partially explain the small difference found in the determination of γ , since the estimates of the critical exponents depend slightly on the value of $g^* = g_4^+$. Using $d\gamma/dg^* \simeq 0.011$ [359], we see that by changing the value of g^* from 23.64 (which is the value obtained from the zero of $\beta(g)$) to 23.54, γ changes from 1.2396 to 1.2385, which is closer to the IHT estimate $\gamma = 1.2371(4)$ of Ref. [177]. Similarly, using $d\nu/dg^* \simeq 0.0066$ [359], ν would change from 0.6304 to 0.6297, which is quite acceptable.

Capel model (2.37). Additional results were obtained from HT expansions [163, 663, 791] and MC simulations [471, 472, 736] of the Ising model. The MC results do not agree with the results of other approaches, especially those of Refs. [471, 472], where FSS techniques were employed. But one should consider the difficulty of such calculations due to the subtractions that must be performed to compute the irreducible correlation functions. In the framework of the ϵ -expansion, the $O(\epsilon^3)$ series of r_{2n} were derived from the $O(\epsilon^3)$ expansion of the equation of state [146, 604, 752]. Ref. [641] performed a constrained analysis—the method is described in Sec. 2.4.3—exploiting the known values of r_{2n} for $d = 0, 1, 2$. In the framework of the fixed-dimension expansion, Refs. [358, 359] analyzed the five-loop series computed in Refs. [62, 371]. Rather good estimates of r_{2n} were also obtained in Ref. [570] (see also Ref. [729]) by using the CRG method, although the estimate of g_4^+ by the same method is not as good. CRG methods seem to be quite effective for the determination of zero-momentum quantities such as r_{2n} , but are imprecise for quantities that involve derivatives of correlation functions, as is the case for g_4^+ . This should not come unexpected since the Ansatz used to solve the RG equation is based on a derivative expansion.

3.3.2 Approximate parametric representations of the equation of state: The general formalism

The equation of state is particularly interesting from an experimental point of view and much work has been dedicated to its determination. In order to obtain approximate representations of the equation of state, it is convenient to use the parametric model described in Sec. 1.5.6, i.e. rewriting H , t , and M in terms of the two variables θ and R , see Eq. (1.133). The advantage in using parametric representations is that all the analytic properties of the equation of state are automatically satisfied if $h(\theta)$ and $m(\theta)$ are analytic and satisfy a few simple constraints: (a) $h(\theta) > 0$, $m(\theta) > 0$, $Y(\theta) \neq 0$ for $0 < \theta < \theta_0$; (b) $m(\theta_0) > 0$; (c) $\theta_0 > 1$. Here θ_0 is the positive zero of $h(\theta)$ that is nearest to the origin and $Y(\theta)$ is defined in Eq. (1.134).

In general, in order to obtain an approximation of the equation of state, one can proceed as follows (see, e.g., Refs. [89, 320, 409, 692]):

- (a) One chooses some parametrization of $h(\theta)$ and $m(\theta)$ depending on k parameters such that $h(\theta)$ and $m(\theta)$ are odd and $h(\theta) = \theta + O(\theta^3)$ and $m(\theta) = \theta + O(\theta^3)$ for $\theta \rightarrow 0$.
- (b) One chooses $\tilde{k} \geq k$ universal quantities that can be derived from the equation of state and that are

HT	MC	ϵ -exp.	$d = 3$ exp.	d -exp.	CRG
23.54(4) [this work]	23.6(2) [471]	23.6(2) [643]	23.64(7) [359]	23.66(24) [107]	24.3 [691]
23.49(4) [177]	23.4(2) [79, 640]	23.3 [359]	23.46 [584]		21(4) [570]
23.57(10) [165]	23.3(5) [736]		23.71 [708]		28.9 [729]
23.55(15) [640]	25.0(5) [68]		23.72(8) [505]		
24.69(10) [163]	24.5(2) [472]				
24.45(15) [791]					
23.7(1.5) [663]					

Table 8: Estimates of g_4^+ for the three-dimensional Ising universality class.

	HT	ϵ -exp.	$d = 3$ exp.	MC	CRG
r_6	2.048(5) [177]	2.058(11) [641]	2.053(8) [359]	2.72(23) [736]	2.064(36) [570]
	1.99(6) [163]	2.12(12) [359]	2.060 [708]	3.37(11) [471]	1.92 [729]
	2.157(18) [791]			3.26(26) [472]	
	2.25(9) [496]				
	2.5(5) [663]				
r_8	2.28(8) [177]	2.48(28) [641]	2.47(25) [359]		2.47(5) [570]
	2.7(4) [163]	2.42(30) [359]			2.18 [729]
r_{10}	-13(4) [177]	-20(15) [641]	-25(18) [359]		-18(4) [570]
	-4(2) [163]	-12.0(1.1) [359]			

Table 9: Estimates of r_6 , r_8 , and r_{10} for the three-dimensional Ising universality class. In the case of r_{10} we also mention the estimate $r_{10} = -10(2)$ obtained in Ref. [177] by studying the equation of state.

known independently, for instance from a MC simulation, from the analysis of HT and/or LT series, or directly from experiments. Then one uses them to determine the k parameters defined in (a).

- (c) The scale factors m_0 and h_0 are determined by requiring the equation of state to reproduce two nonuniversal amplitudes.

For the functions $h(\theta)$ and $m(\theta)$, polynomials are often used. There are many reasons for this choice. First, this choice makes the expressions simple and analytic calculations are easy. Moreover, the simplest representation, the so-called “linear” model, is already a very good approximation [687]. Such a model is defined by considering

$$\begin{aligned} m(\theta) &= \theta, \\ h(\theta) &= \theta + h_3\theta^3. \end{aligned} \quad (3.2)$$

Using the above-presented strategy, the value of h_3 can be computed by considering a universal amplitude ratio. Ref. [687] considered $U_2 \equiv C^+/C^-$, and observed that, for all acceptable values of h_3 , the linear model gave values of U_2 that were larger than the HT/LT estimates. The best approximation was obtained by considering the value of h_3 which gave the smallest possible U_2 , i.e. by setting $h_3 = \bar{h}_3$, where \bar{h}_3 was determined from

$$\left. \frac{dU_2}{dh_3} \right|_{h_3=\bar{h}_3} = 0. \quad (3.3)$$

The result was

$$\bar{h}_3 = \frac{\gamma(1-2\beta)}{\gamma-2\beta}. \quad (3.4)$$

Later Ref. [752] showed that the same condition can be obtained by considering any invariant ratio R , i.e. that Eq. (3.3) is satisfied by any R . Numerically, using the results for the critical exponents reported in Sec. 3.1, the choice $h_3 = \bar{h}_3$ gives $U_2 \approx 4.83$ which is in relatively good agreement with the most accurate MC estimate $U_2 = 4.75(3)$ [206]. Thus, the linear parametric model appears as a good zeroth-order approximation. Then one may think that higher-order polynomials provide better approximations.

A second argument in favor of polynomial representations is provided by the ϵ -expansion. Setting

$$\begin{aligned} m(\theta) &= \theta, \\ h(\theta) &= \theta + \sum_{n=1}^k h_{2n+1}\theta^{2n+1}, \end{aligned} \quad (3.5)$$

one can prove [177, 752] that, for each k , one can fix the coefficients of the polynomial $h(\theta)$ so that the representation is exact up to order ϵ^{k+2} .

We mention that alternative nonpolynomial representations have been introduced in the literature. Motivated by the desire of extending the Helmholtz free energy into the unstable two-phase region below the critical temperature, Refs. [318–320] considered trigonometric representations. This will be discussed in Sec. 3.3.4.

Let us now discuss how to determine the parameters appearing in $m(\theta)$ and $h(\theta)$. If $\tilde{k} = k$, the number of unknowns is equal to the number of conditions and thus we can fix the k parameters by requiring the approximate equation of state to reproduce these values. Since the equations are nonlinear, this is not always possible. For example, this is the case of the linear model. In these cases, one may determine the values of the parameters that give the least discrepancy. A different strategy was pursued in Ref. [358]. When it is not possible to obtain a parametrization that exactly reproduces the known values, Ref. [358] suggested to consider a parametrization with one additional free parameter. In this case infinite good choices of the $k + 1$ parameters exist and thus an additional condition is required. Using the parametric representation (3.5), Ref. [358] fixed the $(k + 1)$ parameter h_3, \dots, h_{2k+3} so that $|h_{2k+3}|$ was as small as possible. Finally, one may also consider the case $\tilde{k} > k$. This may be convenient if the input data have large errors. In this case the k parameters are fixed by means of a standard fitting procedure.

A conceptually different approach, which we will call variational approach, was pursued in Refs. [177, 210], to determine the equation of state by using the lowest-order terms of the expansion of the free energy in powers of M in the HT phase, i.e. the coefficients r_{2n} . Few of them are known, and this puts a serious limitation on the order of the polynomials that can be used. Therefore, in order to improve the approximation, one considers the representation (3.5) with k unknown coefficients h_{2n+1} but uses only $k - 1$ amplitude ratios r_{2n} . A coefficient of $h(\theta)$, which is left undetermined in this procedure, is fixed by requiring physical results to have the smallest possible dependence on it. The idea behind this procedure is that in the exact case, i.e. if we were considering $k = \infty$, one parameter in $h(\theta)$ would be arbitrary and could be fixed at will.²² Of course, in the approximate case, the results depend on all parameters introduced. One may then require that they have some approximate independence from one of the parameters appearing in $h(\theta)$. As we said, this procedure is exact for $k \rightarrow \infty$.

In this approach, one first requires the approximate parametric representation to give the correct $(k - 1)$ universal ratios $r_6, r_8, \dots, r_{2k+2}$. One obtains

$$h_{2n+1} = \sum_{m=0}^n c_{nm} 6^m (h_3 + \gamma)^m \frac{r_{2m+2}}{(2m+1)!}, \quad (3.6)$$

²²For instance, if we know $f(x)$ exactly, we can determine $h(\theta)$ from Eq. (1.139). However, the value of $h(1)$ is completely arbitrary. Indeed, one should first choose $h(1)$, then use the fact that $h(\theta) \approx \theta$ for $\theta \rightarrow 0$ to determine θ_0 , and finally set $h(\theta) = h(1)\theta^\theta f(x)$.

where

$$c_{nm} = \frac{1}{(n-m)!} \prod_{k=1}^{n-m} (2\beta m - \gamma + k - 1), \quad (3.7)$$

and we have set $r_2 = r_4 = 1$. By considering $(k - 1)$ universal ratios one determines all coefficients in terms of h_3 , which should then be fixed. If one followed the approach presented at the beginning, one would require that the approximate representation reproduces some additional invariant ratio: for instance, if one wishes to use only HT data, r_{2k+4} could be used. This would completely determine the function $h(\theta)$. As we said, Ref. [177] proposes a different strategy. First, the two scale factors h_0 and m_0 are fixed by requiring the representation (1.133) to give the correct amplitudes for χ and χ_4 in the HT phase. A simple calculation gives

$$\chi = \frac{m_0}{h_0} t^{-\gamma}, \quad (3.8)$$

$$\chi_4 = \frac{6m_0}{h_0^3} (\gamma + h_3) t^{-3\gamma - 2\beta}, \quad (3.9)$$

so that m_0 and h_0 are fixed by requiring

$$C^+ = \frac{m_0}{h_0}, \quad (3.10)$$

$$C_4^+ = \frac{6m_0}{h_0^3} (\gamma + h_3). \quad (3.11)$$

These two requirements are satisfied if we introduce ρ as in Eq. (1.136) and set²³

$$h_3 = -\gamma + \frac{\rho^2}{6}. \quad (3.12)$$

Using Eq. (3.12), we can reexpress all coefficients h_{2n+1} in terms of ρ . Then, the coefficient ρ is fixed by requiring an additional optimization condition. In the exact parametric representation $h(\theta)$ depends on ρ in such a way to make $F(z)$, which is a universal function (see Eqs. (1.137) and (1.138)), independent of ρ . Of course, this is no longer true when we use our truncated function $h(\theta)$, and the related approximate function $F_{\text{approx}}^{(k)}(z, \rho)$ depends on ρ . We then set $\rho = \rho_k$, where ρ_k is a solution of the global stationarity condition

$$\left. \frac{\partial F_{\text{approx}}^{(k)}(z, \rho)}{\partial \rho} \right|_{\rho=\rho_k} = 0 \quad (3.13)$$

²³In Refs. [177, 210] the conditions (3.6) and (3.12) were obtained by requiring the approximate representation to reproduce the small- z expansion (1.101). The procedure is equivalent, but it hides the fact that this fixes the metrical factors m_0 and h_0 . Indeed, one starts from Eqs. (1.137) and (1.138) which are obtained by using Eq. (1.136) which, in turn, is obtained by fixing the normalization of χ . The requirement that z is correctly normalized, i.e. $F(z) = z + \frac{1}{6}z^3 + O(z^5)$, fixes the second normalization.

for all z . Equivalently one may require that, for any universal ratio R that can be obtained from the equation of state, its approximate expression $R_{\text{approx}}^{(k)}$ obtained by using the parametric representation satisfies

$$\left. \frac{dR_{\text{approx}}^{(k)}(\rho)}{d\rho} \right|_{\rho=\rho_k} = 0. \quad (3.14)$$

In other words, one chooses ρ in such a way to minimize the ρ -dependence. The existence of such a value of ρ is a nontrivial mathematical fact. The stationary value of ρ is the solution of the algebraic equation

$$\left[(2\beta - 1)\rho \frac{\partial}{\partial \rho} - 2\gamma + 2k \right] h_{2k+1} = 0. \quad (3.15)$$

It is interesting to note that, for $k = 1$, this variational method reproduces the linear model with the specific choice (3.4).

At this point the reader may be puzzled by the fact that a metrical factor like ρ plays an important role in the procedure. However, this is just apparent: no metrical factor plays any role here and every reference to m_0 , h_0 , and ρ can be avoided. Indeed, ρ can be interchanged with h_3 by simply using Eq. (3.12). Avoiding any reference to m_0 , h_0 , and ρ , one can determine the unknown h_3 by requiring that the physical results do not depend on the choice of this parameter, i.e. that for all ratios

$$\left. \frac{dR_{\text{approx}}(h_3)}{dh_3} \right|_{h_3=h_{3,k}} = 0, \quad (3.16)$$

which is the condition we mentioned at the beginning of the discussion. The difference between (3.16) and (3.14) is only at the conceptual level, since in practice $R_{\text{approx}}^{(k)}(h_3)$ is obtained from $R_{\text{approx}}^{(k)}(\rho)$ by using Eq. (3.12), and thus the stationarity condition is identical. In other words, one can still use the parameter ρ which is now *defined* by Eq. (3.12) and it is unrelated to m_0 and h_0 , that can then be fixed independently. By writing the stationarity condition as in Eq. (3.16), the relation between these approximations and the linear-model results of Ref. [687] appears obvious.

The same method was used in Ref. [210], where, beside the coefficients r_{2n} , the universal constant F_0^∞ that parametrizes the large- z behavior of the function $F(z)$, see Eq. (1.104), was used. Here, as before, the parameters h_3, \dots, h_{2k-1} are fixed by using the $(k-2)$ universal parameters r_{2n} , $n = 3, \dots, k$ and Eq. (3.12) as before. They are thus given by Eq. (3.6). Then, one sets

$$h_{2k+1} = \rho^{\delta-1} F_0^\infty - 1 - \sum_{n=1}^{k-1} h_{2n+1}, \quad (3.17)$$

so that, the parametric representation is exact for large values of z , i.e. it gives $F(z) \approx F_0^\infty z^\delta$ with the correct amplitude. The coefficient ρ , related to h_3 by Eq. (3.12), can be still determined by using the global stationarity condition (3.13), which is again a nontrivial property. As before, in practice the value of ρ_k is determined from Eq. (3.15).

The reader may be tempted to employ the variational method using other amplitude ratios as input parameters. However, this fact is far from being obvious. Indeed, the proof that Eq. (3.13) holds independently of z requires identities that are valid only for very specific choices of amplitude ratios. At present, the procedure is known to work only for the two sets of amplitude ratios we mentioned above: (a) r_6, \dots, r_{2k+2} ; (b) $F_0^\infty, r_6, \dots, r_{2k}$. The first set of amplitude ratios was used in Ref. [177] in three dimensions, where no estimate of F_0^∞ exists. The second set was used in Ref. [210] in two dimensions, since in this case F_0^∞ is known to high precision.

3.3.3 Approximate critical equation of state and amplitude ratios

Ref. [177] applied the variational method we presented in the previous section, by using the IHT results for γ , ν , r_6 , r_8 , and r_{10} as input parameters of the approximation scheme. This provides different approximations with $k = 1, 2, 3, 4$. The results show a good convergence with increasing k . Actually, the results for $k = 2, 3, 4$ are already consistent within the errors induced by the uncertainty on the input parameters, indicating that the systematic error due to the truncation is at most of the same order of the error induced by the input data. They are also consistent with the results of Ref. [358], that also determined the equation of state starting from its small- M expansion in the HT phase.

In Table 10 we report the polynomials $h(\theta)$ for $k = 1, 2, 3$, that are obtained in the variational approach for the central values of the input parameters. The fast decrease of the coefficients of the higher-order terms in $h(\theta)$ gives further support to the effectiveness of the approximation scheme. We do not report $h(\theta)$ for $k = 4$, since it requires r_{10} and its available estimate is rather imprecise.

In Figs. 5 and 6 we show respectively the scaling functions $F(z)$ and $f(x)$ —see Sec. 1.5.2 for the definitions—as obtained from $h(\theta)$ for $k = 1, 2, 3$. The differences between the $k = 2, 3$ approximations, which are hardly visible in the figures, show how small the error due to the truncation of $h(\theta)$ is. This is quite impressive, since our procedure is essentially an analytic extension of the expansion of $F(z)$, which should

k	ρ_k	θ_0^2	$h(\theta)/\theta$	$h(\theta)/[\theta(1-\theta^2/\theta_0^2)]$
1	1.73577	1.36064	$1 - 0.734951\theta^2$	1
2	1.74070	1.38794	$1 - 0.732091\theta^2 + 0.008355\theta^4$	$1 - 0.0115965\theta^2$
3	1.72893	1.32483	$1 - 0.738898\theta^2 + 0.008136\theta^4 - 0.000639\theta^6$	$1 - 0.0099591\theta^2 + 0.0008762\theta^4$

Table 10: Polynomial approximations of $h(\theta)$ using the global stationarity condition for various values of the parameter k , cf. Eq. (3.5). The reported expressions are obtained by using the central values of the input parameters. Results from Ref. [177].

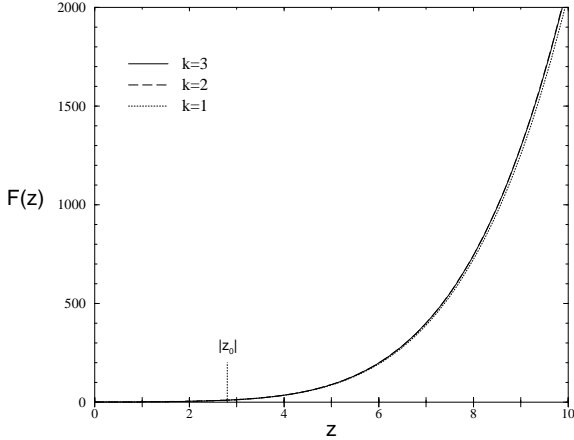


Figure 5: The scaling function $F(z)$ as obtained from the truncations $k = 1, 2, 3$ of the function $h(\theta)$.

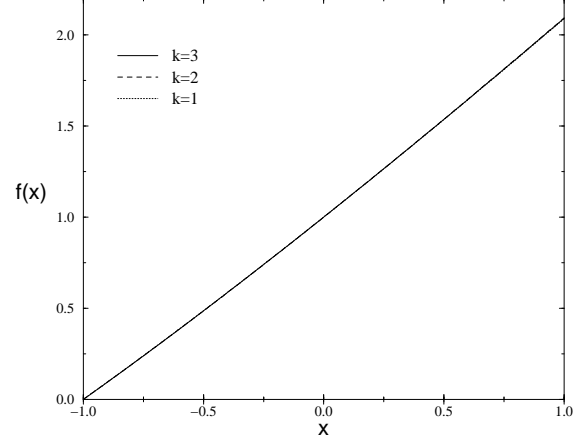


Figure 6: The scaling function $f(x)$ as obtained from the truncations $k = 1, 2, 3$ of the function $h(\theta)$. Differences are not visible.

converge only for $|z| < |z_0|$, to the whole physical domain. From the parametric representation one obtains $F_0^\infty = 0.0377(2)$, $f_0^\infty = R_\chi^{-1} = 0.6017(18)$, $b_{f,1} = \beta U_2/R_\chi = 0.9365(10)$, $b_{f,2} = 0.080(7)$, which are related to the asymptotic behavior of $F(z)$ for large z , cf. Eq. (1.104), to the large- x behavior of $f(x)$, cf. Eq. (1.109), and to the behavior of $f(x)$ at the coexistence curve, cf. Eq. (1.124).

One can also derive accurate estimates of many other universal amplitude ratios. For example, for $k = 1, 2, 3$ one obtains respectively [177]: $U_0 = 0.5222(16)$, $0.5316(21)$, $0.5295(29)$, $U_2 = 4.826(11)$, $4.752(15)$, $4.769(22)$, $U_4 = -9.74(4)$, $-8.92(8)$, $-9.10(18)$, where the errors are only related to the uncertainty of the input parameters. Note that the results oscillate and that the uncertainty due to the input parameters on the $k = 3$ results is approximately the same as the difference between the estimates with $k = 2$ and $k = 3$. Therefore, we may consider the $k = 3$ truncation as the best approximation of the method using the available input parameters and to use the corresponding errors as final uncertainties. Table 11 reports the results obtained in Ref. [177] by using the variational method

with $k = 3$.

Estimates of other universal amplitude ratios can be obtained by supplementing the above results with the estimates of $w^2 \equiv C^-/[B^2(f^-)^3]$ and $Q_\xi^- \equiv f_{\text{gap}}^-/f^-$ obtained by an analysis of the corresponding LT expansions [49, 177, 640, 744]. The results for Q_ξ^- and Q_2 were obtained from approximate parametric representations of the correlation lengths ξ and ξ_{gap} [177]. The parametric functions (1.175) and (1.176) were approximated by

$$\begin{aligned} a(\theta) &= a(0)(1 + c\theta^2), \\ a_{\text{gap}}(\theta) &= a_{\text{gap}}(0)(1 + c_{\text{gap}}\theta^2), \end{aligned} \quad (3.18)$$

where c and c_{gap} were obtained by using the IHT estimates of U_ξ and $U_{\xi_{\text{gap}}}$. The results for Q_ξ^- and Q_2 obtained by using these approximate functions are in reasonable agreement with the HT,LT results in spite of the very crude approximation made in Eq. (3.18).

In Table 11 we also show some experimental results for binary mixtures, liquid-vapor transitions, and uniaxial antiferromagnetic systems. They should give an overview of the level of precision reached by experi-

ments. Most of the experimental data are taken from Ref. [655]. Sometimes, we report a range of values without a corresponding reference: this roughly summarizes the results reported in the corresponding table of Ref. [655] and should give an idea of the range of the experimental results.

In Table 11 we also report results obtained by other lattice techniques, such as HT and LT expansions, and MC simulations. Concerning the HT,LT estimates, we mention Ref. [319] where a review of such results is presented. The results for U_2 and U_ξ of Ref. [167] have been obtained by taking β_c and Δ as external inputs; the reported errors do not take into account the uncertainties on β_c and Δ , which should not be negligible. The IHT+PR estimates agree nicely with the most recent MC results, especially with those reported in Ref. [206], which are quite precise. There is a discrepancy only for U_0 : The estimates reported in Ref. [388] are slightly larger. It is worth mentioning that the result of Ref. [278] for U_2 was obtained by simulating a four-dimensional $SU(2)$ lattice gauge model at finite temperature, whose phase transition is expected to be in the three-dimensional Ising universality class [647].

Table 12 shows the results obtained by FT methods. FT estimates are perfectly consistent, although in general less precise. We mention that the results denoted by “ $d = 3$ exp.” were obtained by using different schemes, see Sec. 2.4: the HT zero-momentum scheme [55,62,358,359], the minimal subtraction without ϵ -expansion [500,683], and the expansion in the LT coupling $u \equiv 3w^2$ [361]. In Refs. [358,359] the authors used the fixed-dimension expansion and the ϵ -expansion to determine the universal coefficients r_6 , r_8 , and r_{10} , which are then used to obtain an approximate parametric representation of the critical equation of state.

For the sake of completeness in Tables 11 and 12 we also report universal amplitude ratios containing the surface-tension amplitude, such as R_σ and R_σ^+ , see Table 2 for the definitions.

3.3.4 Trigonometric parametric representations

Refs. [318–320] considered the possibility of determining a parametric representation of the equation of state that also describes the two-phase region below the critical temperature. In the classical mean-field equation of state that describes a first-order transition, one finds a characteristic van der Waals (vdW) loop that represents an isothermal analytic continuation of the equation of state through the coexistence curve. For $t \rightarrow 0^-$, it approaches the simple cu-

	ϵ -exp.	$d = 3$ exp.	CRG
U_0	0.527(37) [359] 0.524(10) [116,604]	0.537(19) [359] 0.540(11) [500] 0.541(14) [62]	
U_2	4.73(16) [359] 4.9 [604] 4.8 [18,140]	4.79(10) [359] 4.77(30) [62] 4.72(17) [361]	4.966 [691] 4.29 [112]
U_4	-8.6(1.5) [359]	-9.1(6) [359]	
R_c^+	0.0569(35) [359]	0.0574(20) [359]	
R_4^+	8.24(34) [358]	7.84 [359]	
R_χ	1.648(36) [359] 1.67 [116,604]	1.669(18) [359] 1.7 [62]	1.647 [691] 1.61 [112]
w^2		4.73 [361]	
U_ξ	1.91 [140]	2.013(28) [361]	2.027 [691] 1.86 [112]
Q^+	0.0197 [116,117]	0.01968(15) [55]	
Q_c		0.331(9) [62]	
Q_ξ^+	1.00016(2) [177]	1.00021(3) [176]	
Q_2	1.13 [140]		
v_3	5.99(5) [642] 6.07(19) [359]	6.08(6) [359]	
v_4	15.8(1.4) [642]		
g_3^-	13.06(12) [642]		
g_4^-	75(7) [642]		
R_σ	0.055 [138]	0.1065(9) [581]	

Table 12: Estimates of universal quantities, see Table 2 for an explanation of the symbols. The results are obtained by using FT methods: ϵ expansion (ϵ -exp.), the fixed-dimension expansion in $d = 3$ in different schemes (see text) ($d = 3$ exp.), and the continuous RG approach (CRG).

bic form $H \propto M(M^2 - M_0^2)$, which shows the classical critical exponents. The properties of the vdW loop are relevant for classical theories of surface tension, interfaces, spinodal decomposition, etc... (see, e.g., Refs. [168,670]). In Refs. [318–320] the authors search for representations of the equation of state that, on the one hand, describe the nonclassical critical behavior of the system, and, on the other hand, have a good analytic continuation in the two-phase region. As also mentioned by the authors, the existence of a full vdW loop is not guaranteed in nonclassical theories, because of the presence of essential singularities at the coexistence curve [36,301,316,421], which preclude the possibility of performing the required analytic continuation. Nevertheless, in Refs. [318–320] the classical thermodynamic picture was assumed and an analytic continuation of the critical equation of state was performed. They looked for parametric representations that give a reasonable realization of the vdW loop from their analytic continuation to the two-phase region. Polynomial representation do not offer a natural description of vdW loops. This is because the

	IHT-PR [177]	HT,LT	MC	experiments
U_0	0.530(3)	0.523(9) [516] 0.51 [89]	0.560(10) [389] 0.550(12) [389] 0.567(16) [389] 0.45(7) [542]	0.54–0.58 bm 0.47–0.53 lv 0.52–0.56 ms 0.538(17) lv [713] 0.54(2) ms [101]
U_2	4.77(2)	4.762(8) [167] 4.95(15) [516] 5.01 [727]	4.75(3) [206] 4.72(11) [278]	4.3(3) bm [785] 4.5–5.3 lv 4.9(5) ms [232] 4.6(2) ms [102]
U_4	−9.1(2)	−9.0(3) [791]		
R_c^+	0.0564(3)	0.0581(10) [791]		0.050(15) bm [785] 0.04–0.06 lv
R_c^-	0.02235(11)			
R_4^+	7.82(2)	7.94(12) [319]		
R_4^-	93.3(5)	107(13) [319, 791]		
R_χ	1.662(5)	1.57(23) [319, 790]		1.75(30) bm [785] 1.69(14) lv [587]
w^2		4.75(4) [640] 4.71(5) [308, 791]	4.77(3) [206]	
U_ξ	1.961(7)	1.963(8) [167] 1.96(1) [516] 1.96 [727]	1.95(2) [206] 2.06(1) [673]	2.0(4) bm [376] 1.9(2) bm [785] 1.89(4) ms [102] 1.93(10) ms [232]
$U_{\xi_{\text{gap}}}$	1.901(10)			
Q^+	0.01880(8)	0.0202(9) [166] 0.01880(15) [516]	0.0193(10) [389]	0.0174(32) lv [268] 0.023(4) lv [400] 0.018–0.022 bm
Q^-	0.00471(5)	0.00477(20) [319]	0.0463(17) [389]	
Q_c	0.3330(10)	0.324(6) [319]	0.328(5) [206]	0.3–0.4 bm 0.36(3) bm [429] 0.29(4) bm [37] 0.3–0.4 lv
Q_ξ^+	1.000183(2)	1.0001 [319]		
Q_ξ^c	1.024(4)	1.007(3) [319]		
Q_ξ^-		1.032(4) [177] 1.037(3) [319]	1.031(6) [9, 211]	
Q_2	1.195(10)	1.17(2) [319, 790]		1.1(3) bm [785]
v_3	6.041(11)	6.44(30) [319, 791]		
v_4	16.21(11)			
g_3^-	13.17(6)	13.9(4) [791]	13.6(5) [737]	
g_4^-	77.0(8)	85 [791]	108(7) [737]	
R_σ			0.1040(8) [388] 0.1056(19) [9] 0.098(2) [790]	
R_σ^+			0.40(1) [383] 0.377(11) [319, 790]	0.38(3) 0.41(4) bm [540]

Table 11: Estimates of universal quantities, see Table 2 for an explanation of the symbols. The results are obtained by combining HT results and the parametric representation of the equation of state (IHT-PR), from the analysis of high- and low-temperature expansions (HT,LT), and from Monte Carlo simulations (MC). For the experimental results: ms denotes a magnetic system; bm a binary mixture; lv a liquid-vapor transition. Experimental estimates without reference are taken from Ref. [655].

analytic continuation of these equations of state fails to generate a closed, continuous vdW loop inside the two-phase region. To overcome this fact the authors of Ref. [318] proposed an interpolation scheme to supplement these models so as to ensure the expected vdW loop: The traditional parametric representations are retained, but a new angular variable ϕ is introduced to describe the two-phase region only, the values $\phi = \pm 1$ being assigned to the phase boundaries, while $\phi = 0$ corresponds to the coexistence curve diameter $M = 0$, $H = 0$. Thus, new angular functions describing the two-phase region are required, satisfying a matching condition to ensure the smoothness of the equation of state across the phase boundaries $H = 0$, $t < 0$. However, according to the authors, this procedure is not the optimal one. They noted that a natural description of the vdW loop requires analytic periodicity with period $2\theta_p$ with $\theta_p > \theta_0$. Therefore, they proposed an alternative approach based on trigonometric parametric representations:

$$\begin{aligned} M &= m_0 R^\beta m(\theta), \\ t &= R k(\theta), \\ \mathcal{A} &= n_0 R^{2-\alpha} n(\theta), \\ \xi^2/2\chi &= R^{-\eta\nu} a(\theta), \end{aligned} \quad (3.19)$$

where the traditional expression for H is replaced by a direct representation for the free energy \mathcal{A} . The parametric functions $m(\theta)$, $k(\theta)$, $n(\theta)$, and $a(\theta)$ are chosen to guarantee a closed analytic vdW loop:

$$\begin{aligned} m(\theta) &= \frac{\sin(q\theta)}{q}, \\ k(\theta) &= \left[1 - \frac{2b^2}{q^2} (1 - \cos(q\theta)) \right], \\ n(\theta) &= 1 + \sum_{i=1}^j c_i k(\theta)^i, \\ a(\theta) &= a_0 \left[1 + \frac{2a_2}{q^2} (1 - \cos(q\theta)) \right. \\ &\quad \left. + \frac{a_4}{q^4} (1 - \cos(q\theta))^2 \right], \end{aligned} \quad (3.20)$$

where q, b, c_i, a_i are parameters that are determined by using known universal amplitude ratios. As shown in Ref. [320], this parametrization is able to provide a good fit to the universal amplitude ratios and reasonable vdW loops. They found that the shape of the vdW loop for a three-dimensional Ising-like system near criticality differs significantly from the classical form. In particular, the spinodal should be closer to the coexistence curve and the size of the vdW loop is smaller by approximately a factor of two.

3.4 The two-dimensional Ising universality class

3.4.1 General results

In two dimensions a wealth of exact results exists. First, many exact results have been obtained for the simplest model belonging to this universality class, the spin-1/2 Ising model. Among others, we should mention: the exact expression of the free energy along the $H = 0$ axis [613], the two-point correlation function for $H = 0$ [783], and the spontaneous magnetization on the coexistence curve [748]. For a review, see, e.g., Ref. [553]. Moreover, in the critical limit several leading and correction-to-scaling amplitudes are known to high precision, see, e.g., Refs. [600, 617]. Besides, at the critical point one can use conformal field theory. In particular, this gives the exact spectrum of the theory, i.e. all the dimensions of the operators present in the model. One proves that the first rotationally-invariant correction-to-scaling operator has dimension $y_3 = -2$, i.e. $\omega = 2$.²⁴ Also, the exponent ω_{NR} that gives the corrections related to the breaking of the rotational invariance can be exactly predicted [169, 176, 208]: $\omega_{NR} = 2$ on the square lattice and $\omega_{NR} = 4$ on the triangular lattice.

Additional predictions can be obtained by using the S -matrix approach to two-dimensional integrable theories and in particular the thermodynamic Bethe Ansatz (for a review, see, e.g., Ref. [553]). Indeed, one can prove that the quantum field theories that describe the critical regime for $H = 0$ and on the critical isotherm are integrable and one can compute the corresponding S -matrices. While for $H = 0$ the S -matrix is trivial, for two-particle scattering $S = -1$, on the critical isotherm the S -matrix solution is complicated with a nontrivial mass spectrum [786]. A related method is the form-factor approach, which uses the knowledge of the S -matrix to set up a system of recursive functional equations for the form factors. Solving this system one can in principle compute exactly all the form factors, thus continuing the S -matrix off the mass shell [451, 452, 704]. Once the form factors are known, one can express the correlation functions of the basic

²⁴It is interesting to note that such correction does not appear in the lattice Ising model, which is thus an exactly improved model. There is no mathematical proof, but in the years a lot of evidence has been collected. In particular, no such correction is found for the susceptibility for $H = 0$ and $t > 0$ [600, 617] and in the free energy along the critical isotherm [208]. We should also notice that it has been claimed sometimes that $\omega = 4/3$. Such a statement is partially incorrect. Indeed, such exponent only appears in the Wegner expansion of some quantities and correlations that provide a nonunitary extension of the Ising universality class, but not of the standard thermodynamic variables. For a detailed discussion, see App. A of Ref. [169].

fields, as well as of other composite operators, by inserting complete sets of scattering states between them. This gives the correlation functions as infinite series of convolution products of form factors.

In Table 13 we report some exact results and some high-precision estimates of the amplitude ratios that have been obtained by using the approaches we mentioned above. However, many quantities have not yet been computed using these methods and standard numerical techniques have been adopted. In Table 14 we report the best available estimates for some additional universal quantities that have been determined numerically. Expressions for the free energy and for the critical equation of state in the whole (t, H) plane will be reviewed in Sec. 3.4.3.

Let us mention that the two-dimensional Ising universality class is also of interest experimentally. Indeed, there exist several uniaxial antiferromagnets which present a strongly enhanced in-plane coupling and an easy-axis anisotropy (see, e.g., Refs. [399, 655] for some experimental results), and have therefore a two-dimensional Ising critical behavior.

3.4.2 The critical equation of state: exact results

The behavior of the free energy for the two-dimensional Ising model is somewhat different from that described in Sec. 1.5. The reason is that in this case there are resonances among the RG eigenvalues with the subsequent appearance of logarithmic terms. Because of the resonance between the identity and the thermal operator, the singular part of the Gibbs free energy becomes [759]

$$\mathcal{F}_{\text{sing}}(H, t) = t^2 \widehat{\mathcal{F}}_1(Ht^{-15/8}) + t^2 \log |t| \widehat{\mathcal{F}}_{1,\log}(Ht^{-15/8}), \quad (3.21)$$

where irrelevant terms have been discarded. Note that additional resonances involving subleading operators are expected, and thus additional logarithmic terms should be present: such terms, involving higher powers of $\log |t|$, have been found in a high-precision analysis of the susceptibility for $H = 0$ in the HT phase [617]. The exact results for the free energy at $H = 0$ and the numerical results for the higher-order correlation functions at zero momentum show that $\widehat{\mathcal{F}}_{1,\log}(x)$ is constant [16]. Indeed, if this function were nontrivial, then one would obtain $\chi_n \sim |t|^{-\gamma_n} \log |t|$ for $|t| \rightarrow 0$, a behavior which has not been observed. The constant is easily related to the amplitudes of the specific heat for $H \rightarrow 0$ defined in Eq. (1.47). The analyticity for $t = 0$, $H \neq 0$ implies

$$A^+ = A^- \equiv A, \quad (3.22)$$

so that

$$\mathcal{F}_{\text{sing}}(H, t) = t^2 \widehat{\mathcal{F}}_1(Ht^{-15/8}) + \frac{A}{2} t^2 \log |t|. \quad (3.23)$$

For the Helmholtz free energy similar formulae holds. Using the notations of Sec. 1.5.2 we write

$$\begin{aligned} \mathcal{A}_{\text{sing}}(M, t) &= a_{11} t^2 A_1(z) + \frac{A}{2} t^2 \log |t| \\ &= a_{20} M^{16} A_2(x) + \frac{A}{2} t^2 \log |t|, \end{aligned} \quad (3.24)$$

where a_{11} and a_{20} are defined in Eqs. (1.92) and (1.96), the variables z and x in Eqs. (1.88) and (1.94), and the functions $A_1(z)$ and $A_2(x)$ are normalized as in Sec. 1.5.2. The presence of the logarithmic term gives rise to logarithms in the expansions of $A_1(z)$ for $z \rightarrow \infty$ and $A_2(x)$ for $x \rightarrow 0$. Indeed, the analyticity of $\mathcal{A}_{\text{sing}}(M, t)$ for $t = 0$, $|M| \neq 0$ implies

$$A_1(z) = z^{16} \sum_{n=0} a_{1,n} z^{-8n} + a_{1,\log} \log z, \quad (3.25)$$

$$A_2(x) = \sum_{n=0} a_{2,n} x^n + a_{2,\log} x^2 \log |x|. \quad (3.26)$$

The constant $a_{1,\log}$ and $a_{2,\log}$ are easily expressed in terms of invariant amplitude ratios:

$$a_{1,\log} = \frac{4A}{a_{11}} = 4Q^+ g_4^+, \quad (3.27)$$

$$a_{2,\log} = -\frac{A}{2a_{20}B^{16}} = -\frac{8R_c^+}{R_\chi}. \quad (3.28)$$

For the equation of state we have

$$H = \frac{\partial \mathcal{A}}{\partial M} = a_{11} b_1 t^{15/8} F(z) = (B^c)^{-15} M^{15} f(x), \quad (3.29)$$

where $F(z)$ and $f(x)$ are defined in Eq. (1.99). The properties of these two functions are described in Sec. 1.5.3. Using Eqs. (3.25) and (3.26) we can compute the coefficients F_2^∞ and f_2^0 appearing in the expansions of $F(z)$ and of $f(x)$ for $z \rightarrow \infty$ and $x \rightarrow 0$ respectively, cf. Eqs. (1.104) and (1.112). We have

$$F_2^\infty = a_{1,\log}, \quad (3.30)$$

$$f_2^0 = -\frac{1}{2} a_{2,\log}. \quad (3.31)$$

3.4.3 Approximate representations of the equation of state

In spite of the wealth of exact results, there exists no exact expression of the equation of state in the whole (t, H) plane. This problem was addressed in Ref. [210] where parametric representations and the variational

γ	7/4
ν	1
η	1/4
β	1/8
δ	15
ω	2
ω_{NR}	2 (sq), 4 (tr)
$U_0 \equiv A^+/A^-$	1
$U_2 \equiv C^+/C^-$	37.69365201
$R_c^+ \equiv A^+C^+/B^2$	0.31856939
$R_c^- \equiv A^-C^-/B^2$	0.00845154
$R_\chi \equiv Q_1^{-\delta} \equiv C^+B^{\delta-1}/(B^c)^\delta$	6.77828502
$w^2 \equiv C^-/[B^2(f^-)^2]$	0.53152607
$U_\xi \equiv f^+/f^-$	3.16249504
$U_{\xi_{\text{gap}}} \equiv f_{\text{gap}}^+/f_{\text{gap}}^-$	2
$Q^+ \equiv A^+(f^+)^2$	0.15902704
$Q^- \equiv A^-(f^-)^2$	0.015900517
$Q_\xi^+ \equiv f_{\text{gap}}^+/f^+$	1.000402074
$Q_\xi^c \equiv f_{\text{gap}}^c/f^c$	1.0786828
$Q_\xi^- \equiv f_{\text{gap}}^-/f^-$	1.581883299
$Q_2 \equiv (f^c/f^+)^{2-\eta}C^+/C^c$	2.8355305

Table 13: Critical exponents and universal amplitude ratios for the two-dimensional Ising universality class, taken from Refs. [169, 177, 209, 244, 783]. Since the specific heat diverges logarithmically, the specific-heat amplitudes A^\pm are defined by $C_H \approx -A^\pm \log t$. See Sec. 1.3 for the definitions of the other amplitudes. The definition of R_c^\pm and Q^\pm differ from those given in Table 2 because of the absence of α , which is zero in this case. The value of ω_{NR} depends on the lattice that is considered: The reported values refer to the square (sq) and triangular (tr) lattices respectively.

approach presented in Sec. 3.3.2 were used. Specifically, they set $m(\theta) = \theta$,

$$h(\theta) = \theta + \sum_{n=1}^k h_{2n+1} \theta^{2n+1}, \quad (3.32)$$

and determined the k parameters h_3, \dots, h_{2k+1} by requiring the approximate representation to reproduce the $(k-2)$ invariant ratios r_{2n} , $n : 3, \dots, k$, and the large- z behavior of the function $F(z)$, $F(z) \approx F_0^\infty z^\delta$, and to satisfy the global stationarity condition (3.13); see Sec. 3.3.2 for details of the method.

In order to apply the method, good estimates of the coefficients r_{2n} , which parametrize the small-magnetization expansion of the Helmholtz free energy, and of F_0^∞ are needed. The latter constant can be obtained from the results of Table 13 once a precise es-

$g_4^+ \equiv -C_4^+ / [(C^+)^2 (f^+)^2]$	14.697323(20)
r_6	3.67867(7)
r_8	26.041(11)
r_{10}	284.5(2.4)
r_{12}	$4.44(6) \times 10^3$
r_{14}	$8.43(3) \times 10^5$
$R_4^+ \equiv g_4^+ Q^+ / R_c^+$	7.336774(10)
$F_0^\infty \equiv R_\chi (R_4^+)^{1/2-\delta/2}$	$0.592357(6) \times 10^{-5}$
F_1^∞	0.0211(2)
$v_3 \equiv -C_3^- B / (C^-)^2$	33.011(6)
$v_4 \equiv -C_4^- B^2 / (C^-)^3 + 3v_3^2$	48.6(1.2)

Table 14: Universal quantities for the two-dimensional Ising universality class. They have been determined in Refs. [209, 210, 642], by transfer-matrix techniques (g_4^+ , r_6 , r_8 , r_{10}), by using the estimate of g_4^+ and the results of Table 13 (R_4^+ , F_0^∞), by using approximate parametric representations of the equation of state (r_{12} , r_{14} , F_1^∞), and from the analysis of LT expansions (v_3 and v_4). See Sec. 1.3 for definitions of the amplitudes.

timate of the zero-momentum four-point coupling g_4^+ is available, see Eq. (1.105).

In Refs. [209, 210] the zero-momentum four-point coupling g_4^+ and the first coefficients r_{2n} were determined by using transfer-matrix techniques and general RG properties of critical systems, which predicted the scaling behavior for $t > 0$. The estimates of g_4^+ , r_6 , r_8 , and r_{10} obtained in Refs. [209, 210] are reported in Table 14. There, we also report the estimate of F_0^∞ , obtained by using Eq. (1.105), the estimate of the coefficient F_1^∞ , see Eq. (1.104), of r_{12} and r_{14} , obtained in Ref. [210] by using an approximate representation of the equation of state that will be described below, and the estimates of v_3 , v_4 , see Eq. (1.119), obtained in Ref. [642]. In Table 15 we compare the estimates of g_4^+ obtained by various methods. A review of the estimates of the first coefficients r_{2n} can be found in Ref. [210].

We now present the results of Ref. [210] for the equation of state. In Table 16, for $k = 2, 3, 4, 5$, we report the polynomials $h(\theta)$ obtained by using the global stationarity condition (3.13) and the central values of the input parameters F_0^∞ , r_6 , r_8 , r_{10} .

In Fig. 7 we show the scaling function $F(z)$ obtained from $h(\theta)$ for $k = 2, 3, 4, 5$. The convergence is very good, allowing us to determine $F(z)$ for all real $z > 0$ with a relative precision of at least a few per mille (the least precision is found around $z \simeq |z_0| \simeq 2.71$). We recall that the large- z limit corresponds to the critical isotherm $t = 0$, so that positive real values of z describe

k	ρ_k	θ_0^2	$h(\theta)/[\theta(1-\theta^2/\theta_0^2)]$
2	2.01116	1.15278	$1 - 0.208408\theta^2$
3	2.00770	1.15940	$1 - 0.215675\theta^2 - 0.039403\theta^4$
4	2.00770	1.16441	$1 - 0.219388\theta^2 - 0.041791\theta^4 - 0.013488\theta^6$
5	2.00881	1.16951	$1 - 0.222389\theta^2 - 0.043547\theta^4 - 0.014809\theta^6 - 0.007168\theta^8$

Table 16: Polynomial approximations of $h(\theta)$ obtained by using the global stationarity condition for various values of the parameter k , cf. Eq. (3.32). The reported expressions are related to the central values of the input parameters. Results from Ref. [210].

Ref.	Method	g_4^+
[209, 210] 2000	TM+RG	14.697323(20)
[84] 2000	FF	14.6975(1)
[640] 1998	HT	14.694(2)
[162] 1996	HT	14.693(4)
[791] 1996	HT	14.700(17)
[84] 2000	MC	14.69(2)
[471] 1999	MC	14.7(2)
[643] 2000	FT ϵ -exp.	14.7(4)
[616] 2000	FT $d = 2$ exp.	15.4(3)
[505] 1977	FT $d = 2$ exp.	15.5(8)
[107] 1992	d -exp	14.88(17)

Table 15: Estimates of g_4^+ for the two-dimensional Ising universality class. We report the existing results obtained from transfer-matrix techniques combined with RG scaling (TM+RG), the form-factor approach (FF), high-temperature expansions (HT), Monte Carlo simulations (MC), field theory (FT) based on the ϵ -expansion and the fixed-dimension $d = 2$ expansion, and a method based on a dimensional expansion around $d = 0$ (d -exp.).

the HT phase up to $t = 0$. One also obtains rather good estimates of r_{12} and r_{14} , see Table 14, i.e. of two additional coefficients of the expansion (1.101), and of F_1^∞ which is the coefficient of the subleading term in the large- z expansion of $F(z)$, cf. Eq. (1.104). In particular, the result for r_{12} , i.e. $r_{12} = 4.44(6) \times 10^3$, is perfectly consistent with, and much more precise than, the result obtained by using transfer-matrix techniques, see Ref. [210], i.e. $r_{12} = 4.2(7) \times 10^3$.

The convergence of the polynomial representations at the coexistence curve turns out to be slower. For example, the approximate representations give, for $k = 3, 4, 5$, $R_4^+ = 7.396, 7.371, 7.355(5)$, $R_\chi = 7.17, 7.00, 6.90(3)$, $U_2 = 42.4, 40.8, 39.6(3)$ (the reported “errors” are only related to the uncertainty of the corresponding input parameters). These results differ slightly from those appearing in Tables 13 and 14, $R_4^+ = 7.336\dots$,

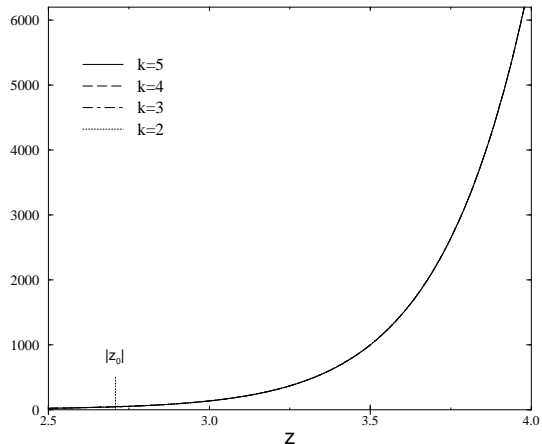


Figure 7: The scaling function $F(z)$ versus z , obtained from the polynomial approximations (3.32) with $k = 2, 3, 4, 5$. Results from Ref. [210].

$R_\chi = 6.778\dots$ and $U_2 = 37.69\dots$, although they appear to monotonically converge to them: the difference is 0.8, 0.3% for R_4^+ , 6, 2% for R_χ , 12, 5% for U_2 for $k = 3, 5$ respectively. The convergence worsens when quantities with more and more derivatives with respect to H are involved in the amplitude ratio, as it can be already seen by comparing the results for R_4^+ and U_2 . However, by estimating the uncertainty on the results from the difference between the last two considered truncations, $k = 4$ and $k = 5$, (the errors induced by the uncertainty on the input parameters are relatively negligible), one obtains reasonable estimates: $R_4^+ = 7.35(2)$, $R_\chi = 6.9(1)$, $U_2 = 39.6(1.5)$.

Fig. 8 shows the scaling function $f(x)$, see Eq. (1.99), obtained by using the polynomial approximations with $k = 2, 3, 4, 5$. The function $f(x)$ is determined with a precision of a few per cent in the whole region. This can be checked by comparing the predictions for f_0^∞ and $b_{f,1}$ that parametrize the behavior for $x \rightarrow \infty$ and $x \rightarrow -1$ respectively, see Eqs. (1.109) and (1.124).

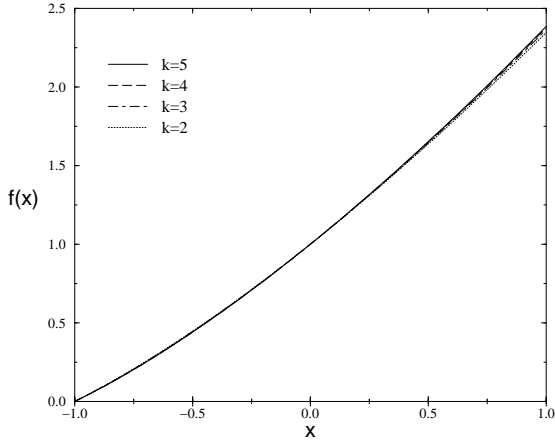


Figure 8: The scaling function $f(x)$ versus x obtained from the polynomial approximations (3.32) with $k = 2, 3, 4, 5$. Results from Ref. [210].

Using the results of Tables 13 and 14, we obtain

$$b_{f,1} = \frac{\beta U_2}{R_\chi} = 0.69511778\dots,$$

$$f_0^\infty = R_\chi^{-1} = 0.14752994\dots$$

This should be compared with the results of the parametric approximations. For $k = 3, 4, 5$ they give: $b_{f,1} = 0.739, 0.729, 0.717$, and $f_0^\infty = 0.139, 0.143, 0.145$. For $k = 5$, the discrepancy is 2% for $x \rightarrow \infty$ and 3% at the coexistence curve. Note that the approximation is also not precise in the large- x region, in spite of the fact that this region corresponds to the HT phase that is described by the function $F(z)$ quite precisely. This is due to the fact that $f(x)$ is normalized at the coexistence curve, i.e. $x = -1$, where our approximation is worse.

3.5 The two-point function of Ising-like systems.

We will review here the results for the two-point function for $H = 0$. Results on the whole (t, H) plane and on the critical isotherm can be found in Refs. [227, 727]. For the two-dimensional case we mention that the large-distance expansion of the two-point function at the critical isotherm, i.e. for $t = 0$ and $H \neq 0$, has been determined using the form-factor approach in Refs. [245, 246].

3.5.1 High-temperature phase

As discussed in Sec. 1.6.1, the two-point correlation function $\tilde{G}(q)$ has the scaling form (1.148). For

HT phase	LT phase
$c_2^+ = -0.7936796064 \times 10^{-3}$	$c_2^- = -0.42989191603$
$c_3^+ = 0.109599108 \times 10^{-4}$	$c_3^- = 0.5256121845$
$c_4^+ = -0.3127446 \times 10^{-6}$	$c_4^- = -0.8154613925$
$c_5^+ = 0.126670 \times 10^{-7}$	$c_5^- = 1.422603449$
$c_6^+ = -0.62997 \times 10^{-9}$	$c_6^- = -2.663354573$
$S_M^+ = 0.999196337056$	$S_M^- = 0.399623590999$

Table 18: Values of c_i^\pm and S_M^\pm for the two-dimensional Ising model. Results from Refs. [177, 735].

$y \equiv q^2 \xi^2 \rightarrow 0$ the function $g^+(y)$ has the expansion (1.150). In Table 17 we report the estimates of the first few coefficients c_n^+ , obtained in various approaches, from the analysis of HT expansions, from the FT fixed-dimension expansion, and from the ϵ -expansion. There, we also report the invariant ratios S_M^+ and S_Z^+ , see Eqs. (1.153) and (1.154), that parametrize the large-distance behavior of $G(x)$.

The coefficients c_n^+ show the pattern

$$|c_n^+| \ll |c_{n-1}^+| \ll \dots \ll |c_2^+| \ll 1 \quad \text{for } n \geq 3. \quad (3.33)$$

Therefore, a few terms of the expansion of $g^+(y)$ in powers of y provide a good approximation in a relatively large region around $y = 0$, larger than $|y| \lesssim 1$. This is in agreement with the theoretical expectation that the singularity of $g^+(y)$ nearest to the origin is the three-particle cut [136, 293]. If this is the case, the convergence radius r_g of the Taylor expansion of $g^+(y)$ is $r_g = 9S_M^+$. Since $S_M^+ \simeq 1$, at least asymptotically we should have

$$c_{n+1}^+ \simeq -\frac{1}{9}c_n^+. \quad (3.34)$$

This behavior was checked explicitly in the large- N limit of the N -vector model [176]. In two dimensions, the critical two-point function can be written in terms of the solutions of a Painlevé differential equation [783] and it can be verified explicitly that $r_g = 9S_M^+$. In Table 18 we report the values of c_i^+ for the two-dimensional Ising model. They are taken from Refs. [177, 735].

Assuming the pattern (3.33) and using Eqs. (1.155) and (1.156), one may estimate S_M^+ and S_Z^+ from the available estimates of c_n^+ [177]. Indeed

$$S_M^+ = 1 + c_2^+ - c_3^+ + \dots \quad (3.35)$$

$$S_Z^+ = 1 - 2c_2^+ + 3c_3^+ + \dots \quad (3.36)$$

where the ellipses indicate contributions that are negligible with respect to c_3^+ . In Ref. [176] the relation (3.35) was confirmed by a direct analysis of the HT series of S_M^+ .

	HT	ϵ -exp	$d = 3$ exp
c_2^+	$-3.576(13) \times 10^{-4}$ [177] $-3.0(2) \times 10^{-4}$ [176] $-5.5(1.5) \times 10^{-4}$, $-7.1(1.5) \times 10^{-4}$ [727]	$-3.3(2) \times 10^{-4}$ [177]	$-4.0(5) \times 10^{-4}$ [176]
c_3^+	$0.87(4) \times 10^{-5}$ [177] $1.0(1) \times 10^{-5}$ [176] $0.5(2) \times 10^{-5}$, $0.9(3) \times 10^{-5}$ [727]	$0.7(1) \times 10^{-5}$ [177]	$1.3(3) \times 10^{-5}$ [176]
c_4^+	$-10^{-6} \lesssim c_4^+ < 0$	$-0.3(1) \times 10^{-6}$ [177]	$-0.6(2) \times 10^{-6}$ [176]
S_M^+	$0.999634(4)$ [177] $0.99975(10)$ [176]	$0.99968(4)$ [177]	$0.99959(6)$ [176]
S_Z^+	$1.000741(7)$ [177]		

Table 17: Estimates of c_i^+ , S_M^+ , and S_Z^+ for the three-dimensional Ising model.

For large y the function $g^+(y)$ follows the Fisher-Langer law (1.151). The coefficients A_n^+ have been computed to three loops in Ref. [136]. In three dimensions one obtains the estimates $A_1^+ \approx 0.92$, $A_2^+ \approx 1.8$, and $A_3^+ \approx -2.7$. In two dimensions the Fisher-Langer law must be modified since $\alpha = 0$. In this case, for large values of y , $g^+(y)$ behaves as

$$g^+(y)^{-1} \approx \frac{A_1^+}{y^{7/8}} \left(1 + \frac{A_2^+}{y^{1/2}} \log y + \frac{A_3^+}{y^{1/2}} \right), \quad (3.37)$$

where the coefficients are [735] $A_1^+ = 0.413840$, $A_2^+ = 0.802998$, and $A_3^+ = 0.395345$. In the years, several parametrizations of the scaling function $g^+(y)$ have been proposed, see, e.g., Refs. [136, 314, 727, 735]. The most successful approximation is the one proposed by Bray [136]. Indeed, by definition, it has the correct large- y behavior (1.151) and has the pattern (3.34) built in. In this approach one fixes the values of the exponents and of the sum $A_2^+ + A_3^+$ and determines an approximation of $g^+(y)$. The accuracy of the results can be evaluated by comparing the predictions for c_n^+ and for the coefficients A_i^+ with those obtained above. Using Bray's parametrization one obtains $A_1^+ \approx 0.918$, $A_2^+ \approx 2.55$, $A_3^+ \approx -3.45$, $c_2^+ \approx -4.2 \times 10^{-4}$, and $c_3^+ \approx 1.0 \times 10^{-5}$. These estimates are in reasonable agreement with those reported in Table 17 and with the ϵ -expansion results.

Bray's approach was also applied in two dimensions. A slightly different approximation that makes use of the high-precision results for A_1^+ , A_2^+ , and A_3^+ reproduces the results of Ref. [735] with a maximum error of 0.03%.

The scaling function $g^+(y)$ has also been determined experimentally, see, e.g., Ref. [98]. A recent study appears in Ref. [236] (older results appear in Ref. [216]). The coefficients c_n^+ are too small to be determined and the experiments are only able to check that the Ornstein-Zernicke behavior $g^+(y) \approx 1+y$ is a very good approximation for $y \lesssim 1$. In Ref. [236] the large- y behavior of $g^+(y)$ was studied. Fixing $A_2^+ + A_3^+ = -0.9$,

the ϵ -expansion result, they found $A_1^+ = 0.915(21)$, $A_2^+ = 2.05(80)$, and $A_3^+ = -2.95(80)$, which reproduce nicely the ϵ -expansion results and the results of Bray's approximation.

3.5.2 Low-temperature phase

In the LT phase, one introduces a scaling function $g^-(y)$ that is defined as $g^+(y)$ in Eq. (1.148). For $y \rightarrow 0$, also $g^-(y)$ admits a regular expansion of the form (1.150) with different coefficients c_n^- . With respect to the HT case, for y small the deviations from the Gaussian behavior are larger. From the ϵ -expansion at two loops, Ref. [227] obtains $c_2^- \approx -2.4 \times 10^{-2}$ and $c_3^- \approx 3.9 \times 10^{-3}$, in reasonable agreement with the series estimates of Ref. [727]: $c_2^- \approx -1.2(6) \times 10^{-2}$ and $c_3^- \approx 7(3) \times 10^{-3}$. Similarly large differences are observed for S_M^- . From the analysis of the LT series (in particular those published in Ref. [49]) one obtains $S_M^- = 0.938(8)$ [177] and $S_M^- = 0.930(6)$ [319], while MC simulations [9, 211] give $S_M^- = 0.941(11)$. Such a different behavior is probably related to the different analytic structure of the two-point function in the LT phase. Indeed, perturbative arguments indicate the presence of a two-particle cut in the LT phase [136, 227, 293]. Thus, the convergence radius of the small- y expansion is expected to be at most $4S_M^-$, and asymptotically $c_{n+1}^- \simeq -0.27 c_n^-$. For large values of y , $g^-(y)$ follows the Fisher-Langer law (1.151) with different coefficients A_n^- . They can be derived from A_n^+ by using Eq. (1.157). These relations have been checked in Ref. [227] to two-loop order in the ϵ -expansion.

The mass spectrum of the model in the LT phase was investigated in Refs. [9, 211, 656] using numerical techniques. Performing simulations of the standard Ising model and of the improved ϕ^4 lattice model (1.7) at $\lambda = 1.10$ (see Sec. 2.3.2), the authors found a state with $M_2 < 2M$, i.e. below the pair-production thresh-

old. They found [211]

$$\frac{M_2}{M} = 1.83(3), \quad (3.38)$$

and argued that this state is not a spurious effect due to the nearby two-particle cut. This second state should appear as a pole in the Fourier transform of the two-point function.

The two-dimensional Ising model shows even larger deviations from Eq. (1.149), as one can see from the values of S_M^- and c_i^- reported in Table 18. Note that in the LT phase of the two-dimensional Ising model the singularity at $k^2 = -1/\xi_{\text{gap}}^2$ of $\tilde{G}(k)$ is not a simple pole, but a branch point²⁵ [783]. As a consequence, the convergence radius of the expansion around $y = 0$ is S_M^- .

For large values of y , $g^-(y)$ behaves according to Eq. (3.37), with different coefficients A_n^- . They are given by [735]: $A_1^- = 2.07993$, $A_2^- = -0.253913$, and $A_3^- = -0.709701$.

4 The XY universality class

4.1 The three-dimensional XY universality class

The three-dimensional XY universality class is characterized by a two-component order parameter and effective short-range interactions with O(2) symmetry. The most interesting representative of this class of universality is the superfluid transition of ^4He along the λ -line $T_\lambda(P)$. It provides an exceptional opportunity for a very accurate experimental test of the RG predictions, because of the weakness of the singularity in the compressibility of the fluid, of the purity of the samples, and of the possibility of performing the experiments in a microgravity environment, for instance on the Space Shuttle as the experiment reported in Ref. [513], thereby achieving a significant reduction of the gravity-induced broadening of the transition. Because of these favorable conditions, the specific heat of liquid helium was measured to within a few nK from the λ -transition, i.e. very deep in the critical region, where the corrections to the expected power-law behavior should be small. The experimental LT data for the specific heat were analyzed by assuming for $t \equiv (T - T_c)/T_c \rightarrow 0^-$ the RG behavior

$$C_H(t) = A|t|^{-\alpha} (1 + C|t|^\Delta + Dt) + B. \quad (4.1)$$

²⁵In the particle interpretation of Ref. [783], this is due to the fact that the lowest propagating state in the LT phase is a two-particle state.

Using $\Delta = 1/2$ the estimate $\alpha = -0.01056(38)$ was obtained.²⁶ This result represents a challenge for theorists. Only recently the theoretical estimates have reached a comparable accuracy.

The XY model also describes the critical behavior of a Heisenberg ferromagnet with easy-plane anisotropy, so that the order parameter has effectively only two components. The model is also of interest in two dimensions. Planar ferromagnets are realized by layered compounds such as K_2CuF_4 [407] and Rb_2CrCl_4 [420] which effectively behave as two-dimensional systems. The crossover from two-dimensional to three-dimensional behavior has been observed in CoCl_2 intercalated in graphite [769], below the Kosterlitz-Thouless temperature.

4.2 The critical exponents

In Table 19 we report the most recent experimental and theoretical estimates of the critical exponents. The table should give an overview of the state of the art for the results obtained by the experiments and by the various theoretical approaches.

Accurate results for the critical exponents have been obtained by combining MC simulations based on FSS techniques and HT expansions for improved Hamiltonians [171, 178, 391]. On the one hand, one exploits the effectiveness of MC based on FSS to determine the critical temperature and the parameters of the improved Hamiltonians [171, 391]. On the other hand, using this information, one exploits the effectiveness of IHT to determine the critical exponents [171, 178], especially when a precise estimate of β_c is available. Two improved Hamiltonians were considered in Ref. [171], the lattice ϕ^4 model (1.7) for $\lambda^* = 2.07$, and the dynamically dilute XY model (2.41) (ddXY) for $D^* = 1.02$, cf. Sec. 2.3.2. An accurate MC study [171] employing FSS techniques provided estimates of λ^* and D^* , of the inverse critical temperature β_c for several values of λ and D , and of course estimates of the critical exponents (see Table 19). Using the linked cluster expansion technique, the HT expansions of χ and $\mu_2 = \sum_x |x|^2 G(x)$ were computed to 20th order for these two Hamiltonians. The analyses were performed by using the estimates of λ^* , D^* , and β_c obtained from the MC simulations. The very accurate results that were obtained are denoted by MC+IHT in Table 19. The results obtained using the two lattice models were

²⁶Ref. [513] reported $\alpha = -0.01285(38)$ and $A^+/A^- = 1.054(1)$. But, as mentioned in footnote [15] of Ref. [514], the original analysis was slightly in error. Ref. [514] reports the new estimates $\alpha = -0.01056$ and $A^+/A^- = 1.0442$. The error reported here is a private communication of J. A. Lipa, quoted in Ref. [171].

Ref.	info	γ	ν	η	α	ω
[513, 514] 1996	experiment ${}^4\text{He}$		0.67019(13)*		-0.01056(38)	
[344] 1993	experiment ${}^4\text{He}$		0.6705(6)		-0.0115(18)*	
[720] 1992	experiment ${}^4\text{He}$		0.6708(4)		-0.0124(12)*	
[699] 1984	experiment ${}^4\text{He}$		0.6717(4)		-0.0151(12)	
[512] 1983	experiment ${}^4\text{He}$		0.6709(9)*		-0.0127(26)	
[171] 2000	MC+IHT, ϕ^4 , ddXY	1.3177(5)	0.67155(27)	0.0380(4)	-0.0146(8)*	
[178] 2000	IHT, ϕ^4	1.3179(11)	0.67166(55)	0.0381(3)	-0.0150(17)*	
[164, 166] 1997	HT, XY sc	1.325(3)	0.675(2)	0.037(7)*	-0.014(9)	
[164, 166] 1997	HT, XY bcc	1.322(3)	0.674(2)	0.039(7)*	-0.022(6)	
[287] 1973	HT XY, easy-plane	1.318(10)	0.670(6)	0.04(1)*	-0.02(3)*	
[171] 2000	MC FSS, ϕ^4 , ddXY	1.3177(10)*	0.6716(5)	0.0380(5)	-0.0148(15)*	0.795(9)
[391] 1999	MC FSS, ϕ^4	1.3190(24)*	0.6723(11)	0.0381(4)	-0.0169(33)*	0.79(2)
[493] 1999	MC FSS, easy-plane	1.315(12)*	0.6693(58)	0.035(5)	-0.008(17)*	
[77] 1996	MC FSS, XY	1.316(3)*	0.6721(13)	0.0424(25)	-0.0163(39)*	
[690] 1995	MC FSS, XY		0.6724(17)		-0.017(5)*	
[347] 1994	MC FSS, AF Potts	1.310(10)*	0.664(4)	0.027(9)	-0.008(12)*	
[346] 1993	MC FSS, XY	1.307(14)*	0.662(7)	0.026(6)	-0.014(21)*	
[430] 1990	MC FSS, S, XY	1.316(5)	0.670(2)	0.036(14)*	-0.010(6)*	
[359] 1998	FT $d = 3$ exp	1.3169(20)	0.6703(15)	0.0354(25)	-0.011(4)	0.789(11)
[435] 1999	FT $d = 3$ exp	1.3164(8)	0.6704(7)	0.0349(8)	-0.0112(21)	0.784(3)
[584] 1991	FT $d = 3$ exp	1.3178(10){28}	0.6715(7){17}	0.0377(6){7}	-0.0145(21){51}	
[505] 1977	FT $d = 3$ exp	1.3160(25)	0.669(2)	0.033(4)	-0.007(6)	0.780(27)
[359] 1998	FT ϵ -exp	1.3110(70)	0.6680(35)	0.0380(50)	-0.004(11)	0.802(18)
[595] 1984	SFM	1.31(2)	0.672(15)	0.043(7)	-0.016(45)*	0.85(7)
[113] 1999	CRG	1.299	0.666	0.049	+0.002	
[729] 1994	CRG	1.371	0.700	0.042	-0.100	

Table 19: Estimates of the critical exponents for the three-dimensional XY universality class. We indicate with an asterisk (*) the estimates we obtained by using the hyperscaling relation $2 - \alpha = 3\nu$ or the scaling relation $\gamma = (2 - \eta)\nu$. When the error was not reported by the authors, we used the independent-error formula to estimate it.

in very good agreement, confirming the error estimates. Note the significant increase in precision with respect to earlier works, that confirms the claim that the systematic error due to confluent singularities is largely reduced when analyzing IHT expansions. The critical exponent α was derived by using the hyperscaling relation $\alpha = 2 - 3\nu$, obtaining the accurate estimate $\alpha = -0.0146(8)$ [171]. This result is not consistent with the experimental estimate reported in Refs. [513, 514]. It is not clear whether this disagreement is significant, or it is due to an underestimate of the experimental and/or theoretical errors. This discrepancy calls for further theoretical and experimental investigations. A new generation of experiments in microgravity environment that is currently in preparation [610] should clarify the issue from the experimental side.

The HT results of Refs. [164, 166] were obtained by analyzing 21st-order HT expansions for the standard XY model on the simple (sc) and body-centered (bcc) cubic lattices. To take into account the subleading corrections, they used biased approximants that make use of the MC estimate of β_c and of the FT result for Δ .

Essentially all MC results reported in Table 19 have been obtained by using FSS techniques. Only Ref. [430] determines the critical exponents from the behavior of

infinite-volume quantities near the critical point (“S” in the column info in Table 19). Refs. [77, 346, 430, 690] present results for the standard XY model, Ref. [493] for a classical ferromagnetic XXZ model with no coupling for s_z^2 (this is the model which in the old literature was called XY model; in Table 19 we refer to it as “easy-plane”), and Ref. [347] for the three-state antiferromagnetic Potts model on a simple cubic lattice (AF Potts) which has been conjectured [85] to be in the XY universality class.²⁷

Refs. [359, 435, 505, 584] report FT results obtained by analyzing the fixed-dimension expansion. The perturbative series of the β -function and of the exponents are known to six-loop [70] and seven-loop order [584] respectively. In Refs. [359, 505] the resummation was performed by using the method presented in Sec. 2.4.3 based on a Borel transform and a conformal mapping

²⁷ Actually, the authors of Ref. [85] argue, using RG arguments, that the effective Hamiltonian of the three- and four-state AF Potts models on a simple cubic lattice are respectively in the same universality class of the two- and three-component ϕ^4 theory with cubic anisotropy. As we shall also discuss in Sec. 8.3, in the two-component case the stable fixed point of the cubic Hamiltonian is the $O(2)$ symmetric one. Therefore, the continuous transition of the three-state AF Potts model belongs to the XY universality class.

that makes use of the large-order behavior of the series. Ref. [435] (see also Refs. [480]) employed a resummation method based on a variational technique: as in the Ising case, the errors seem to be rather optimistic, especially for ω . The analysis of Ref. [584] allowed for a more general nonanalytic behavior of the β -function. In Table 6, we quote two errors for the results of Ref. [584]: the first one (in parentheses) is the resummation error, and the second one (in braces) takes into account the uncertainty of g^* , which is estimated to be $\sim 1\%$. To estimate the second error we used the results of Ref. [359] where the dependence of the exponents on g^* is given. Consistent results are also obtained from the analysis of Ref. [359] of the $O(\epsilon^5)$ series computed in the framework of the ϵ -expansion [223, 482]. Similarly to the Ising case, the results obtained by approximately solving continuous RG (CRG) equations are much more imprecise.

In conclusion, the agreement among the theoretical calculations is overall very good. But an improvement of the precision would be very useful, in order to perform a more stringent comparison with the experiments, and partially clarify the apparent discrepancy between the most precise experimental and theoretical results.

4.3 The critical equation of state

In this section we consider the critical equation of state of the three-dimensional XY universality class. Such an equation is of direct experimental interest for magnetic systems, but cannot be observed in the λ -transition in ^4He . Indeed, in this case the order parameter is related to the complex quantum amplitude of helium atoms. Therefore, the “magnetic” field H does not correspond to an experimentally accessible external field. Only universal amplitude ratios of quantities formally defined at zero external field, such as $U_0 \equiv A^+/A^-$, are here of physical relevance.

4.3.1 Small-magnetization expansion of the free energy in the HT phase.

In Table 20 we report a summary of the available results for the zero-momentum four-point coupling g_4^+ , cf. Eq. (1.63), and for the coefficients r_6 , r_8 , and r_{10} that parametrize the small-magnetization expansion of the Helmholtz free energy, cf. Eq. (1.101).

The results of Refs. [171, 179] were obtained by analyzing HT series for two improved Hamiltonians. The slight difference in the results for g_4^+ of Refs. [171] and [179] is essentially due to a different method of analysis. The result of Ref. [171] should be more reliable. Refs. [165, 640, 663] considered the HT expansion

	HT	$d=3$ exp.	ϵ -exp.
g_4^+	21.14(6) [171]	21.16(5) [359]	21.5(4) [640, 643]
	21.05(6) [179]	21.11 [584]	
	21.28(9) [165]	21.20(6) [505]	
	21.34(17) [640]		
r_6	1.950(15) [171]	1.967 [708]	1.969(12) [641, 643]
	1.951(14) [179]		
	2.2(6) [663]		
r_8	1.44(10) [171]	1.641 [708]	2.1(9) [641, 643]
	1.36(9) [179]		
r_{10}	-13(7) [171]		

Table 20: Estimates of g_4^+ , $r_6 = g_6^+/(g_4^+)^2$, $r_8 = g_8^+/(g_4^+)^3$ and $r_{10} = g_{10}^+/(g_4^+)^4$. In the case of r_{10} we also mention the estimate $r_{10} = -10(1)$ obtained by studying the equation of state [171], see Sec. 4.3.2.

of the standard XY model. In the fixed-dimension FT approach, g_4^+ is obtained from the zero of the corresponding Callan-Symanzik β -function. Note the perfect agreement between the HT and the FT estimates. In the same framework $g_6^+ = r_6(g_4^+)^2$ and $g_8^+ = r_8(g_4^+)^3$ were estimated from the analysis of the corresponding four- and three-loop series respectively [708]. The authors of Ref. [708] argued that the uncertainty on their estimate of g_6^+ is approximately 0.3%, while they considered their value for g_8^+ much less accurate. The ϵ -expansion estimates were obtained from constrained analyses of the $O(\epsilon^4)$ series of g_4^+ and of the $O(\epsilon^3)$ series of r_{2j} [640, 641, 643].

4.3.2 Approximate representations of the equation of state.

The results of Sec. 4.3.1 can be used to determine approximate parametric representations of the critical equation of state. In Refs. [171, 179] the parametric representation (1.133) was used, approximating the functions $m(\theta)$ and $h(\theta)$ by polynomials, and requiring $h(\theta) \sim (\theta - \theta_0)^2$ at the coexistence curve. As discussed in Sec. 1.5.6, such a representation gives the correct leading singular behavior at the coexistence curve, but fails to reproduce the logarithmic singularities discussed in Sec. 1.5.5, cf. Eq. (1.131).

Two polynomial schemes were considered: the scheme (A) defined by

$$m(\theta) = \theta \left(1 + \sum_{i=1}^n c_i \theta^{2i} \right), \quad (4.2)$$

$$h(\theta) = \theta (1 - \theta^2/\theta_0^2)^2,$$

and the scheme (B) defined by

$$m(\theta) = \theta, \quad (4.3)$$

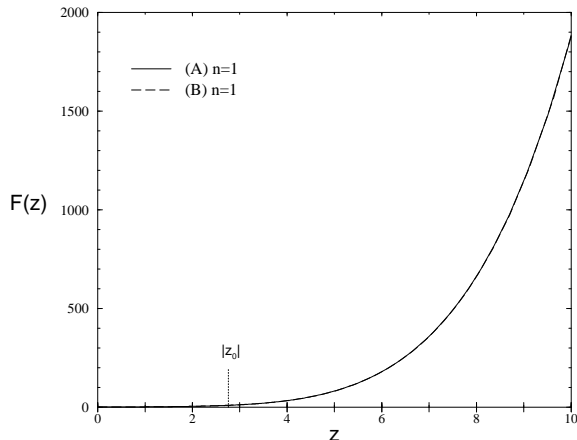


Figure 9: The scaling function $F(z)$ for the XY model. Results from Ref. [171].

$$h(\theta) = \theta \left(1 - \theta^2/\theta_0^2\right)^2 \left(1 + \sum_{i=1}^n c_i \theta^{2i}\right).$$

In both schemes θ_0 and the n coefficients c_i are determined by using the $n + 1$ values of r_{2j} , i.e. r_6, \dots, r_{6+2n} . Notice that in this case a variational approach analogous to that presented in Sec. 3.3.2 cannot be employed. Indeed, for the class of functions that are considered here—with a double zero at θ_0 —there is no globally valid stationary solution.

By using the few known coefficients r_{2j} , see Table 20, and parametric representations, Ref. [171] obtained a satisfactory determination of the scaling function $F(z)$ in the whole real positive axis, describing the HT phase up to $t = 0$. In Fig. 9 we show the curves obtained by using the schemes (A) and (B) with $n = 1$, which use the coefficients r_6 and r_8 . The two approximations of $F(z)$ are practically indistinguishable in Fig. 9. The $n = 1$ polynomial representations are less precise at the coexistence curve. This is evident in Fig. 10, where we show the results for $f(x)$ obtained in Ref. [171]. Indeed, there are sizeable differences between the approximations of $f(x)$ given by schemes (A) and (B) for $n = 1$, especially in the region $x < 0$ corresponding to $t < 0$ (i.e. the region which is not described by real values of z).

A more precise determination of the equation of state near the coexistence curve was achieved by numerical MC simulations of the standard XY model [276]. The MC data are very well interpolated in a relatively large region of values of x around $x = -1$ by a power-law behavior of the type (1.129), taking into account the first few terms of the expansion. This fact does not nec-

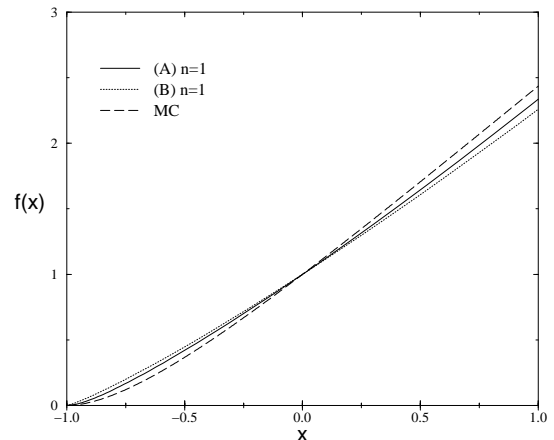


Figure 10: The scaling function $f(x)$ for the XY model. We report the results of Ref. [171] for scheme (A) and (B) and the MC results of Ref. [276].

essarily rule out the presence of the logarithms found in the $1/N$ expansion, cf. Eq. (1.131). Since they are associated with the next-next-to-leading term of the expansion, i.e. $O(v^2)$ with respect to the leading term, in a numerical work it would be very difficult to distinguish them from simple power terms. In Fig. 10 we also plot the curve used in Ref. [276] to fit the MC data.

In Table 21 we report results for some universal amplitude ratios that can be derived from the equation of state. As already mentioned, the most interesting quantity is the specific-heat amplitude ratio $U_0 \equiv A^+/A^-$, because its estimate can be compared with the accurate experimental results for the superfluid transition in ^4He . We note that most of the theoretical and experimental estimates of U_0 reported in Table 21 are strongly correlated with the value of α considered. In particular, the difference between the experimental estimate $U_0 = 1.0442$ of Refs. [513, 514] and the theoretical result $U_0 = 1.062(4)$ of Ref. [171] is a direct consequence of the difference in the values of α used in the respective analyses, i.e. $\alpha = -0.1056(38)$ in the analysis of the experimental data of Refs. [513, 514], and $\alpha = -0.0146(8)$ in the theoretical study of the equation of state of Ref. [171]. We mention also that the IHT-PR result of Ref. [179] and the FT result of Ref. [500] were obtained using $\alpha = -0.01285(38)$, while the FT analysis of Ref. [486] used the value $\alpha = -0.1056$. In all cases the correlation between the estimate of U_0 and that of α is well described by the phenomenological relation $U_0 \approx 1 - 4\alpha$ [409], which was derived in the framework of the ϵ -expansion.

For the sake of completeness, in Table 21 we also re-

port the available estimates of the universal ratio R_ξ^T . We mention that Refs. [159, 684] present two-loop FT calculations of R_ξ^T in the framework of the minimal-subtraction scheme without ϵ -expansion. But it is not clear how to obtain an estimate of R_ξ^T since the two-loop contribution is comparable to the one-loop one, and therefore further terms or an appropriate resummation are required to get a reliable estimate.

4.4 The two-point function in the high-temperature phase

The two-point function of the order-parameter in the HT phase has been studied in Refs. [171, 176] by means of HT expansions and FT calculations. Its small-momentum scaling behavior is qualitatively similar to the Ising case. Indeed, the coefficients c_i^+ of the small-momentum expansion of the scaling function $g^+(y)$, see Eq. (1.150), satisfy the relations (3.33). Their best estimates are [171]

$$\begin{aligned} c_2^+ &= -3.99(4) \times 10^{-4}, \\ c_3^+ &= 0.09(1) \times 10^{-4}, \\ |c_4^+| &< 10^{-6}. \end{aligned} \quad (4.4)$$

Using Eqs. (3.35) and (3.36), one also obtains

$$\begin{aligned} S_M^+ &= 0.999592(6), \\ S_Z^+ &= 1.000825(15). \end{aligned} \quad (4.5)$$

Other results can be found in Ref. [176]. They are obtained by using HT methods in the standard XY model and FT methods, such as the ϵ and $d = 3$ fixed-dimension expansions.

For large values of y , the function $g^+(y)$ follows the Fisher-Langer law reported in Eq. (1.151). The coefficients A_1^+ , A_2^+ and A_3^+ have been computed in the ϵ expansion to three loops [136], obtaining $A_1^+ \approx 0.92$, $A_2^+ \approx 1.8$, and $A_3^+ \approx -2.7$. Bray's phenomenological function [136] provides the estimates [171] $A_1^+ \approx 0.915$, $A_2^+ \approx -24.7$, $A_3^+ \approx 23.8$, $c_2^+ \approx -4.4 \cdot 10^{-4}$, $c_3^+ \approx 1.1 \cdot 10^{-5}$, $c_4^+ \approx -5 \cdot 10^{-7}$. The results for A_1^+ , c_2^+ , c_3^+ , and c_4^+ are in good agreement with the above-reported estimates, while A_2^+ and A_3^+ differ significantly from the ϵ -expansion results. Note, however, that, since $|\alpha|$ is very small, the relevant quantity in the Fisher-Langer formula is the sum $A_2^+ + A_3^+$. In other words, the function does not change significantly if one uses the ϵ -expansion results or the approximations determined using Bray's method. Therefore, Bray's approximation provides a good interpolation both in the large- y and small- y regions.

4.5 The two-dimensional XY universality class.

4.5.1 The Kosterlitz-Thouless critical behavior

The two-dimensional XY universality class is characterized by the Kosterlitz-Thouless (KT) critical behavior [490, 491] (see, e.g., Refs. [424, 792] for reviews on this issue). According to the KT scenario the free energy has an essential singularity at T_c and the correlation length diverges as

$$\xi \sim \exp(b/t^\sigma) \quad (4.6)$$

for $t \equiv T/T_c - 1 \rightarrow 0^+$. The value of the exponent is $\sigma = 1/2$ and b is a nonuniversal positive constant. At the critical temperature, the asymptotic behavior for $r \rightarrow \infty$ of the two-point correlation function should be

$$G(r)_{\text{crit}} \sim \frac{(\ln r)^{2\theta}}{r^\eta} \left[1 + O\left(\frac{\ln \ln r}{\ln r}\right) \right], \quad (4.7)$$

with $\eta = 1/4$ and $\theta = 1/16$. Near criticality, i.e., for $0 < t \ll 1$, the behavior of the magnetic susceptibility can be deduced from Eq. (4.7):

$$\begin{aligned} \chi &\sim \int_0^\xi dr G(r)_{\text{crit}} \\ &\sim \xi^{2-\eta} (\ln \xi)^{2\theta} \left[1 + O\left(\frac{\ln \ln \xi}{\ln \xi}\right) \right] \\ &\sim \xi^{2-\eta} t^{-2\sigma\theta} [1 + O(t^\sigma \ln t)]. \end{aligned} \quad (4.8)$$

In addition, the 2- d XY model is characterized by a line of critical points, starting from T_c and extending to $T = 0$, with $\eta \sim T$ for $T \rightarrow 0$. At criticality the 2- d XY model corresponds to a conformal field theory with $c = 1$, see, e.g., Ref. [424].

Transitions of KT type occur in a number of effectively two-dimensional systems with $O(2)$ symmetry, such as thin films of superfluid helium and of easy-plane magnetic materials. Moreover, the KT critical scenario describes roughening transitions, i.e. phase transitions from a smooth to a rough surface, which are for example observed in the equilibrium structure of crystal interfaces. For a general introduction to roughening, see, e.g., Refs. [4, 328, 424, 740]. At a roughening transition, the large-scale interface behavior changes from being smooth at low temperature to being rough at high temperature. This qualitative picture can be made quantitative, for example by looking at the dependence of the interfacial width on the size L of the interface: in the smooth phase the interfacial width remains finite when $L \rightarrow \infty$, while it diverges logarithmically in the rough phase.

	IHT-PR	HT	MC	$d=3$ exp.	ϵ -exp.	experiments
U_0	1.062(4) [171] 1.055(3) [179]			1.056(4) [500] 1.045 [486]	1.029(13) [116]	1.0442 [513, 514] 1.067(3) [699] 1.058(4) [512] 1.088(7) [725]
R_ξ^+	0.355(3) [171]	0.361(4) [166]		0.3606(20) [55, 117]	0.36 [115]	
R_c	0.127(6) [171]			0.123(3) [715] 0.130 [486]	0.106	
R_χ	1.35(7) [171]		1.356(4) [276]		1.407	
R_A	7.5(2) [171]					
F_0^∞	0.0302(3) [171]					
c_f	4(2) [171]		2.85(7) [276]			
R_ξ^T					1.0(2) [115, 409, 655]	0.85(2) [699]

Table 21: Estimates of universal amplitude ratios obtained using different approaches. The ϵ -expansion estimates of R_c and R_χ have been obtained by setting $\epsilon = 1$ in the $O(\epsilon^2)$ series calculated in Refs. [2, 3, 18].

4.5.2 The roughening transition and Solid-on-Solid models

The interfacial thermodynamic behavior can be modeled by solid-on-solid (SOS) models defined on two-dimensional lattices. The partition function of a SOS model is

$$Z = \sum_{\{h\}} \exp \left[- \sum_{\langle x,y \rangle} V(h_x - h_y) \right] \quad (4.9)$$

where the Hamiltonian is a sum over nearest-neighbor pairs. The variable h_x can be interpreted as heights with respect to a certain base. The summation is over equivalence classes of height configurations $\{h\}$, defined by identifying two configurations that differ only by a global vertical shift. Several realizations of SOS model have been proposed, see, e.g., Refs. [4, 388, 740]. We mention:

- (i) The absolute-value SOS model (ASOS). It can be considered as the SOS approximation of a lattice plane interface of an Ising model on a simple cubic lattice, and it is defined by the function

$$V_{\text{ASOS}} = k|h_x - h_y|, \quad (4.10)$$

where h_x takes integer values. For finite positive k the Hamiltonian suppresses configurations with large differences between nearest-neighbor sites. If k is below a certain critical value, the surface becomes rough, and the surface thickness diverges when the size of the system goes to infinite.

- (ii) The body-centered SOS model (BCSOS). It represents a SOS approximation of an interface in an Ising model on a bcc lattice [739].
- (iii) The discrete Gaussian (DG) model defined by

$$V_{\text{ASOS}} = k(h_x - h_y)^2, \quad (4.11)$$

where h_x takes integer values. It is dual to the Villain formulation of the XY model [679].

- (iv) The dual of the standard XY model,

$$H_{XY} = -\beta \sum_{\langle x,y \rangle} \vec{s}_x \cdot \vec{s}_y, \quad (4.12)$$

can be considered as a SOS model with partition function

$$Z = \sum_{\{h\}} \prod_{\langle x,y \rangle} I_{|h_x - h_y|}(\beta), \quad (4.13)$$

where h_x are integer variables and I_n are modified Bessel functions.

The BCSOS model is the only one that has been proved to undergo a KT transition [739]. It can be transformed into the F model [739], which is a special six-vertex model that can be solved exactly by using transfer-matrix methods [91, 510, 511]. The transitions in the other models, including the standard XY model, are conjectured to be of the KT type as well, and numerical evidences support this fact.

A much studied prototype of roughening is the Ising interface transition, which occurs in the LT phase of the three-dimensional Ising model, i.e. for $T_r < T_c$ where T_c is the bulk critical temperature [387, 758]. The SOS approximation amounts to neglecting overhangs of the Ising interface and bubbles in the two phases separated by the interface. Lattice studies of the interfacial properties use the fact that an interface of size L can be realized on a $L^2 \times T$ lattice by imposing antiperiodic boundary conditions along T .

Roughening transitions occur also in the lattice formulation of four-dimensional nonabelian gauge theories [773], and in particular of QCD that is the theory of strong interactions, whose critical limit for $g_0^2 \equiv T \rightarrow 0$ realizes the continuum theory. See, e.g., Refs. [233, 568]

for an introduction to lattice gauge theories. An important issue concerning nonabelian gauge theories is related to confinement. In the absence of quarks, the question of confinement is related to the behavior of Wilson loops in the limit of large area. Confinement requires a nonzero string tension σ . In the HT region one may systematically expand σ in powers of $1/T$. In particular the leading term is $\sigma \sim \ln T$. Theoretical arguments show that, independently of the gauge group, the string tension is affected by a weak singularity associated with the roughening transition [263, 393, 426, 528, 529, 583, 621] (see also Ref. [424]). However the roughening transition does not imply deconfinement, and the string tension should not vanish in weak coupling region, and therefore in the continuum limit. The change is essentially related to the fact that at strong coupling the contributions to the string tension come from smooth surfaces, while in the weak coupling region the relevant surfaces become rough.

4.5.3 Numerical studies

Numerical studies of the XY model based on MC simulation techniques and HT expansions support the KT behavior [72, 122, 386, 388, 431, 432, 463, 469, 612, 689]. FSS investigations at criticality are required to be very precise in order to pinpoint the logarithm in the two-point Green's function. On the other hand, if this logarithmic correction is neglected, the precise check of the prediction $\eta = 1/4$ at β_c may be quite hard. The relevance of such logarithmic corrections and some of the consequences of neglecting them have been examined in Refs. [431, 463].

HT expansion calculations [160, 161, 174] supports the KT mechanism as well. In Ref. [174] the two-point correlation function was calculated on the square, triangular and honeycomb lattices respectively up to 21th, 15th and 30th order. The results from all lattices considered were consistent with universality and the KT exponential approach to criticality, characterized by an exponent $\sigma = 1/2$. The value $\sigma = 1/2$ has been confirmed within an uncertainty of few per cent. The prediction $\eta = 1/4$ has been also substantially verified.

On the other hand, the value of θ predicted by the KT theory, i.e. $\theta = 1/16$, has not yet got a direct robust numerical confirmation. Some discrepancies have been noted in the results of MC simulations [431, 463] and HT expansions [174]. But one should be cautious in considering these results as a real inconsistency, since it is difficult to exclude a substantial underestimate of the error.

The most accurate verification of the KT critical pattern was achieved in Refs. [386, 387], by numerically

matching the RG trajectory of the dual of the XY model with that of the BCSOS model, which has been proven to exhibit a KT transition. The advantage of this strategy is that such a matching occurs much earlier than the onset of the asymptotic regime, where numerical simulations can provide quite accurate results. Indeed, the authors argued that their method is subject to corrections due to irrelevant operators, which are of order $L^{-\omega}$ with $\omega = 2$, while standard MC techniques to verify the asymptotic behaviors predicted by the KT mechanism are affected by logarithmic corrections. In Refs. [386, 387] the same method was applied to the ASOS model, the DG model and the interface in a simple-cubic Ising model to demonstrate that they all belong to the same universality class, and therefore undergo a KT transition.

Finally, we mention the results available for the zero-momentum four-point coupling g_4^+ , defined in Eq. (1.63), and the small-magnetization expansion of the Helmholtz free energy. In Table 22 we review the estimates of g_4^+ obtained by various approaches: high-temperature series (HT), Monte Carlo simulations (MC), field-theoretical methods (FT), and the form-factor approach (FF). According to the authors of Ref. [84], the FF estimate should be overestimated probably by 2–4%. The first few coefficients r_{2j} of the small-magnetization expansion of the scaling equation of state, cf. Eq. (1.101), were estimated in Ref. [643] by a constrained analysis of their $O(\epsilon^3)$ series, obtaining $r_6 = 3.53(4)$ and $r_8 \approx 23$.

We also mention that results concerning the small-momentum behavior of the two-point function in the HT phase can be found in Ref. [174].

5 Critical behavior of N -vector models with $N \geq 3$

5.1 Three-dimensional models

Among the three-dimensional N -vector models with $N \geq 3$, the physically most relevant ones are those with $N = 3$ and $N = 4$. Indeed, the $N = 3$ case describes many transitions in isotropic magnetic materials. The $N = 4$ is relevant for high-energy physics because it describes the finite-temperature transition in the strong-interaction theory, i.e. quantum chromodynamics (QCD), with two light degenerate flavored quarks. In this section we mainly review the results concerning the $N = 3$ and $N = 4$ universality classes, in Sec. 5.1.1 and 5.1.2 respectively.

For larger values of N , estimates of the critical exponents can be found in Refs. [164] and [46]. They are obtained by analyzing 21st-order expansions for the N -

HT	MC	FT $d = 2$ exp	FT ϵ -exp	FF
13.65(8) [640]	13.71(18) [84]	13.57(23) [616]	13.7(2) [643]	13.97 [84]
13.72(16) [162]	13.3(3) [470]			

Table 22: Estimates of g_4^+ for the two-dimensional XY universality class.

vector model, and the field-theoretic six-loop series at fixed dimension $d = 3$.

In the large- N limit one can obtain analytic results based on a $1/N$ expansion. These results are very useful to obtain a qualitative understanding of the critical behavior, but, from a quantitative point of view, they become predictive only for rather large values of N , $N \gtrsim 10$ say. We do not further discuss this approach, but we signal the recent excellent review of Zinn-Justin [794], where many results and references can be found.

We mention that the critical equation of state for the N -vector models has been computed to $O(\epsilon^2)$ in the framework of the ϵ -expansion [146], and to $O(1/N)$ in the framework of the $1/N$ expansion [145].

5.1.1 The Heisenberg universality class

The Heisenberg universality class corresponds to three-component models with $O(3)$ symmetry. It describes the critical behavior of isotropic magnets. The Curie transition in isotropic ferromagnets such as Ni and EuO, and the transitions of antiferromagnets such as RbMnF_3 at the Néel point. Experimental results are reported for example in Ref. [655, 792] and references therein. Typical experimental values of the critical exponents are [792] in the ranges [1.36, 1.42] for γ , [0.700, 0.725] for ν , $[-0.07, -0.14]$ for α . Uncertainties in the analysis, as well as in the precise treatment of weak dipolar interaction effects and of other effects that smear the transition, are the main experimental problems. We also mention that the isotropic model for such transition neglects the presence of cubic anisotropies due to the lattice structure, which, as we shall see in the Sec. 8.3, are relevant in the RG sense.

In Table 23 we report the theoretical results for the critical exponents of the $O(3)$ symmetric model. The global agreement is satisfactory. Most MC results concern the standard Heisenberg model and were obtained using FSS techniques [77, 151, 221, 255, 412, 413, 609, 632]. The results of Ref. [385] were obtained simulating the improved ϕ^4 model, which has been already mentioned in Sec. 2.3.2. Ref. [181] presents results for an isotropic ferromagnets with double-exchange interaction, whose Hamiltonian is given by [35]

$$\mathcal{H} = -\beta \sum_{\langle i,j \rangle} \sqrt{1 + s_i \cdot s_j}. \quad (5.1)$$

The result of Ref. [609] was obtained by transfer-matrix techniques. We only note the quite anomalous result of Ref. [151], which is further discussed in Refs. [152, 414]. Ref. [481] presents an analysis of the FT expansion in powers of $\epsilon \equiv d - 2$ in the framework of the nonlinear σ model, which is known to $O(\epsilon^4)$ [114, 404, 405].

Finally, we mention that the critical equation of state for $N = 3$ was studied in Ref. [112] by analyzing approximate solutions of RG equations (CRG). Some theoretical results for the universal amplitude ratios were reported in Ref. [655].

5.1.2 The $O(4)$ universality class

The three-dimensional $O(4)$ model is of importance for the theory of strong interactions, quantum chromodynamics, with two light-quark flavors at finite temperature. In this transition the order parameter is the quark condensate $\langle \bar{\psi}\psi \rangle$, and the quark mass plays the role of external field. If the finite-temperature transition is continuous, it should belong to the same universality class of the three-dimensional $O(4)$ model [647, 657, 770]. Finite-temperature simulations of lattice QCD [22, 48, 427] support a continuous phase transition. They also find substantial agreement with the three-dimensional $O(4)$ critical behavior.

In Table 24 we report the theoretical results for the critical exponents of the $O(4)$ symmetric model. The critical equation of state for $N = 4$ was studied by MC simulations in Refs. [277, 734].

5.2 Two-dimensional systems

Two-dimensional systems with $N \geq 3$ are somewhat special since in this case there is no phase transition at finite values of T . The correlation length is always finite and a critical behavior is observed only when $T \rightarrow 0$.²⁸

For $T \rightarrow 0$ the behavior of long-distance quantities is predicted by the perturbative RG applied to the N -vector model. One finds that these systems are asymptotically

²⁸One can rigorously prove that systems with a vector order parameter do not have a magnetized LT phase in two dimensions [562]. This does not exclude a LT phase with algebraically decaying correlation functions, as it happens for $N = 2$. However, numerical and theoretical works indicate that this is not the case for $N \geq 3$. For a critical discussion of this issue, see Refs. [23, 190, 238, 605, 629] and references therein.

Ref.	info	γ	ν	η	ω
[385] 2000	MC FSS ϕ^4	1.393(4)*	0.710(2)	0.0380(10)	0.773
[181] 2000	MC FSS double-exchange	1.3909(30)*	0.6949(38)		
[77] 1996	MC FSS	1.396(3)*	0.7128(14)	0.0413(16)	
[151] 1996	MC FSS	1.270(1)*	0.642(2)	0.020(1)	
[413] 1994	MC FSS		0.706(8)*		
[412] 1993	MC FSS	1.389(14)*	0.704(6)	0.027(2)	
[221] 1993	MC FSS sc, bcc	1.3873(85)*	0.7048(30)	0.0250(35)	
[632] 1991	MC FSS	1.390(23)*	0.706(9)	0.031(7)	
[255] 1991	MC FSS		0.73(4)		
[609] 1988	MC FSS		0.716(40)		
[164] 1997	HT sc	1.406(3)	0.716(2)		
[164] 1997	HT bcc	1.402(3)	0.714(2)		
[7] 1993	HT sc	1.40(1)	0.712(10)		
[286] 1986	HT fcc	1.40(3)	0.72(1)		
[557] 1982	HT sc	1.395(5)			
[665] 1972	HT sc, bcc, fcc	1.375 ^{+0.02} _{-0.01}	0.7025 ^{+0.010} _{-0.005}	0.043(14)	
[359] 1998	FT $d = 3$ exp	1.3895(50)	0.7073(35)	0.0355(25)	0.782(13)
[359] 1998	FT ϵ -exp	1.382(9)	0.7045(55)	0.0375(45)	0.794(18)
[481] 2000	FT ϵ -exp		0.695(10)		
[595] 1984	SFM	1.40(3)	0.715(20)	0.044(7)	0.84(7)
[113] 1999	CRG	1.374	0.704	0.049	

Table 23: Estimates of the critical exponents for the Heisenberg model. We indicate with an asterisk (*) the estimates that have been obtained by using the scaling relations $\gamma = (2 - \eta)\nu$, $2 - \alpha = 3\nu$, $\beta = \nu(1 + \eta)/2$.

Ref.	info	γ	ν	η	ω
[385] 2000	MC FSS ϕ^4		0.749(2)	0.0365(10)	0.765
[77] 1996	MC FSS	1.476(2)*	0.7525(10)	0.0384(12)	
[450] 1995	MC FSS	1.477(18)*	0.748(9)	0.0254(38)	
[164] 1997	HT sc	1.491(4)	0.759(3)		
[164] 1997	HT bcc	1.484(4)	0.756(3)		
[359] 1998	FT $d = 3$ exp	1.456(10)	0.741(6)	0.0350(45)	0.774(20)
[359] 1998	FT ϵ -exp	1.448(15)	0.737(8)	0.036(4)	0.795(30)
[113] 1999	CRG	1.443	0.739	0.047	

Table 24: Estimates of the critical exponents for the $O(4)$ -vector model. We indicate with an asterisk (*) the estimates that have been obtained by using the scaling relations $\gamma = (2 - \eta)\nu$, $2 - \alpha = 3\nu$, $\beta = \nu(1 + \eta)/2$.

totically free with a nonperturbatively generated mass gap [88, 147, 149, 651]. Such a property is present also in QCD, i.e. the theory of strong interactions, and thus these two-dimensional theories are often used as toy models in order to understand nonperturbative properties and to test numerical methods that are of interest for the more complex theory of QCD (see, e.g., Ref. [650]).

The two-dimensional N -vector model is also important in condensed-matter physics. For $N = 3$ it describes the LT behavior of the two-dimensional spin- S Heisenberg quantum antiferromagnet [213]. Indeed, at finite temperature T this quantum spin system is described by a $(2+1)$ -dimensional $O(3)$ classical theory in which the Euclidean time direction has a finite extent $1/T$. For $T \rightarrow 0$ the system becomes effectively two-dimensional since $1/T \ll \xi$, and thus it is described by the two-dimensional three-vector model.

Moreover, the non-linear FT formulation of the two-

dimensional N -vector model with $N \geq 3$ is the starting point for the $\epsilon \equiv d - 2$ expansion (see, e.g., Ref. [792] and references therein), which provides information of the critical properties of N -vector models for $d \gtrsim 2$. The ϵ -expansion of the critical exponents is known to $O(\epsilon^4)$ [114, 404, 405]. But its application to the study of the physical three-dimensional transitions is limited due to the fact that this expansion is not Borel summable [405], and we do not know how to resum it. An attempt based on a variational approach was presented in Ref. [481].

Beside being asymptotically free, the two-dimensional N -vector model with $N \geq 3$ has another remarkable property. The corresponding quantum field theory is integrable, in the sense that, assuming asymptotic freedom, one can establish the existence of nonlocal conserved charges and the absence of particle production [157, 158, 527]. This implies the existence of a factorized S -matrix [787] and allows the applications of powerful

techniques, such as the thermodynamic Bethe Ansatz and the form-factor bootstrap approach (although the latter has been applied only to the $N = 3$ case). These approaches have led to exact predictions for several nonperturbative quantities [82–84, 394, 395, 451, 532].

5.2.1 The critical behavior

The critical behavior for $T \rightarrow 0$ can be computed in perturbation theory for a particular class of $O(N)$ models that, in this context, are usually called σ -models. On the lattice one can consider Hamiltonians

$$\mathcal{H} = -\frac{1}{T} \sum_{ij} K(i-j) \vec{s}_i \cdot \vec{s}_j, \quad (5.2)$$

where $K(x)$ is a short-range coupling and $|\vec{s}_i| = 1$. If only nearest-neighbor spins are coupled, we reobtain the N -vector model (1.4). It is also possible to add couplings that involve more than two spins without changing the universality class. The only important requirement is that the ground state of the system is ferromagnetic.

For this class of systems we can use spin-wave perturbation theory and the RG to obtain the behavior for $T \rightarrow 0$. See e.g. Ref. [792] for a general reference. For the true correlation length ξ_{gap} and the susceptibility χ one has

$$\xi_{\text{gap}}(T) = \xi_0 (\beta_0 T)^{\beta_1/\beta_0^2} \exp\left(\frac{1}{\beta_0 T}\right) \times \exp\left[\int_0^T dt \left(\frac{1}{\beta(t)} + \frac{1}{\beta_0 t^2} - \frac{\beta_1}{\beta_0^2 t}\right)\right], \quad (5.3)$$

$$\chi(T) = \chi_0 (\beta_0 T)^{2\beta_1/\beta_0^2 + \gamma_0/\beta_0} \exp\left(\frac{2}{\beta_0 T}\right) \times \exp\left[\int_0^T dt \left(\frac{2}{\beta(t)} + \frac{2}{\beta_0 t^2} - \frac{2\beta_1}{\beta_0^2 t} - \frac{\gamma(t)}{\beta(t)} - \frac{\gamma_0}{\beta_0 t}\right)\right], \quad (5.4)$$

where $\beta(T)$ is the β -function, defined by $\beta(T) = -adT/da$ with a being the lattice spacing, and $\gamma(T)$ is the anomalous dimension of the field. These functions describe how the temperature and the fundamental field should vary with the lattice spacing a to keep the renormalized Green's functions fixed. They have a perturbative expansion of the form

$$\beta(T) = -T^2 \sum_{n=0} \beta_n T^n, \quad (5.5)$$

$$\gamma(T) = T \sum_{n=0} \gamma_n T^n, \quad (5.6)$$

and are model-dependent. However, two particular combinations of the perturbative coefficients are uni-

versal,²⁹ β_1/β_0^2 and γ_0/β_0 , that appear as universal exponents in the critical behavior of ξ and χ . Explicitly:

$$\frac{\beta_1}{\beta_0^2} = \frac{1}{N-2}, \quad (5.7)$$

$$\frac{\gamma_0}{\beta_0} = \frac{N-1}{N-2}. \quad (5.8)$$

The perturbative expansions of $\beta(T)$ and $\gamma(T)$ have been determined for several different models: to four-loop order for the continuum theory in the minimal subtraction scheme [114] and for the standard N -vector model [25, 195], and to three-loop order for several other theories [27, 194, 282].

The nonperturbative constants ξ_0 and χ_0 are also nonuniversal. However, for the models (5.2) their ratio can be computed in one-loop perturbation theory. For the N -vector model with nearest-neighbour interactions, ξ_0 was computed exactly by means of the thermodynamic Bethe Ansatz [394, 395]:

$$\xi_0 = \left(\frac{e}{8}\right)^{1/(N-2)} \Gamma\left(\frac{N-1}{N-2}\right) 2^{-5/2} \exp\left(-\frac{\pi}{2(N-2)}\right). \quad (5.9)$$

For $N = 3$, there exists also a precise estimate of χ_0 obtained by combining the form-factor approach and HT expansions [175] $\chi_0 = 0.01452(5)$. Of course, one can consider other thermodynamic functions. In order to obtain the corresponding low- T behavior the anomalous dimensions are needed. For some composite operators, perturbative expressions can be found in Refs. [148, 193, 194].

The predictions (5.3) and (5.4) apply also to more general models in which the fields do not satisfy the condition $\vec{\phi} \cdot \vec{\phi} = 1$, for instance to the ϕ^4 theory (1.7). In this case, however, the functions $\beta(T)$ and $\gamma(T)$ cannot be determined analytically.

The perturbative predictions have been checked in several different ways. The results for χ and ξ have been checked in the large- N limit, including the non-perturbative constant (5.9), to order $1/N$ [126]. Several simulations checked the predictions for $N = 3, 4$, and 8 [24, 26, 180, 187, 189, 269, 561, 780] for the standard N -vector model and some other lattice versions in the same class of universality. For $N = 3$ there are significant discrepancies (of order 15-20%) between MC results and 4-loop perturbation results at correlation

²⁹ Often the claim is made that β_0 , β_1 , and γ_0 are universal. This is not strictly correct, since these quantities depend on the normalization of the temperature T . What it is usually meant is that, once a universal normalization is fixed, these constants are universal. The standard normalization of T is such that at tree level the two-point function is $\tilde{G}^{-1}(q) = q^2/T$. Note that the product $(\beta_0 T)$ is independent of the normalization of T .

lengths of order 100. This discrepancy decreases significantly at $\xi \approx 10^5$ where it is $\sim 4\%$. For larger values of N the agreement is better and for $\xi \approx 100$ 4-loop perturbation theory differs from MC by 4% ($N = 4$) and 1% ($N = 8$). The agreement improves if one considers the so-called ‘‘improved’’ perturbation theory [622,624] in terms of effective temperature variables, which take somehow into account a large part of the perturbative contributions (see the discussions of Refs. [194,668]). The corresponding perturbative results are in better agreement with the numerical ones [24,26,187].

It is interesting to mention that much of what has been obtained numerically by MC methods can also be determined by using the $1/N$ expansion. At variance with the three-dimensional case, it is indeed quite predictive even for $N = 3$ [173,323].

As already mentioned, the above results can be extended to the antiferromagnetic quantum Heisenberg model on a square lattice, with Hamiltonian

$$\mathcal{H} = \frac{1}{T} \sum_{\langle xy \rangle} \vec{s}_x \cdot \vec{s}_y, \quad (5.10)$$

where \vec{s}_i is a spin operator satisfying the commutation relations $[s_{x,i}, s_{y,j}] = \delta_{xy} \epsilon_{ijk} s_{x,k}$ and the condition $s_x^2 = S(S+1)$. For $T \rightarrow 0$, the correlation length can be computed obtaining [213,392,396]

$$\xi_{\text{gap}} = \frac{e}{8} \frac{c}{2\pi\rho_s} \exp\left(\frac{2\pi\rho_s}{T}\right) \left(1 - \frac{T}{4\pi\rho_s} + O(T^2)\right) f(\gamma), \quad (5.11)$$

where ρ_s is the spin stiffness, c the spin-wave velocity, $\gamma = 2S/T$, and $f(\gamma)$ a function computed numerically in Ref. [392] and which has the limit values: $f(\infty) = 1$, $f(\gamma) = e^{-\pi/2}/(8\gamma)$ for $\gamma \rightarrow 0$. Of course, for $S \rightarrow \infty$ we reobtain the low- T behavior of the classical model. These results have been compared with the experimental and the numerical results obtained for the antiferromagnet. Similarly to the classical model, good agreement is observed only for very large values of the correlation length [94,95,473,477].

5.2.2 Amplitude ratios and two-point function

The RG predictions (5.3) and (5.4) are quite difficult to test because the neglected corrections are powers of T , thus corresponding to powers of $\log \xi$. As a consequence, numerical determinations of the nonperturbative constants ξ_0 and χ_0 are extremely difficult. On the other hand, in the case of RG invariant quantities scaling corrections are depressed by integer powers of ξ . Indeed, models with $N \geq 3$ are essentially Gaussian and thus the operators have canonical dimensions. For a generic RG invariant quantity we expect:

$$R(T) = R^* + b \frac{X^p}{\xi^2} \left(1 + \frac{a_1}{X} + \frac{a_2 \log X}{X^2} + \frac{a_3}{X^2} + \dots\right)$$

$$+ O(\xi^{-4}), \quad (5.12)$$

where $X = \log \xi$. Apart from logarithmic corrections, the exponent associated with the leading scaling corrections is given by $\omega = 2$. Such a behavior is verified explicitly in large- N calculations, see, e.g., Ref. [169]. This means that accurate estimates of the universal constants R^* can be obtained already by determining $R(T)$ at values of T corresponding to relatively small ξ .

Similarly to the standard power-law critical behaviors, the approach to scaling can be somehow improved by considering models in which some terms in the scaling corrections are depressed. In the context of asymptotically free theories, one can determine analytically, using perturbation theory, the Hamiltonian parameters that provide the cancellation of the leading logarithms associated with each power correction [718,719]. However, in practice the obtainable improvement using this approach is rather modest: the scaling corrections change only by powers of $\log \xi$. Several improved models of this type have been considered in Refs. [192,397,669,719]. On the other hand, a complete removal of the $O(\xi^{-2})$ scaling corrections would require the tuning of an infinite numbers of parameters.

In Table 25 we review the estimates of the four-point coupling constant g_4^+ defined in Eq. (1.63), obtained by various approaches, such as the form-factor approach (FF), Monte Carlo simulations (MC), high-temperature series (HT), and field-theoretical methods (FT). The agreement is globally good. We only note that the HT results of Refs. [173,640] are slightly smaller than the precise FF and MC estimates. The HT estimates were taken at a value of the temperature corresponding to a correlation length $\xi \simeq 10$, where the HT analysis was reliable. The difference with the other results should be essentially due to an underestimate of the scaling corrections. Concerning the coefficients r_{2n} that parametrize the equation of state for $M \rightarrow 0$, we mention the estimates $r_6 = 3.33(2)$ and $r_8 \simeq 19$, obtained by a constrained analysis of their $O(\epsilon^3)$ series [643]. For $N \geq 4$, some estimates of g_4^+ and of the first few r_{2n} can be found in Refs. [162,173,640,643].

Finally, let us discuss the two-point function. Similarly to three-dimensional models, the scaling function $g^+(y)$ defined in Eq. (1.148) is well approximated by the Ornstein-Zernicke behavior $g^+(y) \approx 1 + y$ up to $y \approx 1$. Indeed, the constants c_n^+ defined in Eq. (1.150) are very small and satisfy (3.34) for large N [172,175]. For instance, for $N = 3$ the HT analysis of Ref. [175] obtained $c_2^+ = -0.0012(2)$, $|c_3| \lesssim 10^{-4}$, $S_M^+ = 0.9987(2)$ and $S_Z^+ = 1.0025(4)$ (cf. Eqs. (1.153) and (1.154) for S_M^+ and S_Z^+ respectively). The most precise estimate of S_M^+ was obtained by means of the

FF	MC	HT	FT $d = 2$ exp	FT ϵ -exp
12.19(3) [83]	12.21(4) [83, 84] 11.9(2) [470]	11.82(6) [640] 11.9(2) [173]	12.00(14) [616] 11.99(11) [281]	12.0(2) [643]

Table 25: Estimates of g_4^+ for the two-dimensional O(3) universality class.

form-factor approach, obtaining $S_M^+ = 0.998350(2)$ [83]. For $N = 3$ S_M^+ has also been determined by means of MC simulations, obtaining $S_M^+ = 0.9985(12)$ [563] and $S_M^+ = 0.996(2)$ [24]. The overall agreement is good.

For large values of q^2 , there are logarithmic deviations from the Ornstein-Zernicke behavior. For $y \rightarrow \infty$ we have

$$g^+(y) \sim y(\ln y)^{-1/(N-2)}. \quad (5.13)$$

In x -space this implies, for $x \rightarrow 0$:

$$G(x) \sim (\ln 1/x)^{\frac{N-1}{N-2}}. \quad (5.14)$$

Finally, we report the result of Ref. [82] for the asymptotic behavior of Z_{gap} , see Eq. (1.152). For $T \rightarrow 0$

$$Z_{\text{gap}}(T) = C(N)(\beta_0 T)^{\frac{N-1}{N-2}} [1 + O(T)]. \quad (5.15)$$

The constant $C(N)$ is exactly known for $N = 3$: $C(3) = 3\pi^3$ [82].

6 The Limit $N \rightarrow 0$

In this section we discuss the limit $N \rightarrow 0$ of the N -vector model. This is not an academic problem as it may appear at first. Indeed, in this limit, the N -vector model describes the statistical properties of linear polymers in dilute solutions and in the good solvent regime, i.e. above the Θ temperature [243, 251, 322, 329].

6.1 Walk models

Several walk models can be mapped into scalar theories with an N -vector field in the limit $N \rightarrow 0$. They belong to the same universality class of linear polymers in dilute solutions in the good solvent regime, and thus their study provides quantitative predictions for the statistical behavior of long macromolecules.

We begin by introducing the random walk (RW) and the self-avoiding walk (SAW). Given a regular lattice Λ , an n -step lattice RW is a collection of lattice points $\{\omega_0, \dots, \omega_n\}$ such that, for all k , $1 \leq k \leq n$, ω_k and ω_{k-1} are lattice nearest neighbors. A lattice SAW is a nonintersecting lattice RW, i.e. a walk such that $\omega_i \neq \omega_j$ for all $i \neq j$. Strictly related is the concept of an n -step self-avoiding (rooted) polygon (SAP) which is defined as a closed n -step RW such that $\omega_0 = \omega_n$ and $\omega_i \neq \omega_j$ for all $0 \leq i \neq j \leq n-1$.

Several quantities are usually introduced for SAWs and SAPs. We define:

- The number $c_n(x, y)$ of n -step SAWs going from x to y and the number c_n of n -step SAWs starting from any given point (by translation invariance it does not depend on the chosen point).
- The number p_n of n -step SAPs starting at a given point.
- The squared end-to-end distance of a SAW ω

$$R_e^2(\omega) = (\omega_n - \omega_0)^2, \quad (6.1)$$

and its mean-value $R_e^2(n)$ over all n -step SAWs, i.e.

$$R_e^2(n) = \frac{1}{c_n} \sum_{\{\omega\}} R_e^2(\omega) = \frac{1}{c_n} \sum_{x \in \Lambda} |x|^2 c_n(0, x). \quad (6.2)$$

- The radius of gyration of a SAW or SAP ω

$$R_g^2(\omega) = \frac{1}{(n+1)^2} \sum_{i,j=0}^n (\omega_i - \omega_j)^2, \quad (6.3)$$

and its mean value $R_g^2(n)$ over all n -step SAWs.

- The end-to-end distribution function of n -step SAWs

$$P_n(x) = \frac{c_n(0, x)}{c_n}. \quad (6.4)$$

- The form factor of n -step SAWs or SAPs

$$H_n(q) = \frac{1}{(n+1)^2} \left\langle \sum_{i,j=0}^n \exp[iq \cdot (\omega_i - \omega_j)] \right\rangle, \quad (6.5)$$

where the average is over all n -step SAWs.

- The number b_n of pairs of n -step SAWs (ω_1, ω_2) such that ω_1 starts at the origin, ω_2 starts anywhere, and ω_1 and ω_2 have at least one point in common.

The quantities we have defined have a natural interpretation. The end-to-end distance and the radius of gyration define the typical dimension of the walk and correspond to the correlation length in spin systems.

The end-to-end distribution function is the walk analogue of the two-point function in spin systems, while the form factor is the quantity which is relevant in scattering experiments. Finally, the number b_n is related to the second virial coefficient $B_n = b_n/c_n^2$ and is a measure of the excluded volume between a pair of SAWs. For $n \rightarrow \infty$, these quantities obey general scaling laws:

$$\begin{aligned} c_n &\sim \mu^n n^{\gamma-1}, \\ p_n &\sim \mu^n n^{\alpha-2}, \\ b_n &\sim \mu^{2n} n^{d\nu+2\gamma-2}, \\ R_e^2(n) &\approx a_e n^{2\nu}, \\ R_g^2(n) &\approx a_g n^{2\nu}. \end{aligned} \quad (6.6)$$

The constants γ , α , and ν are critical indices. They are universal in the sense that any walk model which includes the basic property of SAWs, the local self-repulsion, has the same scaling behavior with exactly the same critical indices. The names of the indices were given for analogy with the N -vector model. Indeed, as we shall discuss in the next section, γ , α , and ν are respectively the exponents of the susceptibility, of the specific heat, and of the correlation length in the corresponding spin system in the limit $N \rightarrow 0$. The quantities μ , a_e , and a_g are instead nonuniversal and depend on the specific model one is considering. Some amplitude ratios are however universal, such as

$$\begin{aligned} A &= \frac{a_g}{a_e} = \lim_{n \rightarrow \infty} \frac{R_g^2(n)}{R_e^2(n)}, \\ \Psi &= \left(\frac{d}{12\pi} \right)^{d/2} \lim_{n \rightarrow \infty} \frac{b_n}{c_n^2 [R_g^2(n)]^{d/2}}. \end{aligned} \quad (6.7)$$

The universality of A is obvious: It follows immediately from the existence of a unique length scale at criticality. On the other hand, the universality of the interpenetration ratio Ψ is more subtle, and it is related to a hyperscaling relation among critical indices—such a relation has already been used in writing the scaling of b_n in Eq. (6.6).

The SAW is a good model for dilute linear polymers in a good solvent. Indeed, many properties of dilute polymers in the limit of a large number of monomers are universal and depend essentially on the following properties [243, 251, 322, 329]:

- The polymer can be considered as a continuous completely flexible chain above the persistence-length scale.
- The interaction between monomers is strongly repulsive at small distances: Clearly two monomers cannot occupy the same position in space.

- Above the Θ -temperature (good-solvent regime) the effective long-range attractive interaction between monomers can be neglected: The energetic attraction is much smaller than the entropic repulsion.

The SAW satisfies these properties, and therefore it belongs to the same universality class of real polymers. However, this is not the only model one can consider, and indeed, many others have been introduced in the literature:

- *Domb-Joyce model.* This is again a lattice walk model, in which one considers RWs with Hamiltonian

$$H(\omega) = w \sum_{i,j} \delta_{\omega_i, \omega_j}. \quad (6.8)$$

For $w \rightarrow \infty$, all intersections are suppressed and one recovers the SAW model. The Domb-Joyce model interpolates between the RW and the SAW model, and offers the possibility of constructing an improved lattice walk model, i.e. a model in which the leading correction to scaling has a vanishing amplitude [106].

- *Off-lattice models.* The SAW and the Domb-Joyce models are defined on a lattice. However, it is also possible to consider models of paths in continuous space. For instance, one can consider a model of off-lattice SAWs defined as a collection of points $\{\omega_0, \dots, \omega_n\}$, $\omega_i \in \mathbb{R}^d$, such that $|\omega_i - \omega_j| \geq 2a$ for all $i \neq j$, where a is the excluded radius. These walks are weighted with Hamiltonian

$$H(\omega) = \sum_{i=0}^{n-1} V(\omega_i - \omega_{i+1}), \quad (6.9)$$

where $V(x)$ is an attractive potential. Two common choices are: $V(x) = \delta(|x| - b)$ (stick-and-ball model) and $V(x) = \frac{b}{2}x^2$.

- *Continuous models.* For theoretical considerations it is useful to consider continuous paths, i.e. generic functions $r(s)$ with $0 \leq s \leq n$, n being the length of the path, with Hamiltonian [267]

$$\begin{aligned} H[r(s)] &= -\frac{1}{4} \int_0^n ds \left(\frac{dr(s)}{ds} \right)^2 \\ &\quad - \frac{w}{2} \int_0^n ds \int_0^n dt \delta[r(s) - r(t)]. \end{aligned} \quad (6.10)$$

6.2 N -vector model for $N \rightarrow 0$ and self-avoiding walks

In this section we derive the relation between SAWs and the limit $N \rightarrow 0$ of the N -vector model [237, 243,

273]. Consider N -vector spin variables s , the lattice Hamiltonian

$$H = -N \sum_{\langle ij \rangle} s_i \cdot s_j, \quad (6.11)$$

where the sum is extended over all nearest-neighbor pairs, and the partition function

$$Z = \int \prod_i d\Omega(s_i) e^{-\beta H}, \quad (6.12)$$

where $d\Omega(s_i)$ is the invariant measure on the sphere. The limit $N \rightarrow 0$ follows immediately from a basic result, due to de Gennes:

$$\lim_{N \rightarrow 0} N^{k/2} \int d\Omega(s) s^{\alpha_1} \dots s^{\alpha_k} = \begin{cases} \delta_{\alpha_1 \alpha_2} & \text{if } k = 2, \\ 0 & \text{otherwise.} \end{cases} \quad (6.13)$$

Thus, for $N \rightarrow 0$, we can rewrite the partition function as

$$Z = \int \prod_i d\Omega(s_i) \prod_{\langle ij \rangle} (1 + N\beta s_i \cdot s_j) + O(N^2). \quad (6.14)$$

Then, expanding the product over the links and performing the integration we obtain a sum over a gas of self-avoiding loops. Each closed loop carries a power of N , so that

$$Z = 1 + NV \sum_n \frac{p_n}{n} \beta^n + O(N^2), \quad (6.15)$$

where V is the volume of the lattice, which is assumed to go to infinity. The factor $1/n$ is due to the fact that each loop can be considered as a SAP rooted in n different points. Then, using the asymptotic behavior (6.6), we obtain for $\beta \rightarrow 1/\mu$

$$\lim_{V \rightarrow \infty} \lim_{N \rightarrow 0} \frac{1}{NV} \log Z = \sum_{n=0}^{\infty} \frac{p_n}{n} \beta^n \sim (\beta - 1/\mu)^{2-\alpha}. \quad (6.16)$$

We thus see that α is the specific-heat exponent and we may interpret $1/\mu$ as the critical temperature of the model.

Let us now compute the two-point function. Repeating the argument given above, we obtain

$$\lim_{N \rightarrow 0} G(x-y) = \lim_{N \rightarrow 0} \langle s_x \cdot s_y \rangle = \sum_n \beta^n c_n(x, y). \quad (6.17)$$

Then, using the asymptotic behavior (6.6), for $\beta \rightarrow 1/\mu$ we obtain

$$\lim_{N \rightarrow 0} \chi = \sum_n \beta^n c_n \sim (\beta - 1/\mu)^{-\gamma}, \quad (6.18)$$

that shows that γ is indeed the susceptibility exponent.

Finally note that

$$\lim_{N \rightarrow 0} \sum_x |x|^2 G(x) = \sum_x \sum_n |x|^2 \beta^n c(0, x) = \sum_n c_n \beta^n R_e^2(n) \sim (\beta - 1/\mu)^{-\gamma-2\nu}, \quad (6.19)$$

where we have used the asymptotic formulae (6.6). It follows $\xi^2 \sim (\beta - 1/\mu)^{-2\nu}$, which clarifies the definition of ν .

The interpretation of b_n is less obvious. It can be also related to a quantity defined for a spin system in the the limit $N \rightarrow 0$, but in this case two different fields must be considered [251, 586].

The above-reported discussion clarifies the equivalence between the N -vector model and the SAW model. However, also more general scalar models can be mapped in the limit $N \rightarrow 0$ into walk models [290]. In general one obtains a model of RWs with different weights that depend on the number of self-intersections. Finally, note that the continuous model (6.10) is equivalent to the usual ϕ^4 theory in the continuum [242, 251, 615].

6.3 Critical exponents, universal amplitudes, and scaling functions

In two dimensions exact results have been obtained for SAWs on the honeycomb lattice [92, 607]. In particular, the values of the exponents have been computed:

$$\nu = \frac{3}{4}, \quad \gamma = \frac{43}{32}, \quad \alpha = \frac{1}{2}. \quad (6.20)$$

These predictions have been checked numerically to a very high accuracy, see, e.g., Refs. [110, 182, 197, 365, 369, 438, 508]. In particular, accurate numerical works have shown that the exponents do not depend on the lattice type—several nonstandard lattices, for instance the Manhattan lattice, have also been considered—and on the model—beside SAWs, Domb-Joyce walks, trails (bond-avoiding walks), and neighbor-avoiding walks (note that the list is not exhaustive) have been considered. In two dimensions conformal field theory provides exact predictions for some combinations of critical-amplitude ratios [196, 201, 203]. These predictions have been verified numerically to a very high accuracy. Results obtained using the form-factor approach can be found in Ref. [202].

Extensive work has been performed in three dimensions to determine the critical exponents. A collection of results is reported in Table 26. At present, the most precise results are obtained from MC simulations. Indeed, SAWs and similar walk models are particularly easy to simulate. First, one works directly in infinite

Ref.	Method	γ	ν	η	$\Delta \equiv \omega\nu$
[183] 1998	MC	1.1575(6)			
[106] 1997	MC		0.58758(7)		0.517(7) $_{-0}^{+10}$
[350] 1997	MC	1.157(1)	0.5872(5)		
[633] 1996	MC		0.5880 (18)		
[271] 1996	MC		0.5885(9)		
[508] 1995	MC		0.5877(6)		0.56(3)
[349] 1993	MC	1.608(3)	0.5850(15)		
[270] 1993	MC		0.591(1)		
[191] 1991	MC		0.5867(13)		
[239] 1991	MC		0.5919(2)		
[536] 1988	MC		0.592(2)		
[659] 1985	MC		0.592		
[535] 2000	HT sc	1.1585	0.5875		
[164] 1997	HT sc	1.1594(8)	0.5878(6)		
[164] 1997	HT bcc	1.1582(8)	0.5879(6)		
[534] 1992	HT	1.16193(10)			
[363] 1989	HT	1.161(2)	0.592(3)		
[359] 1998	FT $d=3$ exp	1.1596(20)	0.5882(11)	0.0284(25)	0.478(10)
[584] 1991	FT $d=3$ exp	1.1569(6){10}	0.5872(4){7}	0.0297(9){6}	
[586] 1987	FT $d=3$ exp		0.5886		0.465
[505] 1977	FT $d=3$ exp	1.1615(20)	0.5880(15)	0.027(4)	0.470(24)
[359] 1998	FT ϵ -exp _{free}	1.1575(60)	0.5875(25)	0.0300(50)	0.486(14)
[359] 1998	FT ϵ -exp _{bc}	1.1571(30)	0.5878(11)	0.0315(35)	
[595] 1984	SFM	1.15(1)	0.585(5)	0.034(5)	0.509(35)
[113] 1999	CRG	1.155	0.589	0.0406	
[229] 1980	experiment		0.586		

Table 26: Estimates of the critical exponents for the $N = 0$ universality class.

volume, and thus there are no finite-size systematic errors. Second, there are very efficient algorithms, see, e.g., Refs. [182, 198, 536], such that the autocorrelation time increases linearly with the length of the walk. Translating into the standard language of spin systems, in three dimensions $\tau \sim \xi^{5/3}$ in SAW simulations, to be compared with $\tau \sim \xi^{3+z}$ of spin systems. In practice, simulations with $\xi \sim 10^3$ (corresponding approximately to $n \sim 10^5$) are now feasible. This means that it is now possible to obtain numerical estimates of critical quantities with very good accuracy. We also mention that the older results obtained from MC simulations and exact enumerations were providing larger estimates of ν and γ : typically $\nu \approx 0.592$, $\gamma \approx 1.160$. This was mainly due to the fact that nonanalytic corrections to scaling were neglected in the analysis (see the discussion in, e.g., Refs. [191, 240, 271, 508, 535]).

The FT results for ν are in good agreement with the latest lattice results, while γ is slightly larger, although the discrepancy is not yet significant, being at the level of one error bar. We believe that it is mainly due to the nonanalyticity of the β -function that we discussed in Sec. 2.4.3.

The experimental results for the critical exponents are quite old and, in general, not very precise due to the difficulty to prepare monodisperse solutions. The analysis of the experimental data [332, 566, 747] for polystyrene in benzene gives [229] $\nu \approx 0.586$, in good

agreement with the theoretical estimates. The exponent ν has also been determined from the experimental measurement of the second virial coefficient, obtaining $\nu \approx 0.582$ [251]. Another important class of experiments determine ν from the diffusion of polymers [5, 714], obtaining $\nu = 0.55(2)$. This result is lower than the theoretical estimates and the experimental results we have presented above. This is probably due to the fact that the quantity that is measured in these experiments, the hydrodynamic radius of the polymer, scales approximately as n^ν (n is here the number of monomers) only for values of n that are much larger than those of the macromolecules that are used (see the discussion in Ref. [762]). Therefore, these experiments only measure effective exponents, strongly affected by corrections to scaling.

Beside critical exponents, one can measure several amplitude ratios. The ratio A and the interpenetration ratio Ψ defined in Eq. (6.7) are of particular interest. Theoretical and experimental estimates are reported in Table 27. All results are in good agreement.

Finally, we wish to discuss the distribution functions $P_n(x)$ and $H_n(q)$. In d dimensions, for $n \rightarrow \infty$, $|x| \rightarrow \infty$, with $|x|n^{-\nu}$ fixed, the function $P_n(x)$ has the scaling form [247, 300, 552, 555, 558]

$$P_n(x) \approx \frac{1}{\xi_n^d} f(\rho), \quad (6.21)$$

Ref.	Method	A	Ψ
[350] 1997	MC	0.15995(10)	
[508] 1995	MC	0.1599(2)	0.2471(3)
[695] 1994	MC	0.16003(3)	
[270] 1993	MC	0.1596(2)	
[599] 1991	MC		0.2465(12)
[536] 1988	MC	0.1603(4)	
[659] 1985	MC sc	0.1597(3)	
[659] 1985	MC bcc	0.1594(2)	
[695] 1994	FT $d=3$ exp	0.16012(30)	
[109] 1986	FT ϵ -exp	0.158	
[746] 1993	experiment		0.245

Table 27: Estimates of the amplitude ratios A and Ψ for the $N = 0$ universality class.

where $\rho = x/\xi_n$, and $\xi_n = R_e^2(n)/(2d)$. For large ρ it behaves as [247, 300, 558]

$$f(\rho) \approx f_\infty \rho^\sigma \exp(-D\rho^\delta), \quad (6.22)$$

where, in three dimensions, [184, 247]

$$\delta = \frac{1}{1-\nu} = 2.4247(4), \quad (6.23)$$

$$\sigma = \frac{6\nu - 2\gamma - 1}{2(1-\nu)} = 0.255(2), \quad (6.24)$$

$$f_\infty = 0.01581(2), \quad (6.25)$$

$$D = 0.1434(2). \quad (6.26)$$

For $\rho \rightarrow 0$, we have [247, 558]

$$f(\rho) \approx f_0 \left(\frac{\rho}{2}\right)^\theta, \quad (6.27)$$

where [184, 247]

$$\theta = \frac{\gamma - 1}{\nu} = 0.2680(10), \quad (6.28)$$

$$f_0 = 0.019(3). \quad (6.29)$$

A phenomenological representation for the function $f(\rho)$ has been proposed in Refs. [251, 558]:

$$f(\rho) \approx f_{\text{ph}}(\rho) = f_{\text{ph}} \rho^\theta \exp(-D_{\text{ph}} \rho^\delta). \quad (6.30)$$

Here δ and θ are fixed by Eqs. (6.23) and (6.28), while f_{ph} and D_{ph} are given by

$$D_{\text{ph}} = 0.14470(14), \quad f_{\text{ph}} = 0.015990(8). \quad (6.31)$$

The phenomenological representation is extremely accurate, differing from the exact one by a few percent in the region in which the distribution function is significantly different from zero, i.e. $\rho \lesssim 6$.

Let us now consider the form factor $H_n(q)$. For $n \rightarrow \infty$, $|q| \rightarrow 0$, with $|q|n^\nu$ fixed, the function $H_n(q)$ has a

scaling form $\widehat{H}(qR_g(n))$. For $qR_g(n) \ll 1$, we obtain the Guinier formula

$$H_n(q) = 1 - \frac{q^2 R_g^2(n)}{d} + O(q^2 R_g^2(n)), \quad (6.32)$$

which is often used in experimental determinations of the gyration radius. For large $qR_g(n)$, we have [250, 251, 265, 611, 777, 778]

$$H_n(q) \approx \frac{h_\infty}{[q^2 R_g^2(n)]^{1/(2\nu)}}, \quad (6.33)$$

where h_∞ is a universal constant: in three dimensions $h_\infty \approx 1.0$. Experiments [230, 283, 660] with neutrons and light sources verified the large- q behavior of $H_n(q)$, obtaining an estimate of ν , $\nu \approx 0.60$.

7 Critical crossover between the Gaussian and the Wilson-Fisher fixed point

7.1 Critical crossover as a two-scale problem

Every physical situation of experimental relevance has at least two scales: one scale is intrinsic to the system, while the second one is related to experimental conditions. In statistical mechanics the correlation length ξ is related to experimental conditions (it depends on the temperature), while the interaction length (Ginzburg parameter) is intrinsic. The opposite is true in quantum field theory: here the correlation length (inverse mass gap) is intrinsic, while the interaction scale (inverse momentum) depends on the experiment. Physical predictions are functions of ratios of these two scales and describe the crossover from the correlation-dominated (ξ/G or p/m large) to the interaction-dominated (ξ/G or p/m small) regime. In a properly defined limit they are universal and define the unique flow between two different fixed points. This universal limit is obtained when these two scales become very large with respect to any other (microscopic) scale. Their ratio becomes the (universal) control parameter of the system, whose transition from 0 to ∞ describes the critical crossover.

In this section we consider the crossover between the Gaussian fixed point where mean-field predictions hold (interaction-dominated regime) to the standard Wilson-Fisher fixed point (correlation-dominated regime). In recent years a lot of work has been devoted to understanding this crossover, either experimentally [42–44, 59, 228, 254, 428] or theoretically [40, 41, 54–56, 62, 105, 185, 222, 306, 523–526, 567, 636, 637, 683, 730]. For

a recent review on crossover phenomena in polymer blends and solutions see, e.g., Ref. [124].

The traditional approach to the crossover between the Gaussian and the Wilson-Fisher fixed point starts from the standard Landau-Ginzburg Hamiltonian. On a d -dimensional lattice, it can be written as

$$H = \sum_{x_1, x_2} \frac{1}{2} J(x_1 - x_2) (\phi_{x_1} - \phi_{x_2})^2 + \sum_x \left[\frac{1}{2} r \phi_x^2 + \frac{u}{4!} \phi_x^4 - h_x \cdot \phi_x \right], \quad (7.1)$$

where ϕ_x are N -dimensional vectors, and $J(x)$ is the standard nearest-neighbour coupling. For this model the interaction scale is controlled by the coupling u and the relevant parameters are the (thermal) Ginzburg number G [342] and its magnetic counterpart G_h [526, 636] defined by:

$$G = u^{2/(4-d)}, \quad G_h = u^{(d+2)/[2(4-d)]}. \quad (7.2)$$

Under a RG transformation G scales like the (reduced) temperature, while G_h scales as the magnetic field. For $t \equiv r - r_c \ll G$ and $h \ll G_h$ one observes the standard critical behaviour, while in the opposite case the behaviour is classical. The critical crossover limit corresponds to considering $t, h, u \rightarrow 0$ keeping

$$\tilde{t} \equiv t/G, \quad \tilde{h} \equiv h/G_h \quad (7.3)$$

fixed. This limit is universal, i.e. independent of the detailed structure of the model: any Hamiltonian of the form (7.1) shows the same universal behaviour as long as the interaction is short-ranged, i.e. for any $J(x)$ such that $\sum_x x^2 J(x) < +\infty$. In the HT phase the crossover functions can be related to the RG functions of the standard continuum ϕ^4 theory if one expresses them in terms of the zero-momentum four-point renormalized coupling g [54, 55, 62, 683]. For the quantities that are traditionally studied in statistical mechanics, for instance the susceptibility or the correlation length, the crossover functions can be computed to high precision in the fixed-dimension expansion in $d = 3$ [54, 55, 62, 637].

7.2 Critical crossover functions in field theory

The critical crossover functions can be computed in the framework of the continuum ϕ^4 theory

$$H = \int d^d x \left[\frac{1}{2} (\partial_\mu \phi)^2 + \frac{r}{2} \phi^2 + \frac{u}{4!} \phi^4 \right], \quad (7.4)$$

where ϕ is an N -dimensional vector, by considering the limit $u \rightarrow 0$, $t \equiv r - r_c \rightarrow 0$, with $\tilde{t} \equiv t/G = tu^{-2/(4-d)}$

fixed. In this limit, we have for the susceptibility χ and the correlation length ξ

$$\tilde{\chi} \equiv \chi G \rightarrow F_\chi(\tilde{t}), \quad (7.5)$$

$$\tilde{\xi}^2 \equiv \xi^2 G \rightarrow F_\xi(\tilde{t}). \quad (7.6)$$

The functions $F_\chi(\tilde{t})$ and $F_\xi(\tilde{t})$ can be accurately computed by means of perturbative FT calculations. There are essentially two methods: (a) the fixed-dimension expansion [54, 55], which is at present the most precise one since seven-loop series are available [70, 584]; (b) the so-called minimal renormalization without ϵ -expansion [257, 492, 683] which uses five-loop ϵ -expansion results [223, 482]. In these two schemes the crossover functions are expressed in terms of various RG functions whose perturbative series can be resummed with high accuracy using standard methods [505, 792]. Here we shall consider the first approach although essentially equivalent results can be obtained using the second method. For $F_\chi(\tilde{t})$ and $F_\xi(\tilde{t})$ one obtains [55]

$$F_\chi(\tilde{t}) = \chi^* \exp \left[- \int_{y_0}^g dx \frac{\gamma(x)}{\nu(x)\beta(x)} \right], \quad (7.7)$$

$$F_\xi(\tilde{t}) = (\xi^*)^2 \exp \left[-2 \int_{y_0}^g dx \frac{1}{\beta(x)} \right], \quad (7.8)$$

where \tilde{t} is related to the zero-momentum four-point renormalized coupling g by

$$\tilde{t} = -t_0 \int_g^{g^*} dx \frac{\gamma(x)}{\nu(x)\beta(x)} \exp \left[\int_{y_0}^x dz \frac{1}{\nu(z)\beta(z)} \right], \quad (7.9)$$

$$\nu(x) = (2 - \eta_\phi(x) + \eta_t(x))^{-1}, \quad (7.10)$$

$$\gamma(x) = (2 - \eta_\phi(x))\nu(x), \quad (7.11)$$

where $\eta_\phi(x)$, $\eta_t(x)$, and $\beta(x)$ are the standard RG functions introduced in Sec.2.4.1. As always, g^* is the critical value of g defined by $\beta(g^*) = 0$, and χ^* , ξ^* , t_0 and y_0 are normalization constants.

The expressions (7.7), (7.8) and (7.9) are valid for any dimension $d < 4$. The first two equations are always well defined, while Eq. (7.9) has been obtained with the additional hypothesis that the integral over x is convergent when the integration is extended up to g^* . This hypothesis is verified when the system becomes critical at a finite value of β and shows a standard critical behaviour. Therefore, Eq. (7.9) is always well defined for $d > 2$, and, in two dimensions, for $N \leq 2$. For $N > 2$, one can still define \tilde{t} by integrating up to an arbitrary point g_0 [637]. For these values of N , \tilde{t} varies between $-\infty$ and $+\infty$.

The functions $F_\chi(\tilde{t})$ and $F_\xi(\tilde{t})$ can be computed using the perturbative results of Refs. [70, 584] and one

of the resummation techniques presented in Sec. 2.4.3. Explicit expressions can be found for $N = 1, 2, 3$ and $d = 3$ in Refs. [54, 55], and for the two-dimensional Ising model in Ref. [637].

The above results apply to the HT phase of the model. For $N = 1$ the critical crossover can also be defined in the LT phase [62] and the crossover functions can be computed in terms of (resummed) perturbative quantities. Using the perturbative results of Ref. [62], $F_\chi(\tilde{t})$ in the LT phase of the three-dimensional Ising model has been calculated in Ref. [636], showing an interesting nonmonotonic behavior.

7.3 Critical crossover in spin models with medium-range interaction

The ϕ^4 Hamiltonian relevant for spin models with medium range interaction can be written as

$$H = \sum_{x_1, x_2} \frac{1}{2} J(x_1 - x_2) (\phi_{x_1} - \phi_{x_2})^2 + \sum_x \left[\frac{1}{2} r \phi_x^2 + \frac{u}{4!} \phi_x^4 - h_x \cdot \phi_x \right], \quad (7.12)$$

where $J(x)$ has the following form [526, 567]

$$J(x) = \begin{cases} J & \text{for } x \in D, \\ 0 & \text{for } x \notin D, \end{cases} \quad (7.13)$$

where D is a lattice domain characterized by some scale R . Explicitly, we define R and the corresponding domain volume V_R by

$$V_R \equiv \sum_{x \in D} 1, \quad R^2 \equiv \frac{1}{2d V_R} \sum_{x \in D} x^2. \quad (7.14)$$

The shape of D is irrelevant in the critical crossover limit as long as $V_R \sim R^d$ for $R \rightarrow \infty$. The constant J defines the normalization of the fields. Here we assume $J = 1/V_R$, since this choice simplifies the discussion of the limit $R \rightarrow \infty$. To understand the connection between the theory with medium-range interactions and the short-range model, we consider the continuum Hamiltonian that is obtained by replacing in Eq. (7.1) the lattice sums with the corresponding integrals. Then, we perform a scale transformation [526] by defining new (“blocked”) coordinates $y = x/R$ and rescaling the fields according to

$$\hat{\phi}_y = R^{d/2} \phi_{Ry}, \quad \hat{h}_y = R^{d/2} h_{Ry}. \quad (7.15)$$

The rescaled Hamiltonian becomes

$$\hat{H} = \int d^d y_1 d^d y_2 \frac{1}{2} \hat{J}(y_1 - y_2) \left(\hat{\phi}_{y_1} - \hat{\phi}_{y_2} \right)^2 + \int d^d y \left[\frac{1}{2} r \hat{\phi}_y^2 + \frac{1}{4!} \frac{u}{R^d} \hat{\phi}_y^4 - \hat{h}_y \cdot \hat{\phi}_y \right], \quad (7.16)$$

where now the coupling $\hat{J}(x)$ is of short-range type in the limit $R \rightarrow \infty$. Being short-ranged, we can apply the previous arguments and define Ginzburg parameters:

$$G = (uR^{-d})^{2/(d-4)} = u^{2/(d-4)} R^{-2d/(4-d)}, \quad (7.17)$$

$$G_h = R^{-d/2} (uR^{-d})^{(d+2)/[2(d-4)]} = u^{(d+2)/[2(d-4)]} R^{-3d/(4-d)}. \quad (7.18)$$

Therefore, in the medium-range model, the critical crossover limit can be defined as $R \rightarrow \infty$, $t, h \rightarrow 0$, with $\tilde{t} \equiv t/G$, $\tilde{h} \equiv t/G_h$ fixed. The variables that are kept fixed are the same, but a different mechanism is responsible for the change of the Ginzburg parameters: in short-range models we vary u keeping the range R fixed and finite, while here we keep the interaction strength u fixed and vary the range R . The important consequence of the argument presented above is that the critical crossover functions defined using the medium-range Hamiltonian and the previous limiting procedure agree with those computed in the short-range model, apart from trivial rescalings.

If we consider the critical limit with R fixed, the Hamiltonian (7.12) defines a generalized $O(N)$ -symmetric model with short-range interactions. If $d > 2$, for each value of R there is a critical point³⁰ $\beta_{c,R}$; for $\beta \rightarrow \beta_{c,R}$ the susceptibility and the correlation length have the standard behaviour

$$\chi_R(\beta) \approx A_\chi(R) t^{-\gamma} (1 + B_\chi(R) t^\Delta), \quad (7.19)$$

$$\xi_R^2(\beta) \approx A_\xi(R) t^{-2\nu} (1 + B_\xi(R) t^\Delta), \quad (7.20)$$

where $t \equiv (\beta_{c,R} - \beta)/\beta_{c,R}$ and we have neglected additional subleading corrections. The exponents γ , ν and Δ do not depend on R . On the other hand, the amplitudes are nonuniversal. For $R \rightarrow \infty$, they behave as [525, 526]

$$A_\chi(R) \approx A_\chi^\infty R^{2d(1-\gamma)/(4-d)},$$

$$B_\chi(R) \approx B_\chi^\infty R^{2d\Delta/(4-d)}, \quad (7.21)$$

and

$$A_\xi(R) \approx A_\xi^\infty R^{4(2-d\nu)/(4-d)},$$

$$B_\xi(R) \approx B_\xi^\infty R^{2d\Delta/(4-d)}. \quad (7.22)$$

The critical point $\beta_{c,R}$ depends explicitly on R . The critical crossover limit is obtained by taking the limit [525, 526] $R \rightarrow \infty$, $t \rightarrow 0$, with $R^{2d/(4-d)} t \equiv \tilde{t}$ fixed. It

³⁰In two dimensions a critical point exists only for $N \leq 2$. Theories with $N \geq 3$ are asymptotically free and become critical only in the limit $\beta \rightarrow \infty$.

has been shown that

$$\tilde{\chi}_R \equiv R^{-2d/(4-d)} \chi_R(\beta) \rightarrow f_\chi(\tilde{t}), \quad (7.23)$$

$$\tilde{\xi}_R^2 \equiv R^{-8/(4-d)} \xi_R^2(\beta) \rightarrow f_\xi(\tilde{t}), \quad (7.24)$$

where the functions $f_\chi(\tilde{t})$ and $f_\xi(\tilde{t})$ are universal apart from an overall rescaling of \tilde{t} and a constant factor, in agreement with the argument presented in the introduction.

There exists an equivalent way to define the crossover limit which is due to Thouless [730]. Let $\beta_{c,R}^{(\text{exp})}$ be the expansion of $\beta_{c,R}$ for $R \rightarrow \infty$ up to terms of order $R^{-2d/(4-d)}/V_R$, i.e. such that

$$\lim_{R \rightarrow \infty} R^{2d/(4-d)} \beta_{c,R}^{-1} (\beta_{c,R} - \beta_{c,R}^{(\text{exp})}) = b_c, \quad (7.25)$$

with $|b_c| < +\infty$. Then introduce

$$\hat{t} = R^{2d/(4-d)} \beta_{c,R}^{(\text{exp})-1} (\beta_{c,R}^{(\text{exp})} - \beta). \quad (7.26)$$

In the standard crossover limit $\tilde{t} = \hat{t} + b_c$. Therefore, the crossover limit can be defined considering the limit $R \rightarrow \infty$, $\beta \rightarrow \beta_{c,R}^{(\text{exp})}$ with \hat{t} fixed. The crossover functions will be identical to the previous ones apart from a shift. Thouless' definition of critical crossover has an important advantage. It allows the definition of the critical crossover limit in models that do not have a critical point for finite values of R : indeed, even if $\beta_{c,R}$ does not exist, one can define a quantity $\beta_{c,R}^{(\text{exp})}$ and a variable \hat{t} such that the limit $R \rightarrow \infty$ with \hat{t} fixed exists. This is the case of two-dimensional models with $N \geq 3$ and of one-dimensional models with $N \geq 1$.

Medium-range spin models can be studied by a systematic expansion around mean field [637]. In this framework one proves the equivalence between the crossover functions computed starting from the continuum ϕ^4 model and the results obtained in the medium-range model. Moreover, the nonuniversal constants relating the two cases can be computed, so that the comparison of the FT predictions with the numerical results obtained by simulating medium-range spin models [522, 523, 525, 526] can be done without any free parameter.

In Figs. 11 and 12 we report the graph of the effective magnetic susceptibility exponent γ_{eff} , defined by

$$\gamma_{\text{eff}}(\tilde{t}) \equiv -\frac{\tilde{t}}{f_\chi(\tilde{t})} \frac{df_\chi(\tilde{t})}{d\tilde{t}}, \quad (7.27)$$

for the Ising model in two and three dimensions respectively. They have been determined using the FT results discussed in Sec. 7.2 with the appropriate rescaling computed using the mean-field approach [637].

In two dimensions the results for $\gamma_{\text{eff}}(\tilde{t})$ can be compared with the numerical ones of Ref. [526], obtained

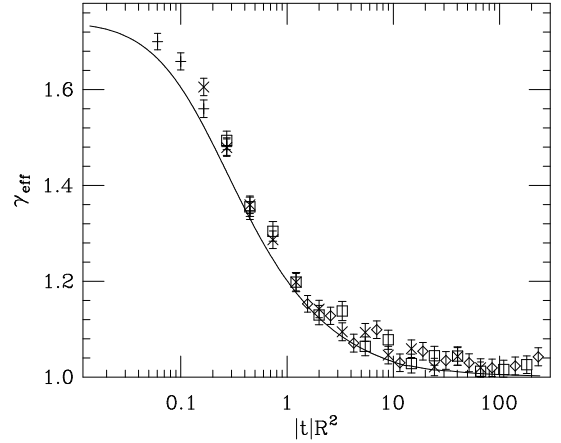


Figure 11: Effective susceptibility exponent as a function of \tilde{t} in the HT phase of the two-dimensional Ising model. The points are the numerical results of Ref. [526]: pluses, crosses, squares, and diamonds correspond to data with $\rho^2 = 10, 72, 140,$ and 1000 respectively. In the mean-field limit $\gamma_{\text{eff}} = 1$, while for $\tilde{t} \rightarrow 0$, $\gamma_{\text{eff}} = 7/4$. Results from Ref. [637].

by simulating the medium-range Ising model with coupling in the domain

$$D = \left\{ x : \sum_{i=1}^d x_i^2 \leq \rho^2 \right\}. \quad (7.28)$$

They are shown in Fig. 11. The agreement is good, showing nicely the equivalence of medium-range and field-theory calculations. In Fig. 12 we report the three-dimensional results for $\gamma_{\text{eff}}(\tilde{t})$ in both phases. MC simulations of the three-dimensional models have been reported in Ref. [523]. In the HT phase, $\gamma_{\text{eff}}(\tilde{t})$ agrees nicely with the MC data in the mean-field region, while discrepancies appear in the neighborhood of the Wilson-Fisher point. However, for $\tilde{t} \rightarrow 0$, only data with small values of ρ are present, so that the differences that are observed should be due to corrections to the universal behavior. The LT phase shows a similar behaviour: good agreement in the mean-field region, and a difference near the Wilson-Fisher point where again only point with small ρ are available.

The leading corrections to the universal scaling behavior were studied analytically in Ref. [637], showing that they are $O(R^{-d})$ in d dimensions if one choose appropriately the scale R , i.e. as in Eq. (7.14). There one

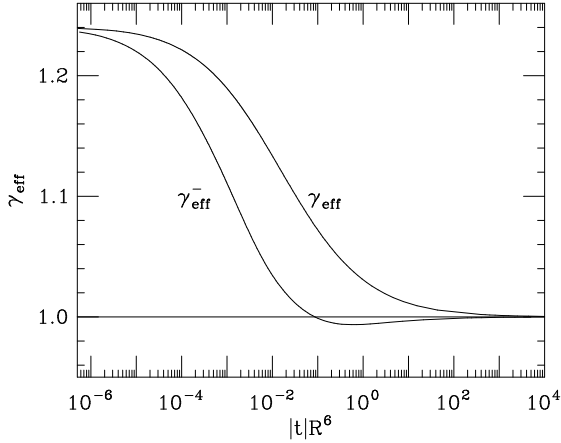


Figure 12: Effective susceptibility exponent as a function of \tilde{t} for the HT (γ_{eff}) and LT (γ_{eff}^-) phase of the three-dimensional Ising model. In the mean-field limit $\gamma_{\text{eff}} = 1$, while for $|\tilde{t}| \rightarrow 0$, $\gamma_{\text{eff}} \approx 1.237$. Results from Ref. [637].

may find also a critical discussion of the phenomenological methods used to describe the nonuniversal effects, such as those proposed in Refs. [40, 41, 43, 219, 222], which have been applied to many different experimental situations [42, 43, 219, 222, 428, 560].

7.4 Critical crossover in self-avoiding walk models with medium-range jumps

The models with medium-range interactions can be studied in the limit $N \rightarrow 0$. In this case, repeating the discussion presented in Sec. 6, one can write the N -vector model with medium-range interactions in terms of self-avoiding walks (SAWs) with medium-range jumps. To be explicit, we define an n -step SAW with range R as a sequence of lattice points $\{\omega_0, \dots, \omega_n\}$ with $\omega_0 = (0, 0, 0)$ and $(\omega_{j+1} - \omega_j) \in D$, such that $\omega_i \neq \omega_j$ for all $i \neq j$. Then, if $c_{n,R}$ is the total number of n -step walks and $R_e^2(n, R)$ is the end-to-end distance—see Sec. 6.1 for definitions—we have

$$\lim_{N \rightarrow 0} \chi(\beta) = \sum_{n=0}^{\infty} \hat{\beta}^n c_{n,R}, \quad (7.29)$$

$$\lim_{N \rightarrow 0} \xi^2(\beta) \chi(\beta) = \frac{1}{2d} \sum_{n=0}^{\infty} \hat{\beta}^n c_{n,R} E_{n,R}^2. \quad (7.30)$$

where $\hat{\beta} = \beta/V_R$ and χ and ξ^2 are defined for the N -vector model with medium-range interaction. The proof is identical to that presented in Sec. 6.2.

Since n is the dual variable (in the sense of Laplace transforms) of t , the critical crossover is obtained by performing the limit $n \rightarrow \infty$, $R \rightarrow \infty$ with $\tilde{n} \equiv nR^{-2d/(4-d)}$ fixed. Using Eqs. (7.23) and (7.24) one infers the existence of the following limits:

$$\tilde{c}_{n,R} \equiv c_{n,R} \beta_c(R)^n \rightarrow g_c(\tilde{n}), \quad (7.31)$$

$$\tilde{R}_e^2(n, R) \equiv R_e^2(n, R) R^{-8/(4-d)} \rightarrow g_E(\tilde{n}), \quad (7.32)$$

where the functions $g_c(\tilde{n})$ and $g_E(\tilde{n})$ are related to $f_\chi(\tilde{t})$ and $f_\xi(\tilde{t})$ by a Laplace transform. Explicitly

$$f_\chi(t) = \int_0^\infty du g_c(u) e^{-ut}, \quad (7.33)$$

$$f_\xi(t) f_\chi(t) = \frac{1}{2d} \int_0^\infty du g_c(u) g_E(u) e^{-ut}. \quad (7.34)$$

Using perturbation theory it is possible to derive predictions for $R_e^2(n, R)$ and $c_{n,R}$. For $R_e^2(n, R)$ we can write

$$g_{E,PT}(\tilde{n}) = a_E \tilde{n} h_E(z), \quad (7.35)$$

where $z = (\tilde{n}/l)^{1/2}$. The function $h_E(z)$ has been computed in perturbation theory to six-loop order [585, 586]. Resumming the series with a Borel-Leroy transform one finds that a very good approximation is provided by [106]

$$h_E(z) = (1 + 7.6118z + 12.05135z^2)^{0.175166}. \quad (7.36)$$

Comparison with a detailed MC simulation for the Domb-Joyce model indicates [106] that this simple expression differs from the exact result by less than 0.02% for $z < 2$.

The constants a_E and l appearing in Eq. (7.35) are non universal. For the specific model considered here they are given by $a_E = 6$, and $l = (4\pi)^3$. Ref. [185] reports results of an extensive simulation of this model of medium-range SAWs, generating walks of length up to $N \approx 7 \cdot 10^4$. The domain D was chosen as follows:

$$D = \left\{ x : \sum_i |x_i| \leq \rho \right\}. \quad (7.37)$$

In the simulation ρ was varied between 2 and 12.

In Fig. 13 the results for $\tilde{R}_e^2(n, R)$ are reported together with the perturbative prediction $g_{E,PT}(\tilde{n})$ defined in Eqs. (7.35) and (7.36). The agreement is very good although one can see clearly the presence of corrections to scaling, which are better seen in Fig. 14 where the ratio $\tilde{R}_e^2(n, R)/g_{E,PT}(\tilde{n})$ is plotted. In this plot the corrections to scaling are clearly visible: points

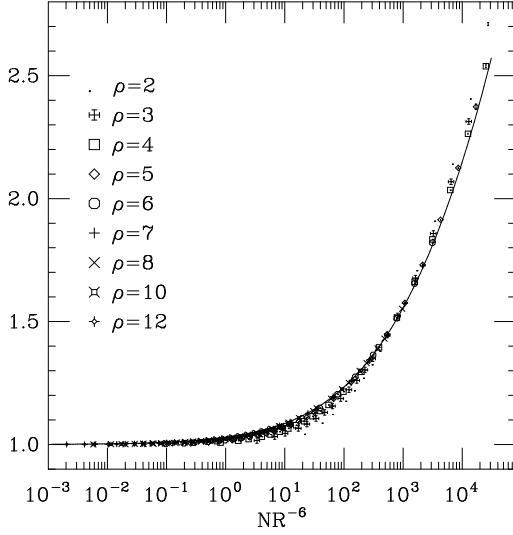


Figure 13: Results for $\tilde{R}_e^2(n, R)/(6\tilde{n})$. The solid line is the theoretical prediction (7.35), (7.36). Results from Ref. [185].

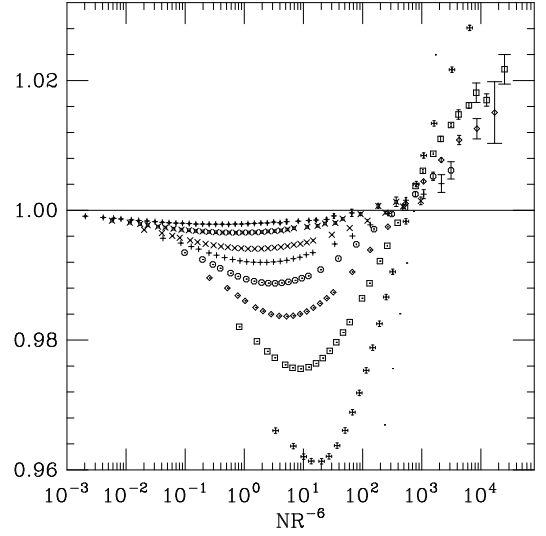


Figure 14: Results for $\tilde{R}_e^2(n, R)/g_{E,PT}(\tilde{n})$. The same symbols as in Fig. 13 are used. Results from Ref. [185].

with different R fall on different curves that converge to 1 as expected. For $\rho = 12$, the deviations are less than 0.2%. A more detailed discussion of the expected scaling corrections can be found in Refs. [185,637]. One may also define an effective exponent ν_{eff}

$$\nu_{\text{eff}} = \frac{1}{2 \log 2} \log \left(\frac{R_e^2(2n, R)}{R_e^2(n, R)} \right). \quad (7.38)$$

The corresponding curve is reported in Fig. 15. It shows the expected crossover behaviour between the mean-field value $\nu = 1/2$ and the self-avoiding walk value $\nu = 0.58758(7)$ [106].

8 Critical phenomena described by Landau-Ginzburg-Wilson Hamiltonians

8.1 Introduction

In the framework of the RG approach to critical phenomena, the critical behavior at many continuous phase transitions can be investigated by considering an effective Landau-Ginzburg-Wilson (LGW) Hamiltonian, having an N -component order parameter ϕ_i as fundamental field, and containing up to fourth-order powers of the field components. The fourth-degree polynomial form of the potential depends essentially on

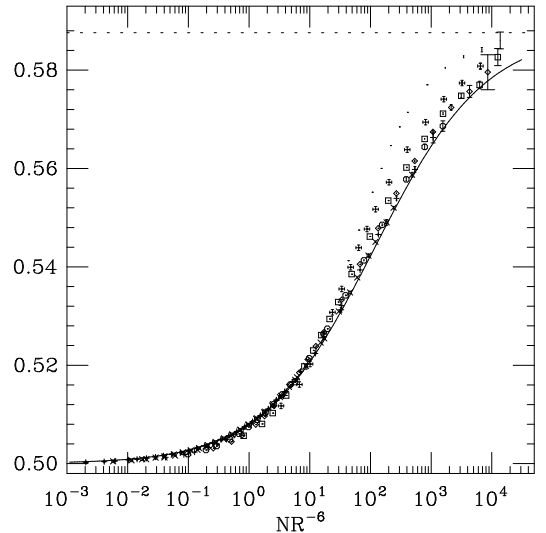


Figure 15: Results for ν_{eff} . The same symbols as in Fig. 13 are used. The dashed line is the self-avoiding walk value $\nu = 0.58758(7)$. The solid line is the theoretical prediction. Results from Ref. [185].

the symmetry of the system. In the previous sections we discussed the classical applications of the $O(N)$ -symmetric ϕ^4 theories, such as the helium superfluid transition, liquid-vapour transitions in classical fluids or critical binary fluids, critical behaviors of many magnetic materials, statistical properties of dilute polymers. We now consider other physically interesting systems whose continuous transitions are described by more complicated ϕ^4 theories.

In general, assuming that all N -components of the order parameter ϕ_i become critical at the transition point (i.e. that the system is characterized by only one diverging length), the quadratic part of the Hamiltonian density must be proportional to

$$\sum_i (\partial_\mu \phi_i)^2 + r \phi_i^2, \quad (8.1)$$

and the quartic term

$$\sum_{ijkl} u_{ijkl} \phi_i \phi_j \phi_k \phi_l \quad (8.2)$$

must be invariant under a symmetry group which possesses only $\sum_i \phi_i^2$ as quadratic invariant. This is achieved by imposing the trace condition [142]

$$\sum_i u_{iikl} \propto \delta_{kl}. \quad (8.3)$$

With increasing N , there are many fourth-order terms that are compatible with the trace condition. In the absence of a sufficiently large symmetry restricting the form of the potential, many quartic couplings must be introduced, see, e.g., Refs. [14, 45, 63, 127, 140, 143, 357, 576–579, 591, 685, 733], and the study of the critical behavior may become quite complicated. In the case of a continuous transition, the critical behavior is described by the infrared-stable fixed point of the theory, which determines a universality class. The absence of a stable fixed-point is instead an indication for a first-order phase transition. Note that even in the presence of a stable fixed point, a first-order phase transition may still occur for systems that are outside its attraction domain.

In this chapter we discuss several examples of continuous transitions in magnetic systems whose critical behavior is described by ϕ^4 LGW Hamiltonians with two or three quartic couplings, such as the Hamiltonian with cubic anisotropy which is relevant for magnets, the so-called MN model whose limit $N \rightarrow 0$ is related to the critical behavior of spin models in the presence of quenched randomness, the $O(M) \times O(N)$ -symmetric Hamiltonian which (in the case $M = 2$) describes the critical behavior of N -component frustrated models with noncollinear order, and, finally, the tetragonal Hamiltonian which is relevant for some structural

phase transitions. We essentially review the results of FT studies, especially the most recent ones. We then compare them with the results of other approaches and with the experiments.

8.2 The field-theoretical method for generic ϕ^4 theories

Let us consider the generic ϕ^4 Hamiltonian

$$\mathcal{H} = \int d^d x \left[\frac{1}{2} \sum_i (\partial_\mu \phi_i)^2 + \frac{1}{2} r \sum_i \phi_i^2 + \frac{1}{4!} \sum_{ijkl} u_{ijkl} \phi_i \phi_j \phi_k \phi_l \right] \quad (8.4)$$

and assume that the quartic coupling satisfies the trace condition (8.3).

The perturbative series of the exponents are obtained by a trivial generalization of the method presented in Sec. 2.4.1. In the fixed-dimension FT approach one renormalizes the theory by introducing a set of zero-momentum conditions for the two-point and four-point correlation functions:

$$\Gamma_{ij}^{(2)}(p) = \delta_{ij} Z_\phi^{-1} [m^2 + p^2 + O(p^4)], \quad (8.5)$$

$$\Gamma_{ijkl}^{(4)}(0) = m Z_\phi^{-2} g_{ijkl}, \quad (8.6)$$

which relate the mass m and the zero-momentum quartic couplings g_{ijkl} to the corresponding Hamiltonian parameters r and u_{ijkl} . In addition, one introduces the function Z_t that is defined by the relation

$$\Gamma_{ij}^{(1,2)}(0) = \delta_{ij} Z_t^{-1}, \quad (8.7)$$

where $\Gamma^{(1,2)}$ is the (one-particle irreducible) two-point function with an insertion of $\frac{1}{2} \sum_i \phi_i^2$.

The fixed points of the theory are given by the common zeros g_{abcd}^* of the β -functions

$$\beta_{ijkl}(g_{abcd}) = m \left. \frac{\partial g_{ijkl}}{\partial m} \right|_{u_{abcd}}. \quad (8.8)$$

In the case of a continuous transition, when $m \rightarrow 0$, the couplings g_{ijkl} are driven toward an infrared-stable zero g_{ijkl}^* of the β -functions. The absence of stable fixed points is usually considered as an indication of a first-order transition.

The stability properties of the fixed points are controlled by the eigenvalues ω_i of the matrix

$$\Omega_{ijkl,abcd} = \frac{\partial \beta_{ijkl}}{\partial g_{abcd}} \quad (8.9)$$

computed at the given fixed point: a fixed point is stable if all eigenvalues ω_i are positive. The smallest

eigenvalue ω determines the leading scaling corrections, which vanish as $m^\omega \sim |t|^\Delta$ where $\Delta = \nu\omega$.

The critical exponents are then obtained by evaluating the RG functions

$$\eta_\phi(g_{ijkl}) = \frac{\partial \ln Z_\phi}{\partial \ln m}, \quad (8.10)$$

$$\eta_t(g_{ijkl}) = \frac{\partial \ln Z_t}{\partial \ln m} \quad (8.11)$$

at the fixed point g_{ijkl}^* :

$$\eta = \eta_\phi(g_{ijkl}^*), \quad (8.12)$$

$$\nu = [2 - \eta_\phi(g_{ijkl}^*) + \eta_t(g_{ijkl}^*)]^{-1}. \quad (8.13)$$

From the perturbative expansion of the correlation functions $\Gamma^{(2)}$, $\Gamma^{(4)}$ and $\Gamma^{(1,2)}$ and the above relations, one derives the expansion of the RG functions β_{ijkl} , η_ϕ and η_t in powers of g_{ijkl} .

In the alternative ϵ -expansion approach one may renormalize the theory using the minimal scheme (or the $\overline{\text{MS}}$ scheme), determine the common zeroes of the β -functions as series in powers of ϵ , and then obtain the ϵ -series of the critical exponents by substituting them in the RG functions $\eta(g_{ijkl})$ and $\nu(g_{ijkl})$, similarly to the fixed-dimension case. In this approach one obtains a different ϵ -expansion for each fixed point. A strictly related scheme is the so-called minimal-subtraction renormalization scheme without ϵ -expansion [683], in which after performing the minimal subtraction one sets $\epsilon = 1$ and analyzes the resulting expansion.

The resummation of the perturbative series can be performed by generalizing to series of more than one variable the methods of Sec. 2.4.3. For this purpose, the knowledge of the large-order behavior of the coefficients is useful. For some models with two quartic couplings, u and v say, the large-order behavior of the perturbative expansion in u and v at v/u fixed is reported in Refs. [204, 638, 644].

8.3 The LGW Hamiltonian with cubic anisotropy

Magnets with cubic symmetry are often described in terms of an $O(3)$ -symmetric Hamiltonian. However, this is correct if the nonrotationally invariant interactions that have only the reduced symmetry of the lattice are irrelevant in the RG sense. Standard considerations based on the canonical dimensions of the operators indicate that there are two terms that one may add to the Hamiltonian and that are cubic invariant: a cubic hopping term $\sum_{\mu=1,3} (\partial_\mu \phi_\mu)^2$ and a cubic interaction term $\sum_{\mu=1,3} \phi_\mu^4$. The first interaction was studied in Refs. [11, 14, 153, 588, 590]. A two-loop $O(\epsilon^2)$ calculation indicates that it is irrelevant at the

symmetric point, although it induces slowly-decaying crossover effects. In order to study the effect of the cubic interaction one considers a three-dimensional ϕ^4 theory with two quartic couplings [12, 14]:

$$\mathcal{H}_{\text{cubic}} = \int d^d x \left\{ \frac{1}{2} \sum_{i=1}^N [(\partial_\mu \phi_i)^2 + r \phi_i^2] + \frac{1}{4!} \sum_{i,j=1}^N (u_0 + v_0 \delta_{ij}) \phi_i^2 \phi_j^2 \right\}. \quad (8.14)$$

The added cubic term breaks explicitly the $O(N)$ invariance of the model, leaving a residual discrete cubic symmetry given by the reflections and permutations of the field components.

The theory defined by the Hamiltonian (8.14) has four fixed points [12, 14]: the trivial Gaussian one, the Ising one in which the N components of the field decouple, the $O(N)$ -symmetric and the cubic fixed points. The Gaussian fixed point is always unstable, and so is the Ising fixed point for any number of components N . Indeed, at the Ising fixed point one may interpret the cubic Hamiltonian as the Hamiltonian of N Ising systems coupled by the $O(N)$ -symmetric interaction, which is the sum of the products of the energy operators of the different Ising models. Therefore, at the Ising fixed point, the crossover exponent associated with the $O(N)$ -symmetric quartic term is given by the specific-heat critical exponent α_I of the Ising model, independently of N [14, 675]. Since $\alpha_I > 0$, the Ising fixed point is unstable independently of N . Thus, the Ising fixed point is a tricritical point with Ising-like exponents. On the other hand, the stability properties of the $O(N)$ -symmetric and of the cubic fixed points depend on N . For sufficiently small values of N , $N < N_c$, the $O(N)$ -symmetric fixed point is stable and the cubic one is unstable. For $N > N_c$, the opposite is true: the RG flow is driven towards the cubic fixed point, which now describes the generic critical behavior of the system, while the $O(N)$ -symmetric fixed point corresponds to a tricritical transition. Figure 16 sketches the flow diagram in the two cases $N < N_c$ and $N > N_c$.

Outside the attraction domain of the fixed points, the flow goes away towards more negative values of u and/or v and finally reaches the region where the quartic interaction no longer satisfies the stability condition. These trajectories should be related to first-order phase transitions. Indeed, in mean-field theory, the violation of the positivity conditions

$$u + v > 0, \quad Nu + v > 0, \quad (8.15)$$

leads to first-order transitions³¹. It is worth men-

³¹ RG trajectories leading to unstable regions have been con-

tioning that, for $v_0 \rightarrow -\infty$, one obtains the model described in Refs. [474, 475] in which the spins align along the lattice axes. A HT analysis on the fcc lattice indicates that these models have a first-order transition for $N \gtrsim 2$. This is consistent with the above argument that predicts the transition to be of first order for any $v_0 < 0$ and $N > N_c$. More general models, that have Eq. (8.14) as their continuous spin limit for $v_0 \rightarrow -\infty$, were also considered in Ref. [15]. The first-order nature of the transition for negative (small) v_0 and large N was also confirmed in Ref. [751].

If $N > N_c$, the cubic anisotropy is relevant and therefore the critical behavior of the system is not described by the $O(N)$ -symmetric theory. In this case, if the cubic interaction favors the alignment of the spins along the diagonals of the cube, i.e. for a positive coupling v , the critical behavior is controlled by the cubic fixed point and the cubic symmetry is retained even at the critical point. On the other hand, if the system tends to magnetize along the cubic axes — this corresponds to a negative coupling v — then the system undergoes a first-order phase transition [14, 15, 724, 751]. Moreover, since the symmetry is discrete, there are no Goldstone excitations in the LT phase. The longitudinal and the transverse susceptibilities are finite for $T < T_c$ and $H \rightarrow 0$, and diverge as $|t|^{-\gamma}$ for $t \propto T - T_c \rightarrow 0$. The equation of state for the cubic-symmetric critical theory has been calculated in Ref. [13] to $O(\epsilon)$ in the framework of the FT ϵ -expansion. For $N > N_c$ the $O(N)$ -symmetric fixed point represents a tricritical point.

One can derive exact expressions for the exponents at the cubic fixed point in the limit $N \rightarrow \infty$, keeping Nu and v fixed. Indeed, for $N \rightarrow \infty$ the system can be reinterpreted as a constrained Ising model [273], leading to a Fisher renormalization of the Ising critical exponents [302]. One has [10, 14, 273]:

$$\begin{aligned} \eta &= \eta_I + O\left(\frac{1}{N}\right), \\ \nu &= \frac{\nu_I}{1 - \alpha_I} + O\left(\frac{1}{N}\right), \end{aligned} \quad (8.16)$$

where η_I , ν_I , and α_I are the critical exponents of the Ising model.

If $N < N_c$, the cubic term in the Hamiltonian is irrelevant, and therefore, it generates only scaling corrections $|t|^{\Delta_c}$ with $\Delta_c > 0$. However, their presence leads to important physical consequences. For instance, the transverse susceptibility at the coexistence curve (i.e. for $T < T_c$ and $H \rightarrow 0$), which is divergent in the

sidered in the study of fluctuation-induced first-order transitions (see, e.g., Refs. [50, 671, 728]).

$O(N)$ -symmetric case, is now finite and diverges only at T_c as $|t|^{-\gamma - \Delta_c}$ [14, 143, 154, 464, 751]. In other words, below T_c , the cubic term is a “dangerous” irrelevant operator. Note that for N sufficiently close to N_c , irrespective of which fixed point is the stable one, the irrelevant interaction bringing from the unstable to the stable fixed point gives rise to very slowly decaying corrections to the leading scaling behavior.

In three dimensions, a simple argument based on the symmetry of the two-component cubic model [489] shows that the cubic fixed point is unstable for $N = 2$. Indeed, for $N = 2$, a $\pi/4$ internal rotation maps $\mathcal{H}_{\text{cubic}}$ into a new one of the same form but with new couplings (u'_0, v'_0) given by $u'_0 = u_0 + \frac{3}{2}v_0$ and $v'_0 = -v_0$. This symmetry maps the Ising fixed point onto the cubic one. Therefore, the two fixed points describe the same theory and have the same stability properties. Since the Ising point is unstable, the cubic point is unstable too, so that the stable point is the isotropic one. In two dimensions, this is no longer true. Indeed, one expects the cubic interaction to be truly marginal for $N = 2$ [441, 594, 635] and relevant for $N > 2$, and therefore $N_c = 2$ in two dimensions.

During the years, the model (8.14) has been the object of several studies [12, 140, 204, 207, 258, 288, 327, 356, 464, 483–485, 550, 551, 573, 588, 590, 592, 594, 694, 696, 743, 745]. In the 70’s several computations were done using the ϵ -expansion [12, 140, 464, 592], and predicted $3 < N_c < 4$, indicating that cubic magnets may be described by the $O(3)$ -invariant Heisenberg model. More recent FT studies have questioned this conclusion, and provided a robust evidence that $N_c < 3$, implying that the critical properties of cubic magnets are not described by the $O(3)$ -symmetric theory, but instead by the cubic model at the cubic fixed point. In Table 28 we report a summary of the results for N_c and, in the physically interesting case $N = 3$, for the smallest eigenvalues ω_2 of the stability matrix Ω .

The most recent FT perturbative analyses are based on the five-loop series in the framework of the ϵ -expansion of Ref. [483] and six-loop expansions in the fixed-dimension approach and of Ref. [204]. In Ref. [204] the analyses of the six-loop fixed-dimension expansions were done by exploiting Borel summability and the knowledge of the large-order behavior of the expansion in u and v at v/u fixed. In the analysis of five-loop ϵ -expansion, beside the large-order behavior of the series, the exact two-dimensional result $N_c = 2$ was also used to perform a constrained analysis [204] (for the method, see Sec. 2.4.3). In Ref. [327] the six-loop fixed-dimension series have been analyzed using the pseudo ϵ -expansion technique [505].

The results of the FT analysis, see Table 28, show that in the Heisenberg case, i.e. $N = 3$, the isotropic

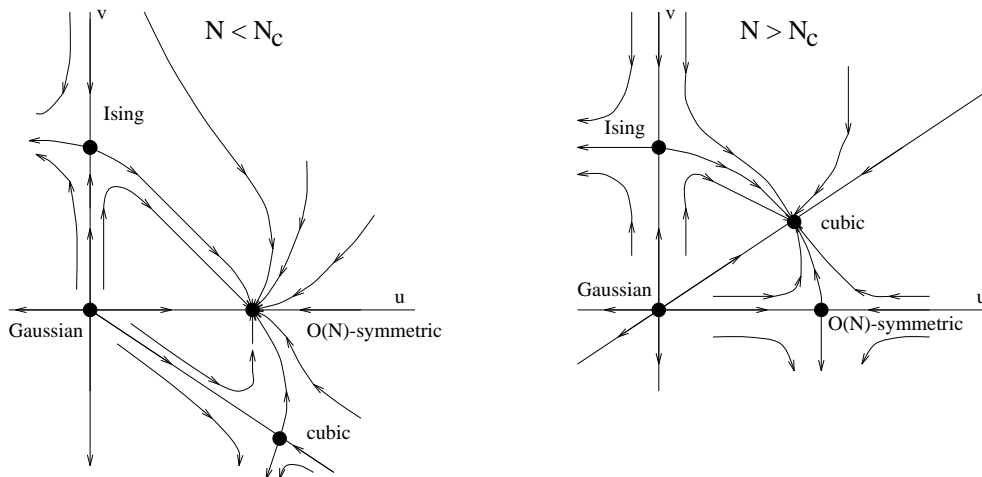


Figure 16: RG flow in the coupling plane (u, v) for $N < N_c$ and $N > N_c$ for magnetic systems with cubic anisotropy.

fixed point is unstable, while the cubic one is stable. Indeed, the smallest eigenvalue ω_2 is positive at the cubic fixed point and negative at the symmetric one, respectively $\omega_2 = 0.010(4)$ and $\omega_2 = -0.013(6)$ from the six-loop fixed-dimension analysis [204]. The other eigenvalue ω_1 turns out to be much larger, i.e. $\omega_1 = 0.781(4)$ at the cubic fixed point [204]. The critical value N_c is therefore smaller than three, but very close to it: all recent analyses indicate $N_c \approx 2.9$.

Note that, for the physically relevant case $N = 3$, the critical exponents do not differ appreciably from those of the isotropic model. The six-loop fixed-dimension analysis leads to the estimates [204]

$$\begin{aligned} \gamma &= 1.390(12), \\ \nu &= 0.706(6), \\ \eta &= 0.0333(26), \end{aligned} \tag{8.17}$$

while a recent reanalysis [359] of the fixed-dimension expansion of the three-dimensional $O(3)$ -symmetric models obtained $\gamma = 1.3895(50)$, $\nu = 0.7073(35)$ and $\eta = 0.0355(25)$, see Sec. 5.1.1. The difference is smaller than the precision of the estimates, which is approximately 1% for the exponents at the cubic fixed point. This tiny difference between the values at the two fixed points would be very difficult to ob-

serve, because of crossover effects decaying as t^Δ with $\Delta = \omega_{2,c}\nu_c = 0.007(3)$. Note that large corrections to scaling appear also for $N = 2$. Indeed, at the XY fixed point (the stable one), the subleading exponent ω_2 is given by $\omega_2 = 0.103(8)$ [204]. Thus, even though the cubic interaction is irrelevant, it induces strong scaling corrections behaving as t^Δ , $\Delta = \omega_2\nu \approx 0.06$.

8.4 The randomly dilute spin models.

The critical behavior of systems with quenched disorder is of considerable theoretical and experimental interest. A typical example is obtained by mixing an (anti)-ferromagnetic material with a non-magnetic one, obtaining the so-called dilute magnets. These materials are usually described in terms of a lattice short-range Hamiltonian of the form

$$\mathcal{H}_x = -J \sum_{\langle ij \rangle} \rho_i \rho_j \vec{s}_i \cdot \vec{s}_j, \tag{8.18}$$

where \vec{s}_i is an M -component spin and the sum is extended over all nearest-neighbor sites. The quantities ρ_i are uncorrelated random variables, which are equal to one with probability x (the spin concentration) and zero with probability $1 - x$ (the impurity concentration). The pure system corresponds to $x = 1$. One

Ref.	Method	Results
[327] 2000	$d = 3$ exp.: $O(g^6)$	$N_c = 2.862(5)$
[204] 2000	$d = 3$ exp.: $O(g^6)$	$\omega_{2,s} = -0.013(6)$, $\omega_{2,c} = 0.010(4)$, $N_c = 2.89(4)$
[204] 2000	ϵ -exp.: $O(\epsilon^5)$	$\omega_{2,s} = -0.003(4)$, $\omega_{2,c} = 0.006(4)$, $N_c = 2.87(5)$
[743] 2000	$d = 3$ exp.: $O(g^4)$	$\omega_{2,s} = -0.0081$, $\omega_{2,c} = 0.0077$, $N_c = 2.89(2)$
[207] 1998	MC	$\omega_{2,s} = 0.0007(29)$, $N_c \approx 3$
[694] 1997	ϵ -exp.: $O(\epsilon^5)$	$N_c \simeq 2.86$
[484, 485] 1995	ϵ -exp.: $O(\epsilon^5)$	$\omega_{2,s} = -0.00214$, $\omega_{2,c} = 0.00213$, $N_c < 3$
[483] 1995	ϵ -exp.: $O(\epsilon^5)$	$N_c \simeq 2.958$
[551] 1989	$d = 3$ exp.: $O(g^4)$	$\omega_{2,c} \simeq 0.008$, $N_c \simeq 2.91$
[594] 1982	scaling-field	$N_c \simeq 3.38$
[288] 1981	H.T. exp.: $O(\beta^{10})$	$\nu_s \omega_{2,s} = -0.63(10)$, $N_c < 3$
[745] 1977	approx. RG	$\nu_s \omega_{2,s} = -0.11$, $N_c \simeq 2.3$
[592] 1974	ϵ -exp.: $O(\epsilon^3)$	$N_c \simeq 3.128$

Table 28: Summary of the results in the literature. The values of the smallest eigenvalues ω_2 of the stability matrix Ω refer to $N = 3$. The subscripts “s” and “c” indicate that it is related to the symmetric and to the cubic fixed point respectively.

considers quenched disorder, since the relaxation time associated with the diffusion of the impurities is much larger than all other typical time scales, so that, for all practical purposes, one can consider the position of the impurities fixed. For sufficiently low spin dilution $1-x$, i.e. as long as one is above the percolation threshold of the magnetic atoms. the system described by the Hamiltonian \mathcal{H}_x undergoes a second-order phase transition at $T_c(x) < T_c(x = 1)$ (see, e.g., Ref. [712] for a review).

The relevant question in the study of this class of systems is the effect of disorder on the critical behavior. The Harris criterion [379] states that the addition of impurities to a system which undergoes a second-order phase transition does not change the critical behavior if the specific-heat critical exponent α_{pure} of the pure system is negative. If α_{pure} is positive, the transition is altered. Indeed the specific-heat exponent α_{random} in a disordered system is expected to be negative [17, 218, 533, 631, 698, 709]. Thus if α_{pure} is positive, α_{random} differs from α_{pure} , so that the pure system and the dilute one have a different critical behavior. In pure M -vector models with $M > 1$, the specific-heat exponent α_{pure} is negative; therefore, according to the Harris criterion, no change in the critical asymptotic behavior is expected in the presence of weak quenched disorder. This means that in these systems disorder leads only to irrelevant scaling corrections. Three-dimensional Ising systems are more interesting, since α_{pure} is positive. In this case, the presence of quenched impurities leads to a new universality class.

Theoretical investigations, using approaches based on the RG [14, 19, 118, 241, 273, 324–326, 353, 354, 380, 415, 416, 433, 437, 444, 465, 521, 547–549, 551, 593, 594,

618, 634, 693, 694, 696, 697, 743], and numerical MC simulations [80, 134, 135, 225, 401–403, 411, 418, 498, 544, 755, 756, 764, 776], support the existence of a new random Ising fixed point describing the critical behavior along the $T_c(x)$ line: the critical exponents are dilution independent (for sufficiently low dilution) and different from those of the pure Ising model.

Experiments confirm this picture. Crystalline mixtures of an Ising-like uniaxial antiferromagnet with short-range interactions (e.g. FeF_2 , MnF_2) with a non-magnetic material (e.g. ZnF_2) provide a typical realization of the random Ising model (RIM) (see, e.g., Refs. [90, 99, 100, 103, 104, 125, 264, 291, 398, 406, 565, 658, 667, 701–703, 731]). Some experimental results are reported in Table 29. This is not a complete list, but it gives an overview of the experimental state of the art. Recent reviews of the experiments can be found in Refs. [97, 98, 326]. The experimental estimates are definitely different from the values of the critical exponents for pure Ising systems. Moreover, they appear to be independent of concentration.

The presence of an external magnetic field along the uniaxial direction, dilute Ising systems present a different critical behavior, equivalent to that of the random-field Ising model [311], which is also the object of intensive theoretical and experimental investigations (see, e.g., Refs. [97, 98, 589]).

Several experiments also tested the effect of disorder on the λ -transition of ^4He that belongs to the XY universality class, corresponding to $M = 2$ [214, 297, 466, 738, 749, 788]. They studied the critical behaviour of ^4He completely filling the pores of porous gold or Vycor glass. The results indicate that the transition is in the same universality class of the λ -transition of

the pure system in agreement with the Harris criterion. Ref. [749] reports $\nu = 0.67(1)$ and Ref. [788] finds that the exponent ν is compatible with $2/3$. These estimates agree with the best results for the pure system reported in Sec. 4.2. Experiments for ${}^4\text{He}$ in aerogels find larger values for the exponent ν [214, 215, 580]. The current explanation of these results is that, in aerogels, the silica network is correlated to long distances, and therefore, the Harris criterion and the model studied in this paper do not apply. A simple model describing these materials has been studied in Ref. [509].

Also, the experiments on disordered magnetic materials of the isotropic random-exchange type show that the critical exponents are unchanged by disorder, see, e.g., Refs. [217, 655].

The randomly dilute Ising model (8.18) has been investigated by many numerical simulations (see, e.g., Refs. [80, 134, 135, 225, 401–403, 411, 498, 544, 755, 756, 764, 776]). The first simulations were apparently finding critical exponents depending on the spin concentration. Later Refs. [403, 433] remarked that this could be simply a crossover effect: the simulations were not probing the critical region and were computing effective exponents strongly affected by corrections to scaling. Recently, the critical exponents were computed using finite-size scaling techniques [80]. The authors found very strong corrections to scaling, decaying with a rather small exponent $\omega = 0.37(6)$, — correspondingly $\Delta = \omega\nu = 0.25(4)$ — which is approximately a factor of two smaller than the corresponding pure-case exponent. By taking into proper account the confluent corrections, they showed that the critical exponents are universal with respect to variations of the spin concentration in a wide interval above the percolation point. Their final estimates are [80]

$$\begin{aligned}\gamma &= 1.342(10), \\ \nu &= 0.6837(53), \\ \eta &= 0.0374(45).\end{aligned}\quad (8.19)$$

The starting point of the FT approach to the study of ferromagnets in the presence of quenched disorder is the LGW Hamiltonian [353]

$$\mathcal{H} = \int d^d x \left\{ \frac{1}{2} (\partial_\mu \phi(x))^2 + \frac{1}{2} r \phi(x)^2 + \frac{1}{2} \psi(x) \phi(x)^2 + \frac{1}{4!} g_0 [\phi(x)^2]^2 \right\}, \quad (8.20)$$

where $r \propto T - T_c$, and $\psi(x)$ is a spatially uncorrelated random field with Gaussian distribution

$$P(\psi) = \frac{1}{\sqrt{4\pi w}} \exp \left[-\frac{\psi^2}{4w} \right]. \quad (8.21)$$

We consider quenched disorder. Therefore, in order to obtain the free energy of the system, we must compute the partition function $Z(\psi, g_0)$ for a given distribution $\psi(x)$, and then average the corresponding free energy over all distributions with probability $P(\psi)$. By using the standard replica trick, it is possible to replace the quenched average with an annealed one. First, the system is replaced by N non-interacting copies with annealed disorder. Then, integrating over the disorder, one obtains the Hamiltonian [353]

$$\mathcal{H}_{MN} = \int d^d x \left\{ \sum_{i,a} \frac{1}{2} [(\partial_\mu \phi_{a,i})^2 + r \phi_{a,i}^2] + \sum_{ij,ab} \frac{1}{4!} (u_0 + v_0 \delta_{ij}) \phi_{a,i}^2 \phi_{b,j}^2 \right\}, \quad (8.22)$$

where $a, b = 1, \dots, M$ and $i, j = 1, \dots, N$. The original system, i.e. the dilute M -vector model, is recovered in the limit $N \rightarrow 0$. Note that the coupling u_0 is negative (being proportional to minus the variance of the quenched disorder), while the coupling v_0 is positive.

In this formulation, the critical properties of the dilute M -vector model can be investigated by studying the RG flow of the Hamiltonian (8.22) in the limit $N \rightarrow 0$, i.e. of \mathcal{H}_{M0} . One can then apply conventional computational schemes, such as the ϵ -expansion, the fixed-dimension $d = 3$ expansion, the scaling-field method, etc... In the RG approach, if the fixed point corresponding to the pure model is unstable and the RG flow moves towards a new random fixed point, then the random system has a different critical behavior.

In the RG approach one assumes that the replica symmetry is not broken. In recent years, however, this picture has been questioned [260–262] on the ground that the RG approach may not take into account other local minimum configurations of the random Hamiltonian (8.20), which may cause the spontaneous breaking of the replica symmetry.

For generic values of M and N , the Hamiltonian \mathcal{H}_{MN} describes M coupled N -vector models and it is usually called MN model [14]. Figure 17 sketches the expected flow diagram for Ising ($M = 1$) and multicomponent ($M > 1$) systems in the limit $N \rightarrow 0$. There are four fixed points: the trivial Gaussian one, an $O(M)$ -symmetric fixed point, a self-avoiding walk (SAW) fixed-point and a mixed fixed point. We recall that the region relevant for quenched disordered systems corresponds to negative values of the coupling u [19, 353]. The SAW fixed point is stable and corresponds to the (MN) -vector theory for $N \rightarrow 0$, but it is not of interest for the critical behavior of randomly dilute spin models, since it is located in the region $u > 0$. The stability of the other fixed points

Ref.	Material	x	γ	ν	α	β
[703] 1999	$\text{Fe}_x\text{Zn}_{1-x}\text{F}_2$	0.93	1.34(6)	0.70(2)		
[701] 1998	$\text{Fe}_x\text{Zn}_{1-x}\text{F}_2$	0.93			-0.10(2)	
[406] 1997	$\text{Fe}_x\text{Zn}_{1-x}\text{F}_2$	0.5				0.36(2)
[104] 1996	$\text{Fe}_x\text{Zn}_{1-x}\text{F}_2$	0.52				0.35
[103] 1995	$\text{Fe}_x\text{Zn}_{1-x}\text{F}_2$	0.5				0.35
[731] 1988	$\text{Mn}_x\text{Zn}_{1-x}\text{F}_2$	0.5				0.33(2)
[658] 1988	$\text{Mn}_x\text{Zn}_{1-x}\text{F}_2$	0.40, 0.55, 0.83			-0.09(3)	
[667] 1988	$\text{Fe}_x\text{Zn}_{1-x}\text{F}_2$	0.9				0.350(9)
[565] 1986	$\text{Mn}_x\text{Zn}_{1-x}\text{F}_2$	0.75	1.364(76)	0.715(35)		
[90] 1986	$\text{Fe}_x\text{Zn}_{1-x}\text{F}_2$	0.925 - 0.950				0.36(1)
[100] 1986	$\text{Fe}_x\text{Zn}_{1-x}\text{F}_2$	0.46	1.31(3)	0.69(1)		
[125] 1983	$\text{Fe}_x\text{Zn}_{1-x}\text{F}_2$	0.5, 0.6	1.44(6)	0.73(3)	-0.09(3)	
[264] 1981	$\text{Mn}_x\text{Zn}_{1-x}\text{F}_2$	0.864				0.349(8)

Table 29: Experimental estimates of the critical exponents for systems in the RIM universality class, taken from Ref. [326].

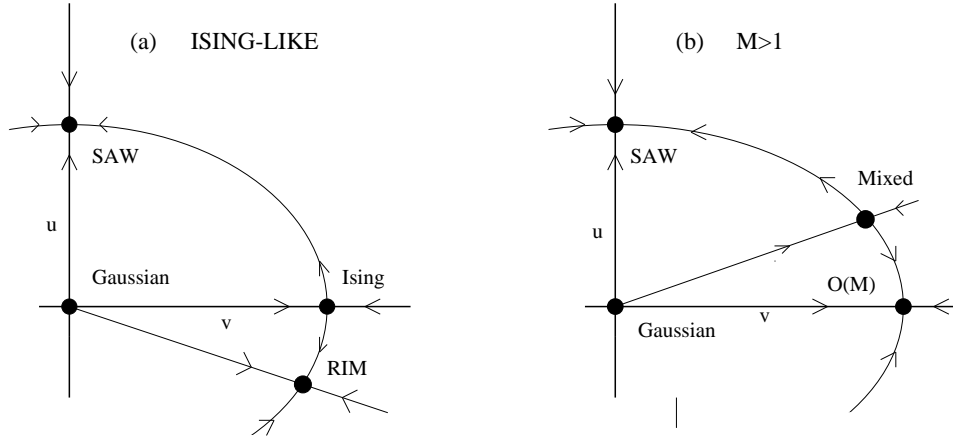


Figure 17: RG flow in the coupling plane (u, v) for (a) Ising ($M = 1$) and (b) M -component ($M > 1$) randomly dilute systems.

depends on the values of M . Simple nonperturbative arguments [14,675] show that the stability of the $O(M)$ fixed point is related to the specific-heat critical exponent of the $O(M)$ -symmetric theory. Indeed, \mathcal{H}_{MN} at the $O(M)$ -symmetric fixed point can be interpreted as the Hamiltonian of N M -vector systems coupled by the $O(MN)$ -symmetric term. Since this interaction is the sum of the products of the energy operators of the different M -vector models, the crossover exponent associated with the $O(MN)$ -symmetric quartic interaction should be given by the specific-heat critical exponent α_M of the M -vector model, independently of N . This implies that for $M = 1$ (Ising-like systems) the pure Ising fixed point is unstable since $\phi = \alpha_I > 0$, while for $M > 1$ the $O(M)$ fixed point is stable given that $\alpha_M < 0$, in agreement with the Harris criterium. For $M > 1$ the mixed fixed point is in the region of positive

u and is unstable [14]. Therefore, the RG flow of the M -component models with $M > 1$ is driven towards the pure $O(M)$ fixed point, and the quenched disorder yields correction to scaling proportional to the spin dilution and to $|t|^{\Delta_r}$ with $\Delta_r = -\alpha_M$. Note that for the physically interesting two- and three-vector models the absolute value of α_M is very small: $\alpha_2 \simeq -0.014$ and $\alpha_3 \simeq -0.12$. Thus, disorder gives rise to very slowly-decaying scaling corrections. For Ising-like systems, the pure Ising fixed point is instead unstable, and the flow for negative values of the quartic coupling u leads to the stable mixed or random fixed point which is located in the region of negative values of u . The above picture emerges clearly in the framework of the ϵ -expansion, although for the Ising-like systems the RIM fixed point is of order $\sqrt{\epsilon}$ [465] rather than ϵ .

The Hamiltonian \mathcal{H}_{MN} has been the object of sev-

eral FT studies, especially for $M = 1$, the case that describes the RIM. Several computations have been done in the framework of the ϵ -expansion and of the fixed-dimension $d = 3$ expansion. In Table 30 we report a summary of the FT results obtained for the RIM universality class.

The analysis of the FT expansions is made more difficult by the more complicated analytic structure of the field theory corresponding to quenched disordered models. This issue has been investigated in zero dimensions. The large-order behavior of the double expansion in the quartic couplings u and v of the free energy shows that the expansion in powers of v , keeping the ratio u/v fixed, is not Borel summable [137]. Ref. [554] showed that the non-Borel summability is a consequence of the fact that, because of the quenched average, there are additional singularities corresponding to the zeroes of the partition function $Z(\psi, g_0)$ obtained from the Hamiltonian (8.20). The problem was reconsidered in Ref. [28]. In the same context of the zero-dimensional model, it was shown that a more elaborate resummation can provide the correct determination of the free energy from its perturbative expansion. The procedure is still based on a Borel summation, which is performed in two steps: first, one resums in the coupling v each coefficient of the series in u ; then, one resums the resulting series in the coupling u . There is no proof that this procedure works also in higher dimensions, since the method relies on the fact that the zeroes of the partition function stay away from the real values of v . This is far from obvious in higher-dimensional systems.

The MN model has been extensively studied in the context of the ϵ -expansion [14, 19, 241, 353, 354, 380, 437, 465, 483, 521, 593, 634, 693, 694, 697]. Several studies also considered the equation of state [354, 593, 697] and the two-point correlation function [354, 634]. In spite of these efforts, studies based on the ϵ -expansion have been not able to go beyond a qualitative description of the physics of three-dimensional randomly dilute spin models. The $\sqrt{\epsilon}$ -expansion [465] turns out not to be effective for a quantitative study of the RIM (see, e.g., the analysis of the five-loop series done in Ref. [694]). The strictly related minimal-subtraction renormalization scheme without ϵ -expansion [683] was also considered. The three-loop [433] and four-loop [324–326] results were in reasonable agreement with the estimates obtained by other methods. At five loops, however, no random fixed point could be found [326] using this method. This negative result was interpreted as a consequence of the non-Borel summability of the perturbative expansion. In this case, the four-loop series could represent the “optimal” truncation.

The most precise FT results have been obtained

using the fixed-dimension expansion in $d = 3$. Several quantities have been computed: the critical exponents [325, 415, 416, 444, 547, 549, 551, 618, 644, 696, 743], the equation of state [118] and the hyperuniversal ratio R_ξ^+ [118, 548]. The RG functions of the MN model were calculated to six-loops in Ref. [644]. In the case relevant for the RIM universality class, i.e. $M = 1$ and $N \rightarrow 0$, several methods of resummation were applied. In Ref. [644] the method proposed in Ref. [28] was used. The analysis of the β -functions for the determination of the fixed point did not lead to a very robust estimate of the random fixed point. Nonetheless, the expansion of the RG functions associated to the exponents was largely insensitive to the exact position of the fixed point, and quite accurate estimates of the critical exponents were obtained, see Table 30.

Earlier analysis of the RIM series up to five-loops were done using Padé-Borel-Leroy approximants [618], thus assuming Borel summability. In spite of the fact that the series are not Borel summable, the results for the critical exponents turned out to be relatively stable, depending very little on the order of the series and the details of the analysis. They are in substantial agreement with the six-loop results of Ref. [644]. This fact may be explained by the observation of Ref. [137] that the Borel resummation applied in the standard way (i.e. at fixed v/u) gives a reasonably accurate result for small disorder if one truncates the expansion at an appropriate point, i.e. for not too long series.

The agreement among FT results, experiments, and MC estimates is overall good: The FT method appears to have a good predictive power, in spite of the complicated analytic structure of the Borel transform, that does not allow the direct application of the resummation methods used successfully in pure systems.

For $M \geq 2$ and $N = 0$ the analysis of the corresponding six-loop series shows that no fixed point exists in the region $u < 0$ and that the $O(M)$ -symmetric fixed point is stable [644], confirming the general argument relating its stability to the sign of the specific-heat critical exponent.

8.5 The critical behavior of frustrated spin models with noncollinear order

The critical behavior of frustrated spin systems with noncollinear or canted order has been the object of intensive theoretical and experimental studies (see, e.g., Refs. [226, 461] for recent reviews on this subject). Their critical behavior has been longly debated, FT RG methods, MC simulations and experiments providing contradictory results in many cases.

In physical magnets noncollinear order is due to frus-

Ref.	Method	γ	ν	η	ω
[644] 2000	$d = 3$ exp. $O(g^6)$	1.330(17)	0.678(10)	0.030(3)	0.25(10)
[618] 2000	$d = 3$ exp. $O(g^5)$	1.325(3)	0.671(5)	0.025(10)	0.32(6)
[325, 326] 2000	$d = 3$ MS $O(g^4)$	1.318	0.675	0.049	0.39(4)
[743] 2000	$d = 3$ exp. $O(g^4)$	1.336(2)	0.681(12)	0.040(11)	0.31
[547] 1989	$d = 3$ exp. $O(g^4)$	1.321	0.671		
	$d = 3$ exp. $O(g^4)$ ϵW	1.318	0.668		
[551] 1989	$d = 3$ exp. $O(g^4)$	1.326	0.670	0.034	
[594] 1982	scaling field	1.38	0.70		0.42

Table 30: FT estimates of the critical exponents for the RIM universality class. Here “ $d = 3$ exp.” denotes the massive scheme in three dimensions, “MS exp.” the minimal subtraction scheme without ϵ -expansion. All perturbative results have been obtained by means of Padé-Borel or Chisholm-Borel resummations, except the results of Ref. [547] indicated by “ ϵW ” obtained using the ϵ -algorithm of Wynn and of Ref. [644].

tration that may arise either because of the special geometry of the lattice, or from the competition of different kinds of interactions. Typical examples of systems of the first type are three-dimensional stacked triangular antiferromagnets (STA), where magnetic ions are located at each site of a three-dimensional stacked triangular lattice. Noncollinear ordering occurs for multicomponent spin systems. Examples are ABX_3 -type compounds, where A denotes elements such as Cs and Rb, B stands for magnetic ions such as Mn, Cu, Ni, and Co, and X for halogens as Cl, Br, and I. Their behavior at the chiral transition³² may be modeled by using short-ranged Hamiltonians for N -component spin variables defined on a stacked triangular lattice as

$$\mathcal{H}_{\text{STA}} = -J \sum_{\langle ij \rangle_{xy}} \vec{s}_i \cdot \vec{s}_j - J' \sum_{\langle ij \rangle_z} \vec{s}_i \cdot \vec{s}_j, \quad (8.23)$$

where $J < 0$, the first sum is over nearest-neighbor pairs within triangular layers (xy planes), and the second one is over orthogonal interlayer nearest neighbors. The sign of J' is not relevant, since there is no frustration along the direction orthogonal to the triangular layers. The condition $N \geq 2$ is essential to have noncollinear ordering. In these N -component spin systems the Hamiltonian is minimized by noncollinear configurations, showing a 120° spin structure. Frustration is partially released by mutual spin canting, and the degeneracy of the ground state is limited to global $O(N)$ spin rotations and reflections. As a consequence, at criticality there is a breakdown of the symmetry from $O(N)$ in the HT phase to $O(N-2)$ in the LT phase, implying a matrix-like order parameter. Frustration due to the competition of interactions may be realized in helimagnets where a magnetic spiral is formed along a

certain direction of the lattice. A simple model Hamiltonian of such systems is (see, e.g., Ref. [461])

$$\mathcal{H}_h = -J_1 \sum_{\langle ij \rangle_{nn}} \vec{s}_i \cdot \vec{s}_j - J_2 \sum_{\langle ij \rangle_{nn,z}} \vec{s}_i \cdot \vec{s}_j, \quad (8.24)$$

where the first sum represents nearest-neighbor ferromagnetic interactions, thus $J_1 > 0$, while the second one describes antiferromagnetic, $J_2 < 0$, next-nearest-neighbor interactions along only one crystallographic axis, z . Depending on the values of J_1 and J_2 , the competition of ferromagnetic and antiferromagnetic interactions may lead the spins to form a helical structure along the z -axis. The rare-earth metals Ho, Dy and Tb provide examples of such systems.

The critical behavior of two- and three-component frustrated spin models with noncollinear order is rather controversial. Many experiments are consistent with a second-order phase transition belonging to a new (chiral) universality class. Some experimental results are reported in Table 31 for two- and three-component systems. These are not complete lists, but they give an overview of the experimental state of the art. For a more extensive discussion, see Ref. [226]. Further experimental evidence in favor of a chiral continuous phase transition has been recently obtained by the experiment described in Ref. [648], where it was shown for an XY STA that chiral and spin order occur simultaneously, confirming the chiral nature of the transition.

On the theoretical side, the situation is less clear. The critical behavior of frustrated spin models with noncollinear order has been much studied by FT RG methods [45, 47, 53, 63, 71, 86, 334, 439, 458, 459, 520, 638, 732, 750, 796].

On the one hand, the perturbative FT approach shows the presence of a stable chiral fixed point in both $N = 2$ and $N = 3$ cases [638], with exponents in substantial agreement with experiments. These re-

³² The phase diagram of these systems is discussed in some detail in Ref. [226].

		γ	ν	β	α
$N = 2$	CsMnBr ₃	1.10(5) [448]	0.57(3) [448]	0.25(1) [448]	0.39(9) [754]
		1.01(8) [545]	0.54(3) [545]	0.22(2) [545]	0.40(5) [252]
	CsNiCl ₃			0.24(2) [336]	
				0.243(5) [275]	0.37(8) [96]
	CsMnI ₃				0.342(5) [274]
FT	1.10(4)	0.57(3)	0.31(2)	0.34(6) [96]	
$N = 3$	VCl ₂	1.05(3) [449]	0.62(5) [449]	0.20(2) [449]	
	VBr ₂				0.30(5) [782]
	RbNiCl ₃			0.28(1) [614]	
	CsNiCl ₃			0.28(3) [275]	0.25(8) [96]
					0.23(4) [274]
	FT	1.06(5)	0.55(3)	0.30(2)	0.28(6) [757]
				0.35(9)	

Table 31: Experimental estimates of the critical exponents for two- and three-component systems. For comparison we also report the field-theoretic (FT) estimates of Ref. [638].

	Ref.	γ	ν	β	α
$N = 2$	[460]	1.13(5)	0.54(2)	0.253(10)	0.34(6)
	[649]	1.03(4)	0.50(1)	0.24(2)	0.46(10)
	[133]	1.15(5)	0.48(2)	0.25(2)	0.46(10)
$N = 3$	[460]	1.17(7)	0.59(2)	0.30(2)	0.24(8)
	[121]	1.176(20)	0.585(9)	0.289(10)	
	[539]	1.185(3)	0.586(8)	0.285(11)	
	[517]	1.25(3)	0.59(1)	0.30(2)	

Table 32: Results of MC simulations for two- and three-component stacked-triangular antiferromagnets.

sults were obtained by an analysis of the six-loop series in the framework of the fixed-dimension expansion [638]. We mention that earlier studies based on three-loop series in the same approach [45, 520] and in the ϵ -expansion framework [47] did not find evidences of such fixed points.

On the other hand, studies based on approximate solutions of continuous RG equations (CRG) [732, 796] favor a weak first order transition, since no evidence of stable fixed points was found. Ref. [796] employed a local potential approximation, while Ref. [732] used a more refined approximation that allowed for an anomalous scaling of the field and therefore for a nontrivial value of η . Since a stable fixed point is not found, these systems should undergo a first-order transition. The authors of Refs. [732, 796] then explained the experimental results by making the hypothesis that the transition is weak enough to effectively appear as a second-order one in experimental works. The weakness of the transition was supported by the observation of a range of parameters in which the flow was very slow, with effective critical exponents close to those found in

experiments: $\nu = 0.53$, $\gamma = 1.03$, $\beta = 0.28$ for $N = 3$.

MC simulations (see, e.g., Refs. [121, 133, 253, 256, 456, 457, 460, 494, 517, 539, 649]) have not been very helpful in setting the question. Simulations of the STA Hamiltonian observe second-order phase transitions but, as it can be seen from Table 32, the numerical results for the critical exponents are not in quantitative agreement among the different authors. This may be taken as evidence that these simulations did not really probe the critical region—in MC studies neglected corrections to scaling may cause large systematic deviations on the final results—but also as evidence for a first-order transition: in this case, in the simulations one would measure effective exponents which depend on the specific Hamiltonian parameters. Additionally, some of the MC simulations of the stacked-triangular antiferromagnetic spin models [133, 517] yield a negative estimate of the critical exponent $\eta = 2 - \gamma/\nu$, see Table 32. But this is not acceptable for a continuous transition, because unitarity would be violated in the corresponding quantum field theory [628, 792] (one may show that the model (8.18) is reflection positive

and thus the corresponding field theory should be unitary). This fact has been interpreted as an additional indication in favor of the first-order transition hypothesis [519, 520].

A clear evidence for a first-order transition was observed in MC investigations [518, 519] of modified lattice spin systems which, according to general universality ideas, should belong to the same universality class of the Hamiltonian (8.23). But, it should be noted that the presence of a stable fixed point does not exclude the possibility that some systems undergo a first-order transition. Indeed, within the RG approach, first-order transitions are still possible for systems that are outside the attraction domain of the chiral fixed point. In this case, the RG flow would run away to a first-order transition. This means that, even if some systems show a universal continuous transition related to presence of a stable fixed point, other systems—for instance, those considered in the numerical MC studies of Refs. [518, 519]—may exhibit a first-order transition (see, e.g., the discussion on this issue of Ref. [461]). The different behavior of these systems is not due to the symmetry, but arises from the particular values of certain microscopic parameters, which may be or not be in the attraction domain of the stable fixed point.

FT studies of systems with noncollinear order are based on the $O(N) \times O(M)$ symmetric Hamiltonian [459, 461]

$$\mathcal{H} = \int d^d x \left\{ \frac{1}{2} \sum_a [(\partial_\mu \phi_a)^2 + r \phi_a^2] + \frac{1}{4!} u_0 \left(\sum_a \phi_a^2 \right)^2 + \frac{1}{4!} v_0 \sum_{a,b} [(\phi_a \cdot \phi_b)^2 - \phi_a^2 \phi_b^2] \right\}, \quad (8.25)$$

where ϕ_a ($1 \leq a \leq M$) are M sets of N -component vectors.³³ The case $M = 2$ with $v_0 > 0$ describes frustrated systems with noncollinear ordering such as STA's. Negative values of v_0 correspond to simple ferromagnetic or antiferromagnetic ordering, and to magnets with sinusoidal spin structures [459]. It is worth mentioning that the Hamiltonian (8.25) with $M = 2$ should be relevant also in other physical contexts, such as the transition from a normal to a superfluid phase of ^3He [71, 440], the superconducting phase transition of the heavy-fermion superconductor such as UPt_3 [443], and the quantum phase transition of a certain Josephson junction array in a magnetic field [348] (see also Ref. [45] for a discussion of these systems).

³³The effective Hamiltonian (8.25) can be obtained from the spin model (8.23) by using the Hubbard-Stratonovich transformation that allows to replace the fixed-length spins with variables of unconstrained length, by expanding around the instability points and dropping terms beyond quartic order [459].

We mention that for $M = 2$ the LGW Hamiltonian (8.25) can be also written in terms of a N -component complex field ψ as [45]

$$\mathcal{H} = \int d^d x \left[\frac{1}{2} (\partial_\mu \psi^* \partial_\mu \psi + r \psi^* \psi) + \frac{1}{4!} y_0 (\psi^* \cdot \psi)^2 + \frac{1}{4!} w_0 |\psi \cdot \psi|^2 \right]. \quad (8.26)$$

The couplings of the models (8.25) and (8.26) are related by $y_0 = u_0 - v_0/2$ and $w_0 = v_0/2$.

For $N = 2$, which is the case relevant for the two-component frustrated systems with noncollinear order, an ϵ -expansion analysis indicates the presence of four fixed points: the Gaussian one, an XY fixed point, an $O(4)$ -symmetric and a mixed fixed point. Using non-perturbative arguments [231], one can show that the XY fixed point is the only stable one among them. This can be easily seen considering the field transformation [45, 348, 459]

$$\begin{aligned} \phi_{11} &= \frac{\phi'_{11} - \phi'_{22}}{\sqrt{2}}, & \phi_{12} &= \frac{\phi'_{12} - \phi'_{21}}{\sqrt{2}}, \\ \phi_{21} &= \frac{\phi'_{12} + \phi'_{21}}{\sqrt{2}}, & \phi_{22} &= \frac{\phi'_{11} + \phi'_{22}}{\sqrt{2}}, \end{aligned} \quad (8.27)$$

which maps, for $N = M = 2$, the $O(M) \times O(N)$ Hamiltonian into the MN model, cf. Eq. (8.22), with couplings $u'_0 = u_0 + v_0/2$ and $v'_0 = -v_0$. One may then use the same argument employed in the previous section to establish the stability of the $O(M)$ fixed point in the MN model, and conclude that the XY fixed point is stable. This fact is confirmed by the analysis of the six-loop fixed-dimension expansion, which also show that the $O(4)$ and mixed fixed points are unstable [638]. However, the region relevant for frustrated models, $v_0 > 0$, thus $v'_0 < 0$, is outside the domain of attraction of the XY fixed point, which is in the region $v_0 < 0$. For $N = 3$, one may easily show the existence of an $O(6)$ fixed point for $v_0 = 0$, which is expected to be unstable [461].

On the other hand, this analysis cannot exclude the existence of other fixed points in the region $v_0 > 0$, which are not predicted by the ϵ -expansion. The six-loop analysis of Ref. [638] in the framework of the fixed-dimension expansion—some details will be presented below—provided a rather robust evidence for the existence of a new stable fixed point in the XY and Heisenberg cases, corresponding to the conjectured chiral universality class, and contradicting earlier FT results based on shorter series, up to three-loops.

The fixed points of the theory are given by the common zeros of the β -functions $\beta_u(u, v)$ and $\beta_v(u, v)$,

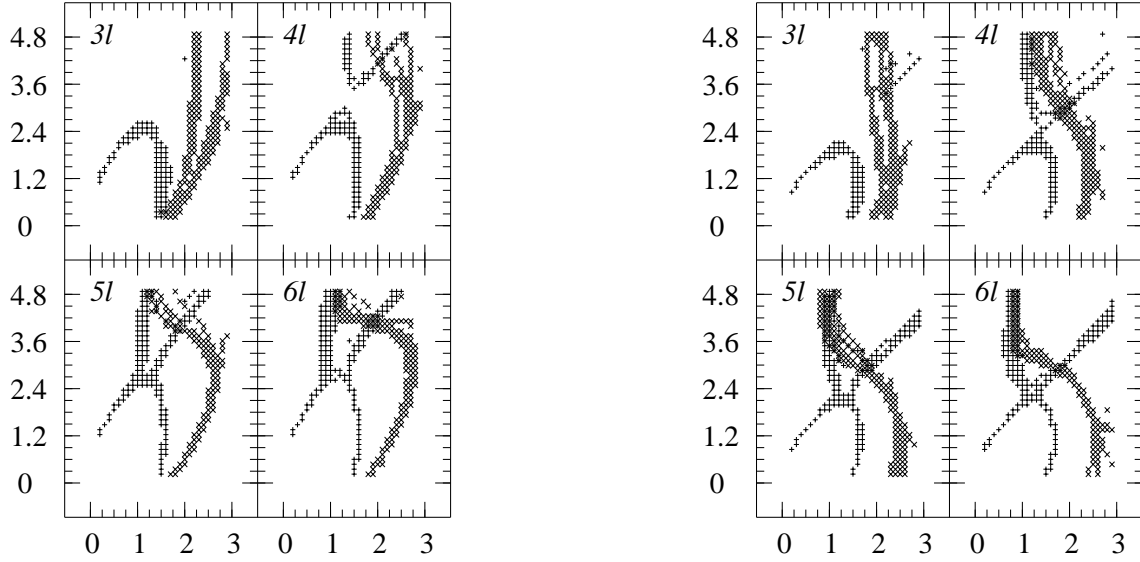


Figure 18: Zeros of the β -functions in the (\bar{u}, \bar{v}) plane. Pluses (+) and crosses (\times) correspond to zeros of $\beta_{\bar{u}}(\bar{u}, \bar{v})$ and $\beta_{\bar{v}}(\bar{u}, \bar{v})$ respectively. On the left we report the results for $N = 2$, on the right those for $N = 3$. Results from Ref. [638].

where u and v are the zero-momentum four-point renormalized couplings normalized so that, at tree level, $u \approx u_0$ and $v \approx v_0$. The six-loop series of the RG functions $\beta_u(u, v)$, $\beta_v(u, v)$, $\eta_\phi(u, v)$, and $\eta_t(u, v)$ and the large-order behavior of the expansion in $\bar{u} = 3u/(16\pi R_{2N})$ (where $R_K \equiv 9/(8 + K)$) and $\bar{v} = 3v/(16\pi)$ at fixed $z \equiv \bar{v}/\bar{u}$ were computed in Ref. [638]. The Borel transform turns out to have a singularity on the positive real axis for $z > 2R_{2N}$, which however is not the closest one for $z < 4R_{2N}$. Thus, for $z > 2R_{2N}$ the expansion is not Borel summable. The perturbative series was resummed by means of an appropriate conformal mapping [505] taking into account the large-order behavior of the perturbative series (at fixed z). The method was also used for those values of z for which the series is not Borel summable. Although in this case the sequence of approximations is only asymptotic, it should provide reasonable estimates as long as $z < 4R_{2N}$, since the leading large-order behavior is taken into account.

Figure 18 shows the zeros of the β -functions (computed for a set of approximants, see Ref. [638] for details), obtained from the analysis of the l -loop series, $l = 3, 4, 5, 6$. No fixed point is observed at three loops, consistently with the three-loop analysis of Ref. [45]. As the number of loops increases, a new fixed point—quite stable with respect to the number of loops—clearly appears for

$$\bar{u}^* = 1.9(1), \quad \bar{v}^* = 4.10(15), \quad \text{for } N = 2, \quad (8.28)$$

$$\bar{u}^* = 1.8(1), \quad \bar{v}^* = 3.00(15), \quad \text{for } N = 3. \quad (8.29)$$

Note that the appearance of such fixed points is essentially related to the appearance of a second upper branch of zeroes of the function $\beta_{\bar{u}}(\bar{u}, \bar{v})$, see Fig. 18. We should mention that the fixed points belong to the region in which the series are not Borel summable, but still satisfy $\bar{v}^*/\bar{u}^* < 4R_{2N}$, indeed $\bar{v}^*/\bar{u}^* \simeq 2.9R_4$ for $N = 2$ and $\bar{v}^*/\bar{u}^* \simeq 2.6R_6$ for $N = 3$. Therefore, the resummations should be still reliable, and the stability of the results with respect to the order of the series seems to confirm it. The analysis of the stability matrix shows that the fixed points (8.28) and (8.29) are stable, although does not provide reasonable estimates of the exponent ω determining the leading scaling corrections.

Figure 18 also suggests the presence of a second fixed point for smaller values of \bar{u} , say $\bar{u} \approx 1$, and thus, a RG flow diagram of the form reported in Fig. 19: indeed, beside the stable chiral fixed point C , an additional unstable (antichiral) one A should be present. In the analysis of the series its position turns out to be rather imprecise. This should be due to the fact that the relevant \bar{u} and \bar{v} belong to the region $\bar{v}/\bar{u} > 4R_{2N}$, where resummation methods should be less effective.

The estimates of the corresponding critical exponents are [638]

$$\begin{aligned} \gamma &= 1.13(5), \\ \nu &= 0.57(3), \\ \eta &= 0.09(1) \end{aligned} \quad (8.30)$$

for $N = 2$, and

$$\begin{aligned}\gamma &= 1.06(5), \\ \nu &= 0.55(3), \\ \eta &= 0.10(1)\end{aligned}\tag{8.31}$$

for $N = 3$. These results are in substantial agreement with the experimental and MC estimates, see Tables 31 and 32. Note that in both $N = 2$ and $N = 3$ cases the values of the exponent η are, although still rather small, considerably larger than those of the Ising and XY universality classes.

In the many-component limit $N \rightarrow \infty$ at fixed M , the $O(M) \times O(N)$ theory can be expanded in powers of $1/N$ [459, 461]. In the $1/N$ -expansion the transition in the noncollinear case, i.e. for $v > 0$, is continuous, and the exponents have been recently computed to $O(1/N^2)$ [638, 639] extending earlier calculations to $O(1/N)$ [459]. For $d = 3$ and $M = 2$ the critical exponents are given by

$$\begin{aligned}\nu &= 1 - \frac{16}{\pi^2} \frac{1}{N} - \left(\frac{56}{\pi^2} - \frac{640}{3\pi^4} \right) \frac{1}{N^2} + O\left(\frac{1}{N^3}\right), \\ \eta &= \frac{4}{\pi^2} \frac{1}{N} - \frac{64}{3\pi^4} \frac{1}{N^2} + O\left(\frac{1}{N^3}\right).\end{aligned}\tag{8.32}$$

In order to check the resummation of the fixed-dimension series, one may compare the above expressions with the six-loop results for sufficiently large values of N . For example, the six-loop analysis gives $\nu = 0.858(4)$ for $N = 16$ and $\nu = 0.936(2)$ for $N = 32$, which are in reasonable agreement with the estimates that one obtains from Eq. (8.32), i.e. $\nu = 0.885$ for $N = 16$ and $\nu = 0.946$ for $N = 32$.

Finally, we mention that for $5 \lesssim N \lesssim 7$ the picture obtained from the analysis of the 6-loop series is less clear and not conclusive. No fixed points appear that are sufficiently stable with respect to the number of loops. Thus, the analysis cannot be considered conclusive. These results may be explained by the traditional picture in which there is a particular value of N , $N_c \approx 6$, such that for $N > N_c$ there is a stable fixed point smoothly related to the large- N and small- ϵ chiral fixed point. For $N < N_c$ a first order transition is usually expected. However, the results of Ref. [638] for $N = 2, 3$ indicate that the situation may be more complicated and that a second value $3 < N_{c2} < N_c$ may exist such that for $N < N_{c2}$ the system shows again a chiral critical behavior with a fixed point unrelated to the small- ϵ chiral fixed point.

It is worth mentioning that for $N = 6$ MC simulations [520] and CRG calculations [732] provide evidence for a second-order phase transition, showing also a good agreement in the estimates of the critical exponents.

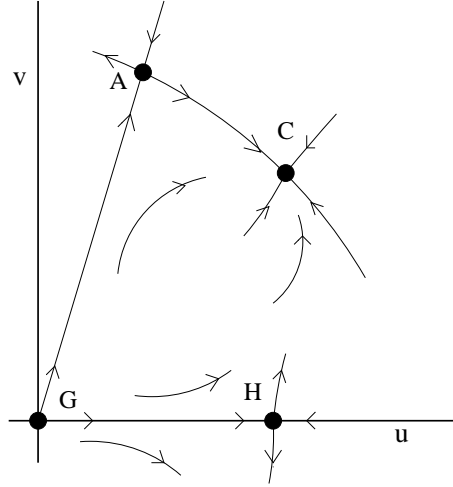


Figure 19: RG flow in the (u, v) plane for $N = 2, 3$.

In conclusion, different theoretical methods, such as MC, CRG and perturbative FT approaches provide contradictory results. Since all of them rely on unproved assumptions and different approximations, their comparison and consistency is essential before considering the issue substantially understood.

8.6 The tetragonal Landau-Ginzburg-Wilson Hamiltonian

In the following we study the critical behavior of statistical systems that are described by the three-coupling LGW Hamiltonian

$$\begin{aligned}\mathcal{H} &= \int d^d x \left\{ \sum_{i,a} \frac{1}{2} [(\partial_\mu \phi_{a,i})^2 + r \phi_{a,i}^2] \right. \\ &\quad \left. + \sum_{ij,ab} \frac{1}{4!} (u_0 + v_0 \delta_{ij} + w_0 \delta_{ij} \delta_{ab}) \phi_{a,i}^2 \phi_{b,j}^2 \right\}\end{aligned}\tag{8.33}$$

where $a, b = 1, \dots, M$ and $i, j = 1, \dots, N$. Note that, as particular cases, one may recover the MN model, for $w_0 = 0$, the $M \times N$ -component model with cubic anisotropy for $v_0 = 0$, and N decoupled M -component cubic models for $u_0 = 0$. The models with $M = 2$ are physically interesting: They should describe the critical properties in some structural and antiferromagnetic phase transitions [14, 63, 357, 576–579, 591, 685, 733]. Therefore, we will restrict ourselves to the case $M = 2$. In the following the Hamiltonian (8.33) with $M = 2$ will be named tetragonal.

We mention that in the literature the tetragonal Hamiltonian is also written in terms of a $2N$ -

component vector field ϕ_i :

$$\mathcal{H} = \int d^d x \left\{ \frac{1}{2} \sum_{i=1}^{2N} [(\partial_\mu \phi_i)^2 + r \phi_i^2] + \frac{1}{4!} z_1 \left(\sum_{i=1}^{2N} \phi_i^2 \right)^2 + \frac{1}{4!} z_2 \sum_{i=1}^{2N} \phi_i^4 + \frac{1}{4!} 2z_3 \sum_{j=1}^N \phi_{2j-1}^2 \phi_{2j}^2 \right\}. \quad (8.34)$$

The relations between the two sets of couplings are $z_1 = u_0$, $z_2 = v_0 + w_0$, and $z_3 = v_0$.

Many physical systems are expected to be described by the tetragonal Hamiltonian. Indeed, for $N = 2$ the tetragonal Hamiltonian should be relevant to the structural phase transitions in the NbO₂ crystal and, for $w_0 = 0$, to antiferromagnetic transitions in TbAu₂ and DyC₂. The case $N = 3$ is related to antiferromagnetic phase transitions in the K₂IrCl₆ crystal and, for $w_0 = 0$, to those in TbD₂ and Nd. Experimental results show continuous phase transitions in all the above-mentioned cases (see, e.g., Ref. [733] and references therein).

The ϵ -expansion analysis of the tetragonal Hamiltonian indicates the presence of eight fixed points [576–578]. In order to understand their physical properties, we observe that the tetragonal Hamiltonian is symmetric under the transformation [489]

$$(\phi_{1,i}, \phi_{2,i}) \longrightarrow \frac{1}{\sqrt{2}}(\phi_{1,i} + \phi_{2,i}, \phi_{1,i} - \phi_{2,i}), \quad (8.35)$$

which leaves it invariant with the change of couplings

$$(u_0, v_0, w_0) \longrightarrow (u_0, v_0 + \frac{3}{2}w_0, -w_0). \quad (8.36)$$

Let us discuss first the special cases when one of the couplings is zero. As already mentioned, the cases $u = 0$ and $v = 0$ reduce to cubic models, with N decoupled two-components in the first case, and with $2N$ components in the latter case. Since N is supposed to be larger than one, using the results reported in Sec. 8.3, we conclude that in the plane $u = 0$ the stable fixed point is the XY one, and the cubic and the Ising fixed points are equivalent because they can be related through the symmetry (8.36). On the other hand, in the plane $v = 0$ the stable fixed point is the cubic one. Figure 20 shows sketches of the flow diagram in the two planes $u = 0$ and $v = 0$.

In the case $w = 0$ the tetragonal Hamiltonian describes N coupled XY models. Such theories have four fixed points [14, 140]: the trivial Gaussian one, the XY one where the N XY models decouple, the $O(2N)$ -symmetric and the mixed tetragonal fixed points. The Gaussian one is never stable again. One

can argue that, at the XY fixed point, the crossover exponent related to the $O(2N)$ -symmetric interaction is given by $\phi = \alpha_{XY}$ [14, 231, 675], where α_{XY} is the specific heat exponent of the XY model. This prediction is again based on the observation that when $w = 0$ the tetragonal Hamiltonian describes N interacting XY models, and the $O(2N)$ -symmetric interaction can be represented as the product of two energy operators of the XY subsystems [675]. Since α_{XY} is negative, the XY fixed point should be stable with respect to the $O(2N)$ -symmetric interaction. In turn, one expects that the $O(2N)$ -symmetric and the tetragonal fixed points are unstable. The resulting sketch of the RG flow in the plane $w = 0$ is given by the case (A) of Fig. 21.

We have so identified seven out of eight fixed points. The eighth one can be obtained by applying the transformation (8.36) to the cubic fixed point lying in the $v_0 = 0$ plane. The cubic fixed point, which is stable in the $v = 0$ plane, turns out to be unstable with respect to the quartic interaction associated with the coupling v . This is clearly seen from the analyses of both the ϵ - and the fixed-dimension expansions.

Putting together all the above pieces of information, the XY fixed point turns out to be a stable fixed point of the tetragonal theory independently of the value of N , and the only one among the eight fixed points predicted by the ϵ -expansion. Thus the systems described by the tetragonal Hamiltonian are expected to have the same XY -like asymptotic critical behavior.

On the other hand, the global stability of the XY fixed point has been apparently contradicted by FT studies. The analysis of the two-loop ϵ -expansion [576–578] predicts a globally stable tetragonal fixed point, which is the one in the plane $w = 0$, and an unstable XY fixed point. In the plane $w = 0$ the predicted RG flow is that of the case (B) in Fig. 21. This fact should not come unexpected because $\alpha_{XY} = \epsilon/10 + O(\epsilon^2)$, so that, according to the arguments of Refs. [14, 231, 675], sufficiently close to $d = 4$ the fixed point describing N decoupled XY models is unstable and the tetragonal fixed point dominates the critical behavior. However, in order to obtain reliable results in three dimensions in the framework of the ϵ -expansion, higher-order calculations with a proper resummation of the series are necessary.

The RG flow (B) of Fig. 21 is further supported by recent higher-loop calculations. The stability of the tetragonal fixed point has been confirmed by calculations up to $O(\epsilon^4)$ in the framework of the ϵ -expansion [241, 572, 575]. The same result has been obtained by a Padè-Borel analysis of the three-loop series in the framework of the fixed-dimension expansion [696, 710]. However, we mention that the authors of Ref. [710],

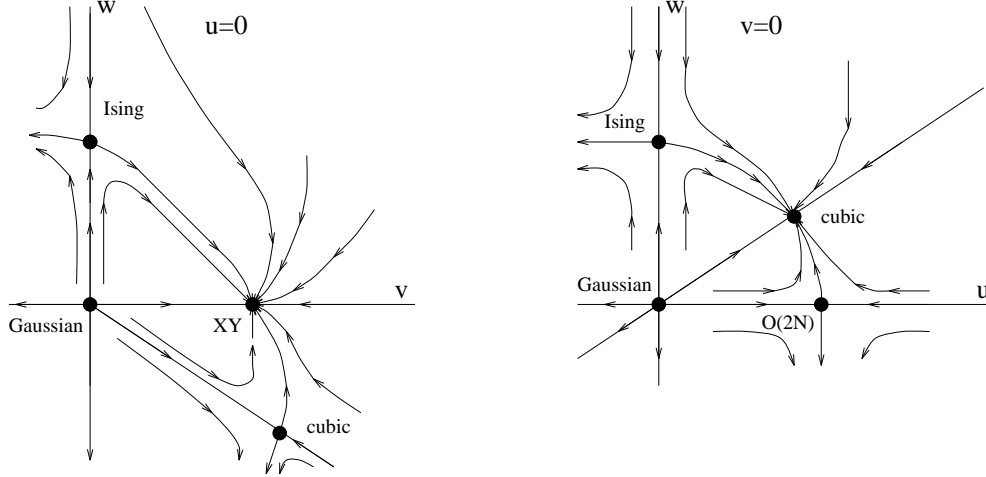


Figure 20: RG flow in the planes $u = 0$ and $v = 0$.

noting the closeness of the apparently stable tetragonal and unstable XY fixed points, argued that the respective stability-instability may be a misleading effect of the relatively few terms of the series.

In order to clarify this issue, we have extended the fixed-dimension expansion of the tetragonal Hamiltonian to six loops. Note that, since the tetragonal model for $w_0 = 0$ is nothing but the MN model with $M = 2$, the results of Sec. 8.5 show that, at least for $N = 2$, there is another stable fixed point in the region $v < 0$, whose presence is not predicted by the ϵ -expansion. In the following we will not investigate this issue, although it would be worthwhile to perform a more systematic study, but we will only focus on the stability properties of the XY fixed point.

The tetragonal FT theory is renormalized by introducing a set of zero-momentum conditions for the (one-particle irreducible) two-point and four-point correlation functions, such as Eq. (8.5) and

$$\Gamma_{ai,bj,ck,dl}^{(4)}(0) = mZ_\phi^{-2} \times (uA_{ai,bj,ck,dl} + vB_{ai,bj,ck,dl} + wC_{ai,bj,ck,dl}) \quad (8.37)$$

where, setting $\delta_{ai,bj} \equiv \delta_{ab}\delta_{ij}$,

$$\begin{aligned} A_{ai,bj,ck,dl} &= \frac{1}{3}(\delta_{ai,bj}\delta_{ck,dl} + \delta_{ai,ck}\delta_{bj,dl} + \delta_{ai,dl}\delta_{bj,ck}), \\ B_{ai,bj,ck,dl} &= \delta_{ij}\delta_{ik}\delta_{il} \frac{1}{3}(\delta_{ab}\delta_{cd} + \delta_{ac}\delta_{bd} + \delta_{ad}\delta_{bc}), \\ C_{ai,bj,ck,dl} &= \delta_{ij}\delta_{ik}\delta_{il} \delta_{ab}\delta_{ac}\delta_{ad}. \end{aligned} \quad (8.38)$$

The mass m , and the zero-momentum quartic couplings u , v and w are related to the corresponding Hamiltonian parameters by

$$u_0 = muZ_uZ_\phi^{-2},$$

$$\begin{aligned} v_0 &= mvZ_vZ_\phi^{-2}, \\ w_0 &= mwZ_wZ_\phi^{-2}. \end{aligned} \quad (8.39)$$

The fixed points of the theory are given by the common zeros of the β -functions $\beta_u(u, v, w)$, $\beta_v(u, v, w)$ and $\beta_w(u, v, w)$, associated with the couplings u , v and w respectively. Their stability properties are controlled by the matrix

$$\Omega = \begin{pmatrix} \frac{\partial\beta_u}{\partial u} & \frac{\partial\beta_u}{\partial v} & \frac{\partial\beta_u}{\partial w} \\ \frac{\partial\beta_v}{\partial u} & \frac{\partial\beta_v}{\partial v} & \frac{\partial\beta_v}{\partial w} \\ \frac{\partial\beta_w}{\partial u} & \frac{\partial\beta_w}{\partial v} & \frac{\partial\beta_w}{\partial w} \end{pmatrix} \quad (8.40)$$

We have computed the perturbative expansion of the two-point and four-point correlation functions to six loops. The diagrams contributing to this calculations are approximately 1000. We handled them with a symbolic manipulation program, which generates the diagrams and computes the symmetry and group factors of each of them. We did not calculate the integrals associated with each diagram, but we used the numerical results compiled in Ref. [602]. Summing all contributions we determined the RG functions to six loops. We report our results in terms of the rescaled couplings

$$u \equiv \frac{16\pi}{3} R_{2N} \bar{u} \quad v \equiv \frac{16\pi}{3} R_{2\bar{v}}, \quad w \equiv \frac{16\pi}{3} \bar{w}, \quad (8.41)$$

where $R_K = 9/(8 + K)$. The resulting series are

$$\begin{aligned} \beta_{\bar{u}} &= -\bar{u} + \bar{u}^2 + \frac{4}{5}\bar{u}\bar{v} + \frac{2}{3}\bar{u}\bar{w} \\ &\quad - \frac{2(95 + 41N)}{27(4 + N)^2}\bar{u}^3 - \frac{80}{27(4 + N)}\bar{u}^2\bar{v} \\ &\quad - \frac{200}{81(4 + N)}\bar{u}^2\bar{w} - \frac{92}{675}\bar{u}\bar{v}^2 - \frac{92}{729}\bar{u}\bar{w}^2 \end{aligned}$$

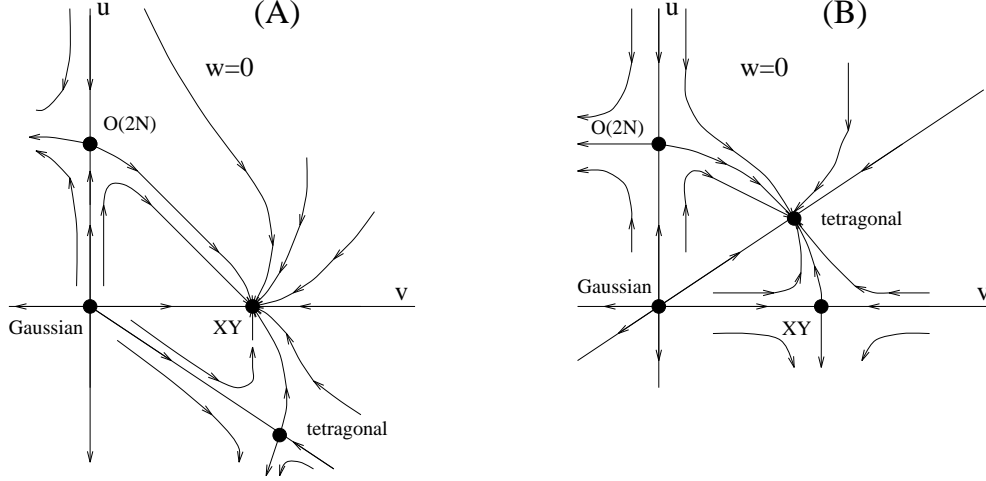


Figure 21: Two possibilities for the RG flow in the plane $w = 0$.

$$+\bar{u} \left(\sum_{i+j+k \geq 3} b_{ijk}^{(u)} \bar{u}^i \bar{v}^j \bar{w}^k \right), \quad (8.42)$$

$$\begin{aligned} \beta_{\bar{v}} = & -\bar{v} + \bar{v}^2 + \frac{6}{4+N} \bar{u}\bar{v} + \frac{2}{3} \bar{v}\bar{w} \\ & - \frac{272}{675} \bar{v}^3 - \frac{724}{135(4+N)} \bar{u}\bar{v}^2 \\ & - \frac{2(185+23N)}{27(4+N)^2} \bar{u}^2 \bar{v} - \frac{40}{81} \bar{v}^2 \bar{w} - \frac{92}{729} \bar{v}\bar{w}^2 \\ & + \bar{v} \left(\sum_{i+j+k \geq 3} b_{ijk}^{(v)} \bar{u}^i \bar{v}^j \bar{w}^k \right), \end{aligned} \quad (8.43)$$

$$\begin{aligned} \beta_{\bar{w}} = & -\bar{w} + \bar{w}^2 + \frac{6}{4+N} \bar{u}\bar{w} + \frac{6}{5} \bar{v}\bar{w} \\ & - \frac{308}{729} \bar{w}^3 - \frac{416}{81(4+N)} \bar{u}\bar{w}^2 \\ & - \frac{416}{405} \bar{v}\bar{w}^2 - \frac{2(185+23N)}{27(4+N)^2} \bar{u}^2 \bar{w} - \frac{416}{675} \bar{v}^2 \bar{w} \\ & + \bar{w} \left(\sum_{i+j+k \geq 3} b_{ijk}^{(w)} \bar{u}^i \bar{v}^j \bar{w}^k \right), \end{aligned} \quad (8.44)$$

$$\begin{aligned} \eta_{\phi} = & \frac{4(1+N)}{27(4+N)^2} \bar{u}^2 + \frac{16}{135(4+N)} \bar{u}\bar{v} \\ & + \frac{8}{81(4+N)} \bar{u}\bar{w} + \frac{8}{675} \bar{v}^2 \\ & + \frac{8}{405} \bar{v}\bar{w} + \frac{8}{729} \bar{w}^2 \\ & + \sum_{i+j+k \geq 3} e_{ijk}^{(\phi)} \bar{u}^i \bar{v}^j \bar{w}^k, \end{aligned} \quad (8.45)$$

$$\begin{aligned} \eta_t = & -\frac{1+N}{4+N} \bar{u} - \frac{2}{5} \bar{v} - \frac{1}{3} \bar{w} \\ & + \frac{1+N}{(4+N)^2} \bar{u}^2 + \frac{4}{5(4+N)} \bar{u}\bar{v} \\ & + \frac{2}{3(4+N)} \bar{u}\bar{w} + \frac{2}{25} \bar{v}^2 + \frac{4}{30} \bar{v}\bar{w} + \frac{2}{27} \bar{w}^2 \\ & + \sum_{i+j+k \geq 3} e_{ijk}^{(t)} \bar{u}^i \bar{v}^j \bar{w}^k. \end{aligned} \quad (8.46)$$

The coefficients $b_{ijk}^{(u)}$, $b_{ijk}^{(v)}$, $b_{ijk}^{(w)}$, $e_{ijk}^{(\phi)}$ and $e_{ijk}^{(t)}$ with $3 \leq i+j+k \leq 6$ are reported in the Tables 33, 34, 35, 36 and 37 respectively.

In the following we limit ourselves to check the stability of the XY fixed point, whose coordinates are $\bar{u}^* = 0$, $\bar{v}_{XY}^* = 1.402(4)$ [171, 359], and $\bar{w}^* = 0$. One can easily see that the eigenvalues of the stability matrix (8.40) at the XY fixed point are given simply by

$$\begin{aligned} \omega_1 &= \frac{\partial \beta_{\bar{u}}}{\partial \bar{u}}(0, \bar{v}_{XY}^*, 0), \\ \omega_2 &= \frac{\partial \beta_{\bar{v}}}{\partial \bar{v}}(0, \bar{v}_{XY}^*, 0), \\ \omega_3 &= \frac{\partial \beta_{\bar{w}}}{\partial \bar{w}}(0, \bar{v}_{XY}^*, 0). \end{aligned} \quad (8.47)$$

Note that ω_i are N -independent, as it can be checked looking at the corresponding series. According to the nonperturbative argument reported above, the XY fixed point is stable, and the smallest eigenvalue of the stability matrix Ω should be given by

$$\omega_1 = -\frac{\alpha_{XY}}{\nu_{XY}}, \quad (8.48)$$

where α_{XY} and ν_{XY} are the critical exponents of the XY model. In the analysis we exploited the knowledge

of the large-order behavior of the series, and therefore of the singularity of the Borel transform closest to the origin, which is determined by the XY fixed point only and therefore it is the same as the one of the $O(2)$ -symmetric theory. We skip the details, since the analysis is identical to that performed in Ref. [644] to study the stability of the $O(M)$ -symmetric fixed point in the MN model. Our estimate is

$$\omega_1 = 0.007(8). \quad (8.49)$$

The stability of the XY fixed point is substantially confirmed, although the apparent error of the analysis does not completely exclude the opposite sign for ω_1 . Moreover, the estimate of ω_1 turns out to be substantially consistent with the value one obtains using Eq. (8.48). Indeed $\alpha_{XY}/\nu_{XY} = -0.0217(12)$ using the recent estimates of the XY critical exponents of Ref. [171], and $\alpha_{XY}/\nu_{XY} = -0.016(7)$ and $\alpha_{XY}/\nu_{XY} = -0.010(9)$ using the estimates respectively of Ref. [359] and [505] obtained by a more similar technique, i.e. the analysis of the fixed-dimension expansion of the $O(2)$ -symmetric model. It is easy to see that ω_3 is equal to the smallest eigenvalue of stability matrix of the two-component cubic model at the XY fixed point, see Sec. 8.3, thus $\omega_3 = 0.103(8)$. The last eigenvalue ω_2 is much larger. It determines the scaling correction in the XY model and it is given by $\omega_2 = 0.789(11)$ [359].

In conclusion the analysis of the six-loop fixed-dimension expansion turns out to be substantially consistent with the nonperturbative prediction indicating the XY fixed point as globally stable independently of N .

i, j, k	$R_2^{-i} R_2^{-j} b_{ijk}^{(u)}$
3,0,0	$0.27385517 + 0.15072806 N + 0.0074016064 N^2$
2,1,0	$0.903231 + 0.072942424 N$
1,2,0	$0.60730385 + 0.0068245729 N$
0,3,0	0.13854816
2,0,1	$0.67742325 + 0.054706818 N$
1,1,1	$0.91095577 + 0.010236859 N$
0,2,1	0.31173336
1,0,2	$0.4154565 + 0.0051184297 N$
0,1,2	0.27646528
0,0,3	0.090448951
4,0,0	$-0.27925724 - 0.1836675 N - 0.021838259 N^2 + 0.00018978314 N^3$
3,1,0	$-1.2584488 - 0.22200749 N + 0.0032992093 N^2$
2,2,0	$-1.4679273 - 0.029437397 N$
1,3,0	$-0.65789001 - 0.0052472383 N$
0,4,0	-0.11873585
3,0,1	$-0.94383662 - 0.16650561 N + 0.002474407 N^2$
2,1,1	$-2.201891 - 0.044156096 N$
1,2,1	$-1.4802525 - 0.011806286 N$
0,3,1	-0.35620754
2,0,2	$-0.96497888 - 0.024920289 N$
1,1,2	$-1.3045513 - 0.010625658 N$
0,2,2	-0.47070809
1,0,3	$-0.42331874 - 0.0035418858 N$
0,1,3	-0.30532865
0,0,4	-0.075446692
5,0,0	$0.35174477 + 0.26485003 N + 0.045288106 N^2 + 0.00043866975 N^3 + 0.000013883029 N^4$
4,1,0	$2.0278677 + 0.51868097 N + 0.0059085942 N^2 + 0.00033898434 N^3$
3,2,0	$3.4214862 + 0.18321912 N + 0.0024313106 N^2$
2,3,0	$2.4773377 + 0.034202317 N$
1,4,0	$0.92541748 + 0.0039821066 N$
0,5,0	0.1462366
4,0,1	$1.5209008 + 0.38901073 N + 0.0044314456 N^2 + 0.00025423826 N^3$
3,1,1	$5.1322293 + 0.27482868 N + 0.0036469659 N^2$
2,2,1	$5.5740098 + 0.076955213 N$
1,3,1	$2.7762524 + 0.01194632 N$
0,4,1	0.54838726
3,0,2	$2.2073347 + 0.13067265 N + 0.00142597 N^2$
2,1,2	$4.8290973 + 0.066949343 N$
1,2,2	$3.5983005 + 0.016143463 N$
0,3,2	0.94562264
2,0,3	$1.5315693 + 0.021353803 N$
1,1,3	$2.2741668 + 0.010775585 N$
0,2,3	0.89377961
1,0,4	$0.56035196 + 0.0026938962 N$
0,1,4	0.44016041
0,0,5	0.087493302
6,0,0	$-0.5104989 - 0.4297050 N - 0.09535750 N^2 - 0.0040017345 N^3 + 0.00003226842 N^4 + 0.00000141045 N^5$
5,1,0	$-3.5978778 - 1.20182 N - 0.057714496 N^2 + 0.00061831126 N^3 + 0.000043766306 N^4$
4,2,0	$-8.0310329 - 0.80074836 N - 0.0021586547 N^2 + 0.00029396543 N^3$
3,3,0	$-8.2478554 - 0.20470296 N + 0.00055966931 N^2$
2,4,0	$-4.7055601 - 0.028798289 N$
1,5,0	$-1.4837563 - 0.0061256278 N$
0,6,0	-0.20437244
5,0,1	$-2.6984083 - 0.90136504 N - 0.043285872 N^2 + 0.00046373344 N^3 + 0.00003282473 N^4$
4,1,1	$-12.046549 - 1.2011225 N - 0.0032379821 N^2 + 0.00044094814 N^3$
3,2,1	$-18.557675 - 0.46058167 N + 0.0012592559 N^2$
2,3,1	$-14.11668 - 0.086394867 N$
1,4,1	$-5.5640863 - 0.022971104 N$
0,5,1	-0.91967597
4,0,2	$-5.1135549 - 0.53538355 N - 0.0025247004 N^2 + 0.00015530699 N^3$
3,1,2	$-15.854479 - 0.41049007 N + 0.00078044444 N^2$
2,2,2	$-18.106633 - 0.11544087 N$
1,3,2	$-9.5137746 - 0.03966586 N$
0,4,2	-1.964478
3,0,3	$-4.9317312 - 0.13514942 N + 0.00011311235 N^2$
2,1,3	$-11.278684 - 0.075967076 N$
1,2,3	$-8.8867987 - 0.0375632 N$
0,3,3	-2.4446492
2,0,4	$-2.754683 - 0.019167341 N$
1,1,4	$-4.3412061 - 0.01856332 N$
0,2,4	-1.7904475
1,0,5	$-0.86229463 - 0.003712664 N$
0,1,5	-0.71141747
0,0,6	-0.1179508

Table 33: The coefficients $b_{ijk}^{(u)}$, cf. Eq. (8.42).

i, j, k	$R_{2N}^{-i} R_{2N}^{-j} b_{ijk}^{(v)}$
3,0,0	0.64380517 + 0.11482552 N - 0.0068647863 N^2
2,1,0	1.97782 - 0.000039427734 N
1,2,0	1.5893912
0,3,0	0.43198483
2,0,1	1.2813995 - 0.0062019643 N
1,1,1	1.8846568
0,2,1	0.73213007
1,0,2	0.56468457
0,1,2	0.42057493
0,0,3	0.090448951
4,0,0	-0.76706177 - 0.17810933 N + 0.00016284548 N^2 - 0.00070068894 N^3
3,1,0	-3.2372708 - 0.11004576 N - 0.0010508505 N^2
2,2,0	-4.2003729 + 0.017778007 N
1,3,0	-2.3041302
0,4,0	-0.48457321
3,0,1	-2.117322 - 0.066630894 N - 0.0014713371 N^2
2,1,1	-5.1751293 + 0.019981131 N
1,2,1	-4.0752638
0,3,1	-1.1078678
2,0,2	-1.6595755 + 0.00505486 N
1,1,2	-2.4989894
0,2,2	-0.98989917
1,0,3	-0.5483926
0,1,3	-0.42686062
0,0,4	-0.075446692
5,0,0	1.0965348 + 0.31582586 N + 0.0094338525 N^2 - 0.00049177077 N^3 - 0.000086193996 N^4
4,1,0	5.9292953 + 0.40901849 N - 0.010102522 N^2 - 0.00031594921 N^3
3,2,0	10.739283 - 0.0048408111 N + 0.00072672306 N^2
2,3,0	9.0637188 - 0.058086499 N
1,4,0	3.8277762
0,5,0	0.66233546
4,0,1	3.9073944 + 0.26207189 N - 0.0068664349 N^2 - 0.00031886052 N^3
3,1,1	13.511919 - 0.017385016 N + 0.00047240741 N^2
2,2,1	16.458953 - 0.10118022 N
1,3,1	9.0245987
0,4,1	1.9145972
3,0,2	4.4690201 - 0.0072615868 N - 0.000071990874 N^2
2,1,2	10.482169 - 0.060013651 N
1,2,2	8.4121105
0,3,2	2.3394333
2,0,3	2.3860591 - 0.012232105 N
1,1,3	3.7649897
0,2,3	1.5529231
1,0,4	0.6859313
0,1,4	0.56304585
0,0,5	0.087493302
6,0,0	-1.774553 - 0.6080863 N - 0.03773523 N^2 + 0.0005359509 N^3 - 0.0001051598 N^4 - 0.00001200996 N^5
5,1,0	-11.741739 - 1.2643992 N + 0.011113177 N^2 - 0.0013773749 N^3 - 0.000070170026 N^4
4,2,0	-27.537411 - 0.39161313 N - 0.0024557833 N^2 - 0.000052719756 N^3
3,3,0	-31.89832 + 0.25340217 N - 0.0042556584 N^2
2,4,0	-20.465063 + 0.12482592 N
1,5,0	-7.0723339
0,6,0	-1.0395295
5,0,1	-7.7827796 - 0.8288997 N + 0.0078564644 N^2 - 0.0010207165 N^3 - 0.000063719952 N^4
4,1,1	-35.145003 - 0.47099755 N - 0.0052695631 N^2 - 0.00017352674 N^3
3,2,1	-59.094258 + 0.45356273 N - 0.0074832062 N^2
2,3,1	-49.340075 + 0.28869185 N
1,4,1	-20.9357
0,5,1	-3.6425627
4,0,2	-11.831866 - 0.15794071 N - 0.0024381429 N^2 - 0.00010567985 N^3
3,1,2	-38.56208 + 0.27559695 N - 0.0045217676 N^2
2,2,2	-47.222342 + 0.26270351 N
1,3,2	-26.292061
0,4,2	-5.6513079
3,0,3	-8.9681447 + 0.05667789 N - 0.00095212462 N^2
2,1,3	-21.590806 + 0.11456243 N
1,2,3	-17.822421
0,3,3	-5.0667675
2,0,4	-3.9823089 + 0.020527147 N
1,1,4	-6.5311036
0,2,4	-2.7738504
1,0,5	-1.0205971
0,1,5	-0.8660073
0,0,6	-0.1179508

Table 34: The coefficients $b_{ijk}^{(v)}$, cf. Eq. (8.43).

i, j, k	$R_{2N}^{-i} R_{2N}^{-j} b_{ijk}^{(w)}$
3,0,0	$0.64380517 + 0.11482552 N - 0.0068647863 N^2$
2,1,0	$2.2471073 + 0.0081904303 N$
1,2,0	2.2552977
0,3,0	0.75176591
2,0,1	$1.6853305 + 0.0061428227 N$
1,1,1	3.3829466
0,2,1	1.6914733
1,0,2	1.3138294
0,1,2	1.3138294
0,0,3	0.3510696
4,0,0	$-0.76706177 - 0.17810933 N + 0.00016284548 N^2 - 0.00070068894 N^3$
3,1,0	$-3.6514455 - 0.13125033 N - 0.00013991835 N^2$
2,2,0	$-5.7009462 + 0.026692512 N$
1,3,0	-3.7828358
0,4,0	-0.94570894
3,0,1	$-2.7385841 - 0.098437749 N - 0.00010493876 N^2$
2,1,1	$-8.5514193 + 0.040038768 N$
1,2,1	-8.5113805
0,3,1	-2.8371268
2,0,2	$-3.3477204 + 0.015083679 N$
1,1,2	-6.6652735
0,2,2	-3.3326368
1,0,3	-1.8071874
0,1,3	-1.8071874
0,0,4	-0.37652683
5,0,0	$1.0965348 + 0.31582586 N + 0.0094338525 N^2 - 0.00049177077 N^3 - 0.000086193996 N^4$
4,1,0	$6.6487314 + 0.46860779 N - 0.011049797 N^2 - 0.00020675107 N^3$
3,2,0	$14.201957 + 0.0086575882 N + 0.0015502926 N^2$
2,3,0	$14.309604 - 0.097439028 N$
1,4,0	7.1060826
0,5,0	1.4212165
4,0,1	$4.9865485 + 0.35145584 N - 0.0082873478 N^2 - 0.0001550633 N^3$
3,1,1	$21.302936 + 0.012986382 N + 0.0023254389 N^2$
2,2,1	$32.19661 - 0.21923781 N$
1,3,1	21.318248
0,4,1	5.329562
3,0,2	$8.3645284 + 0.0079241123 N + 0.00085452488 N^2$
2,1,2	$25.291106 - 0.17118531 N$
1,2,2	25.119921
0,3,2	8.373307
2,0,3	$6.8946012 - 0.046174799 N$
1,1,3	13.696853
0,2,3	6.8484264
1,0,4	2.8857918
0,1,4	2.8857918
0,0,5	0.49554751
6,0,0	$-1.774553 - 0.6080863 N - 0.03773523 N^2 + 0.0005359509 N^3 - 0.0001051598 N^4 - 0.00001200996 N^5$
5,1,0	$-13.10644 - 1.4235988 N + 0.011751068 N^2 - 0.0013937944 N^3 - 0.000055380116 N^4$
4,2,0	$-35.75223 - 0.54684266 N - 0.00034126582 N^2 + 0.000073209725 N^3$
3,3,0	$-48.800935 + 0.40885839 N - 0.0070450255 N^2$
2,4,0	$-36.538548 + 0.23920711 N$
1,5,0	-14.519736
0,6,0	-2.4199561
5,0,1	$-9.8298296 - 1.0676991 N + 0.0088133007 N^2 - 0.0010453458 N^3 - 0.000041535087 N^4$
4,1,1	$-53.628345 - 0.82026399 N - 0.00051189873 N^2 + 0.00010981459 N^3$
3,2,1	$-109.8021 + 0.91993139 N - 0.015851307 N^2$
2,3,1	$-109.61564 + 0.71762134 N$
1,4,1	-54.449012
0,5,1	-10.889802
4,0,2	$-21.073538 - 0.33257393 N - 0.000059310729 N^2 + 0.000035990819 N^3$
3,1,2	$-86.32735 + 0.71521067 N - 0.012400534 N^2$
2,2,2	$-129.28253 + 0.84571708 N$
1,3,2	-85.62454
0,4,2	-21.406135
3,0,3	$-23.569724 + 0.19143373 N - 0.00335616 N^2$
2,1,3	$-70.60619 + 0.46125161 N$
1,2,3	-70.144939
0,3,3	-23.381646
2,0,4	$-14.927998 + 0.097362599 N$
1,1,4	-29.661271
0,2,4	-14.830635
1,0,5	-5.1298717
0,1,5	-5.1298717
0,0,6	-0.74968893

Table 35: The coefficients $b_{ijk}^{(w)}$, cf. Eq. (8.44).

i, j, k	$R_{2N}^{-i} R_2^{-j} e_{ijk}^{(\phi)}$
3,0,0	0.00054176134 + 0.00067720168 N + 0.00013544034 N^2
2,1,0	0.0032505681 + 0.00081264201 N
1,2,0	0.0040632101
0,3,0	0.0013544034
2,0,1	0.002437926 + 0.00060948151 N
1,1,1	0.0060948151
0,2,1	0.0030474076
1,0,2	0.0027426668
0,1,2	0.0027426668
0,0,3	0.00091422227
4,0,0	0.00099254838 + 0.0014050361 N + 0.0004072464 N^2 - 0.00000524135 N^3
3,1,0	0.007940387 + 0.003299902 N - 0.000041930807 N^2
2,2,0	0.015997874 + 0.00079966371 N
1,3,0	0.011198358
0,4,0	0.0027995896
3,0,1	0.0059552903 + 0.0024749265 N - 0.000031448105 N^2
2,1,1	0.023996811 + 0.0011994956 N
1,2,1	0.025196306
0,3,1	0.0083987687
2,0,2	0.01046567 + 0.0006233387 N
1,1,2	0.022178008
0,2,2	0.011089004
1,0,3	0.0071848915
0,1,3	0.0071848915
0,0,4	0.0017962229
5,0,0	-0.00036659735 - 0.0005144234 N - 0.00012810644 N^2 + 0.000017944562 N^3 - 0.00000177505 N^4
4,1,0	-0.0036659735 - 0.0014782605 N + 0.00019719609 N^2 - 0.000017750472 N^3
3,2,0	-0.0099203383 - 6.3273844 10^{-6} N - 2.9110681 10^{-6} N^2
2,3,0	-0.010144693 + 0.00021511594 N
1,4,0	-0.0049647884
0,5,0	-0.00099295767
4,0,1	-0.0027494801 - 0.0011086954 N + 0.00014789707 N^2 - 0.000013312854 N^3
3,1,1	-0.014880507 - 0.0000094910766 N - 0.0000043666022 N^2
2,2,1	-0.022825558 + 0.00048401086 N
1,3,1	-0.014894365
0,4,1	-0.0037235913
3,0,2	-0.0064696069 - 0.0001404214 N + 0.000011129553 N^2
2,1,2	-0.020218951 + 0.00042225431 N
1,2,2	-0.019796696
0,3,2	-0.0065988988
2,0,3	-0.0066046286 + 0.00013518666 N
1,1,3	-0.012938884
0,2,3	-0.0064694419
1,0,4	-0.0032685176
0,1,4	-0.0032685176
0,0,5	-0.00065370353
6,0,0	0.0006956804 + 0.001131719 N + 0.0004822921 N^2 + 0.00004597358 N^3 - 6.141629 $\times 10^{-7}$ N^4 - 3.341208 $\times 10^{-7}$ N^5
5,1,0	0.0083481645 + 0.0052324614 N + 0.0005550435 N^2 - 0.000003360506 N^3 - 0.000004009449 N^4
4,2,0	0.029681932 + 0.0055879907 N + 0.000063895445 N^2 - 0.000013069175 N^3
3,3,0	0.045255621 + 0.0018393536 N - 0.000000643354 N^2
2,4,0	0.035188192 + 0.00013255707 N
1,5,0	0.014128299
0,6,0	0.0023547166
5,0,1	0.0062611234 + 0.0039243461 N + 0.00041628263 N^2 - 0.00000252038 N^3 - 0.00000300709 N^4
4,1,1	0.044522897 + 0.0083819861 N + 0.000095843167 N^2 - 0.000019603762 N^3
3,2,1	0.10182515 + 0.0041385456 N - 0.00000144755 N^2
2,3,1	0.10556457 + 0.00039767121 N
1,4,1	0.052981123
0,5,1	0.010596225
4,0,2	0.018957129 + 0.0036966089 N + 0.000049929976 N^2 - 0.00000604303 N^3
3,1,2	0.087124313 + 0.0036578184 N + 0.00000836604 N^2
2,2,2	0.13565945 + 0.00052629518 N
1,3,2	0.090790498
0,4,2	0.022697624
3,0,3	0.027158805 + 0.0011914092 N + 0.00000681736 N^2
2,1,3	0.084729031 + 0.00034206266 N
1,2,3	0.085071093
0,3,3	0.028357031
2,0,4	0.020775681 + 0.000082959153 N
1,1,4	0.041717279
0,2,4	0.02085864
1,0,5	0.0083268641
0,1,5	0.0083268641
0,0,6	0.0013878107

Table 36: The coefficients $e_{ijk}^{(\phi)}$, cf. Eq. (8.45).

i, j, k	$R_{2N}^{-i} R_2^{-j} e_{ijk}^{(t)}$
3,0,0	-0.025120499 - 0.033959839 N - 0.0088393396 N ²
2,1,0	-0.15072299 - 0.053036037 N
1,2,0	-0.19693446 - 0.0068245729 N
0,3,0	-0.067919677
2,0,1	-0.11304225 - 0.039777028 N
1,1,1	-0.29540169 - 0.010236859 N
0,2,1	-0.15281927
1,0,2	-0.13037154 - 0.0051184297 N
0,1,2	-0.13548997
0,0,3	-0.044310253
4,0,0	0.021460047 + 0.031381665 N + 0.0096237093 N ² - 0.0002979085 N ³
3,1,0	0.17168038 + 0.079372942 N - 0.002383268 N ²
2,2,0	0.34992416 + 0.023080916 N
1,3,0	0.24342282 + 0.0052472383 N
0,4,0	0.062167514
3,0,1	0.12876028 + 0.059529707 N - 0.001787451 N ²
2,1,1	0.52488625 + 0.034621375 N
1,2,1	0.54770134 + 0.011806286 N
0,3,1	0.18650254
2,0,2	0.22779178 + 0.018651276 N
1,1,2	0.48226044 + 0.010625658 N
0,2,2	0.24644305
1,0,3	0.15630733 + 0.0035418858 N
0,1,3	0.15984922
0,0,4	0.039519569
5,0,0	-0.022694287 - 0.035970337 N - 0.014334154 N ² - 0.0010852931 N ³ - 0.000027188944 N ⁴
4,1,0	-0.22694287 - 0.1327605 N - 0.010581042 N ² - 0.00027188944 N ³
3,2,0	-0.63724955 - 0.10204751 N - 0.001815526 N ²
2,3,0	-0.71184836 - 0.029264231 N
1,4,0	-0.36657419 - 0.0039821066 N
0,5,0	-0.074111259
4,0,1	-0.17020715 - 0.099570372 N - 0.0079357814 N ² - 0.00020391708 N ³
3,1,1	-0.95587433 - 0.15307127 N - 0.002723289 N ²
2,2,1	-1.6016588 - 0.06584452 N
1,3,1	-1.0997226 - 0.01194632 N
0,4,1	-0.27791722
3,0,2	-0.40917573 - 0.069076759 N - 0.0011577274 N ²
2,1,2	-1.3803599 - 0.057870795 N
1,2,2	-1.4220872 - 0.016143463 N
0,3,2	-0.47941022
2,0,3	-0.43464785 - 0.018711401 N
1,1,3	-0.89594291 - 0.010775585 N
0,2,3	-0.45335925
1,0,4	-0.22065482 - 0.0026938962 N
0,1,4	-0.22334872
0,0,5	-0.044400355
6,0,0	0.02945062 + 0.04974916 N + 0.02291359 N ² + 0.002524629 N ³ - 0.0000937390 N ⁴ - 0.00000331952 N ⁵
5,1,0	0.35340743 + 0.24358247 N + 0.031380583 N ² - 0.001085034 N ³ - 0.000039834265 N ⁴
4,2,0	1.2683391 + 0.29843736 N + 0.0015241225 N ² - 0.00018653681 N ³
3,3,0	1.9585171 + 0.13258978 N - 0.00028820443 N ²
2,4,0	1.5348918 + 0.033222225 N
1,5,0	0.62111998 + 0.0061256277 N
0,6,0	0.10454094
5,0,1	0.26505557 + 0.18268685 N + 0.023535437 N ² - 0.00081377552 N ³ - 0.000029875699 N ⁴
4,1,1	1.9025086 + 0.44765603 N + 0.0022861838 N ² - 0.00027980522 N ³
3,2,1	4.4066635 + 0.298327 N - 0.00064845996 N ²
2,3,1	4.6046754 + 0.099666674 N
1,4,1	2.3291999 + 0.022971104 N
0,5,1	0.47043421
4,0,2	0.80694662 + 0.19596488 N + 0.0021277046 N ² - 0.00010255799 N ³
3,1,2	3.7550798 + 0.26508626 N - 0.00041952119 N ²
2,2,2	5.8982254 + 0.13139443 N
1,3,2	3.9800807 + 0.039665859 N
0,4,2	1.0049366
3,0,3	1.1638111 + 0.086942068 N - 0.000071468404 N ²
2,1,3	3.6670783 + 0.084966643 N
1,2,3	3.7144818 + 0.037563199 N
0,3,3	1.2506817
2,0,4	0.89481393 + 0.021268461 N
1,1,4	1.8136015 + 0.01856332 N
0,2,4	0.9160824
1,0,5	0.36032293 + 0.003712664 N
0,1,5	0.3640356
0,0,6	0.060363211

Table 37: The coefficients $e_{ijk}^{(t)}$, cf. Eq. (8.46).

References

- [1] I. M. Abdulagatov, N. G. Polikhsonidi, and R. G. Batyrova, *J. Chem. Therm.* **26**, 1031 (1994).
- [2] R. Abe and S. Hikami, *Prog. Theor. Phys.* **54**, 1693 (1977).
- [3] R. Abe and M. Masutani, *Prog. Theor. Phys.* **59**, 672 (1978).
- [4] D. B. Abraham, in *Phase Transitions and Critical Phenomena*, edited by C. Domb and J. Lebowitz (Academic Press, New York, 1986), Vol. 10.
- [5] M. Adam and M. Delsanti, *J. Physique* **37**, 1045 (1976).
- [6] J. Adler, *J. Phys. A* **16**, 3585 (1983).
- [7] J. Adler, C. Holm, and W. Janke, *Physica A* **201**, 581 (1993).
- [8] J. Adler, M. Moshe, and V. Privman, *Phys. Rev. B* **26**, 1411 (1982); **26**, 3958 (1982).
- [9] V. Agostini, G. Carlino, M. Caselle, and M. Hasenbusch, *Nucl. Phys. B* **484**, 331 (1997).
- [10] A. Aharony, *Phys. Rev. Lett.* **31**, 1494 (1973).
- [11] A. Aharony, *Phys. Rev. B* **8**, 3349 (1973).
- [12] A. Aharony, *Phys. Rev. B* **8**, 4270 (1973).
- [13] A. Aharony, *Phys. Rev. B* **10**, 3006 (1974).
- [14] A. Aharony, in *Phase Transitions and Critical Phenomena*, edited by C. Domb and J. Lebowitz (Academic Press, New York, 1976), Vol. 6, p. 357.
- [15] A. Aharony, *J. Phys. A* **10**, 389 (1977).
- [16] A. Aharony and M. F. Fisher, *Phys. Rev. B* **27**, 4394 (1983).
- [17] A. Aharony, A. B. Harris, and S. Wiseman, *Phys. Rev. Lett.* **81**, 252 (1998).
- [18] A. Aharony and P. C. Hohenberg, *Phys. Rev. B* **13**, 3081 (1976).
- [19] A. Aharony, Y. Imry, and S. K. Ma, *Phys. Rev. B* **13**, 466 (1976).
- [20] M. Aizenman, *Phys. Rev. Lett.* **47**, 1 (1981); *Comm. Math. Phys.* **86**, 1 (1982).
- [21] M. Aizenman and R. Fernández, *J. Stat. Phys.* **44**, 393 (1986).
- [22] A. Ali Khan et al. (CP-PACS Collaboration), *Nucl. Phys. B (Proc. Suppl.)* **83**, 319 (2000) [e-print hep-lat/9909075]; “Phase structure and critical temperature of two-flavor QCD with renormalization group improved gauge action and clover improved Wilson quark action”, e-print hep-lat/0008011.
- [23] B. Allés, J. J. Alonso, C. Criado, and M. Pepe, *Phys. Rev. Lett.* **83**, 3669 (1999).
- [24] B. Allés, A. Buonanno, and G. Cella, *Nucl. Phys. B* **500**, 513 (1997).
- [25] B. Allés, S. Caracciolo, A. Pelissetto, and M. Pepe, *Nucl. Phys. B* **562**, 581 (1999).
- [26] B. Allés, G. Cella, M. Dilaver, and Y. Gündüç, *Phys. Rev. D* **59**, 067703 (1999).
- [27] B. Allés and M. Pepe, *Nucl. Phys. B (Proc. Suppl.)* **83**, 348 (2000).
- [28] G. Álvarez, V. Martín-Mayor, and J. J. Ruiz-Lorenzo, *J. Phys. A* **33**, 841 (2000).
- [29] N. A. Alves, B. A. Berg, and R. Villanova, *Phys. Rev. B* **41**, 383 (1990).
- [30] N. A. Alves, J. R. Drugowich de Felicio, and U. H. E. Hansmann, *J. Phys. A* **33**, 7489 (2000).
- [31] T. Ambrose and C. L. Chien, *Phys. Rev. Lett.* **76**, 1743 (1996).
- [32] T. Ambrose and C. L. Chien, *J. Appl. Phys.* **79**, 5920 (1996).
- [33] X. An and W. Shen, *J. Chem. Therm.* **26**, 461 (1994).
- [34] X. An, W. Shen, H. Wang, and G. Zheng, *J. Chem. Therm.* **25**, 1373 (1994).
- [35] P. W. Anderson and H. Hasegawa, *Phys. Rev.* **100**, 675 (1955).
- [36] A. F. Andreev, *Sov. Phys. JETP* **18**, 1415 (1964).
- [37] W. V. Andrew, T. B. K. Khoo, and D. T. Jacobs, *J. Chem. Phys.* **85**, 3985 (1986).
- [38] T. Andrews, *Phil. Trans. R. Soc.* **159**, 575 (1869).
- [39] M. A. Anisimov, *Critical Phenomena in Liquids and Liquid Crystals* (Gordon and Breach, New York, 1991).

- [40] M. A. Anisimov, S. B. Kiselev, J. V. Sengers, and S. Tang, *Physica A* **188**, 487 (1992).
- [41] M. A. Anisimov, E. Luijten, V. A. Agayan, J. V. Sengers, and K. Binder, *Phys. Lett. A* **264**, 63 (1999).
- [42] M. A. Anisimov, A. A. Povodyrev, V. D. Kulikov, and J. V. Sengers, *Phys. Rev. Lett.* **75**, 3146 (1995).
- [43] M. A. Anisimov, A. A. Povodyrev, V. D. Kulikov, and J. V. Sengers, *Phys. Rev. Lett.* **76**, 4095 (1996).
- [44] M. A. Anisimov and J. V. Sengers, Critical and crossover phenomena in fluids and fluid mixtures, in *Supercritical Fluids - Fundamentals and Applications*, edited by E. Kiran, P. G. Debenedetti, and C. J. Peters (Kluwer Acad. Pub., 2000); Critical region, in *Equations of State for Fluids and Fluid Mixtures*, edited by J. V. Sengers, R. F. Kayser, C. J. Peters, and H. J. White Jr. (Elsevier, Amsterdam, 2000) p. 381.
- [45] S. A. Antonenko and A. I. Sokolov, *Phys. Rev. B* **49**, 15901 (1994).
- [46] S. A. Antonenko and A. I. Sokolov, *Phys. Rev. E* **51**, 1894 (1995).
- [47] S. A. Antonenko, A. I. Sokolov and V. B. Varnashev, *Phys. Lett. A* **208**, 161 (1995).
- [48] S. Aoki, Y. Iwasaki, K. Kanaya, S. Kaya, A. Ukawa, and T. Yoshié, *Nucl. Phys. B (Proc. Suppl.)* **63**, 397 (1998).
- [49] H. Arisue and K. Tabata, *Nucl. Phys. B* **435**, 555 (1995).
- [50] P. Arnold, S. Sharpe, L. G. Yaffe, and Y. Zhang, *Phys. Rev. Lett.* **68**, 2062 (1997).
- [51] R. Aschauer and D. Beysens, *J. Chem. Phys.* **98**, 8194 (1993).
- [52] R. Aschauer and D. Beysens, *Phys. Rev. E* **47**, 1850 (1993).
- [53] P. Azaria, B. Delamotte, F. Delduc, and Th. Jolicoeur, *Nucl. Phys. B* **408**, 585 (1993).
- [54] C. Bagnuls and C. Bervillier, *J. Physique Lett.* **45**, L-95 (1984).
- [55] C. Bagnuls and C. Bervillier, *Phys. Rev. B* **32**, 7209 (1985).
- [56] C. Bagnuls and C. Bervillier, *Phys. Rev. Lett.* **58**, 435 (1987).
- [57] C. Bagnuls and C. Bervillier, *Phys. Rev. B* **41**, 402 (1990).
- [58] C. Bagnuls and C. Bervillier, *Phys. Lett. A* **195**, 163 (1994).
- [59] C. Bagnuls and C. Bervillier, *Phys. Rev. Lett.* **76**, 4094 (1996).
- [60] C. Bagnuls and C. Bervillier, *J. Phys. Stud.* **1**, 366 (1997).
- [61] C. Bagnuls and C. Bervillier, “Exact Renormalization Group Equations. An Introductory Review,” e-print hep-th/0002034.
- [62] C. Bagnuls, C. Bervillier, D. I. Meiron, and B. G. Nickel, *Phys. Rev. B* **35**, 3585 (1987); addendum-erratum e-print hep-th/0006187.
- [63] P. Bak and D. Mukamel, *Phys. Rev. B* **13**, 5086 (1976).
- [64] G. A. Baker, Jr., *Phys. Rev. Lett.* **34**, 268 (1975).
- [65] G. A. Baker Jr., *Phys. Rev. B* **15**, 1552 (1976).
- [66] G. A. Baker, Jr., *Quantitative Theory of Critical Phenomena* (Academic Press, San Diego, 1990).
- [67] G. A. Baker, Jr. and N. Kawashima, *Phys. Rev. Lett.* **75**, 994 (1995).
- [68] G. A. Baker, Jr. and N. Kawashima, *J. Phys. A* **29**, 7183 (1996).
- [69] G. A. Baker Jr. and J. M. Kincaid, *Phys. Rev. Lett.* **42**, 1431 (1979); *J. Stat. Phys.* **24**, 469 (1981).
- [70] G. A. Baker, Jr., B. G. Nickel, M. S. Green, and D. I. Meiron, *Phys. Rev. Lett.* **36**, 1351 (1977); G. A. Baker, Jr., B. G. Nickel, and D. I. Meiron, *Phys. Rev. B* **17**, 1365 (1978).
- [71] D. Bailin, A. Love, and M. A. Moore, *J. Phys. C* **10**, 1159 (1977).
- [72] C. F. Baillie and R. Gupta, *Phys. Rev. B* **45**, 2883 (1992).
- [73] C. F. Baillie, R. Gupta, K. A. Hawick, and G. S. Pawley, *Phys. Rev. B* **45**, 10438 (1992).
- [74] V. Balevicius, N. Weiden, and A. Weiss, *Z. Naturforsch. A* **47**, 583 (1992).

- [75] C. A. Ballentine, R. L. Fink, J. Araya-Pochet and J. L. Erskine, *Phys. Rev. B* **41**, 2631 (1990).
- [76] H. G. Ballesteros, L. A. Fernández, V. Martín-Mayor, and A. Muñoz Sudupe, *Phys. Lett. B* **378**, 207 (1996).
- [77] H. G. Ballesteros, L. A. Fernández, V. Martín-Mayor, and A. Muñoz Sudupe, *Phys. Lett. B* **387**, 125 (1996).
- [78] H. G. Ballesteros, L. A. Fernández, V. Martín-Mayor, and A. Muñoz Sudupe, *Nucl. Phys. B* **483**, 707 (1997).
- [79] H. G. Ballesteros, L. A. Fernández, V. Martín-Mayor, and A. Muñoz Sudupe, *Phys. Lett. B* **441**, 330 (1998).
- [80] H. G. Ballesteros, L. A. Fernández, V. Martín-Mayor, A. Muñoz Sudupe, G. Parisi, and J. J. Ruiz-Lorenzo, *Phys. Rev. B* **58**, 2740 (1998).
- [81] H. G. Ballesteros, L. A. Fernández, V. Martín-Mayor, A. Muñoz Sudupe, G. Parisi, and J. J. Ruiz-Lorenzo, *J. Phys. A* **32**, 1 (1999).
- [82] J. Balog and M. Niedermaier, *Nucl. Phys. B* **500**, 421 (1997).
- [83] J. Balog, M. Niedermaier, F. Niedermayer, A. Patrascioiu, E. Seiler, and P. Weisz, *Phys. Rev. D* **60**, 094508 (1999).
- [84] J. Balog, M. Niedermaier, F. Niedermayer, A. Patrascioiu, E. Seiler, and P. Weisz, *Nucl. Phys. B* **583**, 614 (2000).
- [85] J. R. Banavar, G. S. Grest, and D. Jasnow, *Phys. Rev. Lett.* **45**, 1424 (1980); *Phys. Rev. B* **25**, 4639 (1982).
- [86] Z. Barak and M. B. Walker, *Phys. Rev. B* **25**, 1969 (1982).
- [87] M. N. Barber, in *Phase Transitions and Critical Phenomena*, Vol. 8, edited by C. Domb and J. L. Lebowitz (Academic Press, New York, 1983).
- [88] W. A. Bardeen, B. W. Lee, and R. E. Schrock, *Phys. Rev. D* **14**, 985 (1976).
- [89] M. Barmatz, P. C. Hohenberg, and A. Kornblit, *Phys. Rev. B* **12**, 1947 (1975).
- [90] P. H. Barrett, *Phys. Rev. B* **34**, 3513 (1986).
- [91] R. J. Baxter, *Exactly Solved Models in Statistical Mechanics* (Academic Press, New York, 1982).
- [92] R. J. Baxter, *J. Phys. A* **19**, 2821 (1986).
- [93] R. J. Baxter and I. G. Enting, *J. Stat. Phys.* **21**, 103 (1979).
- [94] B. B. Beard, R. J. Birgeneau, M. Greven, and U.-J. Wiese, *Phys. Rev. Lett.* **80**, 1742 (1998).
- [95] B. B. Beard, V. Chudnovsky, and P. Keller-Marxer, *Nucl. Phys. B (Proc. Suppl.)* **83**, 682 (2000).
- [96] D. Beckmann, J. Wosnitza, and H. von Löhneysen, *Phys. Rev. Lett.* **71**, 2829 (1993).
- [97] D. P. Belanger, in *Spin Glasses and Random Fields*, edited by A. P. Young (World Scientific, Singapore, 1998), p. 251.
- [98] D. P. Belanger, “Experimental Characterization of the Ising Model in Disordered Antiferromagnets”, Ising centennial colloquium, e-print cond-mat/0009029, to be published in the Brazilian Journal of Physics.
- [99] D. P. Belanger, A. R. King, I. B. Ferreira, and V. Jaccarino, *Phys. Rev. B* **37**, 226 (1988).
- [100] D. P. Belanger, A. R. King, and V. Jaccarino, *Phys. Rev. B* **34**, 452 (1986).
- [101] D. P. Belanger, P. Nordblad, A. R. King, V. Jaccarino, L. Lundgren, and O. Beckman, *J. Magn. Magn. Mater.* **31-34**, 1095 (1983).
- [102] D. P. Belanger and H. Yoshizawa, *Phys. Rev. B* **35**, 4823 (1987).
- [103] D. P. Belanger, J. Wang, Z. Slanič, S.-J. Han, R. M. Nicklow, M. Lui, C. A. Ramos, and D. Lerdeman, *J. Magn. Magn. Mater.* **140-144**, 1549 (1995).
- [104] D. P. Belanger, J. Wang, Z. Slanič, S.-J. Han, R. M. Nicklow, M. Lui, C. A. Ramos, and D. Lerdeman, *Phys. Rev. B* **54**, 3420 (1996).
- [105] M. Y. Belyakov and S. B. Kiselev, *Physica A* **190**, 75 (1992).
- [106] P. Belohorec and B. G. Nickel, “Accurate universal and two-parameter model results from a Monte-Carlo renormalization group study”, Guelph University report (1997).
- [107] C. M. Bender and S. Boettcher, *Phys. Rev. D* **48**, 4919 (1992); *D* **51**, 1875 (1995).

- [108] C. M. Bender, F. Cooper, G. S. Guralnik, R. Roskies, and D. H. Sharp, *Phys. Rev. D* **23**, 2999 (1981).
- [109] M. Benhamou and G. Mahoux, *J. Physique* **47**, 559 (1986).
- [110] D. Bennett-Wood, I. G. Enting, D. S. Gaunt, A. J. Guttmann, J. L. Leask, A. L. Owczarek, and S. G. Whittington, *J. Phys. A* **31**, 4725 (1998).
- [111] J. Berges and K. Rajagopal, *Nucl. Phys. B* **538**, 215 (1999).
- [112] J. Berges, N. Tetradis, and C. Wetterich, *Phys. Rev. Lett.* **77**, 873 (1996).
- [113] J. Berges, N. Tetradis, and C. Wetterich, “Non-perturbative renormalization flow in quantum field theory and statistical physics”, e-print hep-ph/0005122.
- [114] W. Bernreuther and F. J. Wegner, *Phys. Rev. Lett.* **57**, 1383 (1986).
- [115] C. Bervillier, *Phys. Rev. B* **14**, 4964 (1976).
- [116] C. Bervillier, *Phys. Rev. B* **34**, 8141 (1986).
- [117] C. Bervillier and C. Godrèche, *Phys. Rev. B* **21**, 5427 (1980).
- [118] C. Bervillier and M. Shpot, *Phys. Rev. B* **46**, 955 (1992).
- [119] G. Bhanot, M. Creutz, U. Glässer, and K. Schilling, *Phys. Rev. B* **49**, 2909 (1994).
- [120] G. Bhanot, M. Creutz, and J. Lacki, *Phys. Rev. Lett.* **69**, 1841 (1992).
- [121] T. Bhattacharya, A. Billoire, R. Lacaze, and Th. Jolicœur, *J. Physique I* **4**, 181 (1994).
- [122] L. Biferale and R. Petronzio, *Nucl. Phys. B* **328**, 677 (1989).
- [123] K. Binder, *Z. Phys. B* **43**, 119 (1981).
- [124] K. Binder, E. Luijten, M. Müller, N. B. Wilding, and H. W. Blöte, *Physica A* **281**, 112 (2000).
- [125] R. J. Birgeneau, R. A. Cowley, G. Shirane, H. Joshizawa, D. P. Belanger, A. R. King, and V. Jaccarino, *Phys. Rev. B* **27**, 6747 (1983).
- [126] P. Biscari, M. Campostrini, and P. Rossi, *Phys. Lett. B* **242**, 225 (1990).
- [127] E. J. Blagoeva, G. Busiello, L. De Cesare, Y. T. Millev, I. Rabuffo, and D. I. Uzunov, *Phys. Rev. B* **42**, 6124 (1990).
- [128] H. W. Blöte, J. de Bruin, A. Compagner, J. H. Croockewit, Y. T. J. C. Fonk, J. R. Heringa, A. Hoogland, and A. L. van Willigen, *Europhys. Lett.* **10**, 105 (1989).
- H. W. Blöte, A. Compagner, J. H. Croockewit, Y. T. J. C. Fonk, J. R. Heringa, A. Hoogland, and A. L. van Willigen, *Physica A* **161**, 1 (1989).
- [129] H. W. J. Blöte, J. R. Heringa, A. Hoogland, E. W. Meyer, and T. S. Smit, *Phys. Rev. Lett.* **76**, 2613 (1996).
- [130] H. W. J. Blöte and G. Kamieniarz, *Physica A* **196**, 455 (1993).
- [131] H. W. J. Blöte, E. Luijten, and J. R. Heringa, *J. Phys. A* **28**, 6289 (1995).
- [132] H. W. J. Blöte, L. N. Shchur, and A. L. Talapov, *Int. J. Mod. Phys. C* **10**, 1137 (1999).
- [133] E. H. Boubcheur, D. Loison, and H. T. Diep, *Phys. Rev. B* **54**, 4165 (1996).
- [134] P. Braun and M. Föhnle, *J. Stat. Phys.* **52**, 775 (1988).
- [135] P. Braun, U. Staaden, T. Holey, and M. Föhnle, *Int. J. Mod. Phys. B* **3**, 1343 (1989).
- [136] A. J. Bray, *Phys. Rev. B* **14**, 1248 (1976).
- [137] A. J. Bray, T. McCarthy, M. A. Moore, J. D. Reger, and A. P. Young, *Phys. Rev. B* **36**, 2212 (1987).
- [138] E. Brézin and S. Feng, *Phys. Rev. B* **29**, 472 (1984).
- [139] E. Brézin, J. Le Guillou, and J. Zinn-Justin, *Phys. Rev. D* **8**, 2418 (1973).
- [140] E. Brézin, J. C. Le Guillou, and J. Zinn-Justin, *Phys. Lett. A* **47**, 285 (1974).
- [141] E. Brézin, J. C. Le Guillou, and J. Zinn-Justin, *Phys. Rev. Lett.* **32**, 473 (1974).
- [142] E. Brézin, J. C. Le Guillou, and J. Zinn-Justin, *Phys. Rev. B* **10**, 893 (1974).
- [143] E. Brézin, J. C. Le Guillou, and J. Zinn-Justin, in *Phase Transitions and Critical Phenomena*, edited by C. Domb and J. Lebowitz (Academic Press, New York, 1976), Vol. 6, p. 125.

- [144] E. Brézin, J. C. Le Guillou, and J. Zinn-Justin, Phys. Rev. D **15**, 1544 (1977); D **15**, 1588 (1977).
- [145] E. Brézin and D. J. Wallace, Phys. Rev. B **7**, 1967 (1973).
- [146] E. Brézin, D. J. Wallace, and K. G. Wilson, Phys. Rev. Lett. **29**, 591 (1972); Phys. Rev. B **7**, 232 (1973).
- [147] E. Brézin and J. Zinn-Justin, Phys. Rev. B **14**, 3110 (1976).
- [148] E. Brézin, J. Zinn-Justin, and J. C. Le Guillou, Phys. Rev. B **14**, 4976 (1976).
- [149] E. Brézin, J. Zinn-Justin, and J. C. Le Guillou, Phys. Rev. D **14**, 2615 (1976).
- [150] R. C. Brower and P. Tamayo, Phys. Rev. Lett. **62**, 1087 (1989).
- [151] R. G. Brown and M. Ciftan, Phys. Rev. Lett. **76**, 1352 (1996).
- [152] R. G. Brown and M. Ciftan, Phys. Rev. Lett. **78**, 2266 (1997).
- [153] A. D. Bruce, J. Phys. C **7**, 2089 (1974).
- [154] A. D. Bruce and A. Aharony, Phys. Rev. B **11**, 478 (1975).
- [155] M. J. Buckingham and J. D. Gunton, Phys. Rev. Lett. **20**, 143 (1967); Phys. Rev. **178**, 848 (1969).
- [156] T. W. Burkhardt and J. M. J. van Leeuwen eds., *Real-Space Renormalization* (Springer, Berlin, 1982).
- [157] D. Buchholz and J. T. Lopuszński, Lett. Math. Phys. **3**, 175 (1979).
- [158] D. Buchholz, J. T. Lopuszński, and S. Z. Rabsztyń, Nucl. Phys. B **263**, 155 (1986).
- [159] S. S. C. Burnett, M. Strösser, and V. Dohm, Nucl. Phys. B **504**, 665 (1997).
- [160] P. Butera and M. Comi, Phys. Rev. B **47**, 11969 (1993).
- [161] P. Butera and M. Comi, Phys. Rev. B **50**, 3052 (1994).
- [162] P. Butera and M. Comi, Phys. Rev. B **54**, 15828 (1996).
- [163] P. Butera and M. Comi, Phys. Rev. E **55**, 6391 (1997).
- [164] P. Butera and M. Comi, Phys. Rev. B **56**, 8212 (1997).
- [165] P. Butera and M. Comi, Phys. Rev. B **58**, 11552 (1998).
- [166] P. Butera and M. Comi, Phys. Rev. B **60**, 6749 (1999).
- [167] P. Butera and M. Comi, Phys. Rev. B **62**, 14837 (2000).
- [168] J. W. Cahn and J. E. Hilliard, J. Chem. Phys. **28**, 258 (1958).
- [169] P. Calabrese, M. Caselle, A. Celi, A. Pelissetto, and E. Vicari, J. Phys. A **33**, 8155 (2000).
- [170] M. Campostrini, “Linked cluster expansion of the Ising Model”, e-print cond-mat/0005130, J. Stat. Phys. in press.
- [171] M. Campostrini, M. Hasenbusch, A. Pelissetto, P. Rossi, and E. Vicari, “Critical behavior of the three-dimensional XY universality class”, e-print cond-mat/0010360.
- [172] M. Campostrini, A. Pelissetto, P. Rossi, and E. Vicari, Phys. Rev. D **54**, 1782 (1996).
- [173] M. Campostrini, A. Pelissetto, P. Rossi, and E. Vicari, Nucl. Phys. B **459**, 207 (1996).
- [174] M. Campostrini, A. Pelissetto, P. Rossi, and E. Vicari, Phys. Rev. B **54**, 7301 (1996).
- [175] M. Campostrini, A. Pelissetto, P. Rossi, and E. Vicari, Phys. Lett. B **402**, 141 (1997).
- [176] M. Campostrini, A. Pelissetto, P. Rossi, and E. Vicari, Europhys. Lett. **38**, 577 (1997); Phys. Rev. E **57**, 184 (1998); Nucl. Phys. B (Proc. Suppl.) **53**, 690 (1997).
- [177] M. Campostrini, A. Pelissetto, P. Rossi, and E. Vicari, Phys. Rev. E **60**, 3526 (1999).
- [178] M. Campostrini, A. Pelissetto, P. Rossi, and E. Vicari, Phys. Rev. B **61** 5905 (2000).
- [179] M. Campostrini, A. Pelissetto, P. Rossi, and E. Vicari, Phys. Rev. B **62**, 5843 (2000).
- [180] M. Campostrini, P. Rossi, and E. Vicari, Phys. Rev. D **46**, 2647 (1992); D **46**, 4643 (1992).
- [181] A. A. Caparica, A. Bunker, and D. P. Landau, Phys. Rev. B **62**, 9458 (2000).
- [182] S. Caracciolo, M. S. Causo, P. Grassberger, and A. Pelissetto, J. Phys. A **32**, 2931 (1999).

- [183] S. Caracciolo, M. S. Causo, and A. Pelissetto, Phys. Rev. E **57**, R1215 (1998).
- [184] S. Caracciolo, M. S. Causo and A. Pelissetto, J. Chem. Phys. **112**, 7693 (2000).
- [185] S. Caracciolo, M. S. Causo, A. Pelissetto, P. Rossi, and E. Vicari, Nucl. Phys. B (Proc. Suppl.) **73**, 757 (1999) [e-print hep-lat/9809101].
- [186] S. Caracciolo, R. G. Edwards, S. J. Ferreira, A. Pelissetto, and A. D. Sokal, Phys. Rev. Lett. **74**, 2969 (1995).
- [187] S. Caracciolo, R. G. Edwards, T. Mendes, A. Pelissetto, and A. D. Sokal, Nucl. Phys. B (Proc. Suppl.) **47**, 763 (1996).
- [188] S. Caracciolo, R. G. Edwards, A. Pelissetto, and A. D. Sokal, Nucl. Phys. B **403**, 475 (1993); Nucl. Phys. B (Proc. Suppl.) **20**, 72 (1991); Nucl. Phys. B (Proc. Suppl.) **26**, 595 (1992).
- [189] S. Caracciolo, R. G. Edwards, A. Pelissetto, and A. D. Sokal, Phys. Rev. Lett. **75**, 1891 (1995); Nucl. Phys. B (Proc. Suppl.) **42**, 752 (1995).
- [190] S. Caracciolo, R. G. Edwards, A. Pelissetto, and A. D. Sokal, Phys. Rev. Lett. **76**, 1179 (1996).
- [191] S. Caracciolo, G. Ferraro, and A. Pelissetto, J. Phys. A **24**, 3625 (1991).
- [192] S. Caracciolo, A. Montanari, and A. Pelissetto, Nucl. Phys. B **556**, 295 (1999).
- [193] S. Caracciolo, A. Montanari, and A. Pelissetto, JHEP **09**, 045 (2000).
- [194] S. Caracciolo and A. Pelissetto, Nucl. Phys. B **420**, 141 (1994).
- [195] S. Caracciolo and A. Pelissetto, Nucl. Phys. B **455**, 619 (1995).
- [196] S. Caracciolo, A. Pelissetto, and A. D. Sokal, J. Phys. A **23**, L969 (1990).
- [197] S. Caracciolo, A. Pelissetto, and A. D. Sokal, J. Phys. A **23**, 4509 (1990).
- [198] S. Caracciolo, A. Pelissetto, and A. D. Sokal, Nucl. Phys. B (Proc. Suppl.) **20**, 68 (1991); J. Stat. Phys. **67**, 65 (1992).
- [199] J. L. Cardy ed., *Finite-Size Scaling* (North-Holland, Amsterdam, 1988).
- [200] J. L. Cardy, *Scaling and Renormalization in Statistical Physics* (Cambridge Univ. Press, Cambridge, 1996).
- [201] J. L. Cardy and A. J. Guttmann, J. Phys. A **26**, 2485 (1993).
- [202] J. L. Cardy and G. Mussardo, Nucl. Phys. B **410**, 451 (1993).
- [203] J. L. Cardy and H. S. Saleur, J. Phys. A **22**, L601 (1989).
- [204] J. M. Carmona, A. Pelissetto, and E. Vicari, Phys. Rev. B **61**, 15136 (2000).
- [205] M. Caselle, R. Fiore, F. Gliozzi, M. Hasenbusch, K. Pinn, and S. Vinti, Nucl. Phys. B **432**, 590 (1994).
- [206] M. Caselle and M. Hasenbusch, J. Phys. A **30**, 4963 (1997).
- [207] M. Caselle and M. Hasenbusch, J. Phys. A **31**, 4603 (1998).
- [208] M. Caselle and M. Hasenbusch, Nucl. Phys. B **579**, 667 (2000).
- [209] M. Caselle, M. Hasenbusch, A. Pelissetto, and E. Vicari, J. Phys. A **33**, 8171 (2000).
- [210] M. Caselle, M. Hasenbusch, A. Pelissetto, and E. Vicari, "The critical equation of state of the 2D Ising model", e-print cond-mat/0011305.
- [211] M. Caselle, M. Hasenbusch, and P. Provero, Nucl. Phys. B **556**, 575 (1999).
- [212] M. Caselle, A. Pelissetto, and E. Vicari, "Non-analyticity of the beta-function and systematic errors in field-theoretic calculations of critical quantities," in *Fluctuating Paths and Fields*, edited by W. Janke (World Scientific, Singapore, 2001) [hep-th/0010228].
- [213] S. Chakravarty, B. I. Halperin, and D. R. Nelson, Phys. Rev. B **39**, 2344 (1989).
- [214] M. H. W. Chan, K. I. Blum, S. Q. Murphy, G. K. S. Wong, and J. D. Reppy, Phys. Rev. Lett. **61**, 1950 (1988).
- [215] M. H. W. Chan, N. Mulders, and J. Reppy, Phys. Today **49**, 30 (1996).
- [216] R. F. Chang, H. Burstyn, and J. V. Sengers, Phys. Rev. A **19**, 866 (1979).
- [217] X. S. Chang and C. Hohenemser, Phys. Rev. B **37**, 261 (1988).
- [218] J. T. Chayes, L. Chayes, D. S. Fisher, and T. Spenser, Phys. Rev. Lett. **57**, 2999 (1986).

- [219] Z. Y. Chen, A. Abbaci, S. Tang, and J. V. Sengers, *Phys. Rev. A* **42**, 4470 (1990).
- [220] J.-H. Chen, M. E. Fisher, and B. G. Nickel, *Phys. Rev. Lett.* **48**, 630 (1982).
- [221] K. Chen, A. M. Ferrenberg, and D. P. Landau, *Phys. Rev. B* **48**, 3249 (1993).
- [222] Z. Y. Chen, P. C. Albright, and J. V. Sengers, *Phys. Rev. A* **41**, 3161 (1990).
- [223] K. G. Chetyrkin, S. G. Gorishny, S. A. Larin, and F. V. Tkachov, *Phys. Lett. B* **132**, 351 (1983).
- [224] Y. S. Choi, J. Machta, P. Tamayo, and L. X. Chayes, *Int. J. Mod. Phys. C* **10**, 1 (1999).
- [225] D. Chowdhury and D. Stauffer, *J. Stat. Phys.* **44**, 203 (1986).
- [226] M. F. Collins and O. A. Petrenko, *Can. J. Phys.* **75**, 605 (1997).
- [227] M. Combescot, M. Droz, and J. M. Kosterlitz, *Phys. Rev. B* **11**, 4661 (1974).
- [228] M. Corti and V. Degiorgio, *Phys. Rev. Lett.* **55**, 2005 (1985).
- [229] J. P. Cotton, *J. Physique Lett.* **41**, L231 (1980).
- [230] J. P. Cotton, D. Decker, B. Farnoux, G. Jannink, R. Ober, and C. Picot, *Phys. Rev. Lett.* **32**, 1170 (1974).
- [231] R. A. Cowley and A. D. Bruce, *J. Phys. C: Solid State Phys.* **11**, 3577 (1978).
- [232] R. A. Cowley and K. Carniero, *J. Phys. C* **13**, 3281 (1980).
- [233] M. Creutz, *Quarks, Gluons and Lattices*, (Cambridge Univ. Press, Cambridge, 1983).
- [234] P. Curie, *Ann. Chim. Phys.* **5**, 289 (1895).
- [235] P. Damay, F. Leclercq, and P. Chieux, *Phys. Rev. B* **40**, 4696 (1989).
- [236] P. Damay, F. Leclercq, R. Magli, F. Formisano, and P. Lindner, *Phys. Rev. B* **58**, 12038 (1998).
- [237] M. Daoud, J. P. Cotton, B. Farnoux, G. Jannink, G. Sarma, H. Benoit, R. Duplessix, C. Picot and P. G. de Gennes, *Macromolecules* **8**, 804 (1975).
- [238] F. David, *Phys. Rev. Lett.* **75**, 2626 (1995).
- [239] J. Dayantis and J. F. Palierne, *J. Chem. Phys.* **95**, 6088 (1991).
- [240] J. Dayantis and J. F. Palierne, *Phys. Rev. B* **49**, 3217 (1994).
- [241] K. De Bell and D. J. W. Geldart, *Phys. Rev. B* **32**, 4763 (1985).
- [242] P. G. de Gennes, *Phys. Lett. A* **38**, 339 (1972).
- [243] P. G. de Gennes, *Scaling Concepts in Polymer Physics* (Cornell University Press, Ithaca, NY, 1979).
- [244] G. Delfino, *Phys. Lett. B* **419**, 291 (1998).
- [245] G. Delfino and G. Mussardo, *Nucl. Phys. B* **455**, 724 (1995).
- [246] G. Delfino, G. Mussardo and P. Simonetti, *Nucl. Phys. B* **473**, 469 (1996).
- [247] J. des Cloizeaux, *Phys. Rev. A* **10**, 1665 (1974); *J. Physique* **41**, 223 (1980).
- [248] J. des Cloizeaux, *J. Physique* **42**, 635 (1981).
- [249] J. des Cloizeaux, R. Conte, and G. Jannink, *J. Physique Lett.* **46**, L-595 (1985).
- [250] J. des Cloizeaux and B. Duplantier, *J. Physique Lett.* **46**, L-457 (1985).
- [251] J. des Cloizeaux and G. Jannink, *Les Polymères en Solution* (Les Editions de Physique, Les Ulis, 1987); English translation: *Polymers in Solution: Their Modeling and Structure* (Oxford University Press, Oxford-New York, 1990).
- [252] R. Deutschmann, H. von Löhneysen, H. Wosnitza, R. K. Kremer, and D. Visser, *Europhys. Lett.* **17**, 637 (1992).
- [253] H. T. Diep, *Phys. Rev. B* **39**, 397 (1989).
- [254] G. Dietler and D. S. Cannel, *Phys. Rev. Lett.* **60**, 1852 (1988).
- [255] I. Dimitrović, P. Hasenfratz, J. Nager, and F. Niedermayer, *Nucl. Phys. B* **350**, 893 (1991).
- [256] A. Dobry and H. T. Diep, *Phys. Rev. B* **51**, 6731 (1995).
- [257] V. Dohm, *Z. Phys. B* **60**, 61 (1985); **61**, 193 (1985).
- [258] E. Domany and E. K. Riedel, *J. Appl. Phys.* **50**, 1804 (1979).
- [259] C. Domb and D. L. Hunter, *Proc. Phys. Soc.* **86**, 1147 (1965).

- [260] V. S. Dotsenko, J. Phys. A **32**, 2949 (1999).
- [261] V. S. Dotsenko and D. E. Feldman, J. Phys. A **28**, 5183 (1995).
- [262] V. S. Dotsenko, B. Harris, D. Sherrington, and R. Stinchcombe, J. Phys. A **28**, 3093 (1995).
- [263] J. M. Drouffe and J. B. Zuber, Nucl. Phys. B **180**, 253 (1981); B **180**, 264 (1981).
- [264] R. A. Dunlap and A. M. Gottlieb, Phys. Rev. B **23**, 6106 (1981).
- [265] B. Duplantier, J. Physique **47**, 1633 (1986).
- [266] J. P. Eckmann, J. Magnen, and R. Sénéor, Comm. Math. Phys. **39**, 251 (1975).
- [267] S. F. Edwards, Proc. Phys. Soc. **85**, 613 (1965).
- [268] T. J. Edwards, thesis, University of Western Australia, 1984 (unpublished), cited in Ref. [400].
- [269] R. G. Edwards, S. J. Ferreira, J. Goodman, and A. D. Sokal, Nucl. Phys. B **380**, 621 (1992).
- [270] N. Eizenberg and J. Klafter, J. Chem. Phys. **99**, 3976 (1993).
- [271] N. Eizenberg and J. Klafter, Phys. Rev. B **53**, 5078 (1996).
- [272] H. J. Elmers, J. Hauschild, H. Höche, U. Gradmann, H. Bethge, D. Heuer and U. Kölher, Phys. Rev. Lett. **73**, 898 (1994).
- [273] V. J. Emery, Phys. Rev. B **11**, 239 (1975).
- [274] M. Enderle, G. Fortuna, and M. Steiner, J. Phys.: Condens. Matter **6**, L385 (1994).
- [275] M. Enderle, R. Schneider, Y. Matsuo, and K. Kakurai, Physica B **234-236**, 554 (1997).
- [276] J. Engels, S. Holtmann, T. Mendes, and T. Schulze, Phys. Lett. B **492**, 219 (2000).
- [277] J. Engels and T. Mendes, Nucl. Phys. B **572**, 289 (2000).
- [278] J. Engels and T. Scheideler, Nucl. Phys. B **539**, 557 (1999).
- [279] J. W. Essam and M. E. Fisher, J. Chem. Phys. **38**, 802 (1963).
- [280] M. Falcioni, E. Marinari, M. L. Paciello, G. Parisi, and B. Taglienti, Phys. Lett. B **108**, 331 (1982).
- [281] M. Falcioni, E. Marinari, M. L. Paciello, G. Parisi, and B. Taglienti, Nucl. Phys. B **225**, 313 (1983).
- [282] M. Falcioni and A. Treves, Nucl. Phys. B **265**, 671 (1986).
- [283] B. Farnoux, Ann. Fr. Phys. **1**, 73 (1976).
- [284] J. S. Feldman and K. Osterwalder, Ann. Phys. **97**, 80 (1976).
- [285] M. Ferer, Phys. Rev. Lett. **33**, 21 (1974).
- [286] M. Ferer and A. Hamid-Aidinejad, Phys. Rev. B **34**, 6481 (1986).
- [287] M. Ferer, M. A. Moore, and M. Wortis, Phys. Rev. B **8**, 5205 (1973).
- [288] M. Ferer, J. P. Van Dyke, and W. J. Camp, Phys. Rev. B **23**, 2367 (1981).
- [289] M. Ferer and M. J. Velgakis, Phys. Rev. B **27**, 2839 (1983).
- [290] R. Fernández, J. Fröhlich, and A. D. Sokal, *Random Walks, Critical Phenomena, and Triviality in Quantum Field Theory*, Text and Monographs in Physics (Springer-Verlag, Berlin, 1992).
- [291] I. B. Ferreira, A. R. King, and V. Jaccarino, Phys. Rev. B **43**, 10797 (1991).
- [292] S. J. Ferreira and A. D. Sokal, J. Stat. Phys. **96**, 461 (1999).
- [293] R. A. Ferrel and D. J. Scalapino, Phys. Rev. Lett. **34**, 200 (1975).
- [294] A. M. Ferrenberg and D. P. Landau, Phys. Rev. B **44**, 5081 (1991).
- [295] A. M. Ferrenberg and R. Swendsen, Phys. Rev. Lett. **63**, 1195 (1989).
- [296] A. E. Filippov and S. A. Breus, Phys. Lett. A **158**, 300 (1991).
- [297] D. Finotello, K. A. Gillis, A. Wong, and M. H. W. Chan, Phys. Rev. Lett. **61**, 1954 (1988).
- [298] M. E. Fisher, Philos. Mag. **7**, 1731 (1962).
- [299] M. E. Fisher, J. Math. Phys. **4**, 278 (1963).
- [300] M. E. Fisher, J. Chem. Phys. **44**, 616 (1966).
- [301] M. E. Fisher, Physics **3**, 255 (1967).

- [302] M. E. Fisher, Phys. Rev. **176**, 257 (1968).
- [303] M. E. Fisher, Phys. Rev. **180**, 594 (1969).
- [304] M. E. Fisher, Rev. Mod. Phys. **46**, 597 (1974).
- [305] M. E. Fisher, in *Renormalization Group in Critical Phenomena and Quantum Field Theory*, edited by J. D. Gunton and M. S. Green (Temple Univ. Press, Philadelphia, 1974) p.65.
- [306] M. E. Fisher, Phys. Rev. Lett. **57**, 1911 (1986).
- [307] M. E. Fisher, Rev. Mod. Phys. **70**, 653 (1998).
- [308] M. E. Fisher, private communications.
- [309] M. E. Fisher and A. Aharony, Phys. Rev. Lett. **31**, 1238 (1973).
- [310] M. E. Fisher and A. Aharony, Phys. Rev. B **10**, 2818 (1974).
- [311] M. E. Fisher and H. Au-Yang, J. Phys. A **12**, 1677 (1979); (E) A **13**, 1517 (1980).
- [312] M. E. Fisher and M. N. Barber, Phys. Rev. Lett. **28**, 1516 (1972).
- [313] M. E. Fisher, M. N. Barber, and D. Jasnow, Phys. Rev. A **8**, 1111 (1973).
- [314] M. E. Fisher and R. J. Burford, Phys. Rev. **156**, 583 (1967).
- [315] M. E. Fisher and J. H. Chen, J. Physique **46**, 1645 (1985).
- [316] M. E. Fisher and B. U. Felderhof, Ann. Phys. **58** 176, 217 (1970).
- [317] M. E. Fisher and J. S. Langer, Phys. Rev. Lett. **20**, 665 (1968).
- [318] M. E. Fisher and P. J. Upton, Phys. Rev. Lett. **65**, 2402 (1990); **65**, 3405 (1990).
- [319] M. E. Fisher and S.-Y. Zinn, J. Phys. A **31**, L629 (1998).
- [320] M. E. Fisher, S.-Y. Zinn, and P. J. Upton, Phys. Rev. B **59**, 14533 (1999).
- [321] S. Fishman and A. Aharony, J. Phys. C **12**, L729 (1979).
- [322] P. J. Flory, *Principles of Polymer Chemistry* (Cornell University Press, Ithaca, NY, 1953).
- [323] H. Flyvbjerg and F. Larsen, Phys. Lett. B **266**, 92 (1991); B **266**, 99 (1991).
- [324] R. Folk, Yu. Holovatch, and T. Yavors'kii, J. Phys. Stud. **2**, 213 (1998).
- [325] R. Folk, Yu. Holovatch, and T. Yavors'kii, Pis'ma v Zh. Eksp. Teor. Fiz. **69**, 698 (1999) [JETP Lett. **69**, 747 (1999)].
- [326] R. Folk, Yu. Holovatch, and T. Yavors'kii, Phys. Rev. B **61**, 15114 (2000).
- [327] R. Folk, Yu. Holovatch, and T. Yavors'kii, Phys. Rev. B **62**, 12195 (2000).
- [328] F. Forgacs, R. Lipowsky, and Th. M. Nieuwenhuizen, in *Phase Transitions and Critical Phenomena*, edited by C. Domb and J. Lebowitz (Academic Press, New York, 1991), Vol. 14.
- [329] K. F. Freed, *Renormalization-Group Theory of Macromolecules* (John Wiley, New York, 1987).
- [330] B. Freedman, P. Smolensky and D. Weingarten, Phys. Lett. B **113**, 481 (1982).
- [331] B. Freedman and G. A. Baker, J. Phys. A **15**, L715 (1982).
- [332] M. Fukuda, M. Fukutomi, Y. Kato, and T. Hashimoto, J. Polym. Sci. Polym. Phys. **12**, 871 (1974).
- [333] E. E. Fullerton, S. Adenwalla, G. P. Felcher, K. T. Riggs, C. H. Sowers, S. D. Bader and J. L. Robertson, Physica B **221**, 370 (1996).
- [334] T. Garel and P. Pfeuty, J. Phys. C **9**, L245 (1976).
- [335] S. Gartenhaus and W. S. Mc Cullough, Phys. Rev. B **38**, 11688 (1988).
- [336] B. D. Gaulin, T. E. Mason, M. F. Collins, and J. Z. Larese, Phys. Rev. Lett. **62**, 1380 (1989).
- [337] D. S. Gaunt, in *Phase Transitions*, edited by M. Lévy, J. C. Le Guillou, and J. Zinn-Justin (Plenum, New York and London, 1982).
- [338] D. S. Gaunt, M. E. Fisher, M. F. Sykes, and J. W. Essam, Phys. Rev. Lett. **13**, 713 (1964).
- [339] R. V. Gavaï, J. Potvin, and S. Sanielevici, Phys. Rev. Lett. **58**, 2519 (1987).
- [340] S. Gavin, A. Gocksh and R. D. Pisarski, Phys. Rev. D **49**, 3079 (1994).
- [341] M. J. George and J. J. Rehr, Phys. Rev. Lett. **53**, 2063 (1984).

- [342] V. L. Ginzburg, Fiz. Tverd. Tela **2**, 2031 (1960) [Sov. Phys. Solid State, **2**, 1824 (1960)].
- [343] J. Glimm and A. Jaffe, Comm. Math. Phys. **52**, 203 (1977).
- [344] L. S. Goldner, N. Mulders, and G. Ahlers, J. Low Temp. Phys. **93**, 131 (1993).
- [345] G. R. Golner and E. K. Riedel, Phys. Lett. A **58**, 11 (1976).
- [346] A. P. Gottlob and M. Hasenbusch, Physica A **201**, 593 (1993).
- [347] A. P. Gottlob and M. Hasenbusch, J. Stat. Phys. **77**, 919 (1994).
- [348] E. Granato and J. M. Kosterlitz, Phys. Rev. Lett. **65**, 1267 (1990).
- [349] P. Grassberger, J. Phys. A **26** 2769 (1993).
- [350] P. Grassberger, P. Sutter, and L. Schäfer J. Phys. A **30**, 7039 (1997).
- [351] R. B. Griffiths, Phys. Rev. **152**, 240 (1966); in *Phase Transitions and Critical Phenomena*, vol. 1, edited by C. Domb and M. S. Green (Academic Press, New York, 1972).
- [352] R. B. Griffiths and P. A. Pierce, Phys. Rev. Lett. **41**, 917 (1978); J. Stat. Phys. **20**, 499 (1979).
- [353] G. Grinstein and A. Luther, Phys. Rev. B **13**, 1329 (1976).
- [354] G. Grinstein, S. K. Ma, and G. F. Mazenko, Phys. Rev. B **15**, 258 (1977).
- [355] G. Grinstein and D. Mukamel, J. Phys. A **15**, 233 (1982).
- [356] M. K. Grover, L. P. Kadanoff, and F. J. Wegner, Phys. Rev. B **6**, 311 (1972).
- [357] Yu. M. Gufan and V. P. Popov, Kristallografiya **25**, 921 (1980) [Sov. Phys. Crystallogr. **25**, 527 (1980)].
- [358] R. Guida and J. Zinn-Justin, Nucl. Phys. B **489**, 626 (1997).
- [359] R. Guida and J. Zinn-Justin, J. Phys. A **31**, 8103 (1998).
- [360] R. Gupta and P. Tamayo, Int. J. Mod. Phys. C **7**, 305 (1996).
- [361] C. Gutfeld, J. Küster, and G. Münster, Nucl. Phys. B **479**, 654 (1996).
- [362] A. J. Guttmann, J. Phys. A **20**, 1839 (1987); A **20**, 1855 (1987).
- [363] A. J. Guttmann, J. Phys. A **22**, 2807 (1989).
- [364] A. J. Guttmann, in *Phase Transitions and Critical Phenomena*, vol. 13, edited by C. Domb and J. Lebowitz (Academic Press, New York, 1989).
- [365] A. J. Guttmann and I. G. Enting, J. Phys. A **21**, L467 (1988); A **22**, 1371 (1989).
- [366] A. J. Guttmann and I. G. Enting, J. Phys. A **26**, 806 (1993).
- [367] A. J. Guttmann and I. G. Enting, J. Phys. A **27**, 8007 (1994).
- [368] A. J. Guttmann and G. S. Joyce, J. Phys. A **5**, L81 (1972).
- [369] A. J. Guttmann and J. Wang, J. Phys. A **24**, 3107 (1991).
- [370] M. A. Halasz, A. D. Jackson, R. E. Shrock, M. A. Stephanov, and J. J. Verbaarschot, Phys. Rev. D **58**, 096007 (1998).
- [371] F. J. Halfkann and V. Dohm, Z. Phys. B **89**, 79 (1992).
- [372] D.G. Hall, J. Chem. Soc. Faraday Trans. **68**, 668 (1972).
- [373] B. I. Halperin and P. C. Hohenberg, Phys. Rev. **177**, 952 (1969).
- [374] K. Hamano, T. Kawazura, T. Koyama, and N. Kuwahara, J. Chem. Phys. **82**, 2718 (1985).
- [375] K. Hamano, N. Kuwahara, I. Mitsushima, K. Kubota, and T. Kamura, J. Chem. Phys. **94**, 2172 (1991).
- [376] K. Hamano, S. Teshigawara, T. Koyama, and N. Kuwahara, Phys. Rev. A **33**, 485 (1986).
- [377] T. Hara, J. Stat. Phys. **47**, 57 (1987).
- [378] T. Hara and H. Tasaki, J. Stat. Phys. **47**, 99 (1987).
- [379] A. B. Harris, J. Phys. C **7**, 1671 (1974).
- [380] A. B. Harris and T. C. Lubensky, Phys. Rev. Lett. **33**, 1540 (1974).
- [381] M. Hasenbusch, J. Physique I **3**, 753 (1993).
- [382] M. Hasenbusch, J. Phys. A **32**, 4851 (1999).

- [383] M. Hasenbusch, Habilitationsschrift, Humboldt-Universität zu Berlin, 1999.
- [384] M. Hasenbusch, private communications.
- [385] M. Hasenbusch, “Eliminating leading corrections to scaling in the three dimensional ϕ^4 model on the lattice”, e-print cond-mat/0010463.
- [386] M. Hasenbusch, M. Marcu, and K. Pinn, *Physica A* **208**, 124 (1994).
- [387] M. Hasenbusch and K. Pinn, *J. Phys. A* **30**, 63 (1997).
- [388] M. Hasenbusch and K. Pinn, *J. Phys. A* **30**, 366 (1997).
- [389] M. Hasenbusch and K. Pinn, *J. Phys. A* **31**, 6157 (1998).
- [390] M. Hasenbusch, K. Pinn, and S. Vinti, *Phys. Rev. B* **59**, 11471 (1999).
- [391] M. Hasenbusch and T. Török, *J. Phys. A* **32**, 6361 (1999).
- [392] P. Hasenfratz, *Eur. Phys. J. B* **13**, 11 (2000).
- [393] A. Hasenfratz, E. Hasenfratz, and P. Hasenfratz, *Nucl. Phys. B* **180**, 353 (1981).
- [394] P. Hasenfratz, M. Maggiore, and F. Niedermayer, *Phys. Lett. B* **245**, 522 (1990).
- [395] P. Hasenfratz and F. Niedermayer, *Phys. Lett. B* **245**, 529 (1990).
- [396] P. Hasenfratz and M. Niedermayer, *Phys. Lett. B* **268**, 231 (1991).
- [397] P. Hasenfratz and F. Niedermayer, *Nucl. Phys. B* **414**, 785 (1994).
- [398] J. M. Hastings, L. M. Corliss, and W. Kunnmann, *Phys. Rev. B* **31**, 2902 (1985).
- [399] I. Hatta and H. Ikeda, *J. Phys. Soc. Japan* **48**, 77 (1980).
- [400] A. Haupt and J. Straub, *Phys. Rev. E* **59**, 1795 (1999).
- [401] M. Hennecke, *Phys. Rev. B* **48**, 6271 (1993).
- [402] H.-O. Heuer, *Phys. Rev. B* **42**, 6476 (1990).
- [403] H.-O. Heuer, *J. Phys. A* **26**, L333 (1993).
- [404] S. Hikami, *Nucl. Phys. B* **215**, 555 (1983).
- [405] S. Hikami and E. Brézin, *J. Phys. A* **11**, 1141 (1978).
- [406] J. P. Hill, Q. Feng, Q. J. Harris, R. J. Birgeneau, A. P. Ramirez, and A. Cassanho, *Phys. Rev. B* **55**, 356 (1997).
- [407] K. Hirakawa and H. Yoshizawa, *J. Phys. Soc. Japan* **47**, 368 (1979).
- [408] R. Hocken and G. Stell, *Phys. Rev. A* **8**, 887 (1973).
- [409] C. Hohenberg, A. Aharony, B. I. Halperin, and E. D. Siggia, *Phys. Rev. B* **13**, 2986 (1976).
- [410] P. C. Hohenberg and P. C. Martin, *Ann. Phys.* **34**, 291 (1965).
- [411] T. Holey and M. Föhnle, *Phys. Rev. B* **41**, 11709 (1990).
- [412] C. Holm and W. Janke, *Phys. Rev. B* **48**, 936 (1993); *Phys. Lett. A* **173**, 8 (1993); *J. Appl. Phys.* **73**, 5488 (1993).
- [413] C. Holm and W. Janke, *J. Phys. A* **27**, 2553 (1994).
- [414] C. Holm and W. Janke, *Phys. Rev. Lett.* **78**, 2265 (1997).
- [415] Yu. Holovatch and M. Shpot, *J. Stat. Phys.* **66**, 867 (1992).
- [416] Yu. Holovatch and T. Yavors’kii, *J. Stat. Phys.* **92**, 785 (1998).
- [417] F. Huang, G. J. Mankey, M. T. Kief, and R. F. Willis, *J. Appl. Phys.* **73**, 6760 (1993).
- [418] K. Hukushima, *J. Phys. Soc. Jpn.* **69**, 631 (2000).
- [419] D. L. Hunter and G. A. Baker, Jr., *Phys. Rev. B* **7**, 3346 (1973); *B* **7**, 3377 (1973); *B* **19**, 3808 (1979).
- [420] M. T. Hutchins, P. Day, E. Janke, and R. Pynn, *J. Magn. Magn. Mater.* **54**, 673 (1986).
- [421] S. N. Isakov, *Comm. Math. Phys.* **95**, 427 (1984).
- [422] E. Ising, *Z. Phys.* **31**, 253 (1925).
- [423] R. B. Israel, in *Random Fields*, Vol. II, J. Fritz, J. L. Lebowitz, and D. Szász (North-Holland, Amsterdam, 1981).
- [424] C. Itzykson and J. M. Drouffe, *Statistical Field Theory*, (Cambridge Univ. Press, Cambridge 1989).

- [425] C. Itzykson, R. B. Pearson, and J. B. Zuber, Nucl. Phys. B **220**, 415 (1983).
- [426] C. Itzykson, M. E. Peskin, and J. B. Zuber, Phys. Lett. B **95**, 259 (1980).
- [427] Y. Iwasaki, K. Kanaya, S. Kaya, and T. Yoshié, Phys. Rev. Lett. **78**, 179 (1997).
- [428] J. Jacob, A. Kumar, M. A. Anisimov, A. A. Povodyrev, and J. V. Sengers, Phys. Rev. E **58**, 2188 (1998).
- [429] D. T. Jacobs, Phys. Rev. A **33**, 2605 (1986).
- [430] W. Janke, Phys. Lett. A **148**, 306 (1990).
- [431] W. Janke, Phys. Rev. B **55**, 3580 (1997).
- [432] W. Janke and K. Nather, Phys. Rev. B **48**, 7419 (1993); Phys. Lett. A **157**, 11 (1991).
- [433] H. K. Janssen, K. Oerding, and E. Sengespeick, J. Phys. A **28**, 6073 (1995).
- [434] H. K. Janssen, B. Schaub, and B. Schmittmann, Z. Phys. B **73**, 539 (1989).
- [435] F. Jasch and H. Kleinert, “Fast convergent re-summation algorithm and critical exponents of φ^4 theory in three dimensions”, e-print cond-mat/9906246v2.
- [436] A. Jaster, J. Mainville, L. Schülke and B. Zheng, J. Phys. A **32**, 1395 (1999).
- [437] C. Jayaprakash and H. J. Katz, Phys. Rev. B **16**, 3987 (1977).
- [438] I. Jensen and A. J. Guttmann, J. Phys. A **32**, 4867 (1999).
- [439] Th. Jolicoer and F. David, Phys. Rev. Lett. **76**, 3148 (1996).
- [440] D. R. T. Jones, A. Love, and M. A. Moore, J. Phys. C **9**, 743 (1976).
- [441] J. V. José, L. P. Kadanoff, S. Kirkpatrick, and D. R. Nelson, Phys. Rev. B **16**, 1217 (1977).
- [442] B. D. Josephson, J. Phys. C **2**, 1113 (1969).
- [443] R. Joynt, Phys. Rev. Lett. **71**, 3015 (1993).
- [444] J. Jug, Phys. Rev. B **27**, 609 (1983).
- [445] L. P. Kadanoff, Nuovo Cimento **44**, 276 (1966); Physics **2**, 263 (1966).
- [446] L. P. Kadanoff, Phys. Rev. Lett. **34**, 1005 (1975); Ann. Phys. (NY) **100**, 359 (1976).
- [447] L. P. Kadanoff, A. Houghton, and M. C. Yalabik, J. Stat. Phys. **14**, 171 (1976).
- [448] H. Kadowaki, S. M. Shapiro, T. Inami, and Y. Ajiro, J. Phys. Soc. Japan **57**, 2640 (1988).
Y. Ajiro, T. Nakashima, Y. Unno, H. Kadowaki, M. Mekata, and N. Achiwa, J. Phys. Soc. Japan **57**, 2648 (1988).
- [449] H. Kadowaki, K. Ubukoshi, K. Hirakawa, J. L. Martinez, and G. Shirane, J. Phys. Soc. Japan **56**, 4027 (1988).
- [450] K. Kanaya and S. Kaya, Phys. Rev. D **51**, 2404 (1995).
- [451] M. Karowski and P. Weisz, Nucl. Phys. B **139**, 455 (1978).
- [452] M. Karowski, in *Field Theoretical Methods in Particle Physics*, edited by W. Ruhl, 1980, p. 307.
- [453] F. Karsch, E. Laermann, A. Peikert, C. Schmidt, and S. Stickan, “QCD thermodynamics with 2 and 3 quark flavors”, e-print hep-lat/0010027.
- [454] F. Karsch and S. Stickan, Phys. Lett. B **488**, 319 (2000).
- [455] S. Katsura, N. Yazaki, and M. Takaishi, Can. J. Phys. **55**, 1648 (1977).
- [456] H. Kawamura, J. Phys. Soc. Japan **54**, 3220 (1985); **56**, 474 (1987).
- [457] H. Kawamura, J. Phys. Soc. Japan **55**, 2095 (1986); **58**, 584 (1989).
- [458] H. Kawamura, J. Phys. Soc. Japan **55**, 2157 (1986).
- [459] H. Kawamura, Phys. Rev. B **38**, 4916 (1988); (E) B **42**, 2610 (1990).
- [460] H. Kawamura, J. Phys. Soc. Japan **61**, 1299 (1992).
- [461] H. Kawamura, J. Phys.: Condens. Matter **10**, 4707 (1998).
- [462] S. Kawase, K. Maruyama, S. Tamaki, and H. Okazaki, J. Phys. Condens. Matter **6**, 10237 (1994).
- [463] R. Kenna and A. C. Irving, Phys. Lett. B **351**, 273 (1995); Nucl. Phys. B **485**, 583 (1997).
- [464] I. J. Ketley and D. J. Wallace, J. Phys. A **6**, 1667 (1973).

- [465] D. E. Khmel'nitskii, Zh. Eksp. Teor. Fiz. **68**, 1960 (1975) [Sov. Phys. JETP **41**, 981 (1976)].
- [466] C. W. Kieweit, H. E. Hall, and J. D. Reppy, Phys. Rev. Lett. **35**, 1286 (1975).
- [467] R. Kikuchi, Phys. Rev. **81**, 988 (1951).
G. An, J. Stat. Phys. **52**, 727 (1988).
T. Morita, J. Stat. Phys. **59**, 819 (1990).
- [468] J.-K. Kim, Phys. Rev. Lett. **70**, 1735 (1993); Nucl. Phys. B (Proc. Suppl.) **34**, 702 (1994).
- [469] J.-K. Kim, Phys. Lett. A **223**, 261 (1996).
- [470] J.-K. Kim, Phys. Lett. B **345**, 469 (1995).
- [471] J.-K. Kim, J. Phys. A **33**, 2675 (2000).
- [472] J.-K. Kim and D. P. Landau, Nucl. Phys. B (Proc. Suppl.) **53**, 706 (1997).
- [473] J.-K. Kim, D. P. Landau, and M. Troyer, Phys. Rev. Lett. **79**, 1583 (1997).
- [474] D. Kim and P. M. Levy, Phys. Rev. B **12**, 5105 (1975).
- [475] D. Kim, P. M. Levy, and L. F. Uffer, Phys. Rev. B **12**, 989 (1975).
- [476] J. K. Kim and A. Patrascioiu, Phys. Rev. D **47**, 2588 (1993).
- [477] J.-K. Kim and M. Troyer, Phys. Rev. Lett. **80**, 2705 (1998).
- [478] H. Kleinert, Phys. Lett. A **173**, 332 (1993).
- [479] H. Kleinert, Phys. Lett. A **207**, 133 (1995).
- [480] H. Kleinert, Phys. Rev. D **57**, 2264 (1998); D **58**, 107702 (1998); D **60**, 085001 (1999).
- [481] H. Kleinert, Phys. Lett. A **264**, 357 (2000).
- [482] H. Kleinert, J. Neu, V. Schulte-Frohlinde, K. G. Chetyrkin, and S. A. Larin, Phys. Lett. B **272**, 39 (1991); (E) B **319**, 545 (1993).
- [483] H. Kleinert and V. Schulte-Frohlinde, Phys. Lett. B **342**, 284 (1995).
- [484] H. Kleinert and S. Thoms, Phys. Rev. D **52**, 5926 (1995).
- [485] H. Kleinert, S. Thoms, and V. Schulte-Frohlinde, Phys. Rev. B **56**, 14428 (1997).
- [486] H. Kleinert and B. Van den Bossche, "Three-loop exponents, amplitude functions and amplitude ratios from variational perturbation theory", e-print cond-mat/0011329.
- [487] M. Kolesik and M. Suzuki, Physica A **215**, 138 (1995).
- [488] X.-P. Kong, H. Au-Yang, and J. H. H. Perk, Phys. Lett. A **116**, 54 (1986); A **118**, 336 (1986).
- [489] A. L. Korzhenevskii, Zh. Eksp. Teor. Fiz. **71**, 1434 (1976) [Sov. Phys. JETP **44**, 751 (1976)].
- [490] J. M. Kosterlitz, J. Phys. C **7**, 1046 (1974).
- [491] J. M. Kosterlitz and D. J. Thouless, J. Phys. C **6**, 1181 (1973).
- [492] H. J. Krause, R. Schloms, and V. Dohm, Z. Phys. B **79**, 287 (1990).
- [493] M. Krech and D. P. Landau, Phys. Rev. B **60**, 3375 (1999).
- [494] H. Kunz and G. Zumbach, J. Phys. A **26**, 3121 (1993).
- [495] S. Kuwabara, H. Aoyama, H. Sato, and K. Watanabe, J. Chem. Eng. Data **40**, 112 (1995).
- [496] S.-N. Lai and M. E. Fisher, Molec. Phys. **88**, 1373 (1996).
- [497] L. D. Landau, Phys. Z. Sowjetunion **11**, 26 (1937); **11**, 545 (1937).
- [498] D. P. Landau, Phys. Rev. B **22**, 2450 (1980).
- [499] J. S. Langer, Ann. Phys. **41**, 108 (1967).
- [500] S. A. Larin, M. Mönnigman, M. Strösser, and V. Dohm, Phys. Rev. B **58**, 3394 (1998).
- [501] A. I. Larkin and D. E. Khmel'nitskii, Zh. Eksp. Teor. Fiz. **56**, 647 (1969) [Sov. Phys. JETP **29**, 1123 (1969)].
- [502] I. D. Lawrie, J. Phys. A **14**, 2489 (1981).
- [503] D. Lawrie and S. Sarbach, in *Phase Transitions and Critical Phenomena*, vol. 9, edited by C. Domb and J. L. Lebowitz (Academic Press, London, 1984).
- [504] D. Lederman, C. A. Ramos, V. Jaccarino, and J. L. Cardy, Phys. Rev. B **48**, 8365 (1993).
- [505] J. C. Le Guillou and J. Zinn-Justin, Phys. Rev. Lett. **39**, 95 (1977); Phys. Rev. B **21**, 3976 (1980).

- [506] J. C. Le Guillou and J. Zinn-Justin, *J. Physique Lett.* **46**, L137 (1985).
- [507] J. C. Le Guillou and J. Zinn-Justin, *J. Physique* **48**, 19 (1987).
- [508] B. Li, N. Madras, and A. D. Sokal, *J. Stat. Phys.* **80**, 661 (1995).
- [509] Y.-H. Li and S. Teitel, *Phys. Rev. B* **41**, 11388 (1990).
- [510] E. H. Lieb, *Phys. Rev.* **162**, 162 (1967).
- [511] E. H. Lieb and F. Y. Wu, in *Phase Transitions and Critical Phenomena*, edited by C. Domb and N. S. Green (Academic Press, New York, 1972), Vol. 1.
- [512] J. A. Lipa and T. C. P. Chui, *Phys. Rev. Lett.* **51**, 2291 (1983).
- [513] J. A. Lipa, D. R. Swanson, J. Nissen, T. C. P. Chui, and U. E. Israelsson, *Phys. Rev. Lett.* **76**, 944 (1996).
- [514] J. A. Lipa, D. R. Swanson, J. Nissen, Z. K. Geng, P. R. Williamson, D. A. Stricker, T. C. P. Chui, U. E. Israelsson, and M. Larson, *Phys. Rev. Lett.* **84**, 4894 (2000).
- [515] L. N. Lipatov, *Zh. Eksp. Teor. Fiz.* **72**, 411 (1977) [*Sov. Phys. JETP* **45**, 216 (1977)].
- [516] A. J. Liu and M. E. Fisher, *Physica A* **156**, 35 (1989).
- [517] D. Loison and H. T. Diep, *Phys. Rev. B* **50**, 16453 (1994).
- [518] D. Loison and K. D. Schotte, *Eur. Phys. J. B* **5**, 735 (1998).
- [519] D. Loison and K. D. Schotte, *Eur. Phys. J. B* **14**, 125 (2000).
- [520] D. Loison, A. I. Sokolov, B. Delamotte, S. A. Antonenko, K. D. Schotte, and H. T. Diep, *Pis'ma v ZhETF* **72**, 487 (2000) [*JETP Lett.* **72**, 337 (2000)].
- [521] T. C. Lubensky, *Phys. Rev. B* **11**, 3573 (1975).
- [522] E. Luijten, *Phys. Rev. E* **59**, 4997 (1999).
- [523] E. Luijten and K. Binder, *Phys. Rev. E* **58**, 4060 (1998); **59**, 7254 (1999).
- [524] E. Luijten and K. Binder, *Europhys. Lett.* **47**, 311 (1999).
- [525] E. Luijten, H. W. J. Blöte, and K. Binder, *Phys. Rev. E* **54**, 4626 (1996).
- [526] E. Luijten, H. W. J. Blöte, and K. Binder, *Phys. Rev. Lett.* **79**, 561 (1997); *Phys. Rev. E* **56**, 6540 (1997).
- [527] M. Lüscher, *Nucl. Phys. B* **135**, 1 (1978) and unpublished errata.
- [528] M. Lüscher, *Nucl. Phys. B* **180**, 317 (1981).
- [529] M. Lüscher, G. Münster, and P. Weisz, *Nucl. Phys. B* **180**, 1 (1981).
- [530] M. Lüscher and P. Weisz, *Nucl. Phys. B* **300**, 325 (1988).
- [531] M. Lüscher, P. Weisz, and U. Wolff, *Nucl. Phys. B* **359**, 221 (1991).
- [532] M. Lüscher and U. Wolff, *Nucl. Phys. B* **339**, 222 (1990).
- [533] S.-k. Ma, *Modern Theory of Critical Phenomena* (The Benjamin/Cummings Publ., 1976).
- [534] D. MacDonald, D. L. Hunter, K. Kelly, and N. Jan, *J. Phys. A* **25**, 1429 (1992).
- [535] D. MacDonald, S. Joseph, D. L. Hunter, L. L. Moseley, N. Jan and A. J. Guttmann, *J. Phys. A* **33**, 5973 (2000).
- [536] N. Madras and A. D. Sokal, *J. Stat. Phys.* **50**, 109 (1988).
- [537] J. Magnen and V. Rivasseau, *Comm. Math. Phys.* **102**, 59 (1985).
- [538] J. Magnen and R. Sénéor, *Comm. Math. Phys.* **56**, 237 (1977).
- [539] A. Mailhot, M. L. Plumer and A. Caillé, *Phys. Rev. B* **50**, 6854 (1994).
- [540] T. Mainzer and D. Woermann, *Physica A* **225**, 312 (1996).
- [541] G. Mana, A. Pelissetto, and A. D. Sokal, *Phys. Rev. D* **54**, 1252 (1996).
- [542] E. Marinari, *Nucl. Phys. B* **235**, 123 (1984).
- [543] M. Marinelli, F. Mercuri, and D. P. Belanger, *J. Magn. Magn. Mater.* **140-144**, 1547 (1995).
- [544] J. Marro, A. Labarta, and J. Tejada, *Phys. Rev. B* **34**, 347 (1986).

- [545] T. E. Mason, M. F. Collins, and B. D. Gaulin, *J. Phys. C: Solid State Phys.* **20**, L945 (1987); *Phys. Rev. B* **39**, 586 (1989).
- [546] J. Mattsson, C. Djurberg, and P. Nordblab, *J. Magn. Magn. Mater.* **136**, L23 (1994).
- [547] I. O. Mayer, *J. Phys. A* **22**, 2815 (1989).
- [548] I. O. Mayer, *Physica A* **252**, 450 (1998).
- [549] I. O. Mayer and A. I. Sokolov, *Fiz. Tverd. Tela* **26**, 3454 (1984) [*Sov. Phys. Solid State* **26**, 2076 (1984)].
- [550] I. O. Mayer and A. I. Sokolov, *Izv. Akad. Nauk SSSR Ser. Fiz.* **51**, 2103 (1987).
- [551] I. O. Mayer, A. I. Sokolov, and B. N. Shalaye, *Ferroelectrics* **95**, 93 (1989).
- [552] J. Mazur, *J. Res. Natl. Bur. Stand. A* **69**, 355 (1965); *J. Chem. Phys.* **43**, 4354 (1965).
- [553] B. M. McCoy, in *Statistical Mechanics and Field Theory*, edited by V.V. Bazhanov and C.J. Burden, (World Scientific, Singapore, 1995).
- [554] A. J. McKane, *Phys. Rev. B* **49**, 12003 (1994).
- [555] D. S. McKenzie, *Phys. Rep.* **27**, 35 (1976).
- [556] D. S. McKenzie, *Can. J. Phys.* **57**, 1239 (1979).
- [557] D. S. McKenzie, C. Domb, and D. L. Hunter, *J. Phys. A* **15**, 3899 (1982).
- [558] D. S. McKenzie and M. A. Moore, *J. Phys. A* **4**, L82 (1971).
- [559] S. Mehtaand and F. M. Gasparini, *Phys. Rev. Lett.* **78**, 2596 (1997).
- [560] Y. B. Melnichenko, M. A. Anisimov, A. A. Povodyrev, G. D. Wignall, J. V. Sengers, and W. A. Van Hook, *Phys. Rev. Lett.* **79**, 5266 (1997).
- [561] T. Mendes, A. Pelissetto, and A. D. Sokal, *Nucl. Phys. B* **477**, 203 (1996).
- [562] N. D. Mermin and H. Wagner, *Phys. Rev. Lett.* **17**, 1133 (1966).
- [563] S. Meyer, unpublished, cited in Ref. [189].
- [564] A. A. Migdal, *Sov. Phys. JETP* **42**, 413 (1976); *Sov. Phys. JETP* **42**, 743 (1976).
- [565] P. W. Mitchell, R. A. Cowley, H. Yoshizawa, P. Böni, Y. J. Uemura, and R. J. Birgeneau, *Phys. Rev. B* **34**, 4719 (1986).
- [566] Y. Miyaki, Y. Einaga, and H. Fujita, *Macromolecules* **11**, 1180 (1978).
- [567] K. K. Mon and K. Binder, *Phys. Rev. E* **48**, 2498 (1993).
- [568] I. Montvay and G. Münster, *Quantum Fields on a Lattice*, (Cambridge Univ. Press, Cambridge, 1994).
- [569] T. Morris, *Phys. Lett. B* **345**, 139 (1995).
- [570] T. Morris, *Nucl. Phys. B* **495**, 477 (1997).
- [571] T. R. Morris, “New Developments in the Continuous Renormalization Group,” in *New Developments in Quantum Field Theory*, edited by P. H. Damgaard and J. Jurkiewicz (Plenum Press, New York–London, 1998) p. 147.
- [572] A. I. Mudrov and K. B. Varnashev, *Phys. Rev. B* **57**, 3562 (1998); *B* **57**, 5704 (1998).
- [573] A. I. Mudrov and K. B. Varnashev, *Phys. Rev. E* **58**, 5371 (1998).
- [574] A. I. Mudrov and K. B. Varnashev, “New approach to summation of field-theoretical series in models with strong coupling,” in *Proceedings of the Conference Problems of Quantum Field Theory*, Dubna (1998); e-print hep-th/9811125.
- [575] A. I. Mudrov and K. B. Varnashev, “Critical thermodynamics and the three-dimensional MN -component field model with cubic anisotropy from higher-loop RG expansions”, e-print cond-mat/0011167.
- [576] D. Mukamel, *Phys. Rev. Lett.* **34**, 481 (1975).
- [577] D. Mukamel and S. Krinsky, *J. Phys. C* **8**, L496 (1975).
- [578] D. Mukamel and S. Krinsky, *Phys. Rev. B* **13**, 5065 (1976).
- [579] D. Mukamel and S. Krinsky, *Phys. Rev. B* **13**, 5078 (1976).
- [580] N. Mulders, R. Mehrotra, L. S. Goldner, and G. Ahlers, *Phys. Rev. Lett.* **67**, 695 (1991).
- [581] G. Münster, *Nucl. Phys. B* **324**, 630 (1989); *B* **340**, 559 (1990).
P. Hoppe and G. Münster, *Phys. Lett. A* **238**, 265 (1998).
- [582] G. Münster and J. Heitger, *Nucl. Phys. B* **424**, 582 (1994).

- [583] G. Münster and P. Weisz, Nucl. Phys. B **180**, 13 (1981); B **180**, 330 (1981).
- [584] D. B. Murray and B. G. Nickel, “Revised estimates for critical exponents for the continuum n -vector model in 3 dimensions”, unpublished Guelph University report (1991).
- [585] M. Muthukumar and B. G. Nickel, J. Chem. Phys. **80**, 5839 (1984).
- [586] M. Muthukumar and B. G. Nickel, J. Chem. Phys. **86**, 460 (1987).
- [587] U. Nürger and D. A. Balzarini, Phys. Rev. B **39**, 9330 (1989).
- [588] T. Nattermann, J. Phys. A **9**, 3337 (1976).
- [589] T. Nattermann, Spin Glasses and Random Fields, edited by A. P. Young (World Scientific, Singapore, 1998), p. 277.
- [590] T. Nattermann and S. Trimper, J. Phys. A **8**, 2000 (1975).
- [591] D. R. Nelson and M. E. Fisher, Phys. Rev. B **11**, 1030 (1975); B **12**, 263 (1975).
- [592] D. R. Nelson, J. M. Kosterlitz, and M. E. Fisher, Phys. Rev. Lett. **33**, 813 (1974).
- [593] S. A. Newlove, J. Phys. C **16**, L423 (1983).
- [594] K. E. Newman and E. K. Riedel, Phys. Rev. B **25**, 264 (1982).
- [595] K. E. Newman and E. K. Riedel, Phys. Rev. B **30**, 6615 (1984).
- [596] G. Nickel and B. Sharpe, J. Phys. A **12**, 1819 (1979).
- [597] B. G. Nickel, in *Phase Transitions*, edited by M. Lévy, J. C. Le Guillou, and J. Zinn-Justin (Plenum, New York and London, 1982).
- [598] B. G. Nickel, Physica A **117**, 189 (1991).
- [599] B. G. Nickel, Macromolecules **24**, 1358 (1991).
- [600] B. G. Nickel, J. Phys. A **32**, 3889 (1999); **33**, 1693 (2000).
- [601] B. G. Nickel and M. Dixon, Phys. Rev. B **26**, 3965 (1981).
- [602] B. G. Nickel, D. I. Meiron, and G. A. Baker, Jr., “Compilation of 2-pt and 4-pt graphs for continuum spin models”, University Guelph Report, 1977, unpublished.
- [603] B. G. Nickel and J. J. Rehr, J. Stat. Phys. **61**, 1 (1990).
- [604] J. F. Nicoll and P. C. Albright, Phys. Rev. B **31**, 4576 (1985).
- [605] F. Niedermayer, M. Niedermaier, and P. Weisz, Phys. Rev. D **56**, 2555 (1997).
- [606] Th. Niemeijer and J. M. J. van Leeuwen, in *Phase Transitions and Critical Phenomena*, vol. 6, edited by C. Domb and M. S. Green (Academic Press, New York, 1976).
- [607] B. Nienhuis, Phys. Rev. Lett. **49**, 1062 (1982).
- [608] M. P. Nightingale, Physica A **83**, 561 (1976); Phys. Lett. A **59**, 486 (1976).
- [609] M. P. Nightingale and H. W. J. Blöte, Phys. Rev. Lett. **60**, 1562 (1988).
- [610] J. A. Nissen, D. R. Swanson, Z. K. Geng, V. Dohm, U. E. Israelsson, M. J. DiPirro, and J. A. Lipa, Low Temp. Phys. **24**, 86 (1998).
- [611] T. Ohta, Y. Oono, and K. Freed, Macromolecules **14**, 1588 (1981); Phys. Rev. A **25**, 2801 (1982).
- [612] P. Olsson, Phys. Rev. Lett. **73**, 3339 (1994); Phys. Rev. B **52**, 4526 (1995).
- [613] L. Onsager, Phys. Rev. **65**, 117 (1944); Nuovo Cimento (Suppl.) **6**, 261 (1949).
- [614] Y. Oohara, H. Kadowaki, and K. Iio, J. Phys. Soc. Japan **60**, 393 (1991).
- [615] Y. Oono, in *Advances in Chemical Physics*, Vol. LXI, edited by I. Prigogine and S. A. Rice, pag. 301, 1985.
- [616] E. V. Orlov and A. I. Sokolov, Fiz. Tverd. Tela **42**, 2087 (2000). A shorter English version appears as e-print hep-th/0003140.
- [617] W. P. Orrick, B. Nickel, A. J. Guttmann, and J. H. H. Perk, “The susceptibility of the square lattice Ising model: New developments,” J. Stat. Phys. in press.
- [618] D. V. Pakhnin and A. I. Sokolov, Phys. Rev. B **61**, 15130 (2000); JETP Lett. **71**, 412 (2000).
- [619] M. Palassini and S. Caracciolo, Phys. Rev. Lett. **82**, 5128 (1999).
- [620] G. Parisi, Cargèse Lectures (1973), J. Stat. Phys. **23**, 49 (1980).

- [621] G. Parisi, in *Recent Developments in Gauge Theories*, Cargèse Lectures (1979), edited by G. 't Hooft, C. Itzkison, A. Jaffe, H. Lehmann, P. K. Mitter, I. M. Singer and R. Stora (Plenum Publishing Corporation, New York, 1980).
- [622] G. Parisi, in *Proc. XXth Conference on High-Energy Physics*, Madison, WI, edited by L. Durand and L. G. Pondrom, AIP Conf. Proc. 68 (AIP, 1981)
- [623] G. Parisi, *Statistical field theory*, (Addison-Wesley, New York, 1988).
- [624] G. Parisi and R. Rapuano, Phys. Lett. B **100**, 485 (1981).
- [625] A. Parola and L. Reatto, Adv. Phys. **44**, 211 (1995).
- [626] A. Z. Patashinskii and V. L. Pokrovskii, Zh. Eksp. Teor. Fiz. **46**, 994 (1964) [Sov. Phys. JETP **19**, 667 (1964)]; Zh. Eksp. Teor. Fiz. **50**, 439 (1966) [Sov. Phys. JETP **23**, 292 (1966)].
- [627] A. Z. Patashinski and V. L. Pokrovski, Zh. Eksp. Teor. Fiz. **64**, 1445 (1973) [Sov. Phys. JETP **37**, 733 (1973)].
- [628] A. Z. Patashinskii and V. L. Pokrovskii, *Fluctuation Theory of Phase Transitions*, (Pergamon Press, New York, 1979).
- [629] A. Patrascioiu and E. Seiler, J. Stat. Phys. **69**, 573 (1992); Nucl. Phys. B (Proc. Suppl.) **30**, 184 (1993); Phys. Rev. Lett. **74**, 1920 (1995); Phys. Rev. Lett. **74**, 1924 (1995); Phys. Rev. D **57**, 1394 (1998); Phys. Rev. Lett. **84**, 5916 (2000).
- [630] G. S. Pawley, R. H. Swendsen, D. J. Wallace, and K. G. Wilson, Phys. Rev. B **29**, 4030 (1984).
- [631] F. Pázmándi, R. T. Scalettar, and G. T. Zimányi, Phys. Rev. Lett. **79**, 5130 (1997).
- [632] P. Peczak, A. M. Ferrenberg, and D. P. Landau, Phys. Rev. B **43**, 6087 (1991).
- [633] J. S. Pedersen, M. Laso, and P. Shurtenberger, Phys. Rev. E **54**, R5917 (1996).
- [634] R. A. Pelcovits and A. Aharony, Phys. Rev. B **31**, 350 (1985).
- [635] R. A. Pelcovits and D. R. Nelson, Phys. Lett. A **57**, 23 (1976).
- [636] A. Pelissetto, P. Rossi, and E. Vicari, Phys. Rev. E **58**, 7146 (1998).
- [637] A. Pelissetto, P. Rossi, and E. Vicari, Nucl. Phys. B **554**, 552 (1999).
- [638] A. Pelissetto, P. Rossi and E. Vicari, "The critical behavior of frustrated spin models with non-collinear order", e-print cond-mat/0007389.
- [639] A. Pelissetto, P. Rossi and E. Vicari, in preparation.
- [640] A. Pelissetto and E. Vicari, Nucl. Phys. B **519**, 626 (1998); Nucl. Phys. B (Proc. Suppl.) **73**, 775 (1999).
- [641] A. Pelissetto and E. Vicari, Nucl. Phys. B **522**, 605 (1998).
- [642] A. Pelissetto and E. Vicari, Nucl. Phys. B **540**, 639 (1999).
- [643] A. Pelissetto and E. Vicari, Nucl. Phys. B **575**, 579 (2000).
- [644] A. Pelissetto and E. Vicari, Phys. Rev. B **62**, 6393 (2000).
- [645] A. Pelizzola, Phys. Rev. E **53**, 5825 (1995); E **61**, 4915 (2000).
- [646] M. W. Pestak and M. H. W. Chan, Phys. Rev. B **30**, 274 (1984).
- [647] R. Pisarsky and F. Wilczek, Phys. Rev. D **29**, 338 (1984).
- [648] V. P. Plakhty, J. Kulda, D. Visser, E. V. Moskvina, and J. Wosnitza, Phys. Rev. Lett. **85**, 3942 (2000).
- [649] M. L. Plumer and A. Mailhot, Phys. Rev. B **50**, 16113 (1994).
- [650] A. M. Polyakov, *Gauge Fields and Strings*, (Harwood Academic Publ., London, 1987).
- [651] A. M. Polyakov, Phys. Lett. B **59**, 79 (1975).
- [652] V. Privman ed., *Finite Size Scaling and Numerical Simulation of Statistical Systems*, (World Scientific, Singapore, 1990).
- [653] V. Privman, J. Phys. A **16**, 3097 (1983).
- [654] V. Privman and M. E. Fisher, Phys. Rev. B **30**, 322 (1984).
- [655] V. Privman, P. C. Hohenberg, and A. Aharony, in *Phase Transitions and Critical Phenomena*, vol. 14, edited by C. Domb and J. L. Lebowitz (Academic Press, New York, 1991).

- [656] P. Provero, Phys. Rev. E **57**, 3861 (1998).
- [657] K. Rajagopal and F. Wilczek, Nucl. Phys. B **399**, 395 (1993).
- [658] C. A. Ramos, A. R. King, and V. Jaccarino, Phys. Rev. B **37**, 5483 (1988).
- [659] D. C. Rapaport, J. Phys. A **18**, 113 (1985).
- [660] M. Rawiso, R. Duplessix, and C. Picot, Macromolecules **20**, 630 (1987).
- [661] P. F. Rebillot and D. T. Jacobs, J. Chem. Phys. **109**, 4009 (1998).
- [662] J. J. Rehr, A. J. Guttman, and G. S. Joyce, J. Phys. A **13**, 1587 (1980).
- [663] T. Reisz, Phys. Lett. B **360**, 77 (1995).
- [664] T. Reisz, Nucl. Phys. B **450**, 569 (1995).
- [665] D. S. Ritchie and M. E. Fisher, Phys. Rev. B **5**, 2668 (1972).
- [666] R. Z. Roskies, Phys. Rev. B **24**, 5305 (1981).
- [667] N. Rosov, A. Kleinhammes, P. Lidbjörk, C. Hohenemser, and M. Eibschütz, Phys. Rev. B **37**, 3265 (1988).
- [668] P. Rossi and E. Vicari, Phys. Rev. D **49**, 6072 (1994); (E) D **50**, 4718 (1994); (E) D **55**, 1668 (1997).
- [669] P. Rossi and E. Vicari, Phys. Lett. B **389**, 571 (1996).
- [670] J. S. Rowlinson and B. Widom, *Molecular Theory of Capillarity* (Oxford University Press, London, 1982).
- [671] J. Rudnick, Phys. Rev. B **11**, 3397 (1975); B **18**, 1406 (1978).
- [672] J. Rudnick, W. Lay, and D. Jasnow, Phys. Rev. E **58**, 2902 (1998).
- [673] C. Ruge, P. Zhu, and F. Wagner, Physica A **209**, 431 (1994).
- [674] K. Rummukainen, M. Tsy-pin, K. Kajantie, M. Laine, and M. Shaposhnikov, Nucl. Phys. B **532**, 283 (1998).
- [675] J. Sak, Phys. Rev. B **10**, 3957 (1974).
- [676] J. Salas, J. Stat. Phys. **80**, 1309 (1995).
- [677] J. Salas and A. D. Sokal, J. Stat. Phys. **98**, 551 (2000); e-print cond-mat/9904038v1.
- [678] M. A. Salgueiro, B. G. Almeida, M. M. Amado, J. B. Sousa, B. Chevalier, and J. Étourneau, J. Magn. Magn. Mater. **125**, 103 (1993).
- [679] R. Savit, Rev. Mod. Phys. **52**, 453 (1980).
- [680] L. Schäfer, Phys. Rev. E **50**, 3517 (1994).
- [681] L. Schäfer and H. Horner, Z. Phys. B **29**, 251 (1978).
- [682] J. Schimtz, L. Belkoura, and D. Woermann, Ann. Phys. (Leipzig) **3**, 1 (1994).
- [683] R. Schloms and V. Dohm, Nucl. Phys. B **328**, 639 (1989).
- [684] R. Schloms and V. Dohm, Phys. Rev. B **42**, 6142 (1990).
- [685] J. Schneck, J. C. Toledano, C. Joffrin, J. Aubree, B. Joukoff, and A. Gabelotaud, Phys. Rev. B **25**, 1766 (1982).
- [686] P. Schofield, Phys. Rev. Lett. **22**, 606 (1969).
- [687] P. Schofield, J. D. Lister and J. T. Ho, Phys. Rev. Lett. **23**, 1098 (1969).
- [688] W. Schröer, S. Wiegand, and H. Weingärtner, Ber. Bunsenges. Phys. Chem. **97**, 975 (1993).
- [689] N. Schultka and E. Manousakis, Phys. Rev. B **49**, 12071 (1994).
- [690] N. Schultka and E. Manousakis, Phys. Rev. B **52**, 7528 (1995).
- [691] S. Seide and C. Wetterich, Nucl. Phys. B **562**, 524 (1999).
- [692] J. V. Sengers and J. M. H. Levelt Sengers, in *Progress in Liquid Physics*, edited by C. A. Croxton (Wiley, Chichester, UK, 1978), p. 103.
- [693] B. N. Shalaev, Zh. Eksp. Teor. Fiz. **73**, 2301 (1977) [Sov. Phys. JETP **46**, 1204 (1977)].
- [694] B. N. Shalaev, S. A. Antonenko, and A. I. Sokolov, Phys. Lett. A **230**, 105 (1997).
- [695] F. Shanes and B. G. Nickel, "Calculation of the radius of gyration for a linear flexible polymer chain with excluded volume interaction", unpublished.
- [696] N. A. Shpot, Phys. Lett. A **133**, 125 (1988); A **142**, 474 (1989).
- [697] N. A. Shpot, Zh. Eksp. Teor. Fiz. **98**, 1762 (1990) [Sov. Phys. JETP **71**, 989 (1990)].

- [698] R. R. P. Singh and M. E. Fisher, Phys. Rev. Lett. **60**, 548 (1988).
- [699] A. Singaas and G. Ahlers, Phys. Rev. B **30**, 5103 (1984).
- [700] C. Sinn and D. Woermann, Ber. Bunsenges. Phys. Chem. **96**, 913 (1992).
- [701] Z. Slanič and D. P. Belanger, J. Magn. Magn. Mater. **186**, 65 (1998).
- [702] Z. Slanič, D. P. Belanger, and J. A. Fernandez-Baca, J. Magn. Magn. Mater. **177-181**, 171 (1998).
- [703] Z. Slanič, D. P. Belanger, and J. A. Fernandez-Baca, Phys. Rev. Lett. **82**, 426 (1999).
- [704] F. A. Smirnov, *Form Factors in Completely Integrable Models of Quantum Field Theory* (World Scientific, Singapore, 1992).
- [705] A. D. Sokal, J. Stat. Phys. **25**, 25 (1981); **25**, 51 (1981).
- [706] A. D. Sokal, Ann. Inst. Henri Poincaré **37**, 317 (1982).
- [707] A. D. Sokal, Europhys. Lett. **27**, 661 (1994); (E) **30**, 123 (1995).
- [708] A. I. Sokolov, E. V. Orlov, V. A. Ul'kov, and S. S. Kashtanov, Phys. Rev. E **60**, 1344 (1999).
- [709] A. I. Sokolov and B. N. Shalaev, Fiz. Tverd. Tela **23**, 2058 (1981) [Sov. Phys. Solid State **23**, 1200 (1981)].
- [710] A. I. Sokolov and K. B. Varnashev, Phys. Rev. B **59**, 8363 (1999).
A. I. Sokolov, K. B. Varnashev, and A. I. Mudrov, Int. J. Mod. Phys. B **12**, 1365 (1998).
K. B. Varnashev and A. I. Sokolov, Fiz. Tverd. Tela **38**, 3665 (1996) [Phys. Solid State **38**, 1996 (1996)].
- [711] H. E. Stanley, *Introduction to phase transitions and critical phenomena*, (Oxford, New York, 1971).
- [712] R. B. Stinchcombe, in *Phase Transitions and Critical Phenomena*, edited by C. Domb and J. Lebowitz (Academic Press, New York, 1983), Vol. 7, p. 152.
- [713] J. Straub and K. Nitsche, Fluid Phase Equilibria **88**, 183 (1993).
- [714] C. Strazielle and H. Benoit, Macromolecules **8**, 203 (1975).
- [715] M. Stroesser, S.A. Larin, and V. Dohm, Nucl. Phys. B **540**, 654 (1999).
- [716] A. M. Strydom, P. de V. du Plessis, D. Kaczorowski, and E. Troć, Physica B **186-188**, 785 (1993).
- [717] M. F. Sykes, D. S. Gaunt, J. L. Martin, S. R. Mattingly, and J. W. Essam, J. Math. Phys. **14**, 1071 (1973).
- [718] K. Symanzik, in *Mathematical Problems in Theoretical Physics*, edited by R. Schrader et al. (Springer, Berlin, 1982).
- [719] K. Symanzik, Nucl. Phys. B **226**, 187 (1983); B **226**, 205 (1983).
- [720] D. R. Swanson, T. C. P. Chui, and J. A. Lipa, Phys. Rev. B **46**, 9043 (1992);
D. Marek, J. A. Lipa, and D. Philips, Phys. Rev. B **38**, 4465 (1988).
- [721] R. H. Swendsen, Phys. Rev. Lett. **42**, 859 (1979).
- [722] R. H. Swendsen and J.-S. Wang, Phys. Rev. Lett. **58**, 86 (1987).
- [723] R. H. Swendsen, in *Real Space Renormalization*, edited by T. W. Burkhardt and J. M. J. van Leeuwen (Springer, Berlin, 1982).
- [724] J. Sznajd and M. Dudziński, Phys. Rev. B **59**, 4176 (1999).
- [725] T. Takada and T. Watanabe, J. Low Temp. Phys. **49**, 435 (1982).
- [726] A. L. Talapov and H. W. J. Blöte, J. Phys. A **29**, 5727 (1996).
- [727] H. B. Tarko and M. E. Fisher, Phys. Rev. Lett. **31**, 926 (1973); Phys. Rev. B **11**, 1217 (1975).
- [728] N. Tetradis, Phys. Lett. B **431**, 380 (1998).
- [729] N. Tetradis and C. Wetterich, Nucl. Phys. B **422**, 541 (1994).
- [730] D. J. Thouless, Phys. Rev. **181**, 954 (1969).
- [731] T. R. Thurston, C. J. Peters, R. J. Birgeneau, and P. M. Horn, Phys. Rev. B **37**, 9559 (1988).
- [732] M. Tissier, B. Delamotte, and D. Mouhanna, Phys. Rev. Lett. **84**, 5208 (2000); "An exact renormalization group approach to frustrated magnets", e-print cond-mat/0101167.

- [733] J. C. Toledano, L. Michel, P. Toledano, and E. Brézin, *Phys. Rev. B* **31**, 7171 (1985).
- [734] D. Toussaint, *Phys. Rev. D* **55**, 362 (1997).
- [735] C. A. Tracy and B. M. McCoy, *Phys. Rev. B* **12**, 368 (1975).
- [736] M. M. Tsypin, *Phys. Rev. Lett.* **73**, 2015 (1994).
- [737] M. M. Tsypin, *Phys. Rev. B* **55**, 8911 (1997).
- [738] A. Tyler, H. A. Cho, and J. D. Reppy, *J. Low Temp. Phys.* **89**, 57 (1992).
- [739] H. van Beijeren, *Phys. Rev. Lett.* **38**, 993 (1977).
- [740] H. van Beijeren and I. Nolden, in *Topics in Current Physics, Vol. 43: Structure and Dynamics of Surfaces II*, edited by W. Schommers and P. van Blanckenhagen (Springer, Berlin, 1987).
- [741] A. C. D. van Enter, R. Fernández, and A. D. Sokal, *J. Stat. Phys.* **72**, 879 (1994); *Nucl. Phys. B (Proc. Suppl.)* **20**, 48 (1991).
- [742] A. C. D. van Enter, R. Fernández, and R. Kotecký, *J. Stat. Phys.* **79**, 969 (1995).
- [743] K. B. Varnashev, *Phys. Rev. B* **61**, 14660 (2000); *J. Phys. A* **33**, 3121 (2000).
- [744] C. Vohwinkel, *Phys. Lett. B* **301**, 208 (1993).
- [745] M. C. Yalabik and A. Houghton, *Phys. Lett. A* **61**, 1 (1977).
- [746] H. Yamakawa, F. Abe, and Y. Einaga, *Macromolecules* **26**, 1898 (1993).
- [747] A. Yamamoto, M. Fuji, G. Tanaka, and H. Yamakawa, *Polym. J.* **2**, 799 (1971).
- [748] C. N. Yang, *Phys. Rev.* **85**, 808 (1952).
- [749] J. Yoon and M. H. W. Chan, *Phys. Rev. Lett.* **78**, 4801 (1997).
- [750] M. Yosefin and E. Domany, *Phys. Rev. B* **32**, 1778 (1985).
- [751] D. J. Wallace, *J. Phys. C* **6**, 1390 (1973).
- [752] D. J. Wallace and R. P. K. Zia, *J. Phys. C* **7**, 3480 (1974).
- [753] D. J. Wallace and R. P. K. Zia, *Phys. Rev. B* **12**, 5340 (1975).
- [754] J.-S. Wang, D. P. Belanger, and B. D. Gaulin, *Phys. Rev. Lett.* **66**, 3195 (1991).
- [755] J.-S. Wang and D. Chowdhury, *J. Phys. (France)* **50**, 2905 (1989).
- [756] J.-S. Wang, M. Wöhlert, H. Mühlenbein, and D. Chowdhury, *Physica A* **166**, 173 (1990).
- [757] H. Weber, D. Beckmann, J. Wosnitza, and H. von Löhneysen, *Int. J. Mod. Phys. B* **9**, 1387 (1995).
- [758] J. D. Weeks, G. H. Gilmer, and H. J. Leamy, *Phys. Rev. Lett.* **31**, 549 (1973).
- [759] F. J. Wegner, in *Phase Transitions and Critical Phenomena*, vol. 6, edited by C. Domb and M. S. Green (Academic Press, New York, 1976).
- [760] F. J. Wegner and A. Houghton, *Phys. Rev. A* **8**, 401 (1973).
- [761] F. J. Wegner and E. Riedel, *Phys. Rev. B* **7**, 248 (1973).
- [762] G. Weill and J. des Cloizeaux, *J. Physique* **40**, 99 (1979).
- [763] R. A. Weston, *Phys. Lett. B* **219**, 315 (1989).
- [764] A. Weyersberg, T. Holey and M. Fähnle, *J. Stat. Phys.* **66**, 133 (1992).
- [765] J. F. Wheeler, *Phys. Lett. B* **136**, 402 (1984).
- [766] B. Widom, *J. Chem. Phys.* **41**, 1633 (1964).
- [767] B. Widom, *J. Chem. Phys.* **43**, 3892 (1965).
- [768] B. Widom, *J. Chem. Phys.* **43**, 3898 (1965).
- [769] D. G. Wiesler, H. Zabel, and S. M. Shapiro, *Z. Phys. B* **93**, 277 (1994).
- [770] F. Wilczek, *Int. J. Mod. Phys. A* **7**, 3911 (1992).
- [771] K. G. Wilson, *Phys. Rev. B* **4**, 3174 (1971).
- [772] K. G. Wilson, *Phys. Rev. B* **4**, 3184 (1971).
- [773] K. G. Wilson, *Phys. Rev. D* **10**, 2445 (1974).
- [774] K. G. Wilson and M. E. Fisher, *Phys. Rev. Lett.* **28**, 240 (1972).
- [775] K. G. Wilson and J. Kogut, *Phys. Rep.* **12**, 75 (1974).
- [776] S. Wiseman and E. Domany, *Phys. Rev. Lett.* **81**, 22 (1998); *Phys. Rev. E* **58**, 2938 (1998).
- [777] T. A. Witten, *J. Chem. Phys.* **76**, 3300 (1982).
- [778] T. A. Witten and L. Schäfer, *J. Chem. Phys.* **74**, 2582 (1981).

- [779] U. Wolff, Phys. Rev. Lett. **62**, 361 (1989); Nucl. Phys. B **322**, 759 (1989);
- [780] U. Wolff, Phys. Lett. B **248**, 335 (1990); Nucl. Phys. B **334**, 581 (1990).
- [781] M. Wortis, “Linked cluster expansion”, in *Phase Transitions and Critical Phenomena*, vol. 3, edited by C. Domb and M. S. Green (Academic Press, London, 1974).
- [782] J. Wosnitza, R. Deutschmann, H.v. Löhneysen and R. K. Kremer, J. Phys.: Condens. Matter **6**, 8045 (1994).
- [783] T. T. Wu, B. M. McCoy, C. A. Tracy, and E. Barouch, Phys. Rev. B **13**, 316 (1976).
- [784] U. Würz, M. Grubić, and D. Woermann, Ber. Bunsenges. Phys. Chem. **96**, 1460 (1992).
- [785] G. Zalczer, A. Bourgou, and D. Beysens, Phys. Rev. A **28**, 440 (1983).
- [786] A. B. Zamolodchikov, Adv. Stud. Pure Math. **19**, 641 (1989); Int. J. Mod. Phys. A **3**, 743 (1988).
- [787] A. B. Zamolodchikov and Al. B. Zamolodchikov, Ann. Phys. **120**, 253 (1979).
- [788] G. M. Zassenhaus and J. D. Reppy, Phys. Rev. Lett. **83**, 4800 (1999).
- [789] A. Zielesny, L. Belkoura, and D. Woermann, Ber. Bunsenges. Phys. Chem. **98**, 579 (1994).
- [790] S.-Y. Zinn and M. E. Fisher, Physica A **226**, 168 (1996).
- [791] S.-Y. Zinn, S.-N. Lai, and M. E. Fisher, Phys. Rev. E **54**, 1176 (1996).
- [792] J. Zinn-Justin, *Quantum Field Theory and Critical Phenomena*, third edition (Clarendon Press, Oxford, 1996).
- [793] J. Zinn-Justin, J. Physique **40**, 969 (1979); J. Physique **42**, 783 (1981).
- [794] J. Zinn-Justin, “Vector models in the large N limit: a few applications”, lecture for the 11th Taiwan Spring School, Taipei 1997, e-print hep-th/9810198.
- [795] J. Zinn-Justin, “Precise determination of critical exponents and equation of state by field theory methods,” e-print hep-th/0002136.
- [796] G. Zumbach, Phys. Rev. Lett. **71**, 2421 (1993); Nucl. Phys. B **413**, 771 (1994).